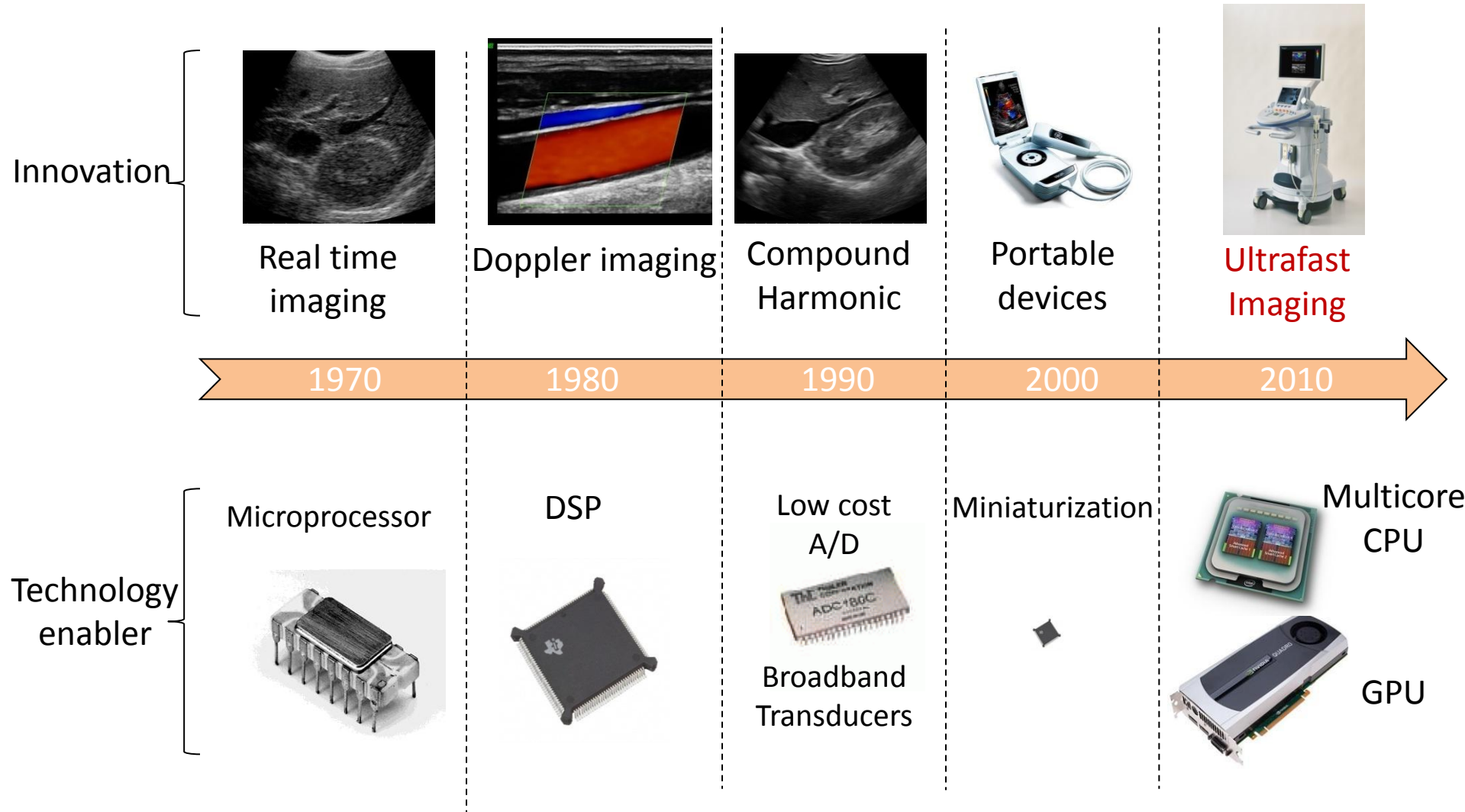


Plane Wave Imaging and Applications for Ultrafast Doppler, Elastography, and Contrast

Mathias Fink & Mickael Tanter

Short Course IEEE IUS, Dresden 2012

Ultrasound Technology Evolution



How to obtain an ultrasonic image ?

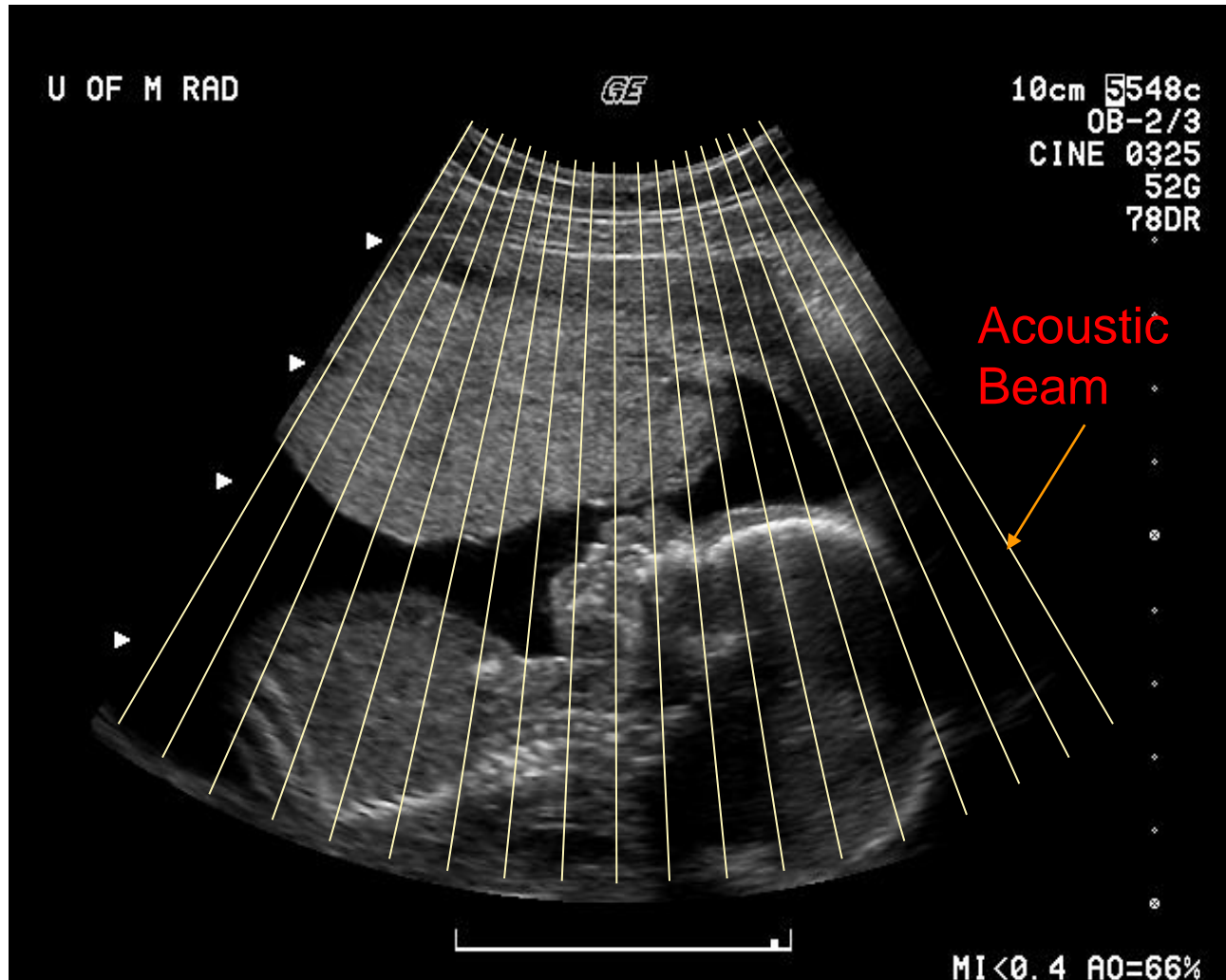
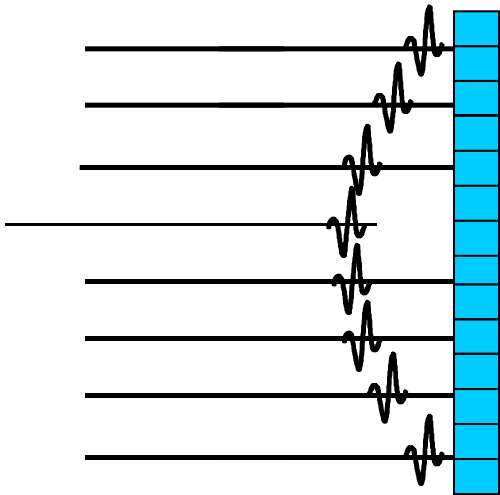
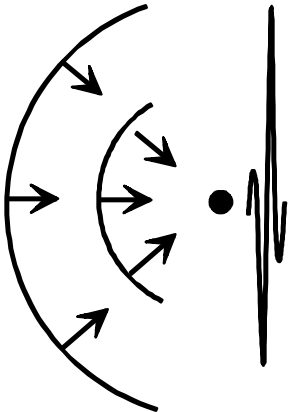


Image formation using sequential transmit beams

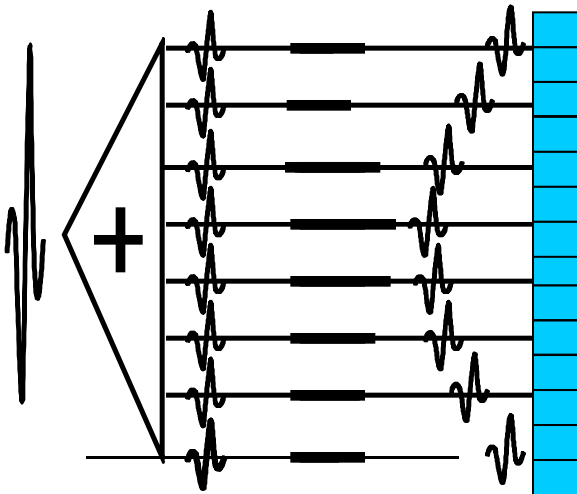
Focusing in transmit/receive mode



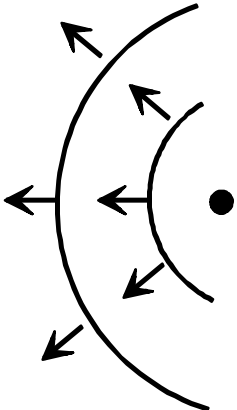
Focusing in transmit



Ultrasonic speed
uniform c

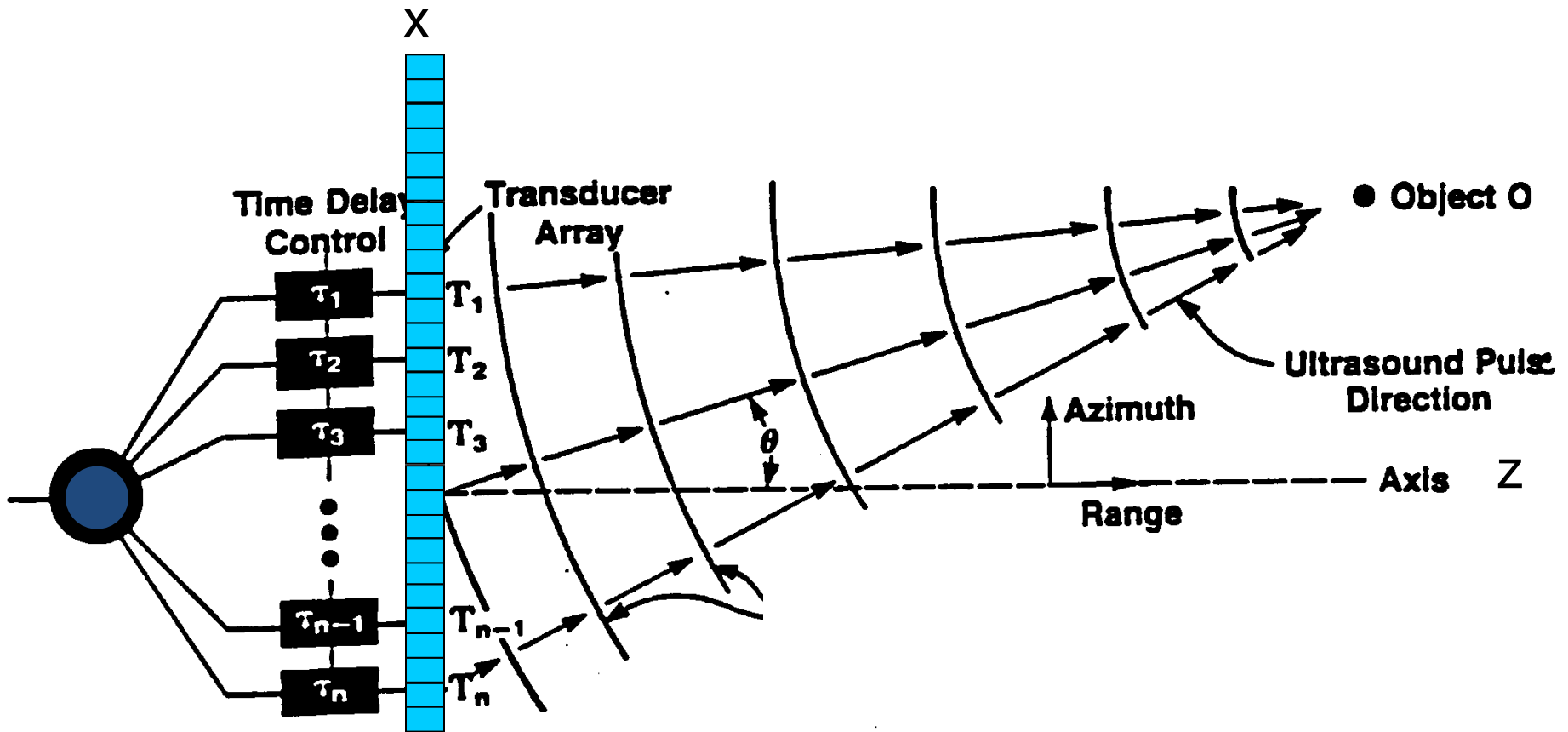


Focusing in receive
Beamforming



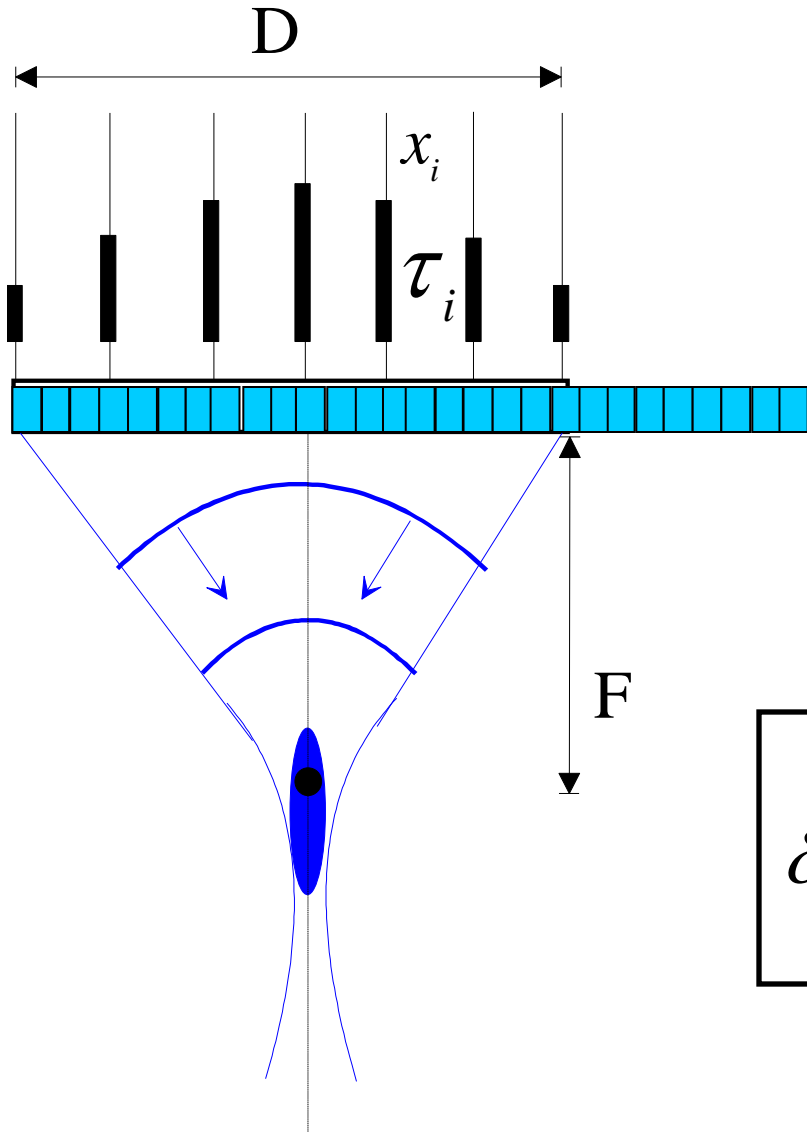
Double focusing

Steering and Focusing



$$\tau(x_i, \sin \theta_m, z_n) = \frac{-x_i \sin \theta_m}{c} + \frac{x_i^2 \cos^2 \theta_m}{2z_n c}$$

Focal spot dimension in transmit mode



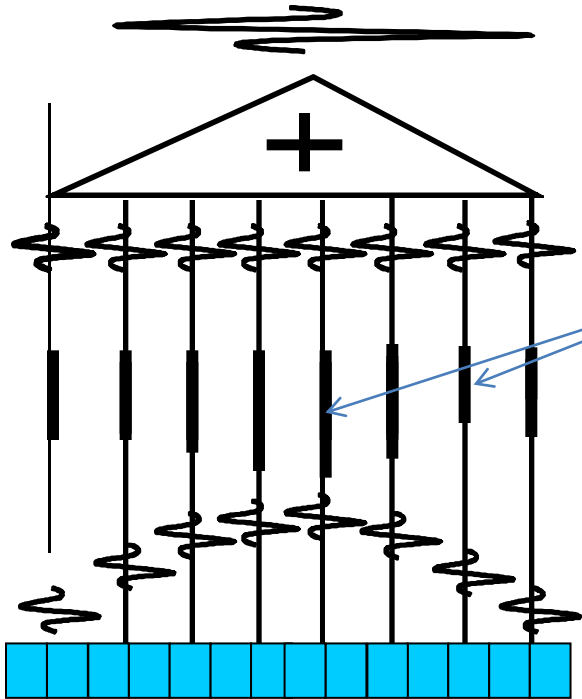
$$\tau_i = \frac{\sqrt{F^2 + (x_i - x)^2}}{c_0}$$

$$\delta_l = \frac{\lambda F}{D} \quad \delta_a = 7\lambda \left(\frac{F}{D} \right)^2$$

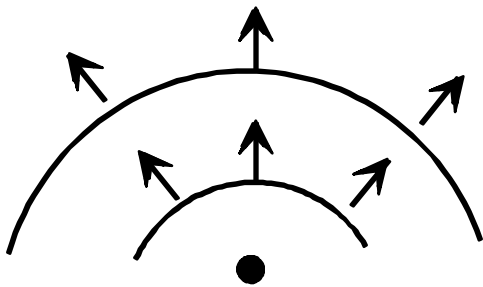
Transmit Beam Forming

- Time Delay Accuracy – typically $\lambda/32$
- Aperture Control – determined by format
- Apodization – primarily for depth of field
- Fixed focus – **multiple zone** / frame rate

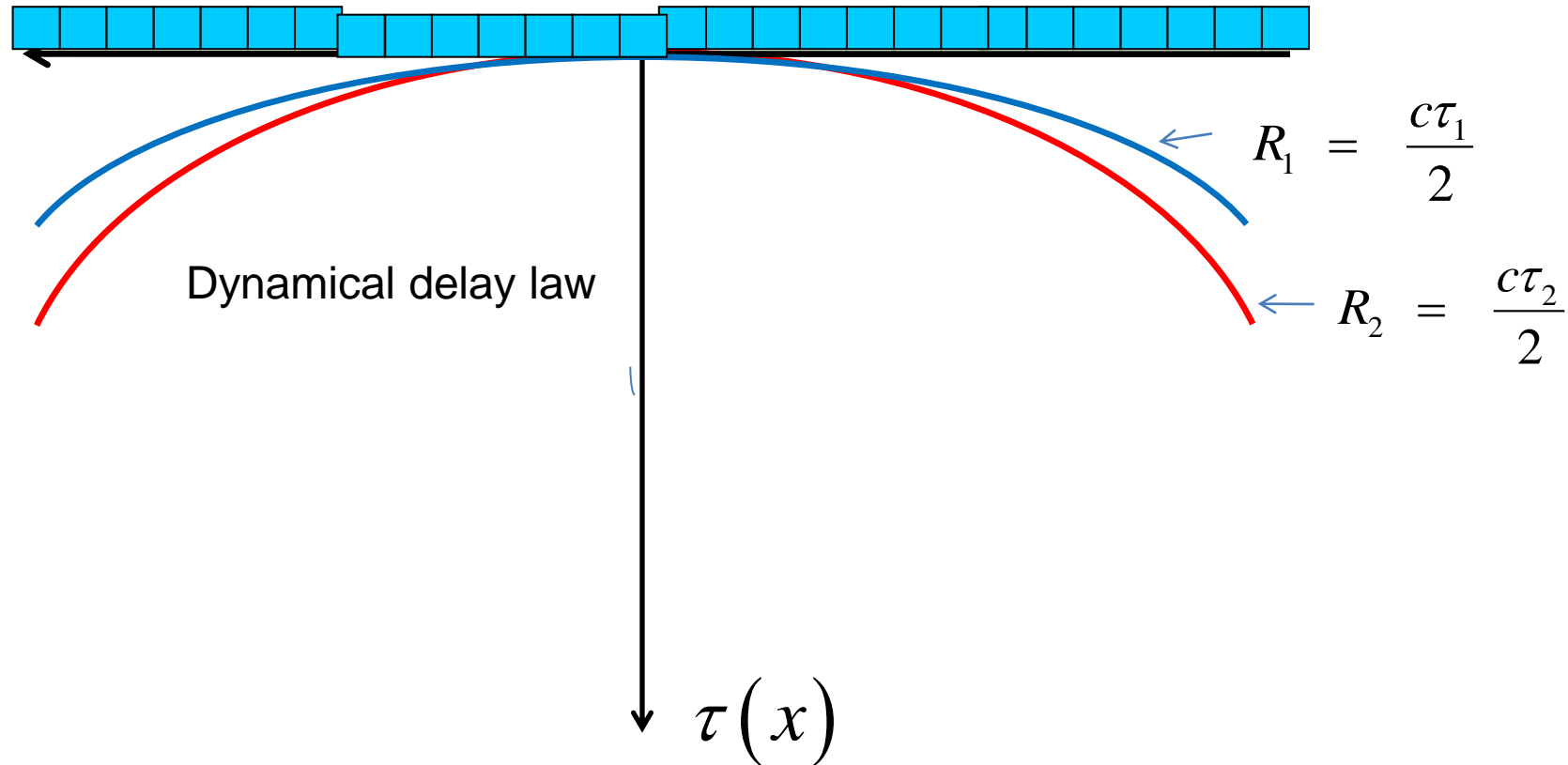
Beam Forming in Receive Mode



$$\tau_i = \frac{\sqrt{F^2 + (x_i - x)^2}}{c_0}$$

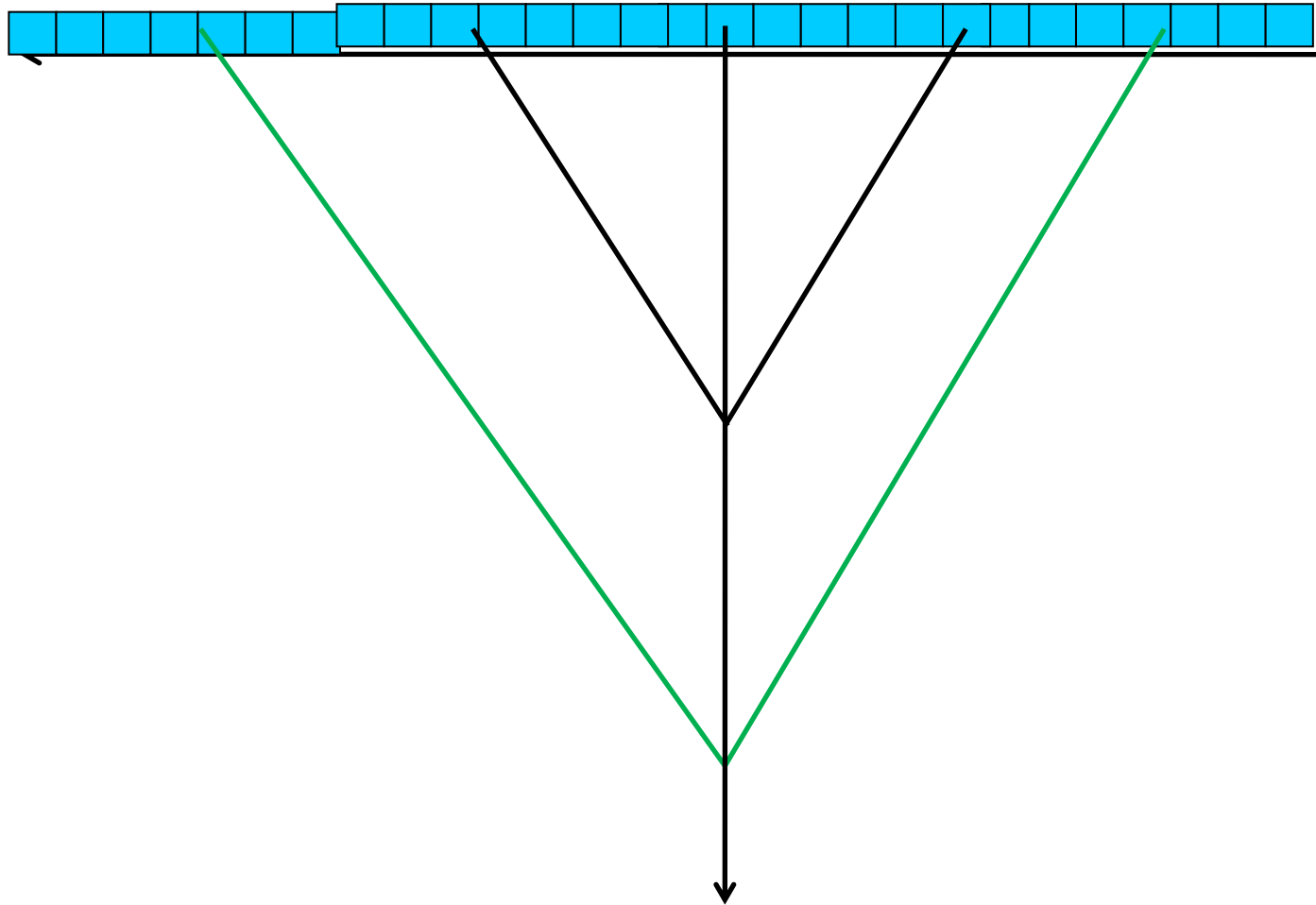


In receive mode, Dynamical Focusing with variable focal depth



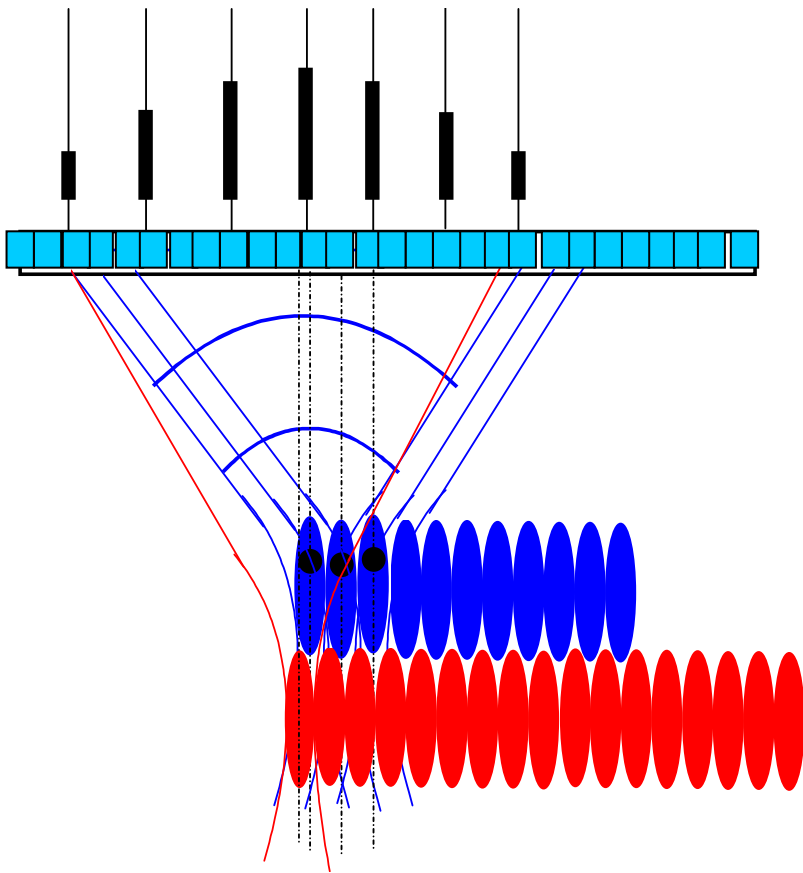
The focal depth is varying continuously with the time of arrival of the echoes

Dynamical Apodization



To get the same spatial resolution at all the depths
 F/D must stay constant on the whole depth of exploration

Frame Rate with Sequential Imaging



Typically, to get an image :
128 shots x 4 focal depths
= 512 ultrasonic shots

Time of flight – two ways:
60 μ s for 5 cm

Time to get a full image:
512 x 60 μ s = 0,032 s

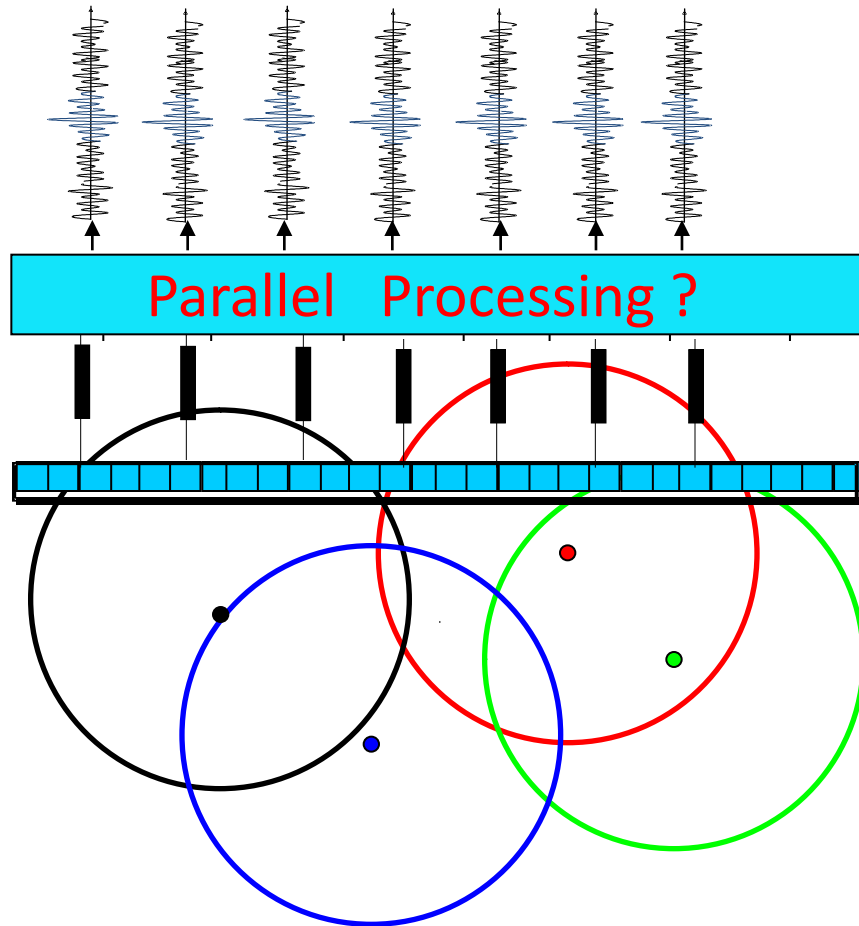
Frame rate:
1/0,032 = 35 frames/ second

25 to 50 frames/sec

How to go faster ?

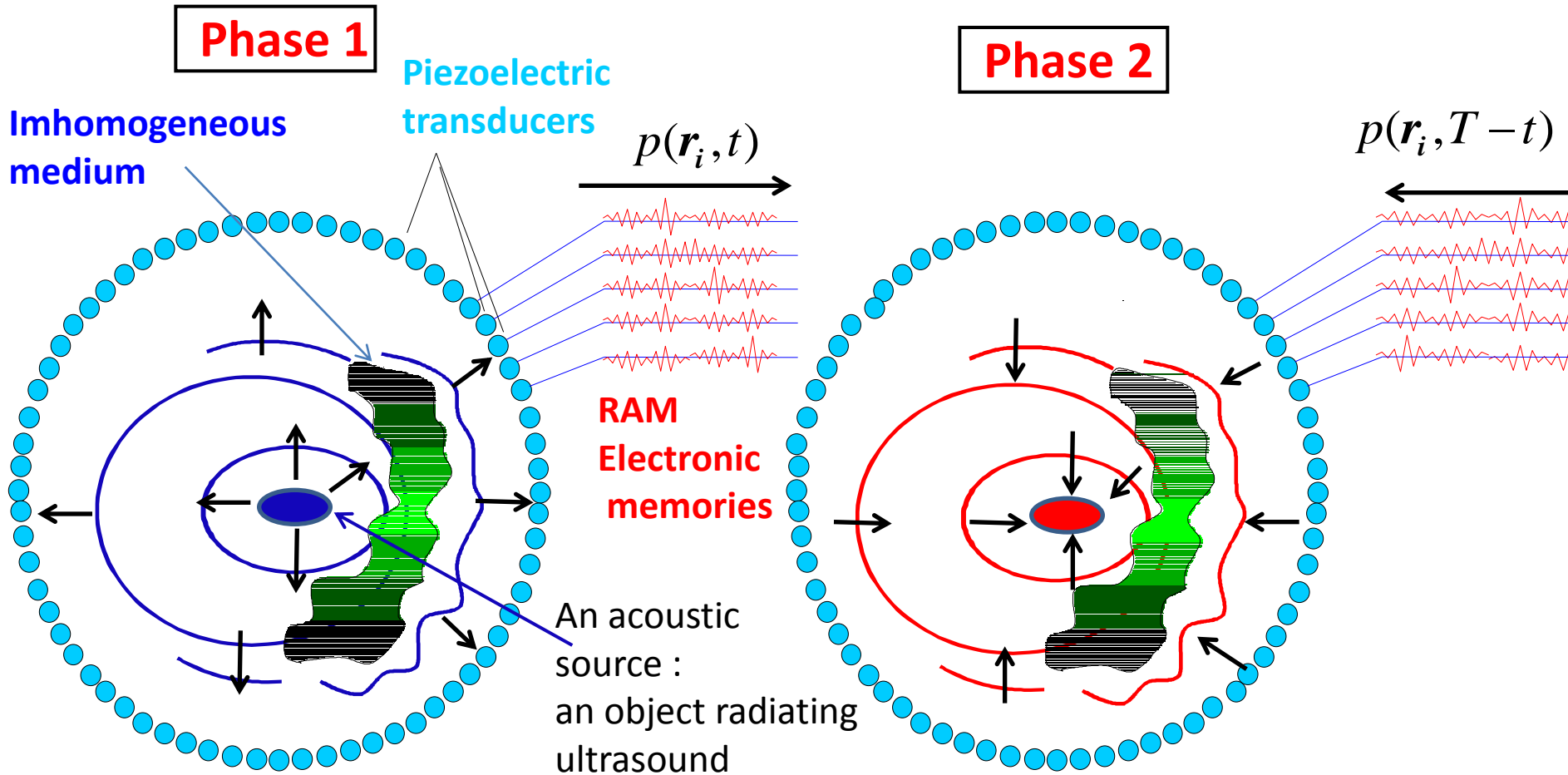
Replace the focused transmit beams by one unfocused transmitted beam that illuminated the whole field of view

Ultrafast Imaging

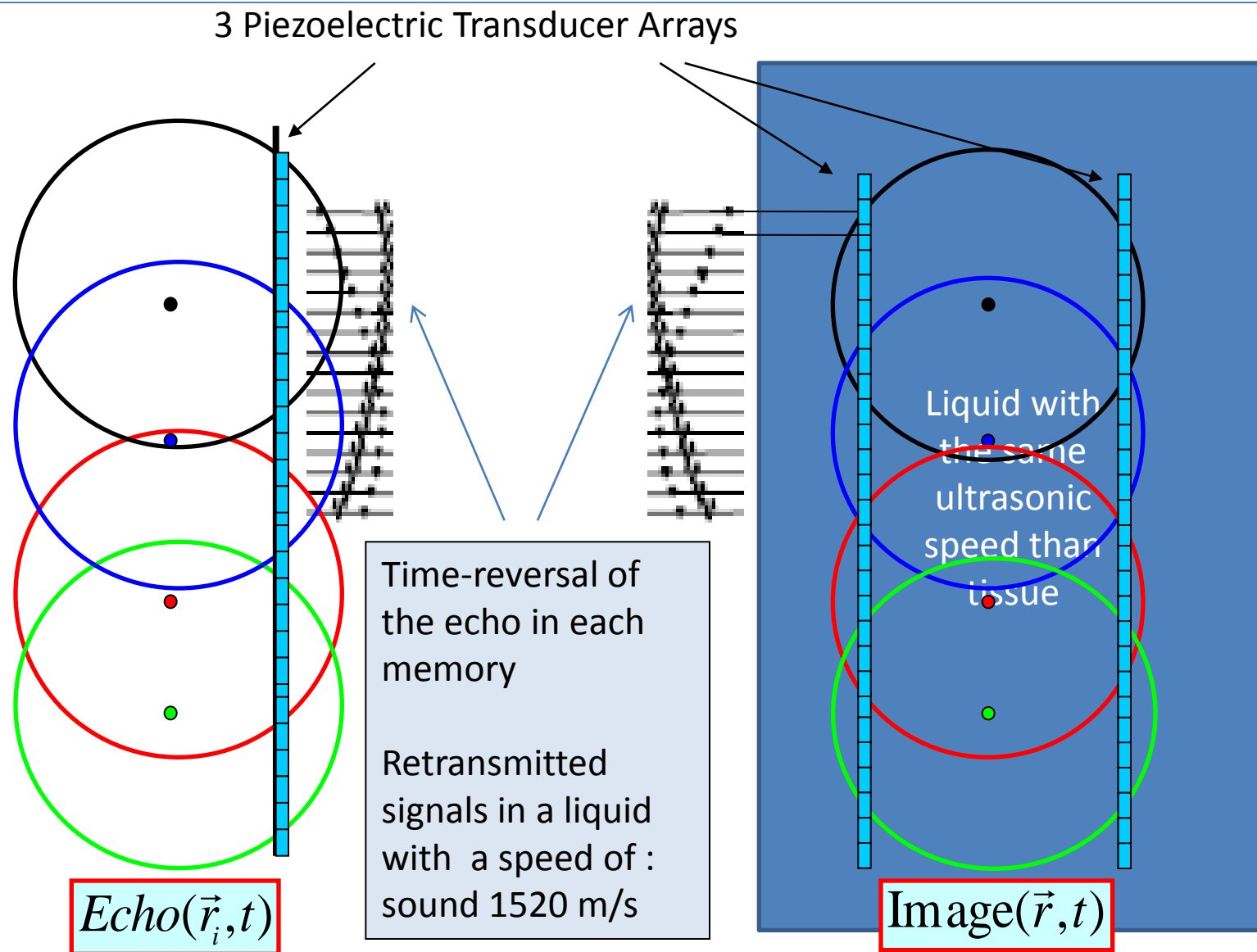


Plane Wave Insonification
One shot : One image

The Time-Reversal approach : An elegant way to build the Acoustic Image of any source radiating ultrasound



Ultrafast Imaging with Time-Reversal



The Dynamic Electronic Lens Approach

446

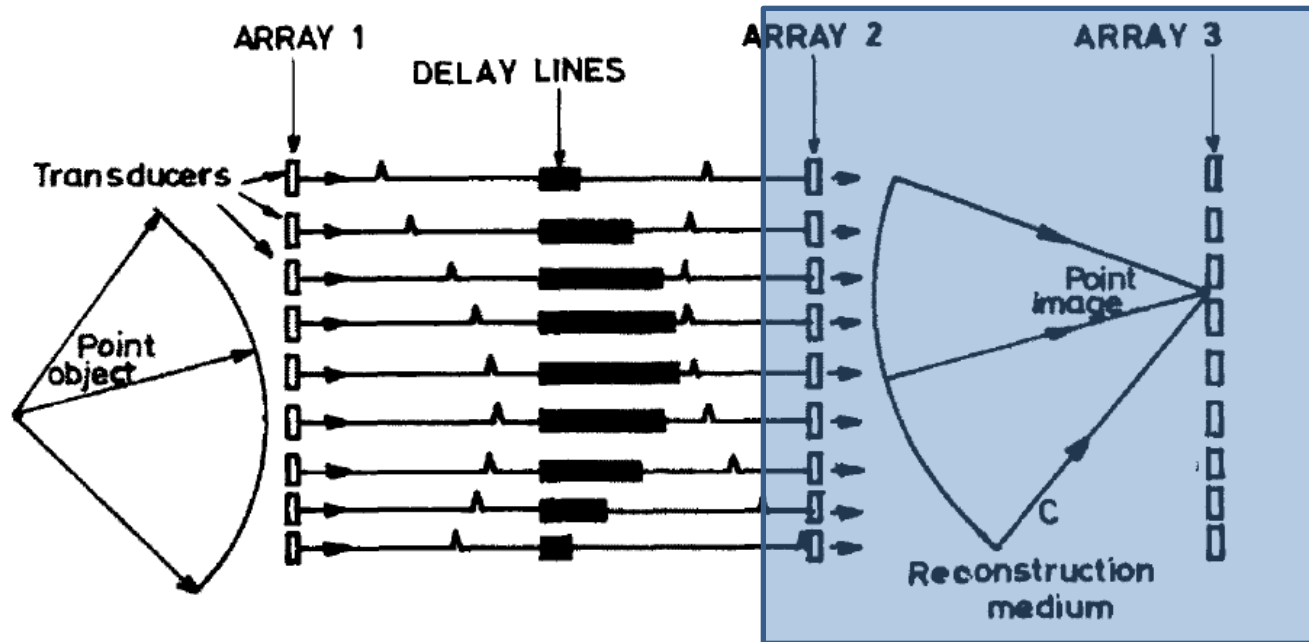


Fig. 3 - Electronic lens with delay lines and 2 transducers arrays,

$$\frac{1}{f} = \frac{1}{z} - \frac{1}{z'} = \frac{2z' - ct}{ctz'} \quad (4)$$

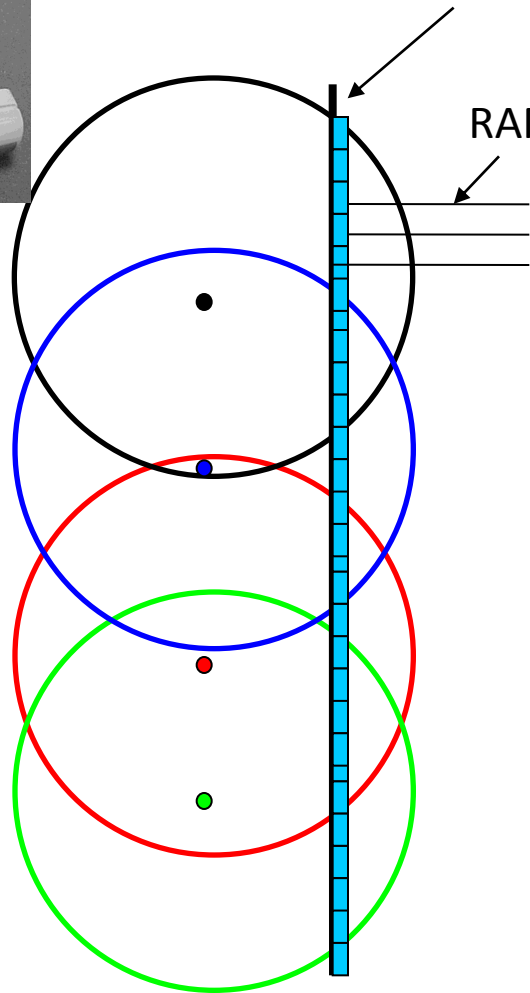
$$\Delta\tau(x_n, t) = \frac{-x_n^2}{2cf} = \frac{-x_n^2}{c^2} \left(\frac{1}{t} \right) + \frac{x_n^2}{2cz'} \quad (5)$$

M. Fink "Principles and techniques of acoustical imaging", Imaging processes and coherence in physics"Springer, Lecture Notes in Physics, 1979, p 438-452

The Computed Time-Reversal Approach



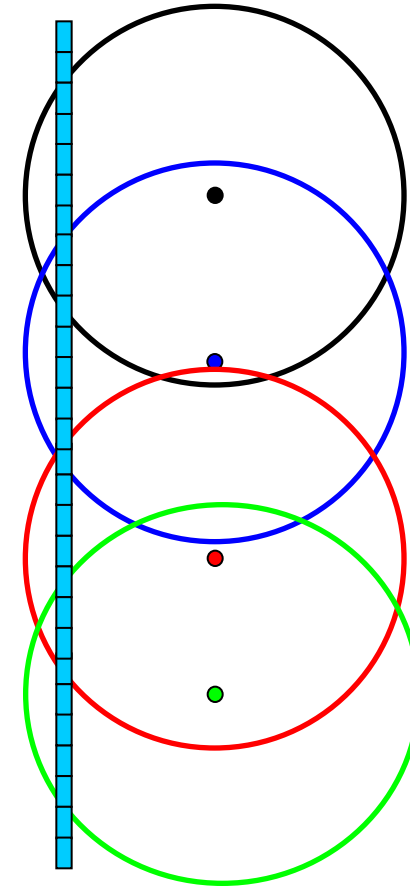
Piezoelectric Transducer Array



$Echo(\vec{r}_i, t)$

Computed Time Reversal and backpropagation

Hypothesis:
 c uniform: 1520 m/s



$Image(\vec{r}, t)$



Echoes and Images

$$Echo_i(t) = \begin{cases} \sum_n \alpha_n e(\vec{r}_i - \vec{r}_n; t - \tau_{ni}) & t \geq 0 \\ 0 & t < 0 \end{cases}$$

$$\text{with } \tau_{ni} = \left\{ z_n + \sqrt{z_n^2 + (x_i - x_n)^2} \right\} / c$$

Time-reversal Imaging

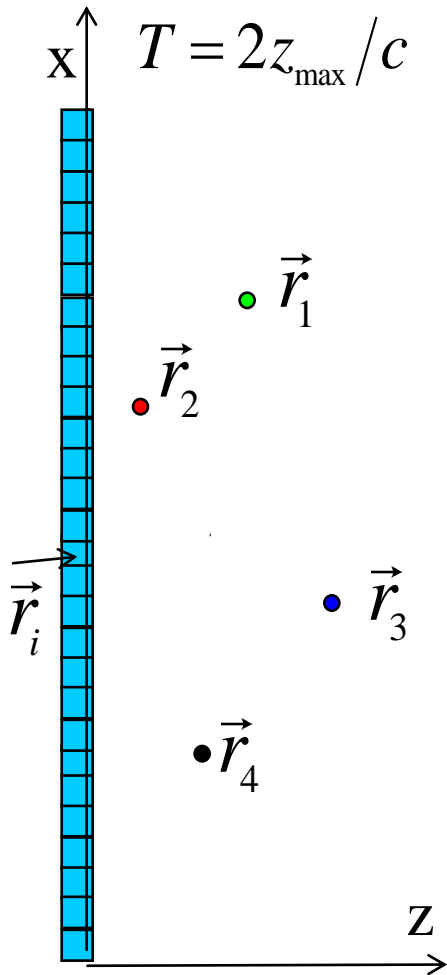
$$\text{Image}(\vec{r}, t) = \sum_i Echo_i(T - t) \otimes G_0(\vec{r} - \vec{r}_i; t) \quad \vec{r} = \{x, z\}$$

with $G_0(\vec{r}; t) = \delta(t - |\vec{r}|/c) / 4\pi|\vec{r}|$ the Green's function

$$\text{IMAGE}(\vec{r}) = \text{Image}(\vec{r}, t = z/c)$$

Parallel beam forming

$$\text{Image}(\vec{r}, T - t) = \sum_i Echo_i(t) \otimes \delta(T - t - |\vec{r} - \vec{r}_i|/c)$$



Conventional Imaging / Ultrafast Imaging

Conventional Imaging

Plane wave Imaging

Image field of view @ 50 Hz

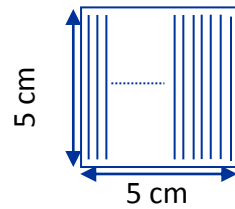
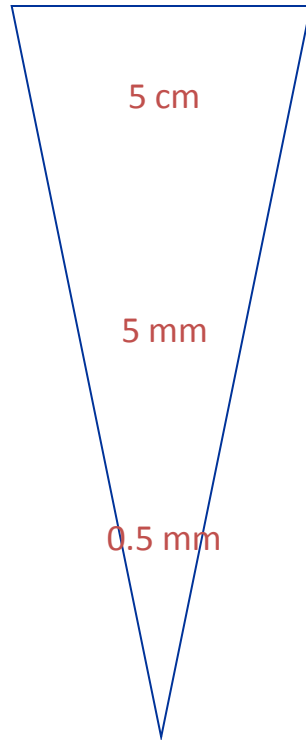


Image field of view @ 500 Hz

5 mm

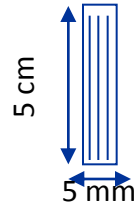
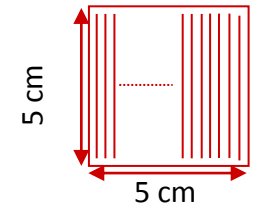
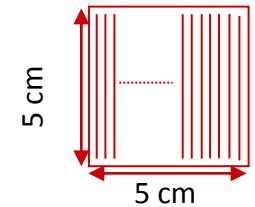
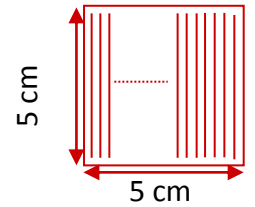
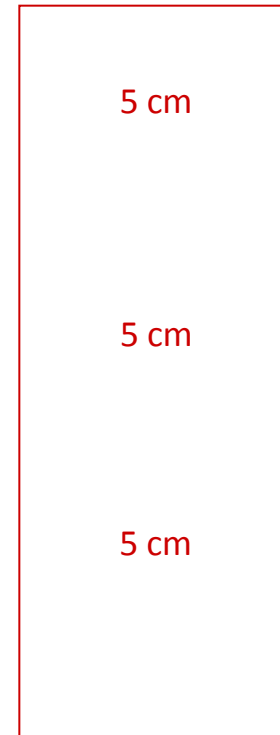
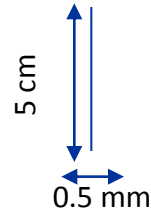


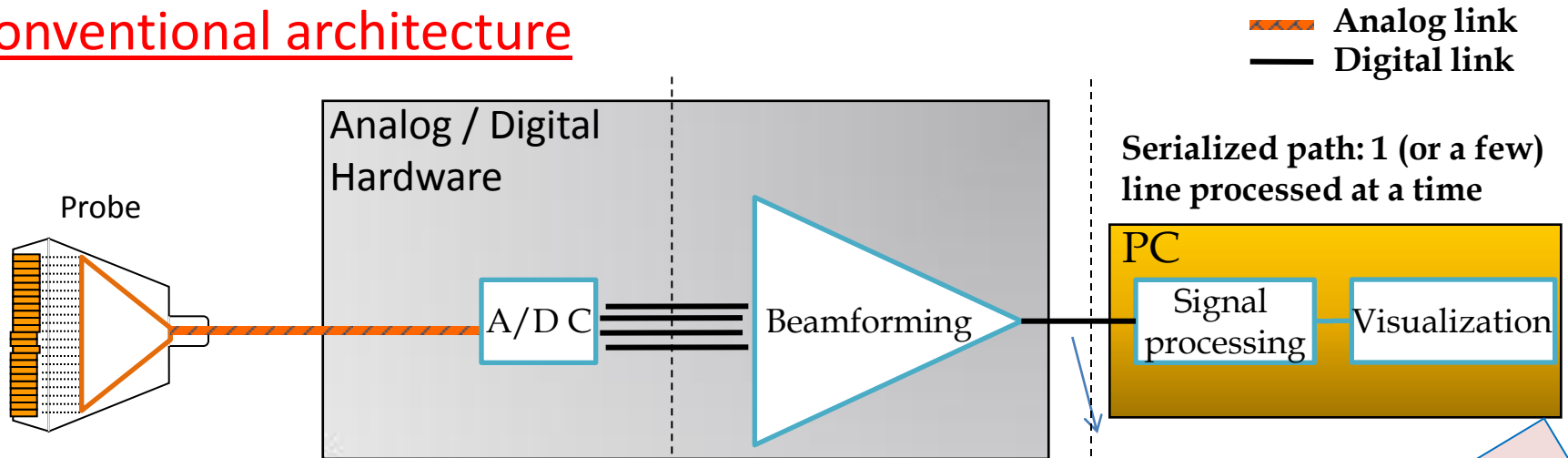
Image field of view @ 5000 Hz

0.5 mm

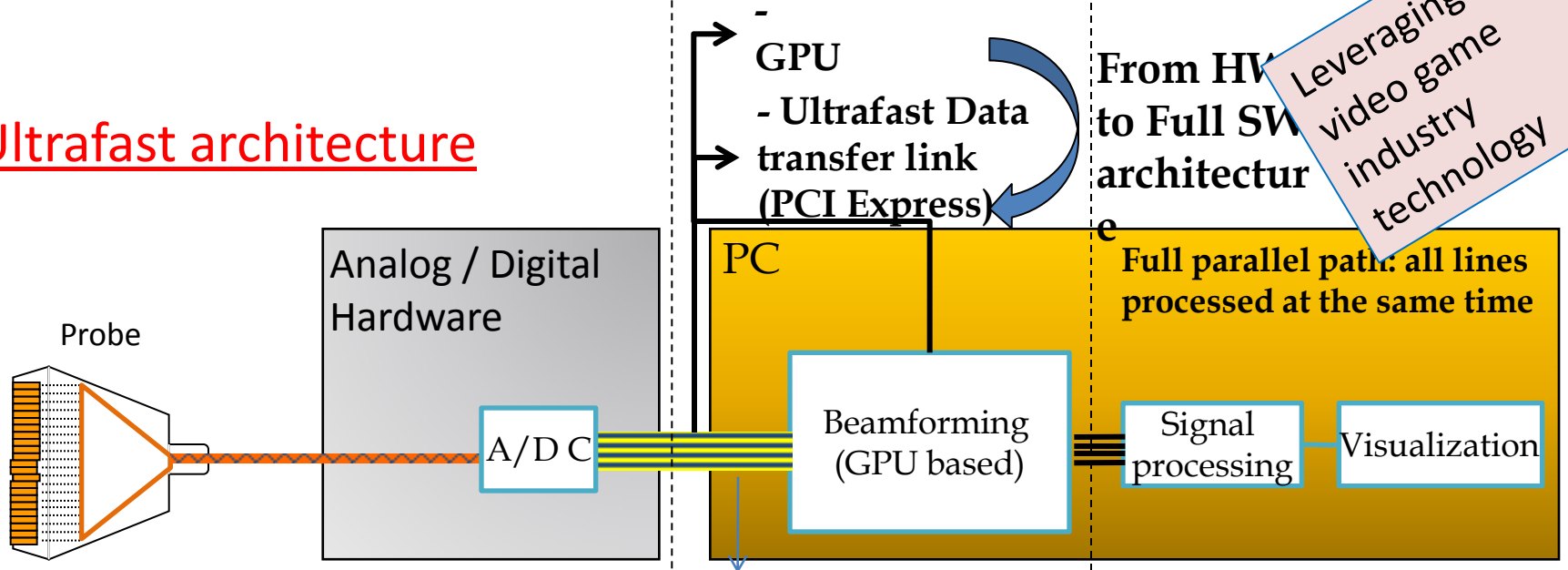


System Architecture

Conventional architecture



Ultrafast architecture



The Ancestors: A 20 transducers array For Ultrafast Imaging

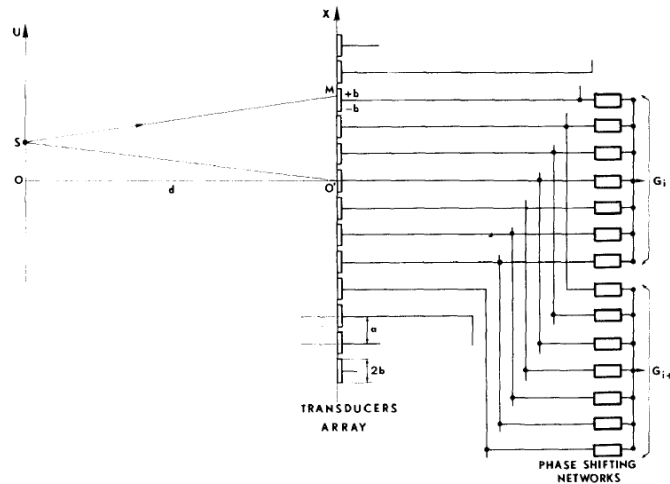


FIG. 1. Receiving array and transducers groups connections.

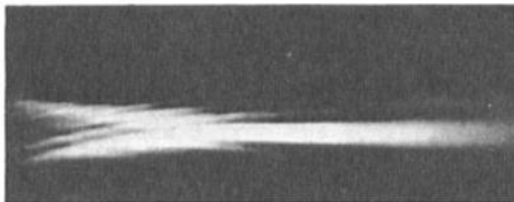


Fig. 3 : Reconstructed acoustical field distribution

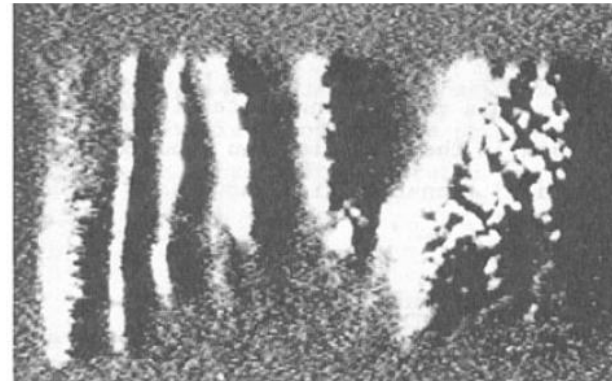


Fig. 4 : Image of the heart

B. Delannoy, R. Torguet, C. Bruneel, E. Bridoux, J. M. Rouvaen, and H. Lasotaa Acoustical image reconstruction in parallel-processing analog electronic systems, J, Appl, Phys, 50(5), May 1979, 3153

*B. Delannoy, R. Torguet, C. Bruneel, and E. Bridoux, **Ultrafast** electronical image reconstruction device, in Echocardiography, edited by C.T. Lancee (Nijhoff, The Hague, 1979), Vol.1, Chap. 3, pp. 447-450. 1273-1282 (1984).*

The Explososcan

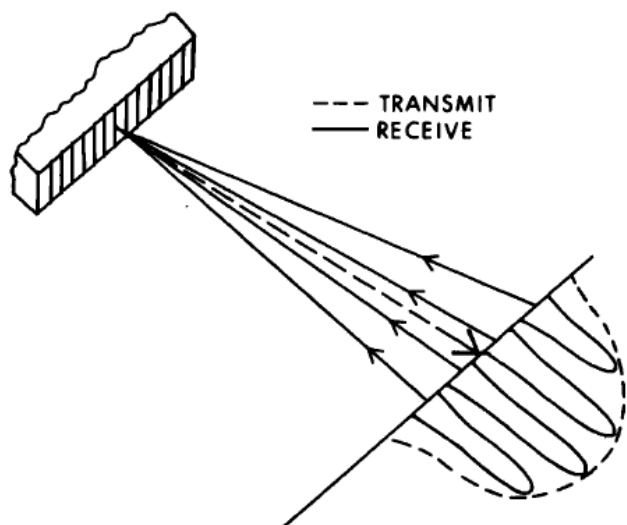


FIG. 1. The Explososcan concept. For each oriented acoustic transmit burst, dashed line, information in four individual receive directions, solid lines, about the transmit direction is acquired simultaneously. Transmit beam response, dashed curve, extends beyond the four receive beam responses, solid curves.

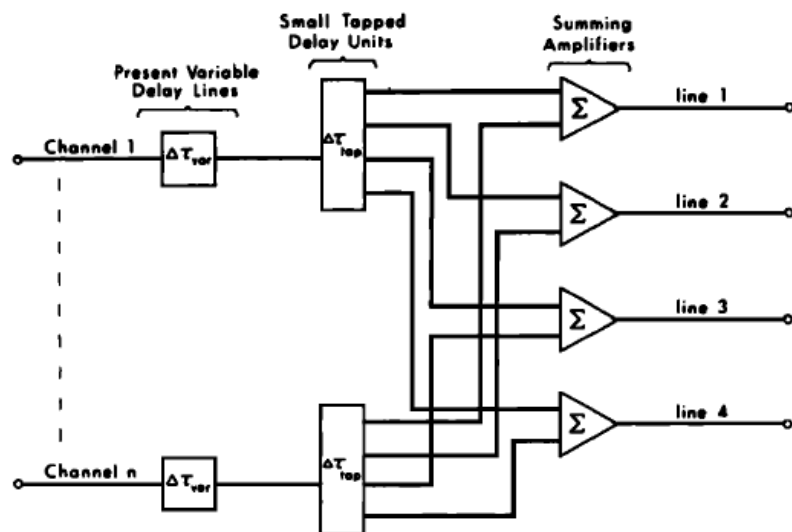
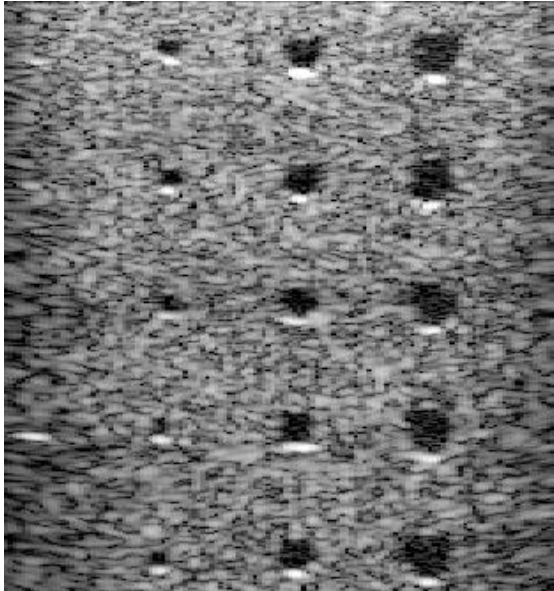


FIG. 6. Schematic of receiver delay processing to achieve four to one parallelism in receive. Note that $\Delta\tau_{tap}$ and the four summing amplifiers are the additional processing circuitry which was connected to the conventional phased array system.

Image Comparison

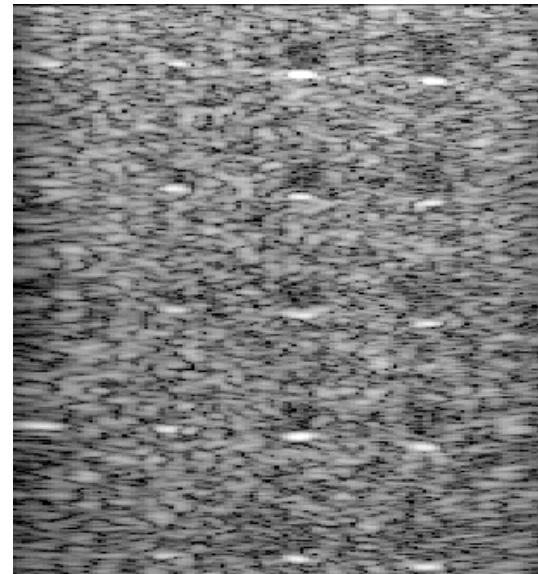
Conventional
4 focal depths
512 beams

25 Frames/s



Ultrafast
Imaging
1 unfocused
beam : 1
Plane Wave

18 000 F/s



- Very High Frame Rate is reached by using plane wave transmissions and Time-reversal processing or parallel receive beamforming

- **Loss of Transmit Focusing degrades image quality**

Slightly Lower Resolution

Much Lower Contrast

- How to reach High Frame Rate without compromising Image Quality ?

- Synthetic recombination of multiple angles plane wave transmissions – **Coherent compounding**

Coherent Plane Wave Compounding

The coherent addition of plane waves with different incident angles allows to synthesize any focused wave

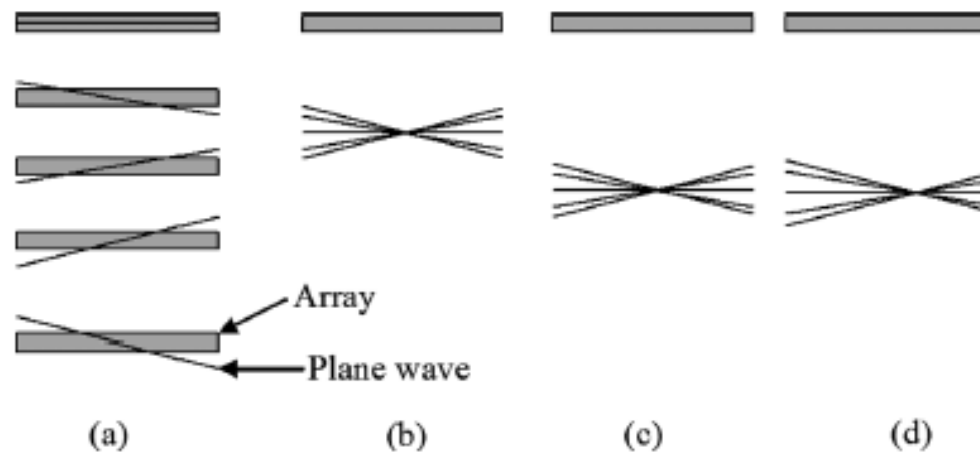
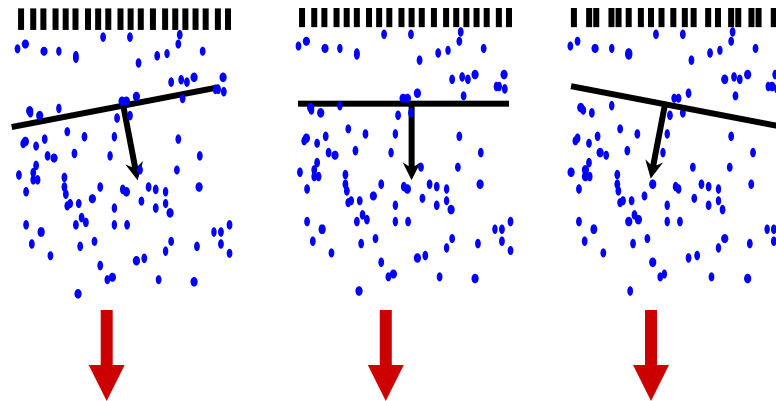


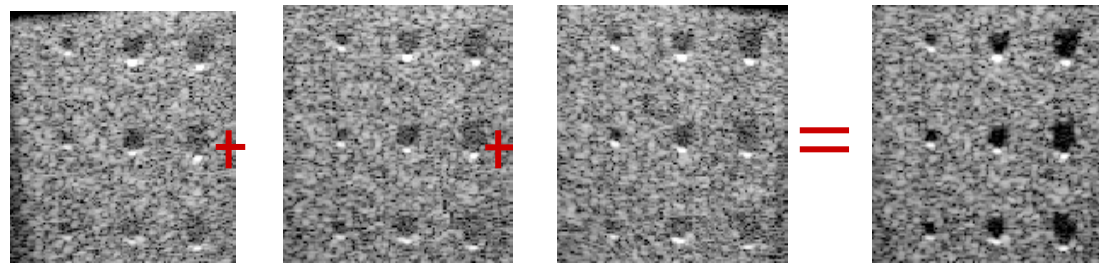
Fig. 4. (a) Individual plane waves send with the compound method. (b), (c), (d) The addition of the plane waves with the adequate delays enables focus at different depths and laterally. This focusing is performed synthetically. If this synthetic focusing is the same as in the standard focusing method, the final image must have the same quality in both methods.

Ultrafast Imaging with coherent plane wave compounding

Illumination with a set of Plane Waves with DIFFERENT ANGLES



Each plane wave gets a LOW QUALITY IMAGE



The coherent addition generates a HIGHER QUALITY IMAGE

Trade-off between speed and quality

Conventional
4 focal depths

25 Frames/s

40 angles

350 F/s

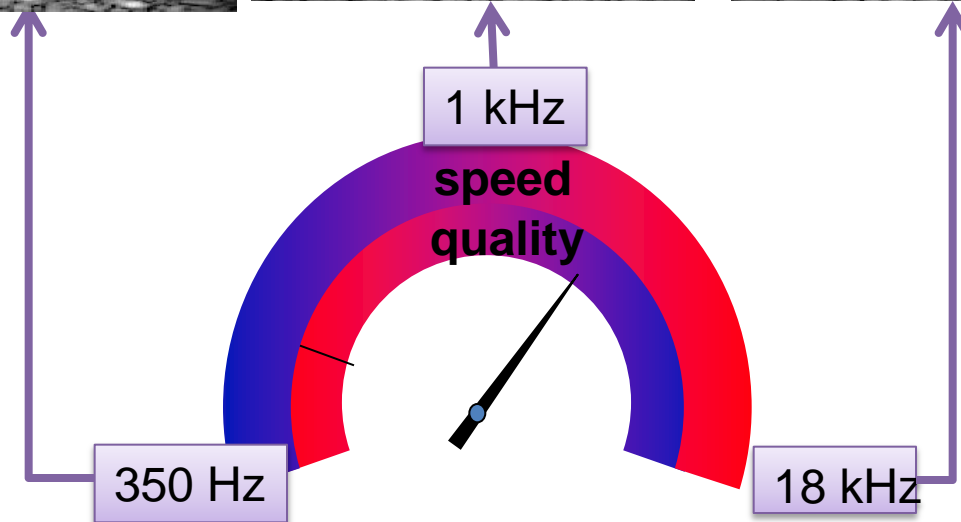
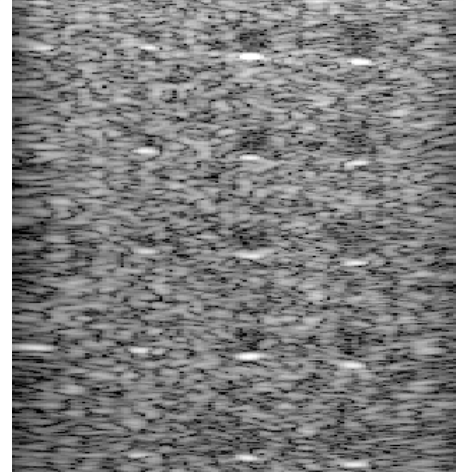
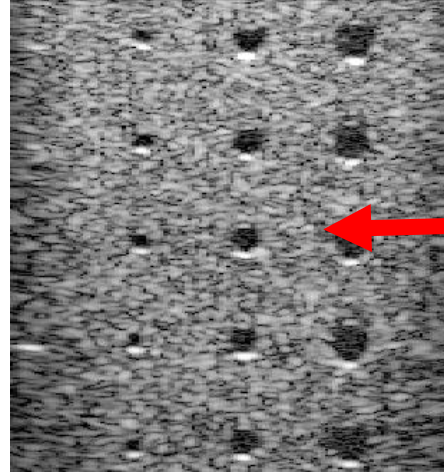
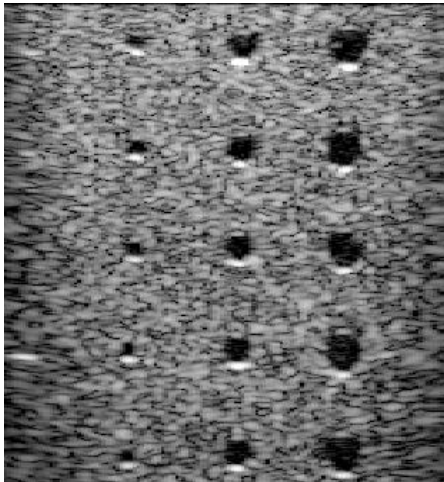
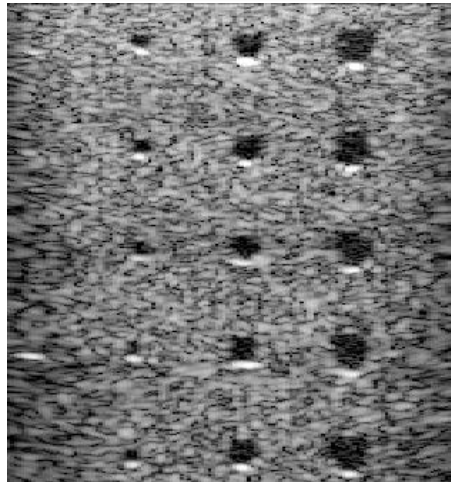
Ultrafast Compound

17 angles

1000 F/s

1 angle

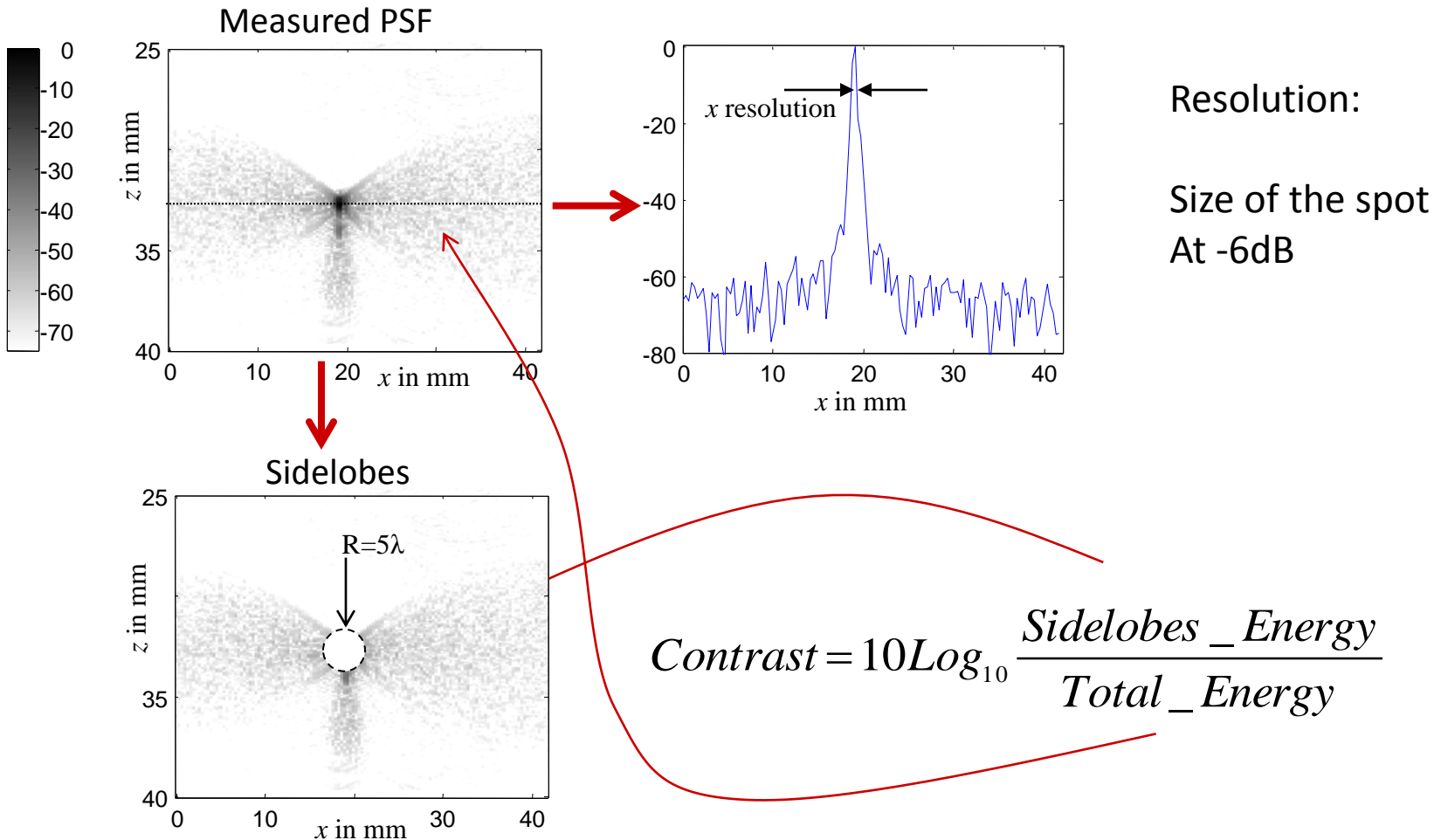
18 000 F/s



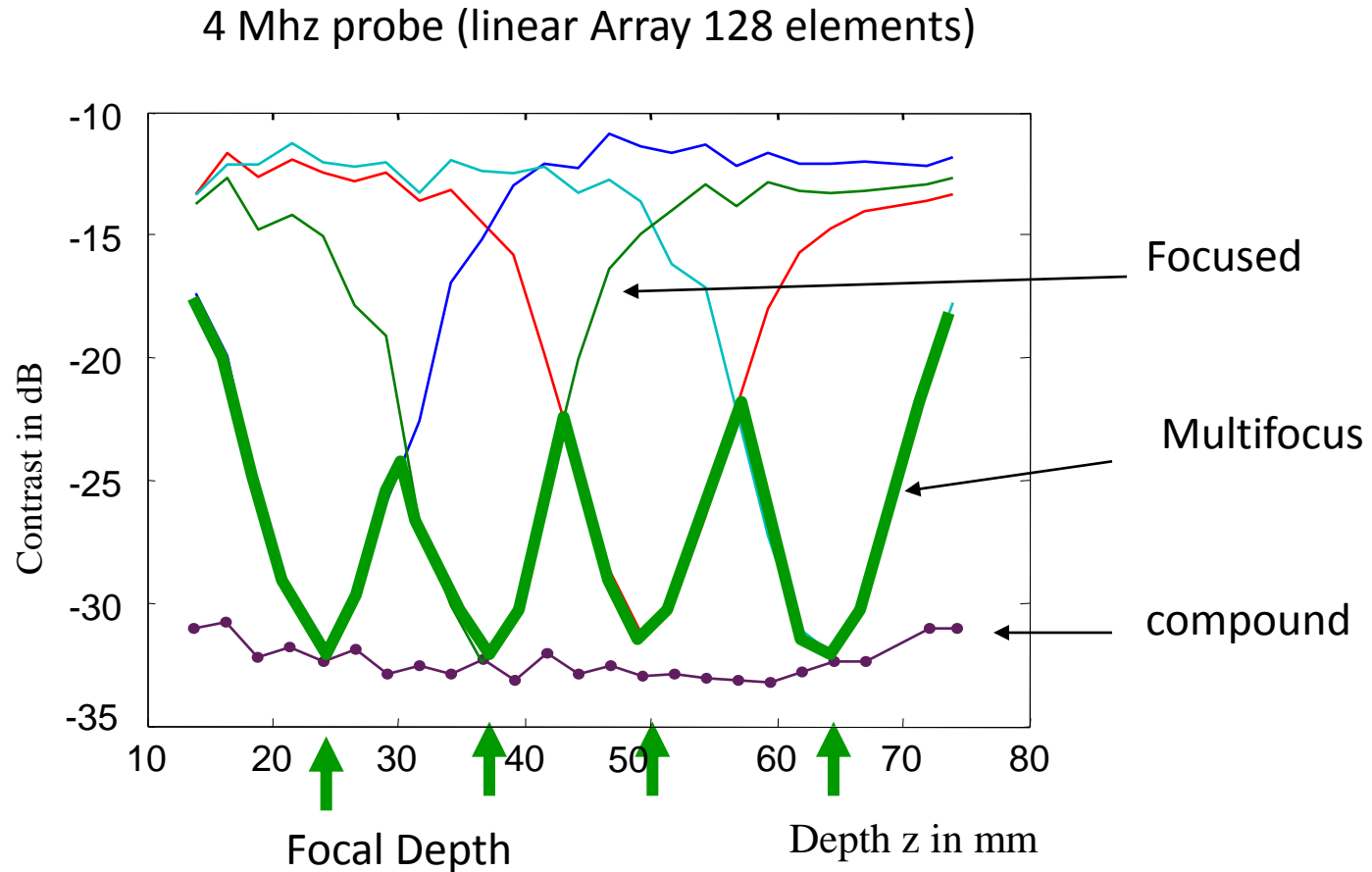
Quantitative Comparison: The PSF function

The Point-Spread-Function is the image of a point-like object

We can measure: **RESOLUTION** and **CONTRAST**



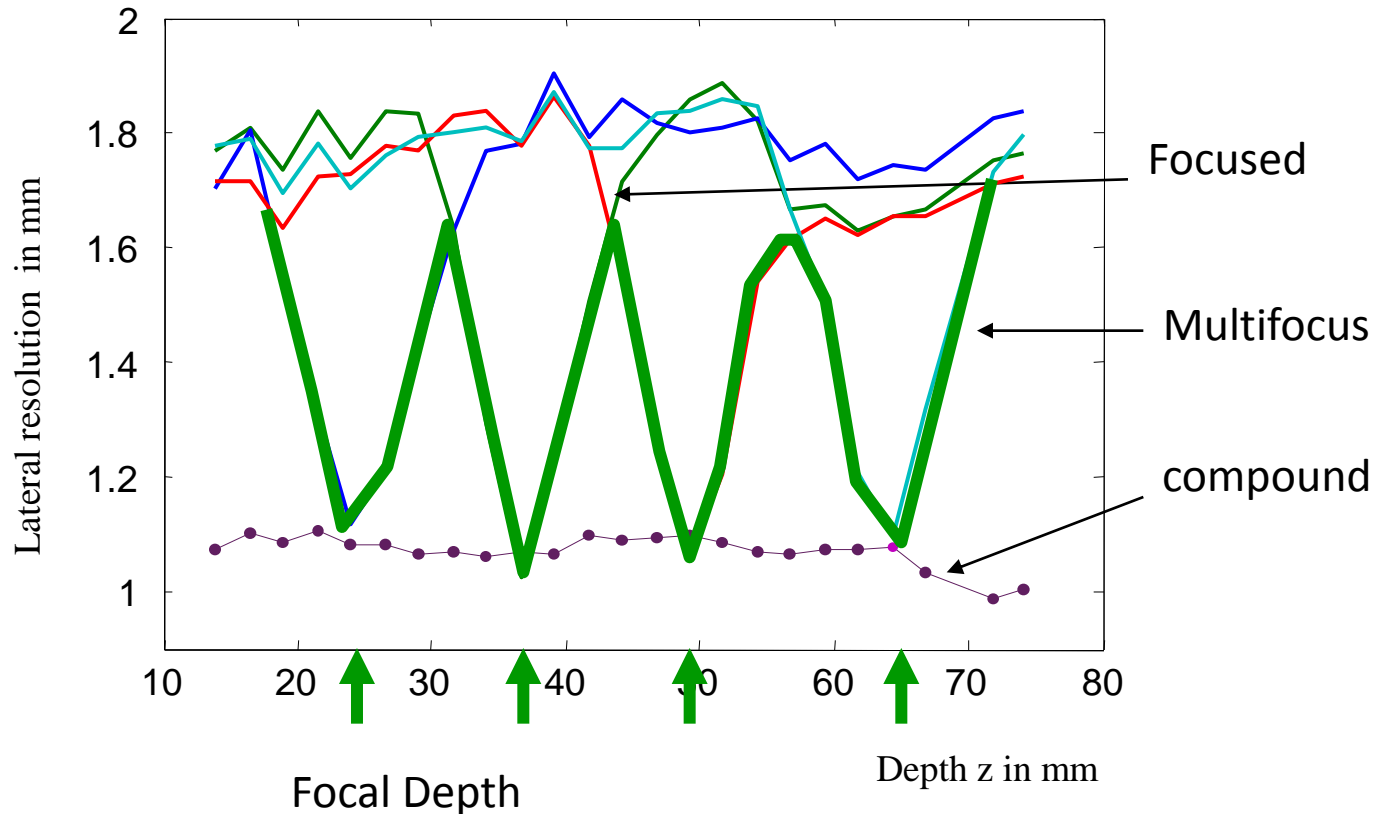
Quantitative Comparison: CONTRAST



Better CONTRAST using Plane Wave Coherent Compounding !

Quantitative Comparison: RESOLUTION

4 Mhz probe (linear Array 128 elements)

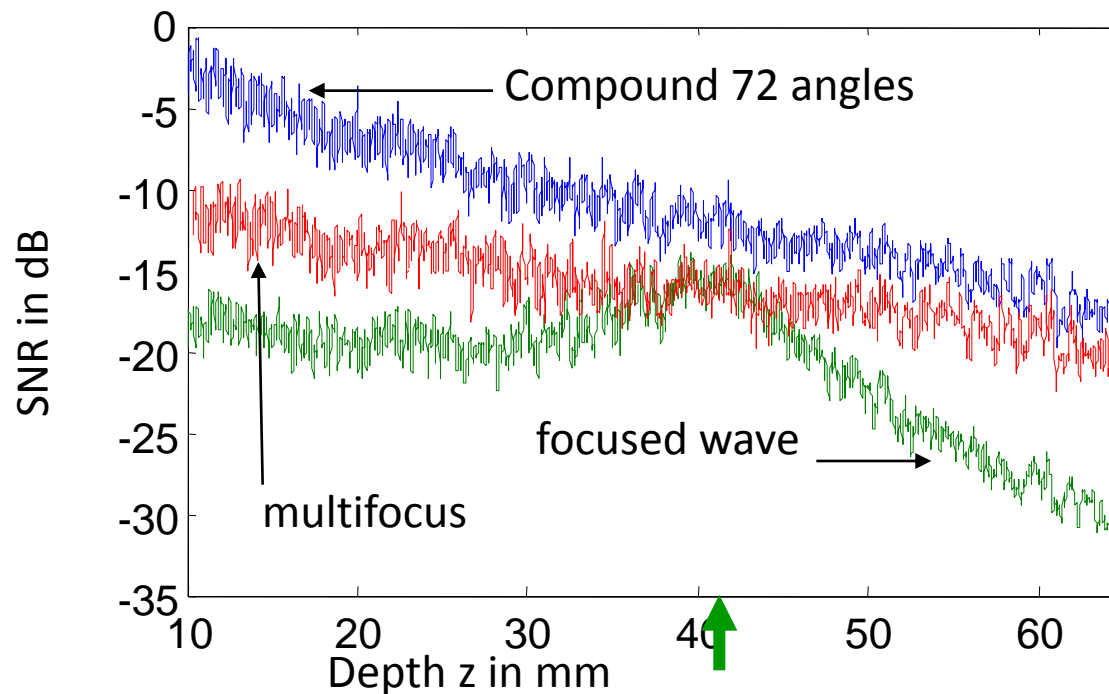


Better RESOLUTION using Plane Wave Coherent Compounding !

Quantitative Comparison: SNR

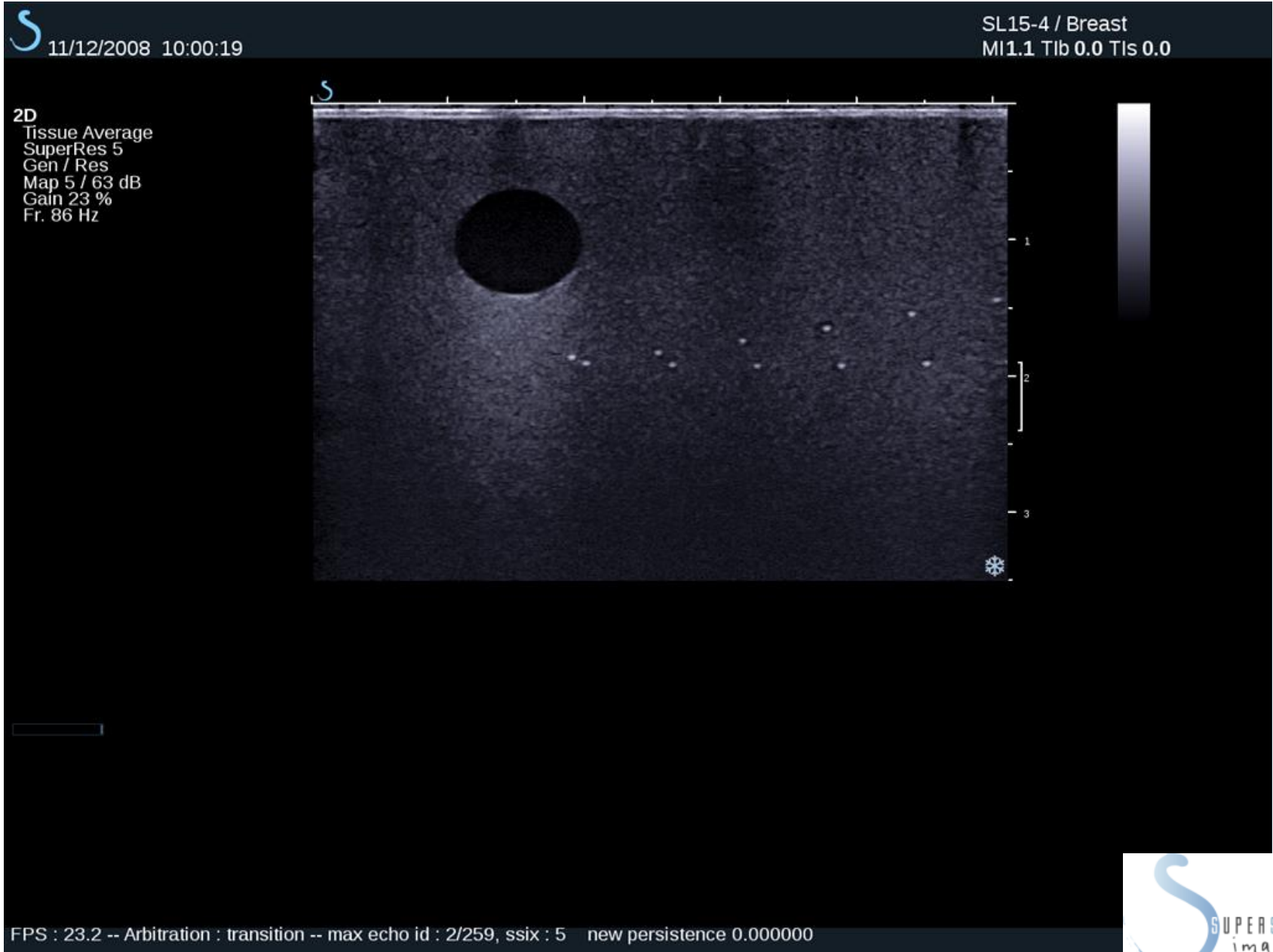
SNR estimation:

- 1) acquisition of 10 images
- 2) for each pixel in the image
 - signal = mean of the 10 images
 - noise = standard deviation of the 10 images



Better SNR using Plane Wave Coherent Compounding

Implementation on Aixplorer® scanner (Supersonic Imagine)

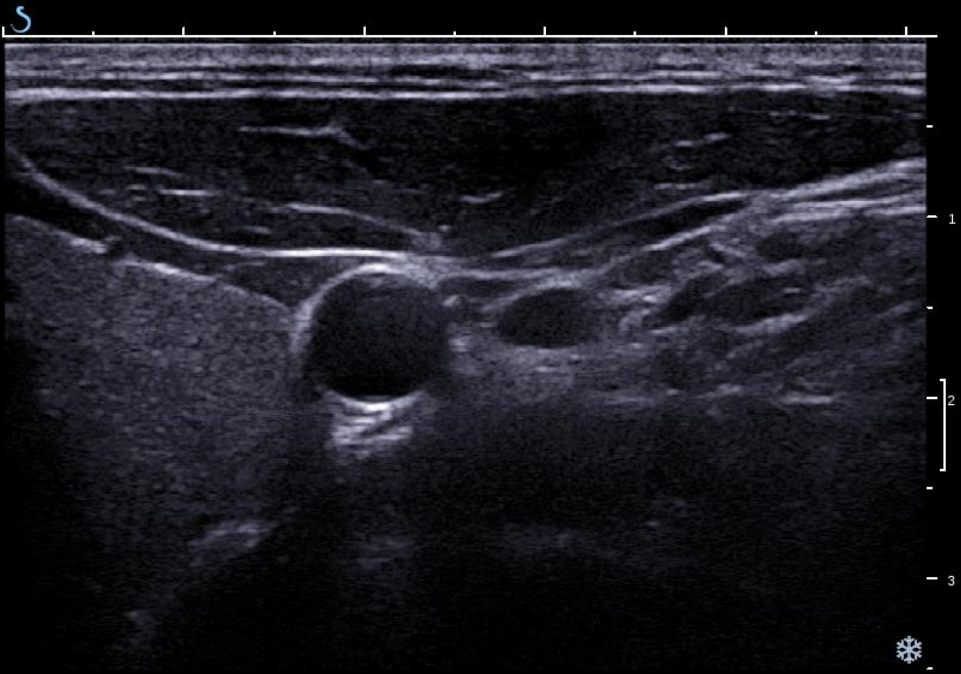


Implementation on Aixplorer® scanner (Supersonic Imagine)

S 11/12/2008 10:28:23

SL15-4 / Breast
MI1.1 Tib 0.0 TIs 0.0

2D
Tissue Average
SuperRes 5
Gen / Res
Map 5 / 63 dB
Gain 23 %
Fr. 86 Hz



FPS : 0.0 -- Arbitration : transition -- max echo id : 1/259, ssix : 5 new persistence 0.000000



Ultrafast Frame Rates Give Access to New Information

Ultrafast Ultrasonic Imaging

(typically more than 1000 fps)

Tissue Motion

Quantitative Elasticity Imaging
Diagnosis Imaging
Temperature and necrosis Imaging
Imaging of natural vibrations
Muscle fibers stimulation
Cardiac Electromechanical waves
Arterial Pulse Wave

Blood Motion

Ultrafast Doppler Imaging
Full field imaging of complex flows
Imaging of the micro-vascularization
(tumor vasc., brain ischemia,...)
Functional imaging of brain activation

Gray scale Modifications

Ultrafast Imaging of bubbles
Cavitation threshold estimation
Information on gas dissolution
Imaging of Drug release
Enhanced Contrast Imaging
Superresolution Imaging

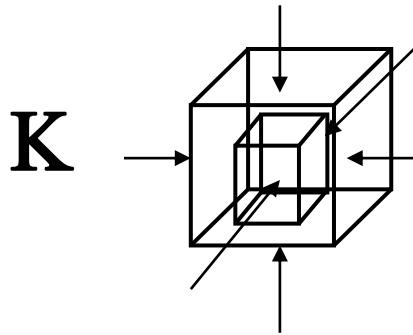
Quantitative Elasticity Imaging

From Transient Elastography
to Shear Wave imaging :

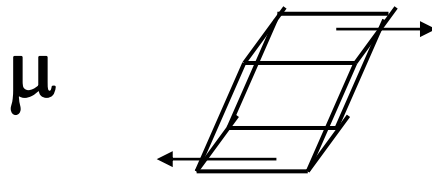
The multiwave approach

What kind of mechanical waves can propagate in soft tissues ?

Two types of waves related to the two mechanical coefficients \mathbf{K} and μ used to define the elasticity of a solid material



\mathbf{K} Bulk Modulus (**Compression**) almost constant, of the order of 10^9 Pa, Fluctuations $\approx 5\%$
Quasi incompressible medium



μ **Shear** Modulus, Strongly heterogeneous, varying between 10^2 and 10^7 Pa
(A. Sarvazian)

$$\mathbf{K} \gg \mu$$

Young modulus
 $E \approx 3 \mu$

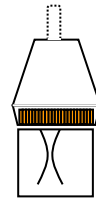
Human Body Seismology : Mechanical waves in soft tissues

$$\left\{ \begin{array}{l} \text{Compressional Waves propagate at } c_p \approx \sqrt{\frac{K}{\rho}} \quad (\approx 1500 \text{ m.s}^{-1}) \\ \text{Shear waves propagates at } c_s = \sqrt{\frac{\mu}{\rho}} \quad (\approx 1-10 \text{ m.s}^{-1}) \end{array} \right.$$

Two kind of waves propagating at totally different speeds !!

At **Ultrasonic** frequency, only Compressional waves can propagate, at 5MHz, **wavelength = 0.3mm**.

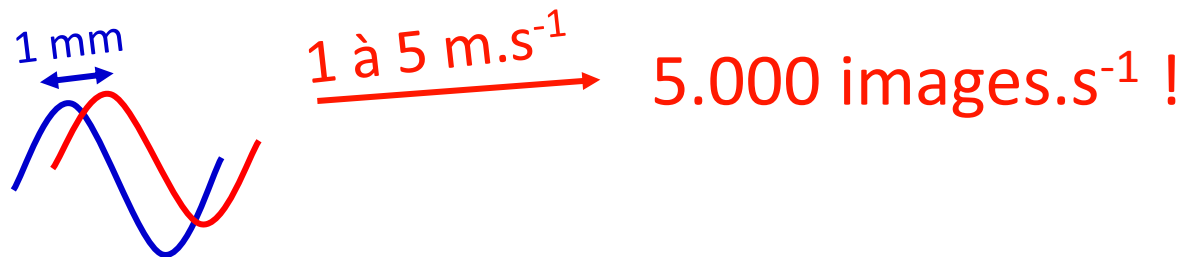
At **Sonic** frequency, Shear waves can propagate < 1000 Hz (High Shear Viscosity), at 200 Hz, **large wavelength = 2cm**



Ultrasonic radiation force

Transient Elastography : Shear Wave Imaging - a Multiwave approach

- Generation of transient low frequency shear wave (10 Hz to 1000 Hz) with some microns amplitude

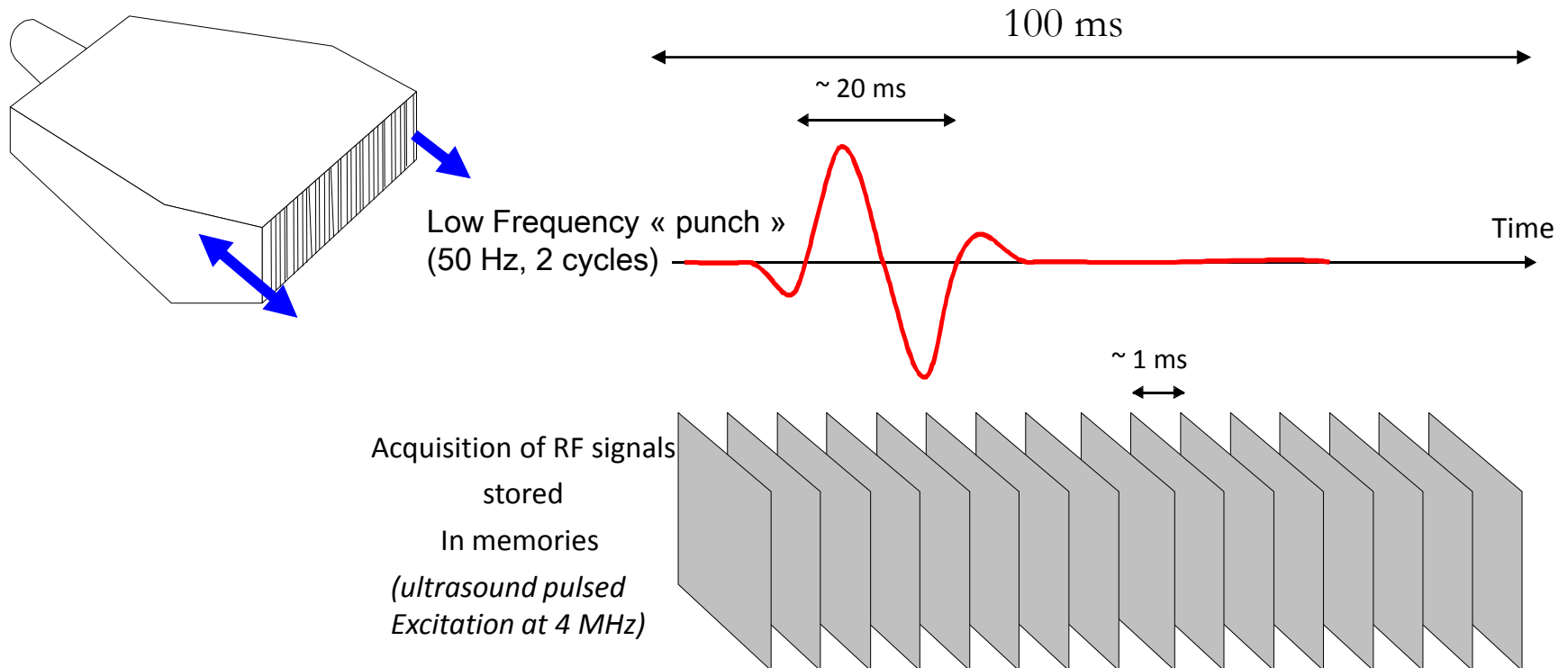


- One follows tissue motion induced by shear waves 5.000 times/s. Local measurement of the shear velocity and E ou μ are deduced by relation :

$$c_s = \sqrt{\frac{\mu}{\rho}} \approx \sqrt{\frac{E}{3\rho}}$$

The Transient Elastography Technique

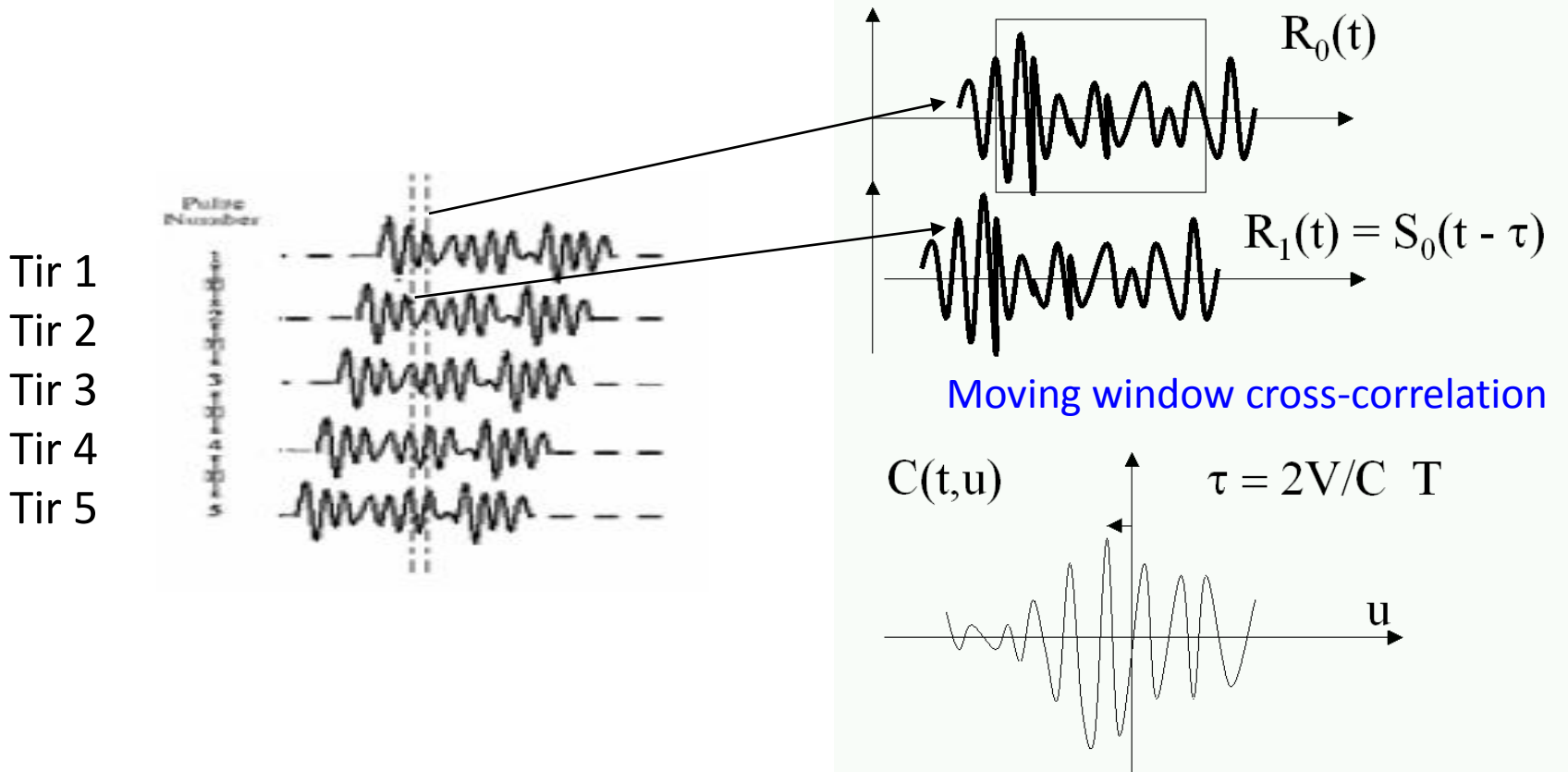
Shear wave generation + Ultrafast Imaging



How to measure the axial displacement induced by shear waves ?

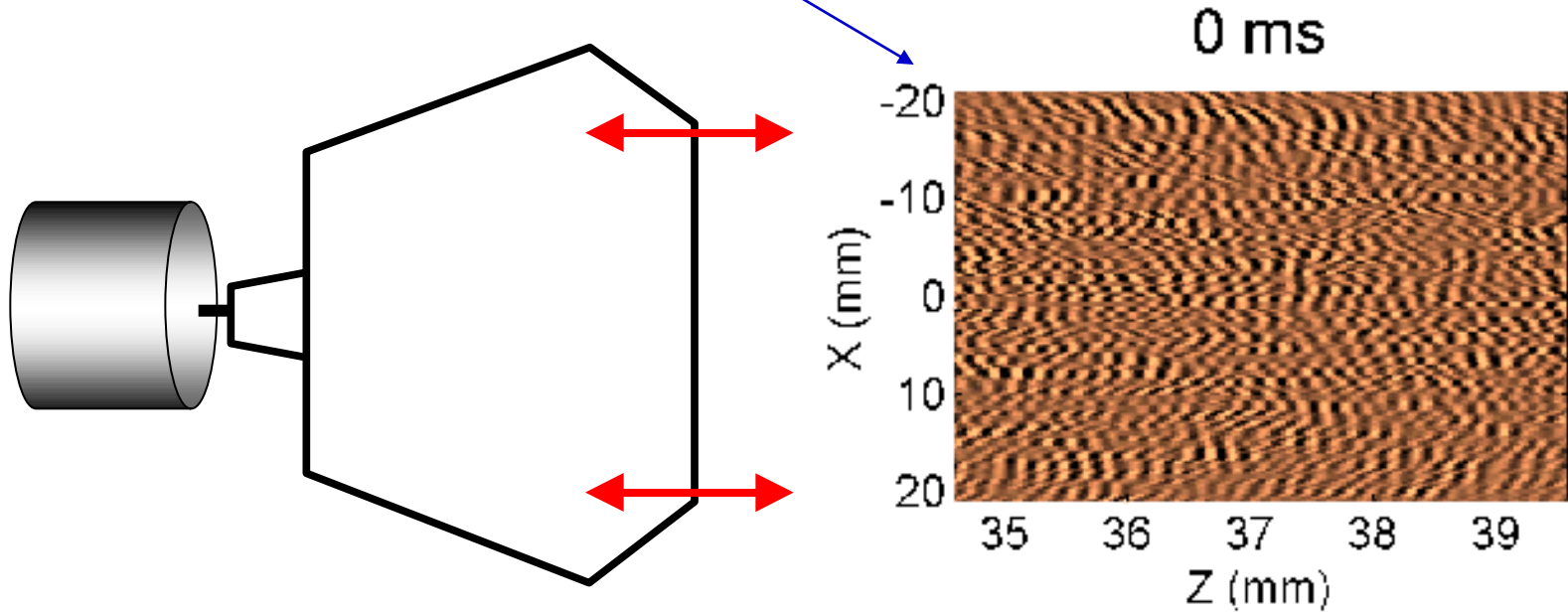
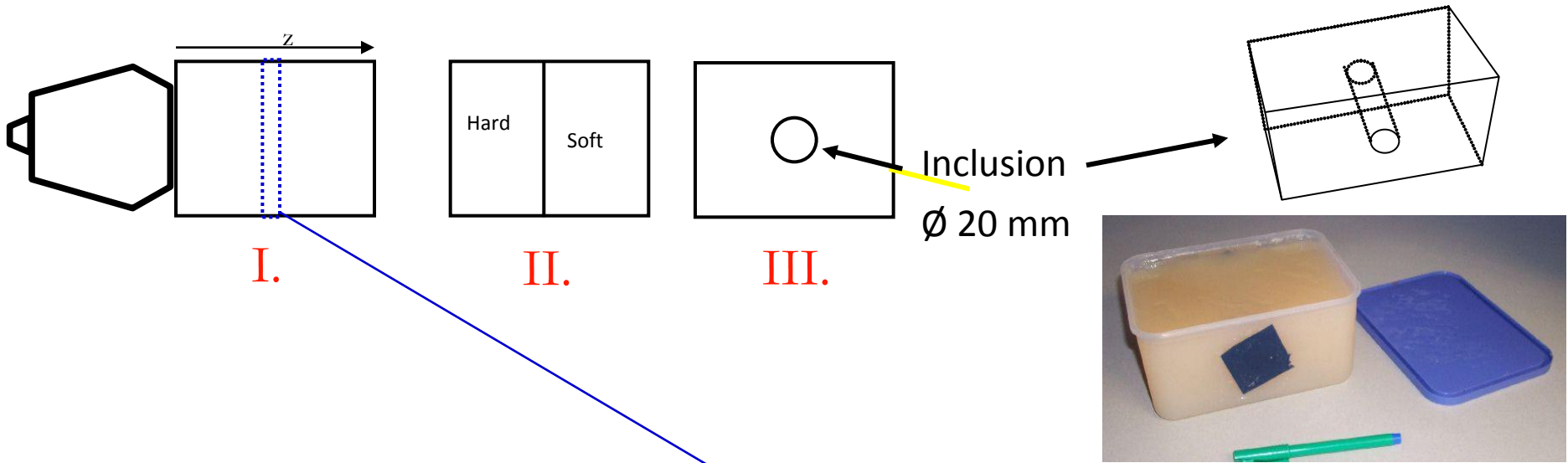
Tissues behave as random distributions of scatterers.

One repeat ultrasonic shots at high rate (less than 200 μs)



It is possible to measure between 2 shots (for example every 200 μs) displacements between 1 and 100 μ (particular velocity between 1 mm/s et 10 cm/s)

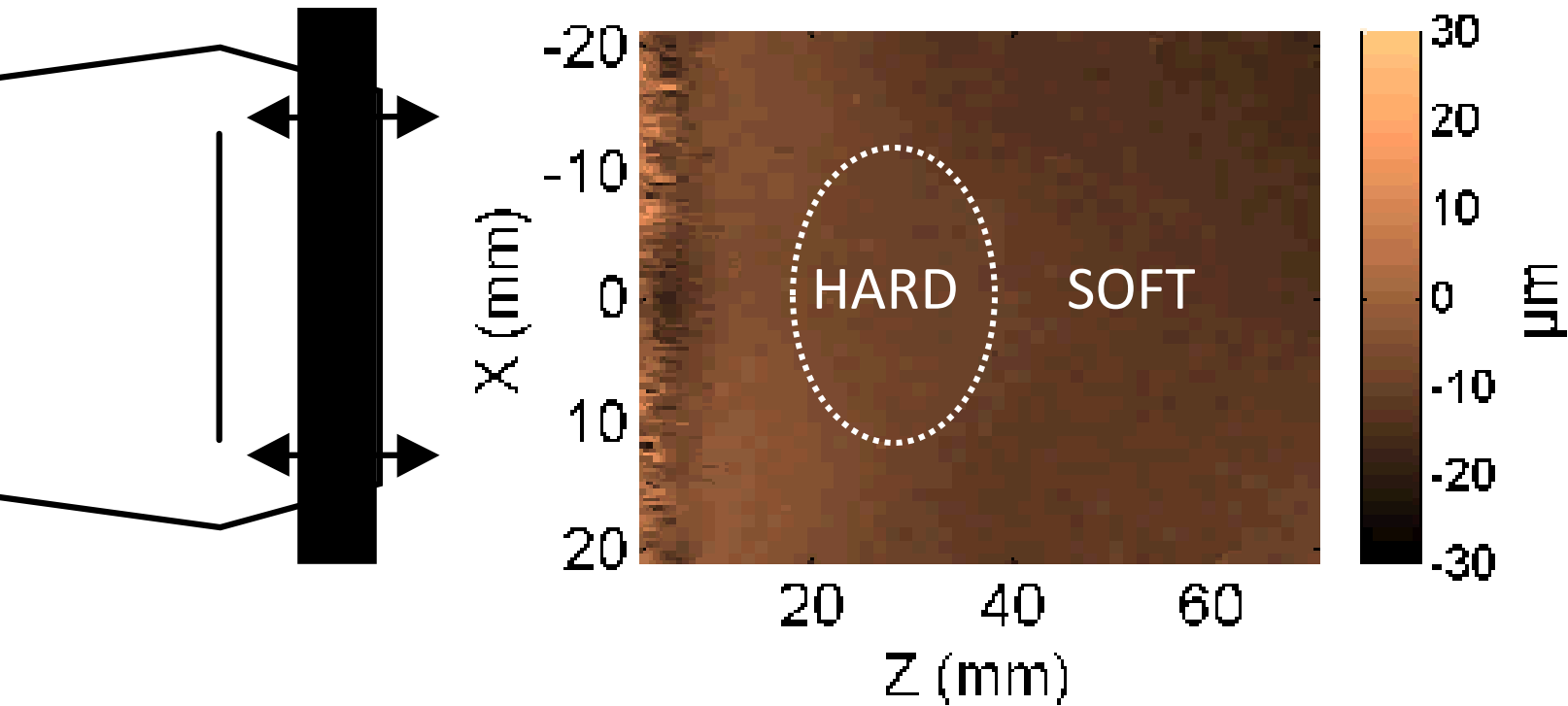
Transient Elastography in Tissue Mimicking Phantoms



Hard inclusion

Movie of U_z component

9 ms



A Simple Inversion Algorithm

- Motion Equation : an ideal model : isotropic solid without dissipation

$$\rho \frac{\partial^2 \vec{u}}{\partial t^2} = (\lambda + \mu) \times \vec{\nabla}(\vec{\nabla} \cdot \vec{u}) + \mu \Delta \vec{u}$$

Compressional shear

- Assumptions:

- 1) The medium is considered as infinite, isotropic, purely elastic and locally homogeneous.
- 2) $\lambda \gg \mu \Rightarrow$ the bulk wave propagates instantaneously, and then:

$$\rho \frac{\partial^2 u_z}{\partial t^2} = \mu \Delta u_z$$

$$3) \frac{\partial^2 u_z}{\partial y^2} \ll \frac{\partial^2 u_z}{\partial x^2} + \frac{\partial^2 u_z}{\partial z^2} \Rightarrow \Delta u_z \approx \frac{\partial^2 u_z}{\partial x^2} + \frac{\partial^2 u_z}{\partial z^2}$$

No diffraction outside the image plane

Inverse Problem

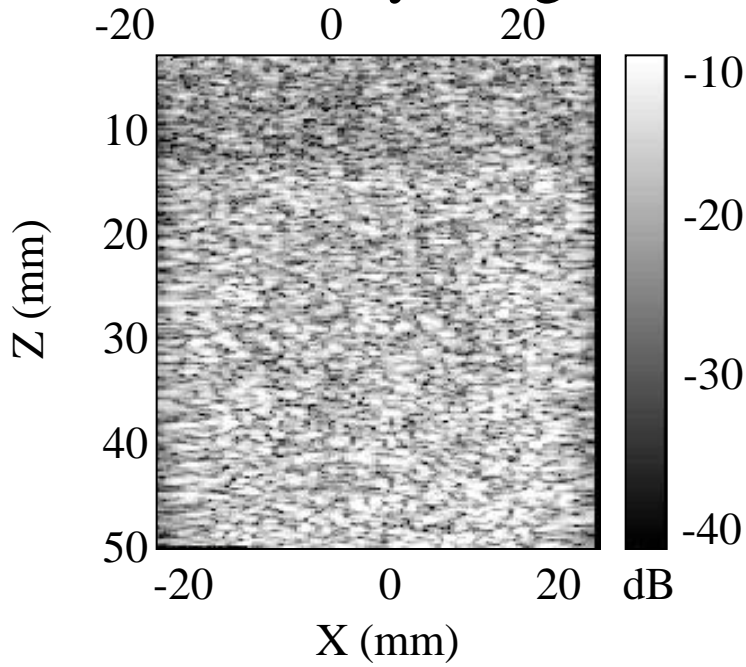
$$\rho \frac{\partial^2 u_z}{\partial t^2} = \mu \Delta u_z$$

- Local inversion algorithm

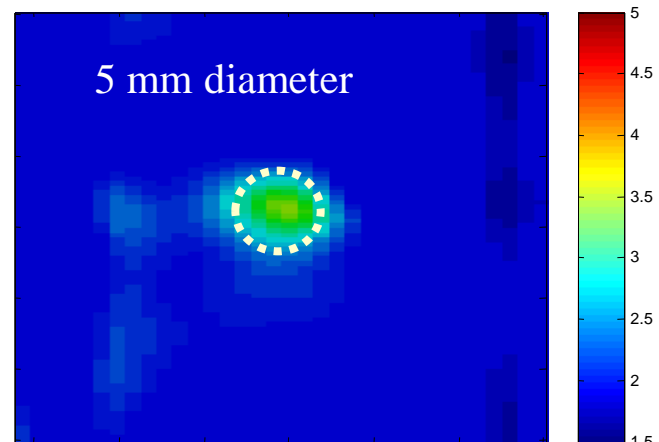
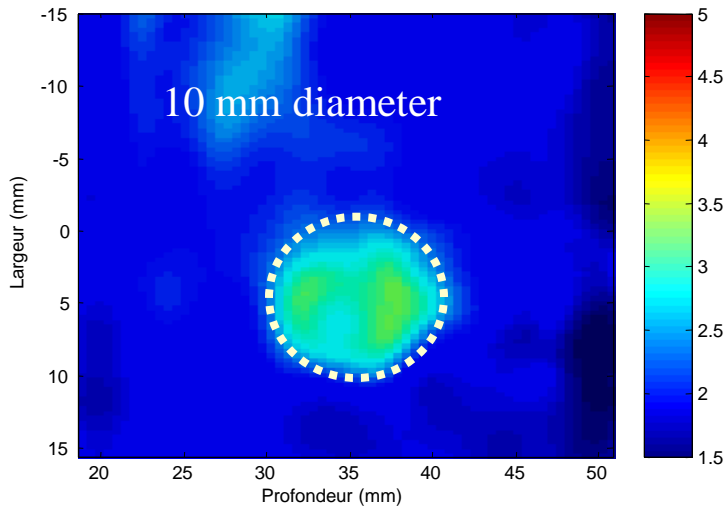
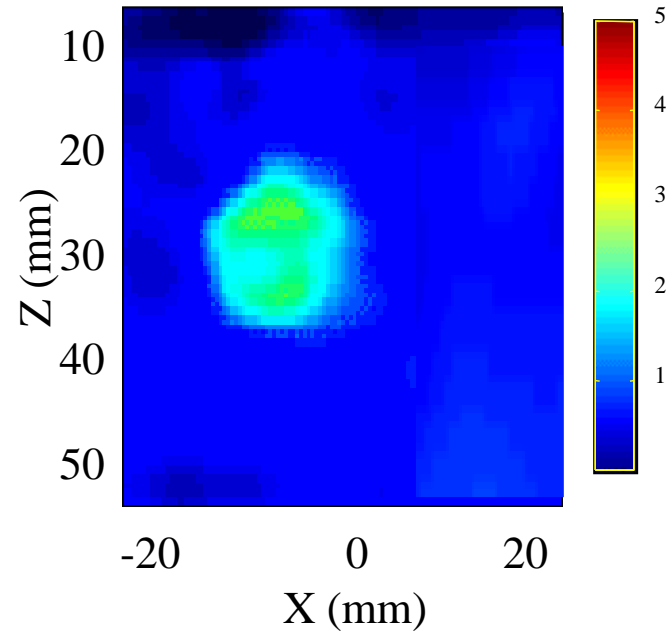
$$\mu(x, z) = \rho \frac{\left(\frac{\partial^2 u_z(x, z)}{\partial t^2} \right)}{\left(\frac{\partial^2 u_z(x, z)}{\partial x^2} + \frac{\partial^2 u_z(x, z)}{\partial z^2} \right)}$$

Inverse Problem – Hard Inclusion

Reflectivity Image



Shear modulus map



Ultrafast Plane Wave Compound Imaging for Vector Tissue Motion Imaging

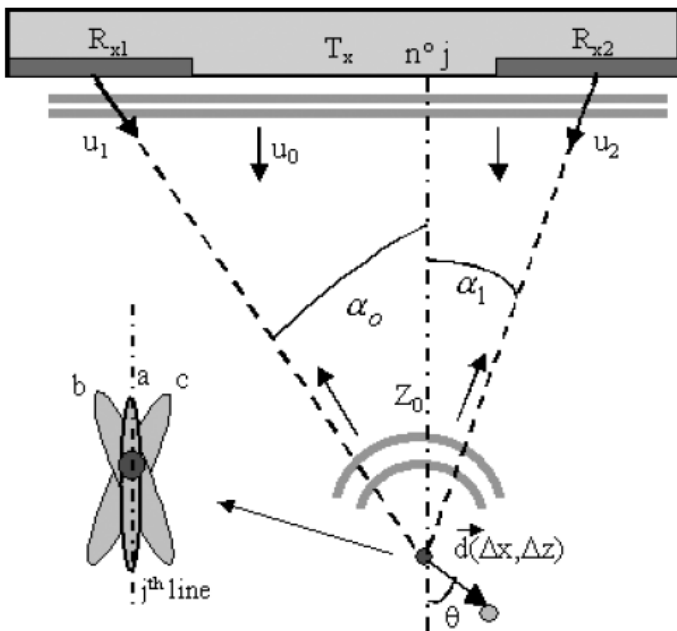


Fig. 3. Left and right subapertures performing two different left and right speckle images. The focal spot allowing one to perform a segment (at depth Z_0) of the j^{th} line of the image is presented: (a) for a classical transmit-receive beamforming, (b) for the left subaperture receive beamforming, (c) for the right subaperture receive beamforming.

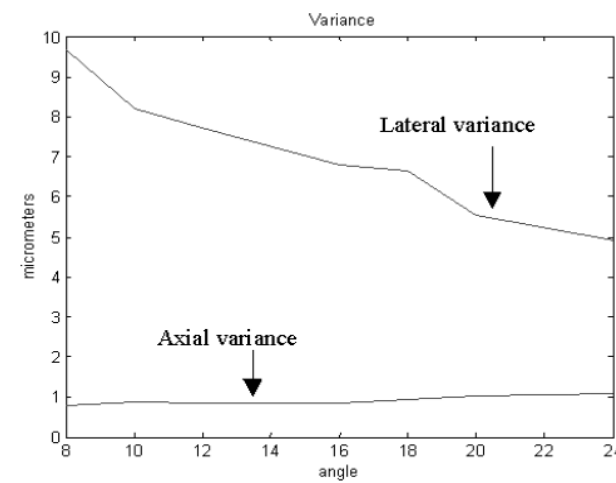
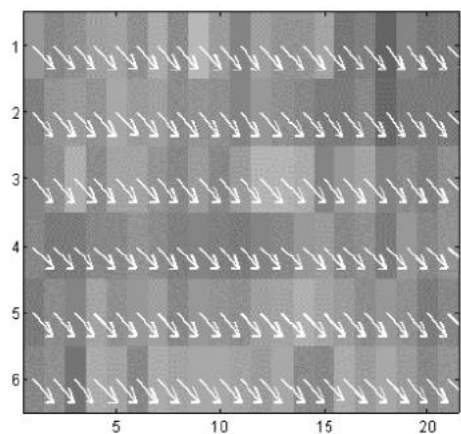
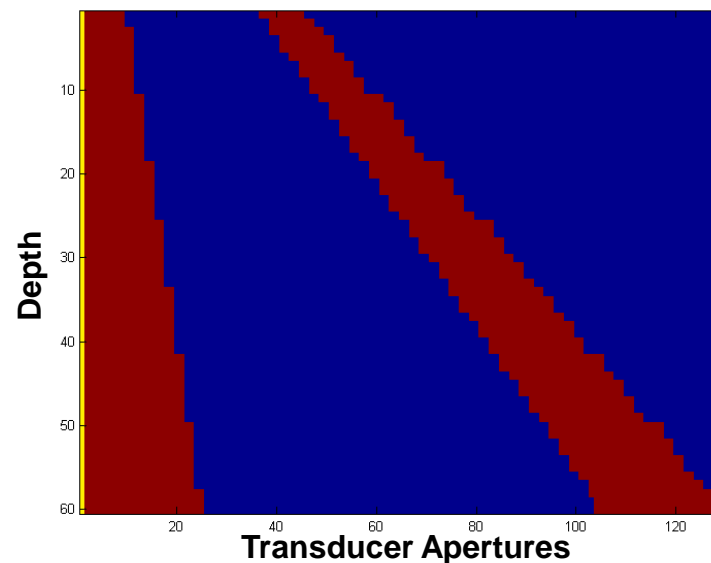


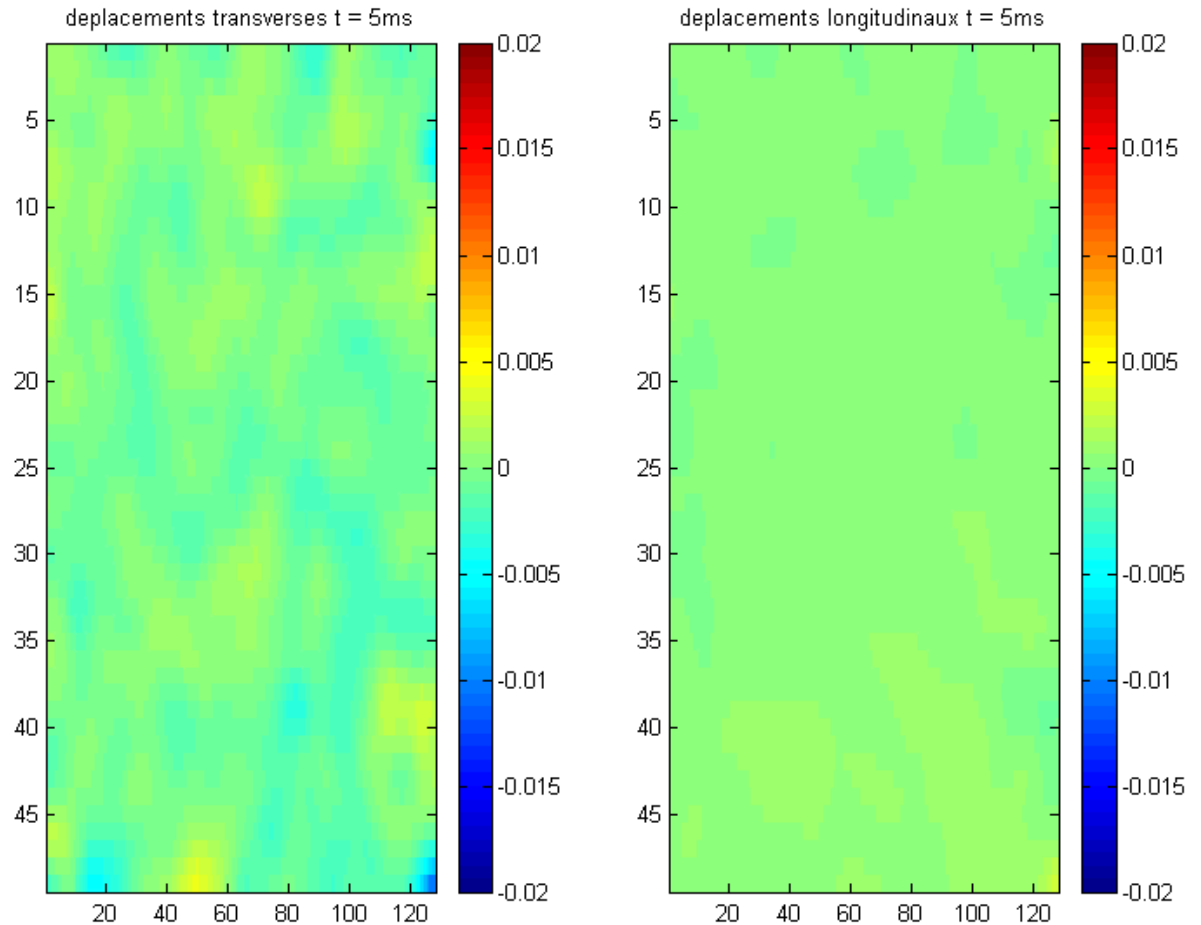
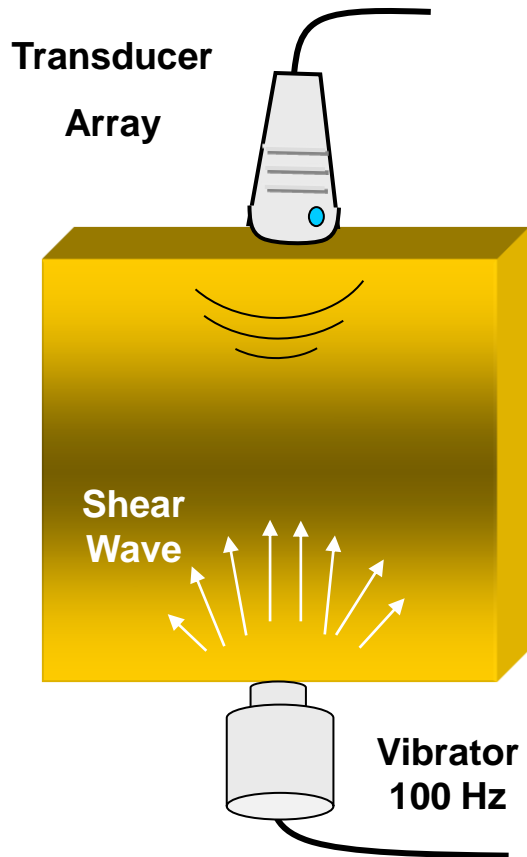
Fig. 10. Dependence of the lateral and longitudinal displacements variance with the angle between subapertures (in degrees). For a 50- μm displacement applied in both directions, the mean estimate of the lateral and longitudinal displacements are, respectively, 48 and 51 μm .

Ultrafast compound imaging for 2D motion vector estimation : Application to transient elastography"

M. Tanter, J. Bercoff, M. Fink, IEEE Ultr., Ferr. And Freq. Ctrl, 49 (10), pp 1363-1374, 2002.

Ultrafast Compound Imaging for Vector Tissue Motion Imaging

Experimental Proof of concept for Transient Elastography

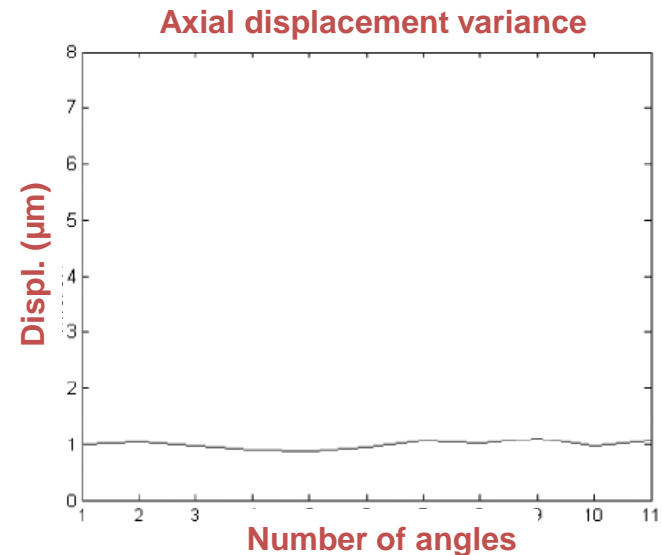
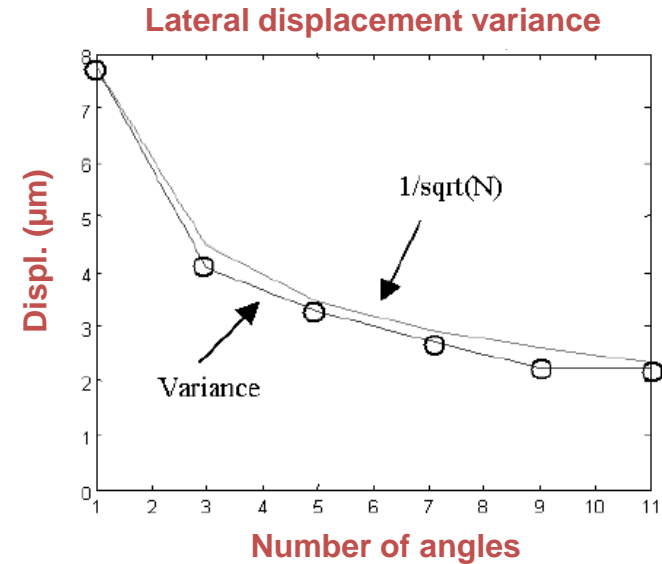
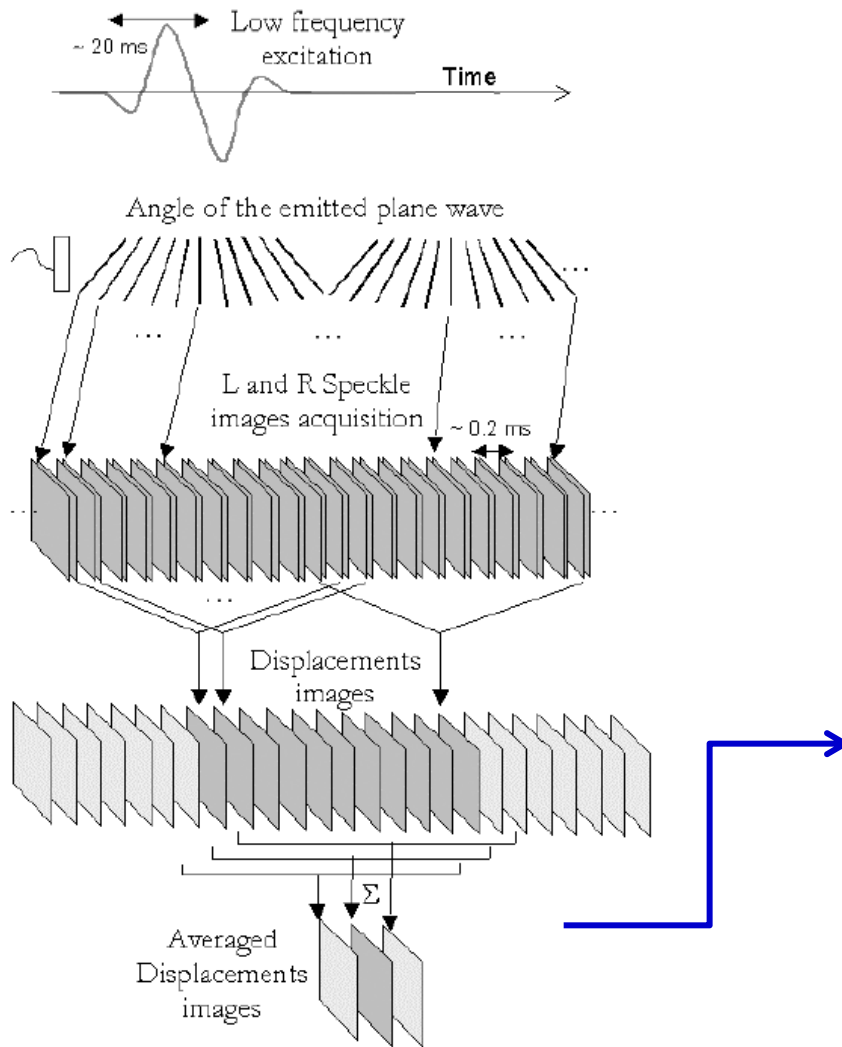


Transient Shear wave at 2000 fps

The extension to Ultrafast Vector Doppler was also proposed in the 2002 paper

Ultrafast compound imaging for 2D motion vector estimation : Application to transient elastography”
M. Tanter, J. Bercoff, M. Fink, IEEE Ultr., Ferr. And Freq. Ctrl, 49 (10), pp 1363-1374, 2002.

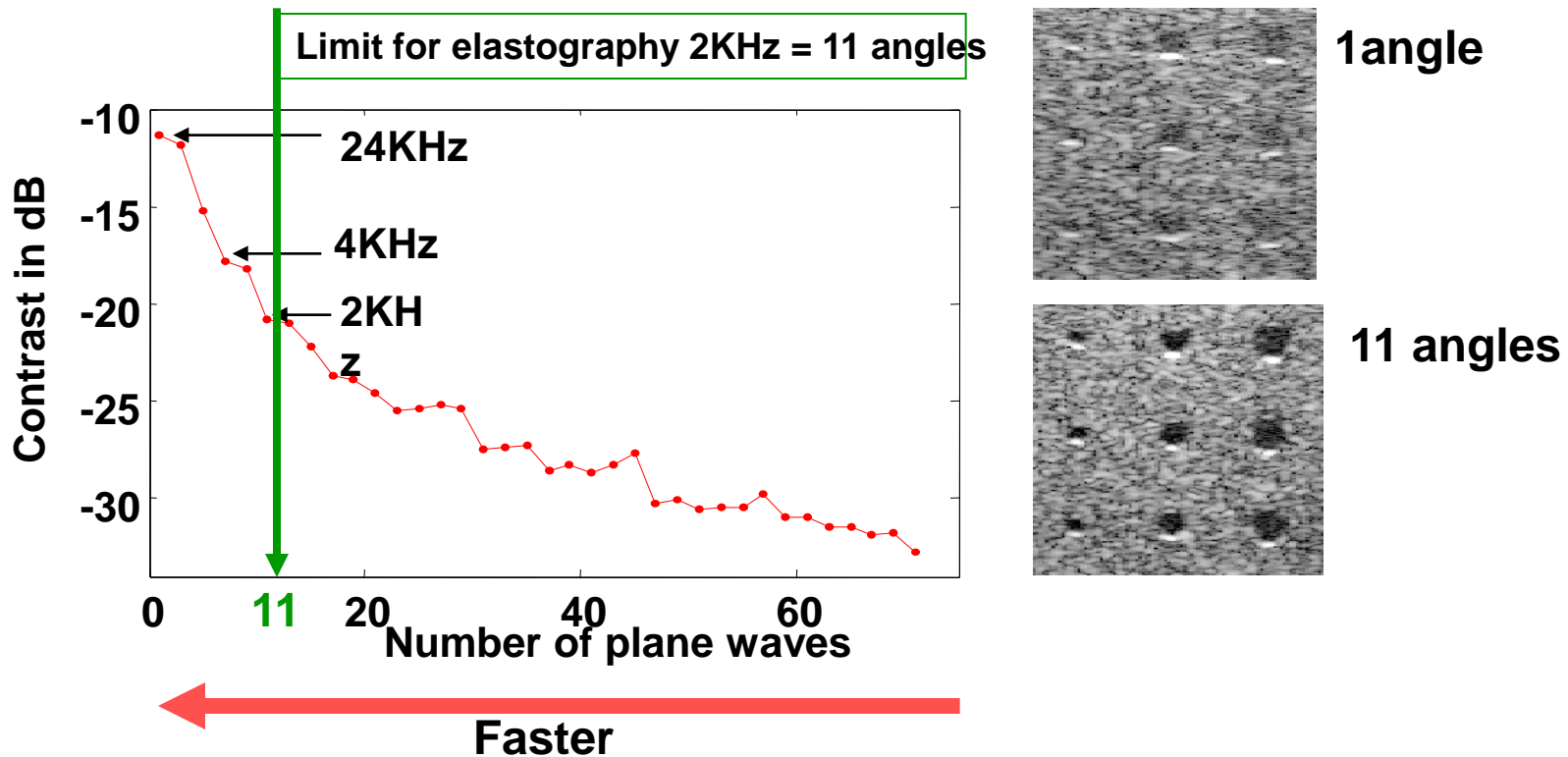
Ultrafast Plane Wave Compounding improves Motion estimation



Ultrafast imaging with Coherent Compounding

Tradeoff between FRAME RATE and IMAGE QUALITY

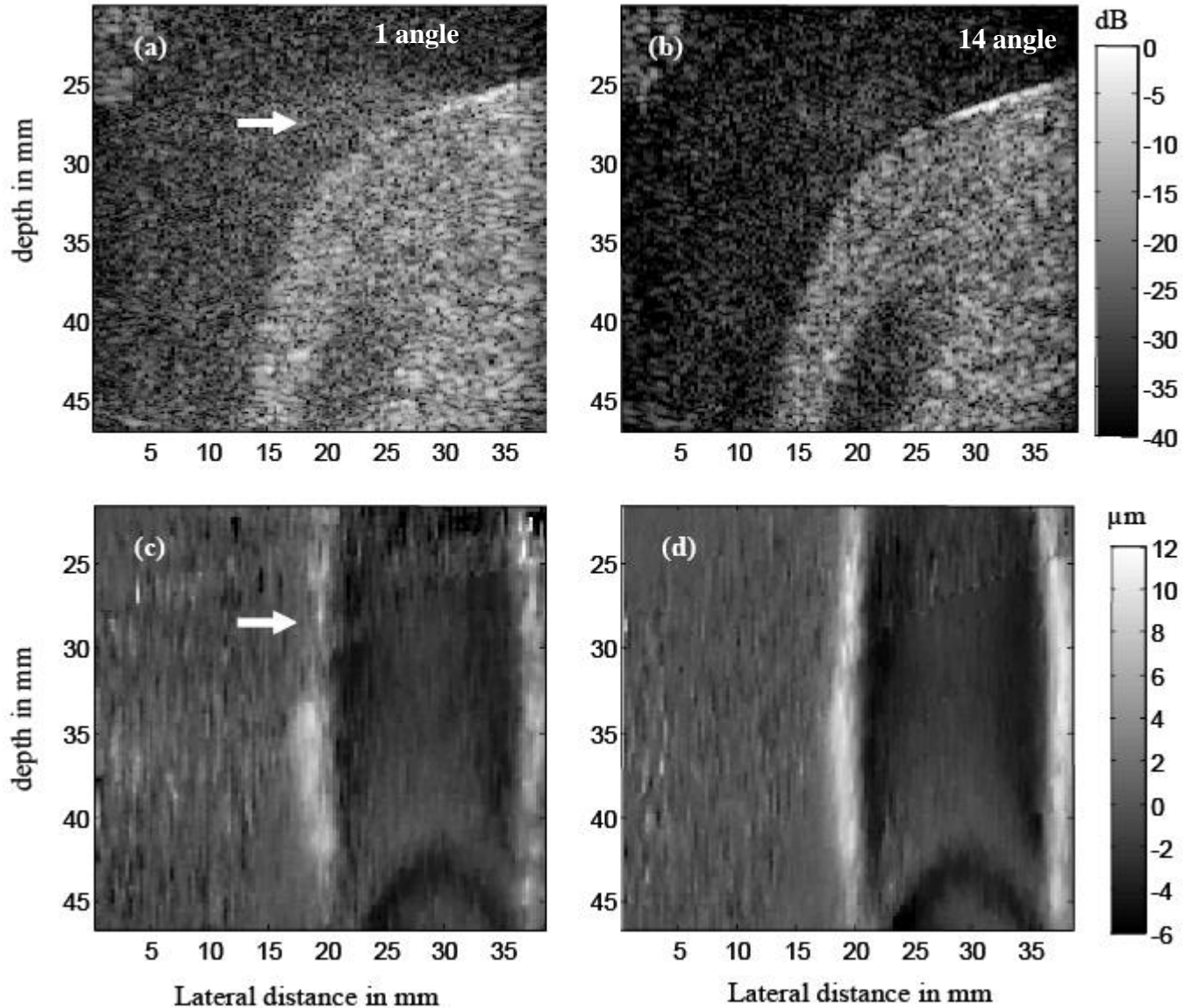
Example in a 3cm depth image



10dB contrast Improvement using Ultrafast Compound for SSI sequence

Supersonic shear Imaging with Coherent compounding

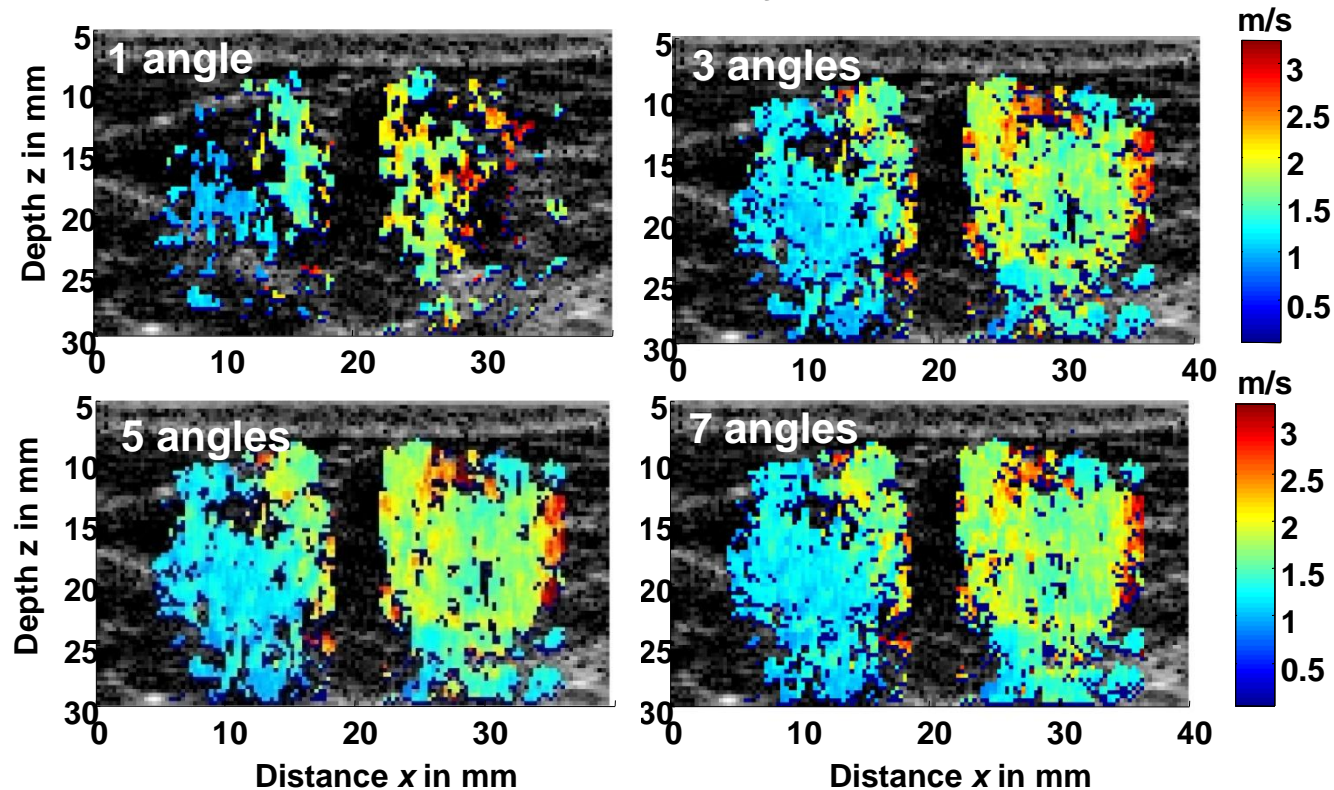
Typical Experiment in Gelatin Phantoms



In Vivo Breast Elasticity map using Coherent Compou

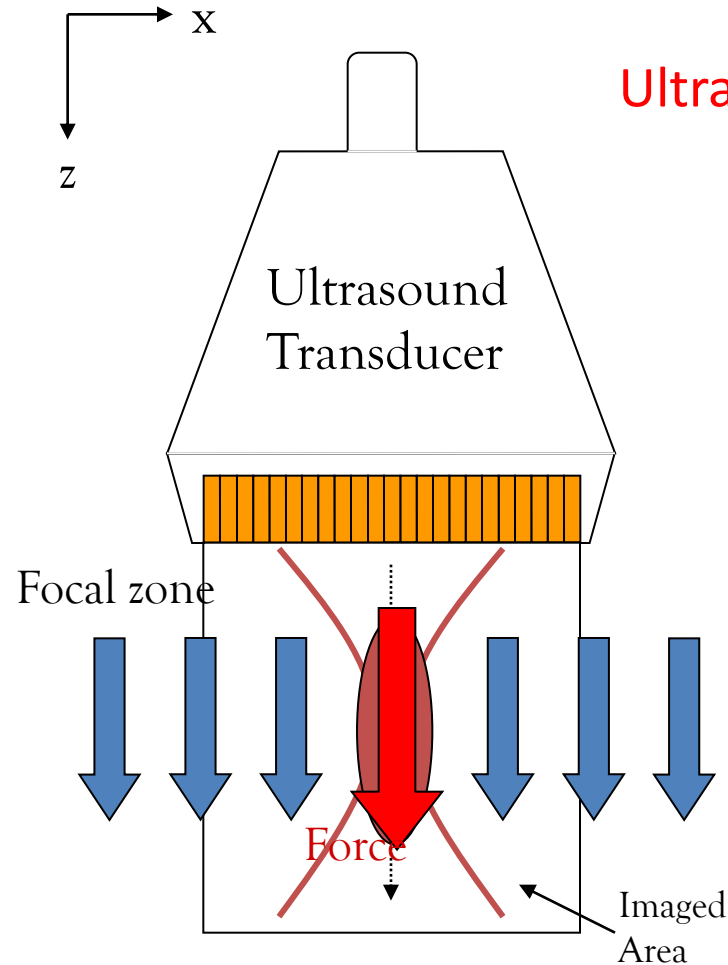
Medium: In Vivo Breast (healthy volunteer)
1 pushing line in the middle of the image

Shear wave velocity maps



Strong Increase of the quality of the shear velocity maps

Transient Elastography and Ultrasonic Radiation Force



Ultrasonic Radiation Force
non-linear effect

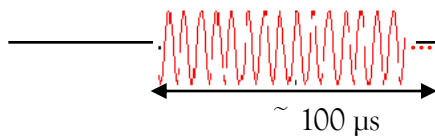
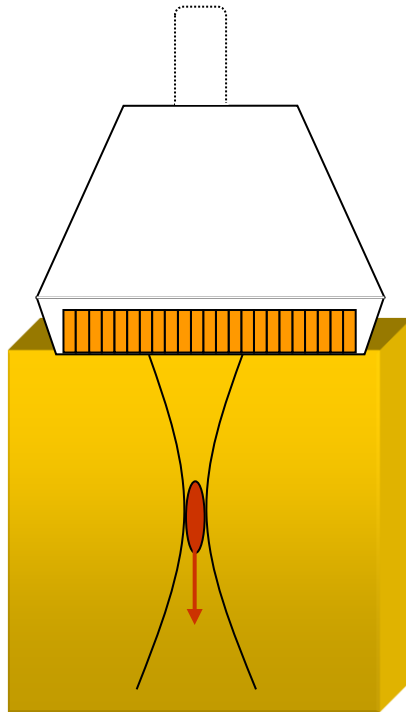
$$F(\vec{r}, t) = \frac{\alpha}{\rho c^2} p^2(\vec{r}, t)$$

Typical ultrasonic bursts of 100 μ s to create low frequency pushes (10 micrometers displacement)

Ultrafast Imaging and Acoustic Radiation Force

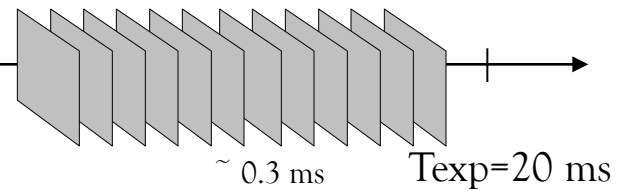
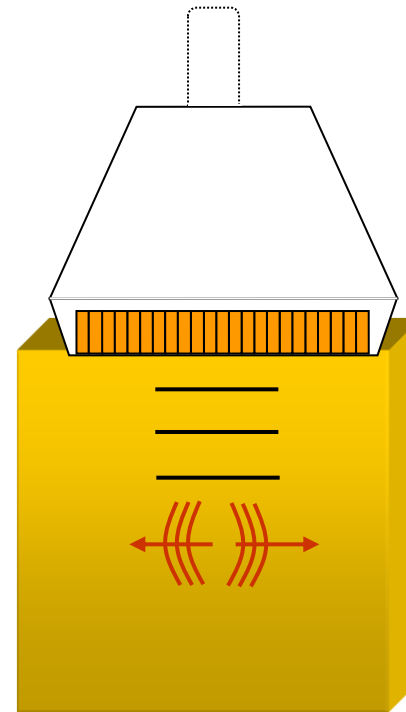
Step 1

Shear wave generation by focusing an ultrasound beam



Step 2

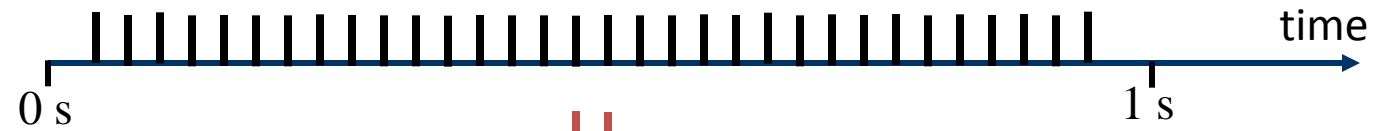
Ultrafast imaging



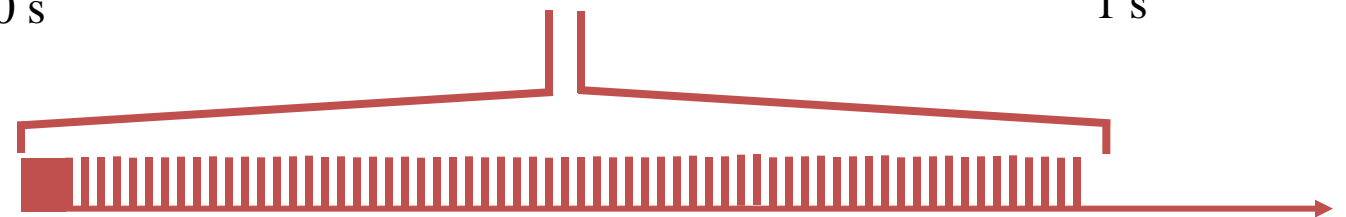
Plane wave insonification at 3000 Hz

The Supersonic Push !!!!!!!

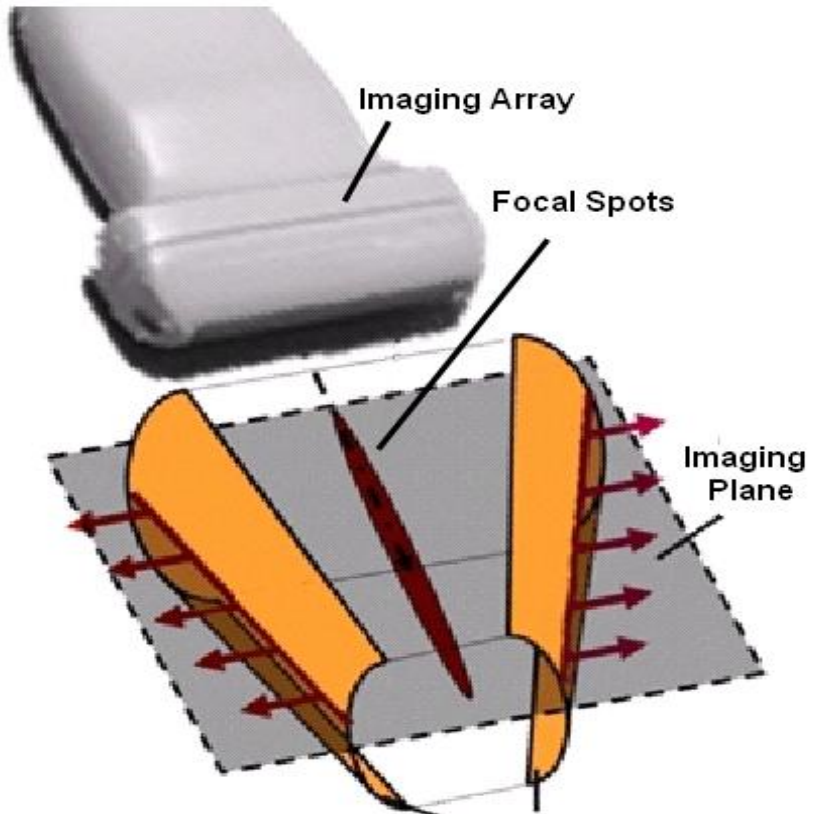
Conventional US



Ultrafast US



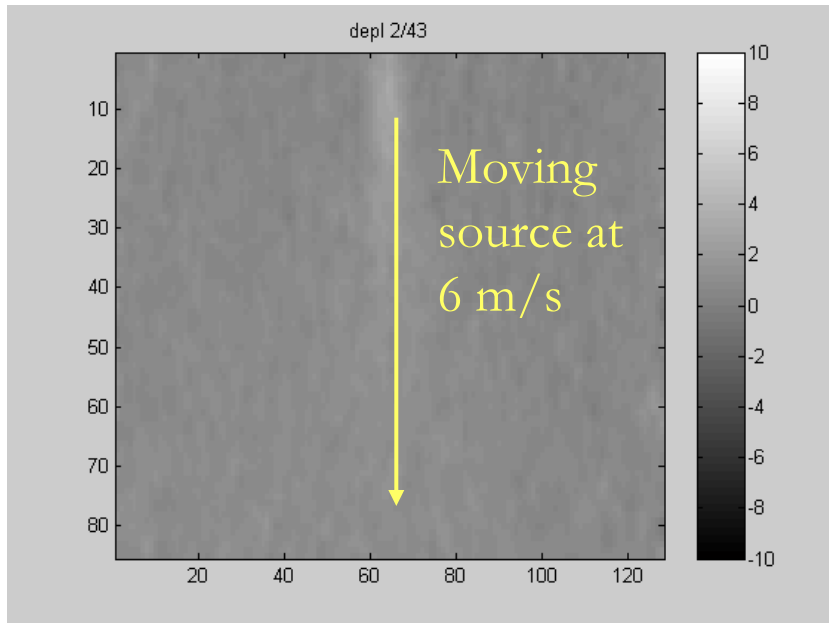
A 30 ms Experiment !!



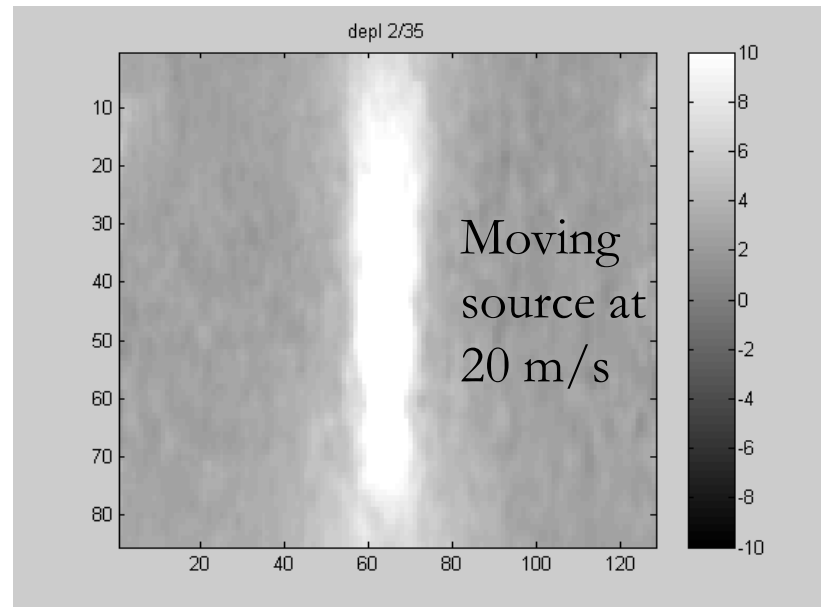
Supersonic moving source

Shear beamforming with a supersonic moving source

Plane wave generation in a
2m/s phantom

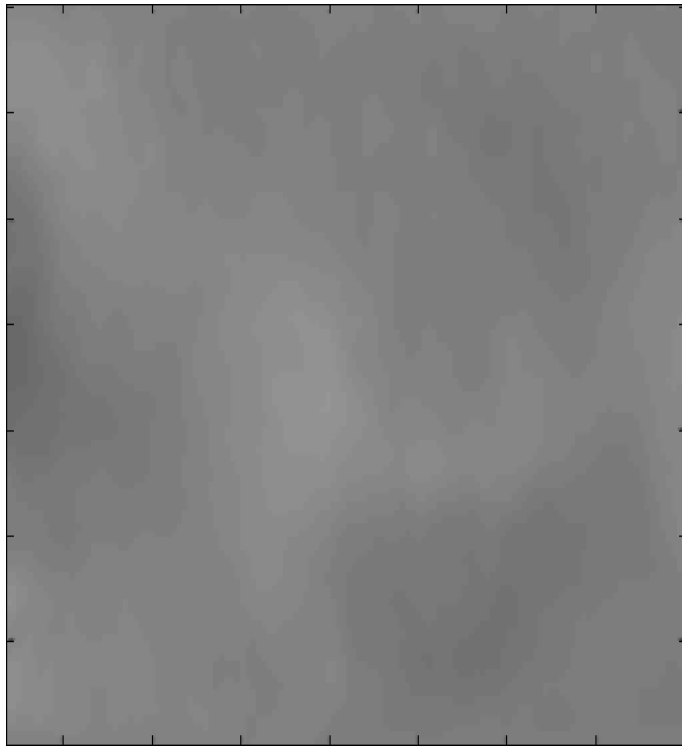


Mach 3

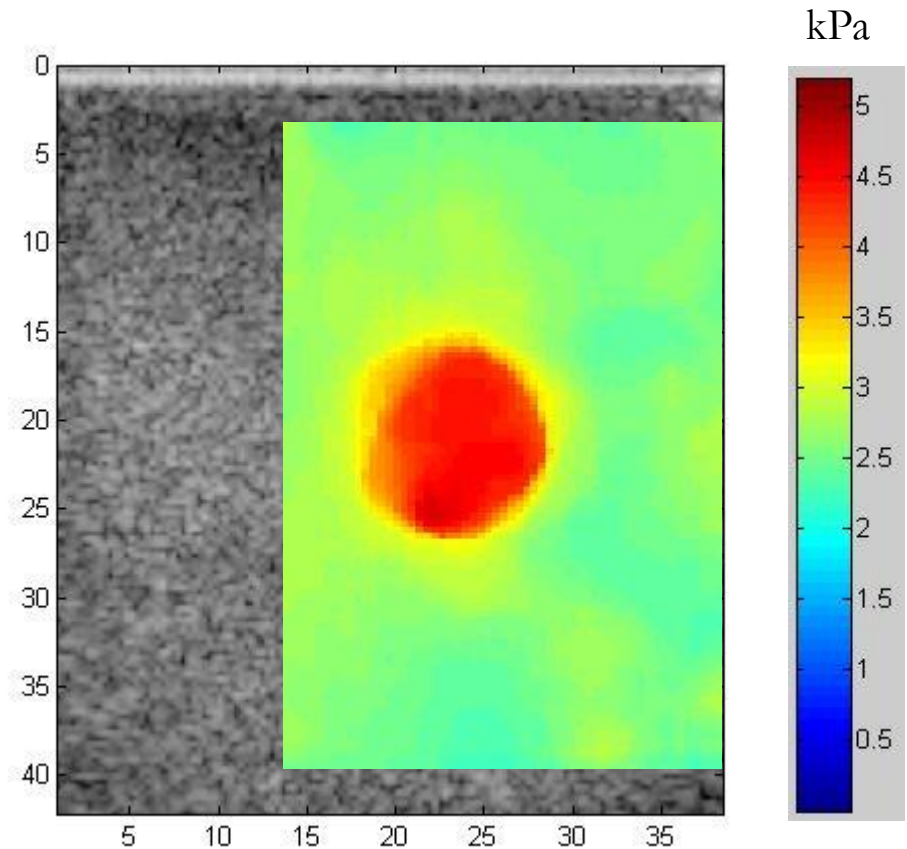


Mach 10

Mapping Elasticity : Inverse problem of Shear Wave Propagation



Movie Duration 20 ms



La résolution des ultrasons
Le contraste des ondes de cisaillement

The goal of Elastography is to estimate tissue elasticity : Multiwave or not Multiwave ?

- Mechanical excitation

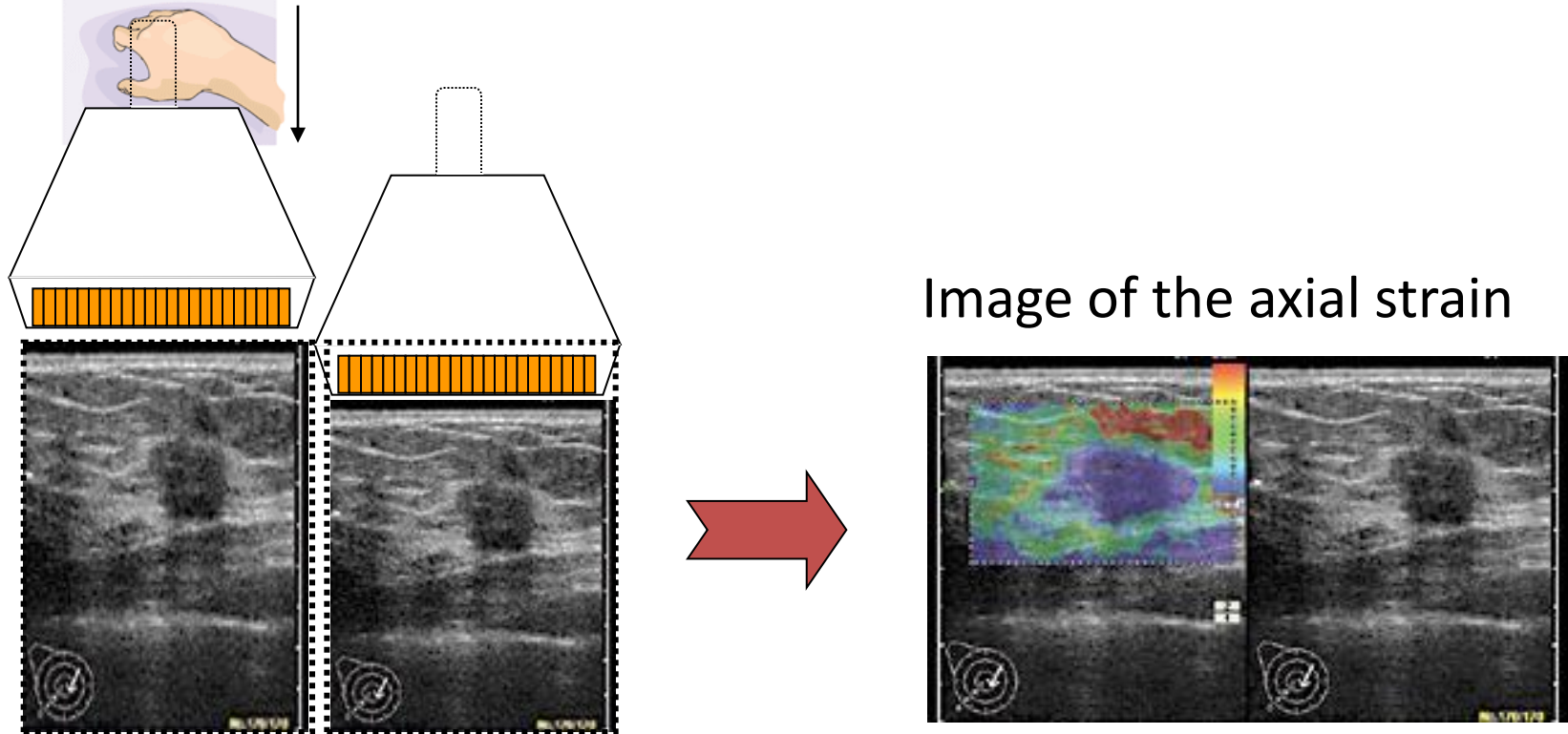
- **Static** (*Ophir, Konofagou, Insana...*)
- **Dynamic** / Harmonic (*Parker, Sato, Greenleaf, Levinson,...*)
- **Transient** (*Fink, Tanter*)
- **Induced remotely by ultrasonic radiation force**
(*Sarvazyan, Trahey, Nightingale (ARFI), Greenleaf, Fink, Tanter*)

- Imaging tissue displacements

- **Ultrasound** Speckle motion (*Sato, Parker, Levinson, Ophir, Fink...*)
- **Magnetic Resonance Imaging** (*Greenleaf,...*)

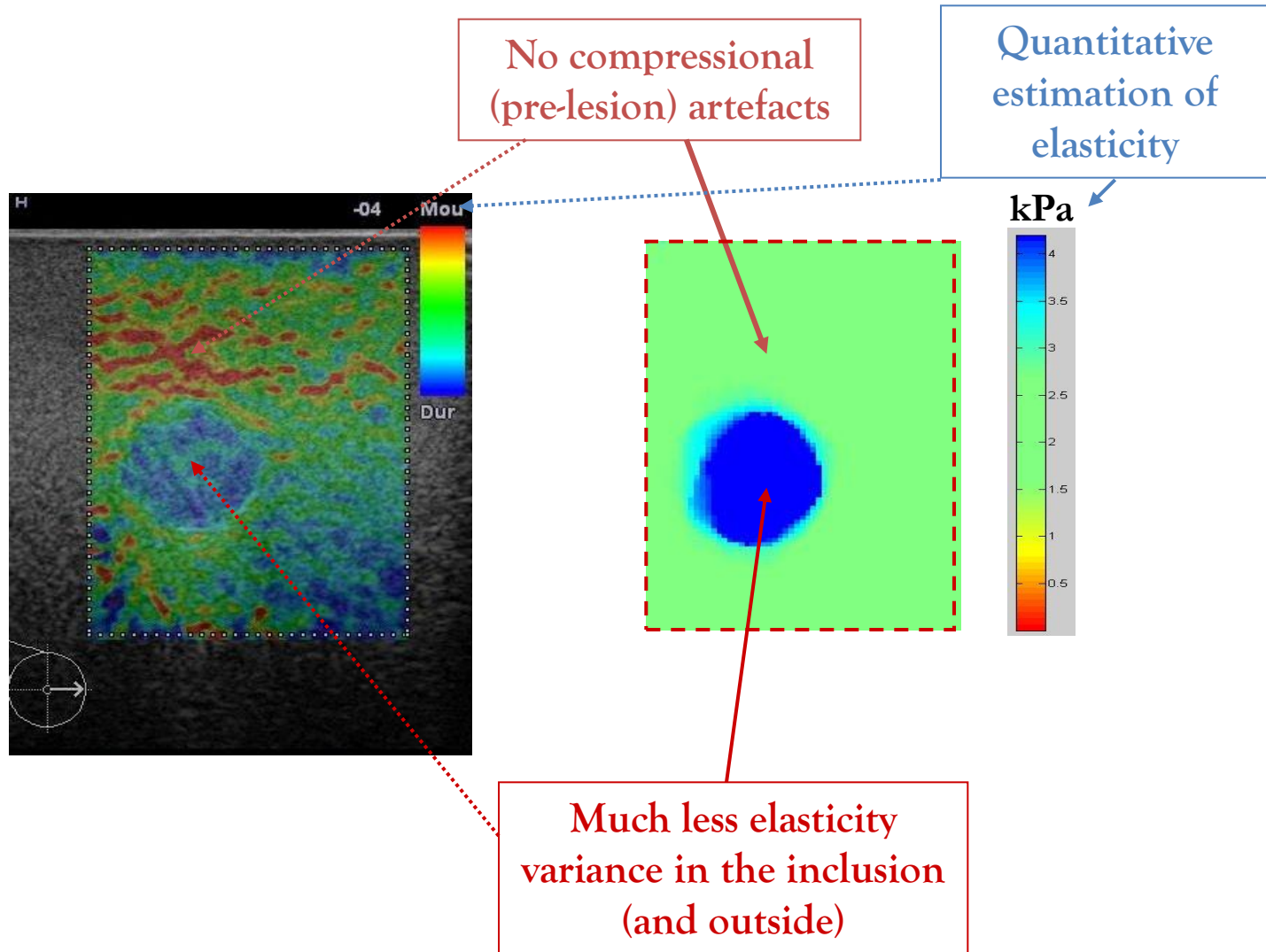
Static Elastography (J. Ophir)

One create a static stress that induces a static strain.
On measure at all locations **the strain (strain imaging)**



Hitachi, Medison, Siemens, Ultrasonix, Zonare, Toshoba...

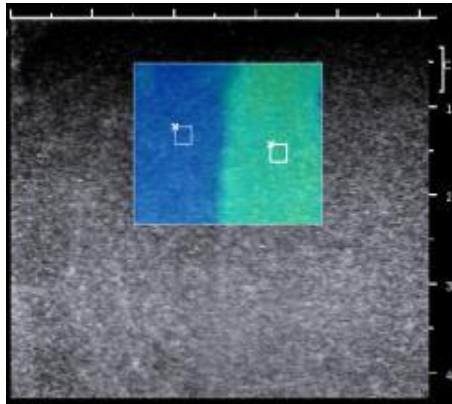
Comparison between the Supersonic Shear Wave Imaging and Static Elastography (strain imaging)



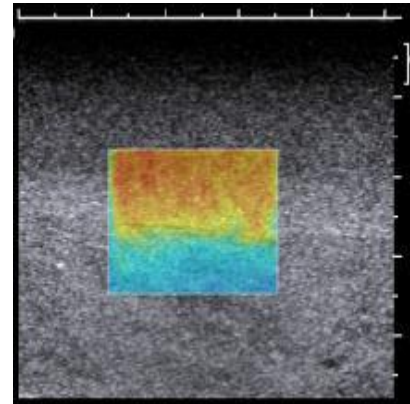
Supersonic Shear Wave Imaging: Spatial resolution

Axial and lateral resolution in a two layers medium :
around 1 mm

Lateral resolution



Axial resolution



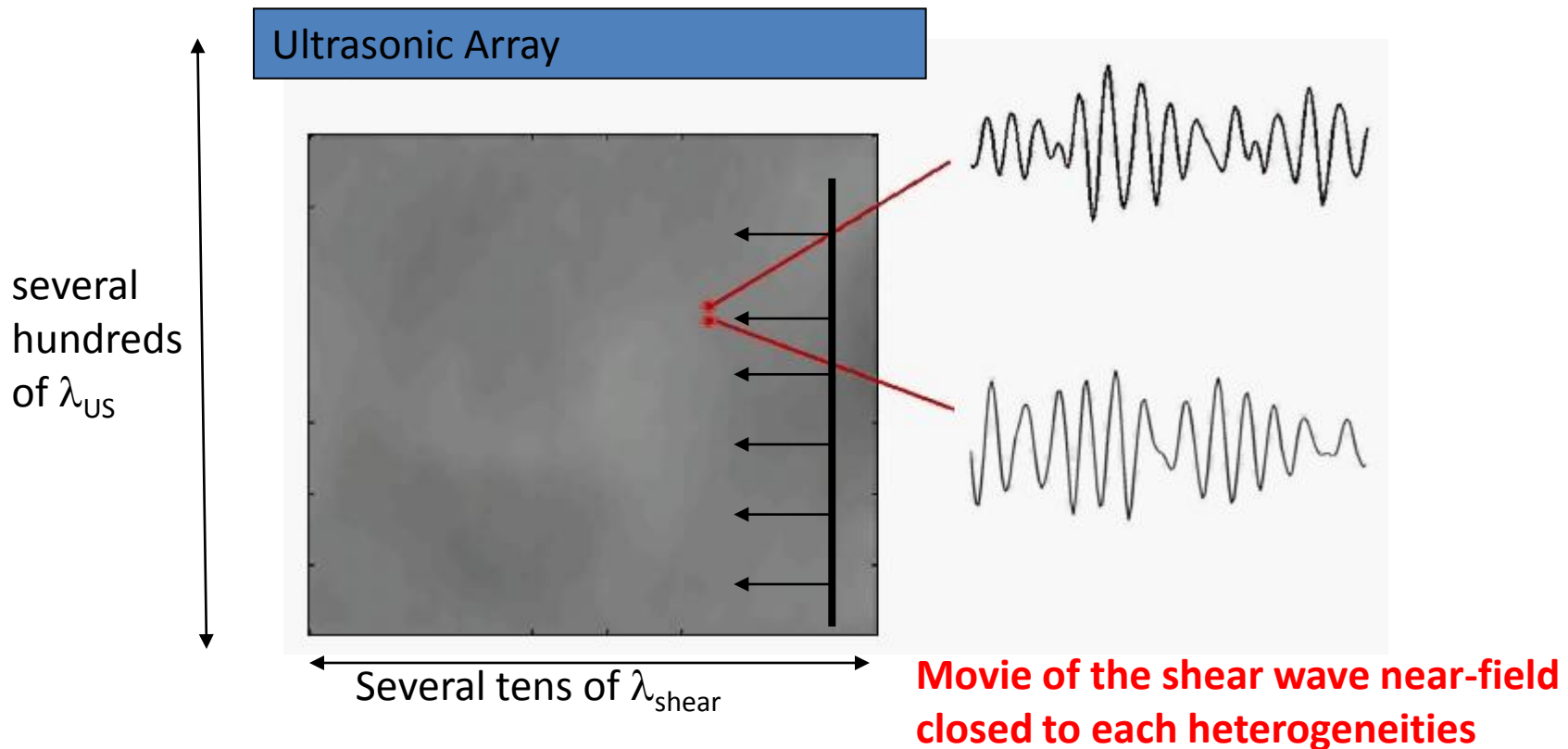
Elasticity contrast	Axial Res (mm)	Lateral Res (mm)
2	1	1.1
3	1.2	1.2
10	1.3	1.1

Multiwave imaging and super-resolution

M. Fink, M. Tanter, "Multiwave Imaging and Superresolution"
Physics Today, 63(2), 28-33, Feb. 2010

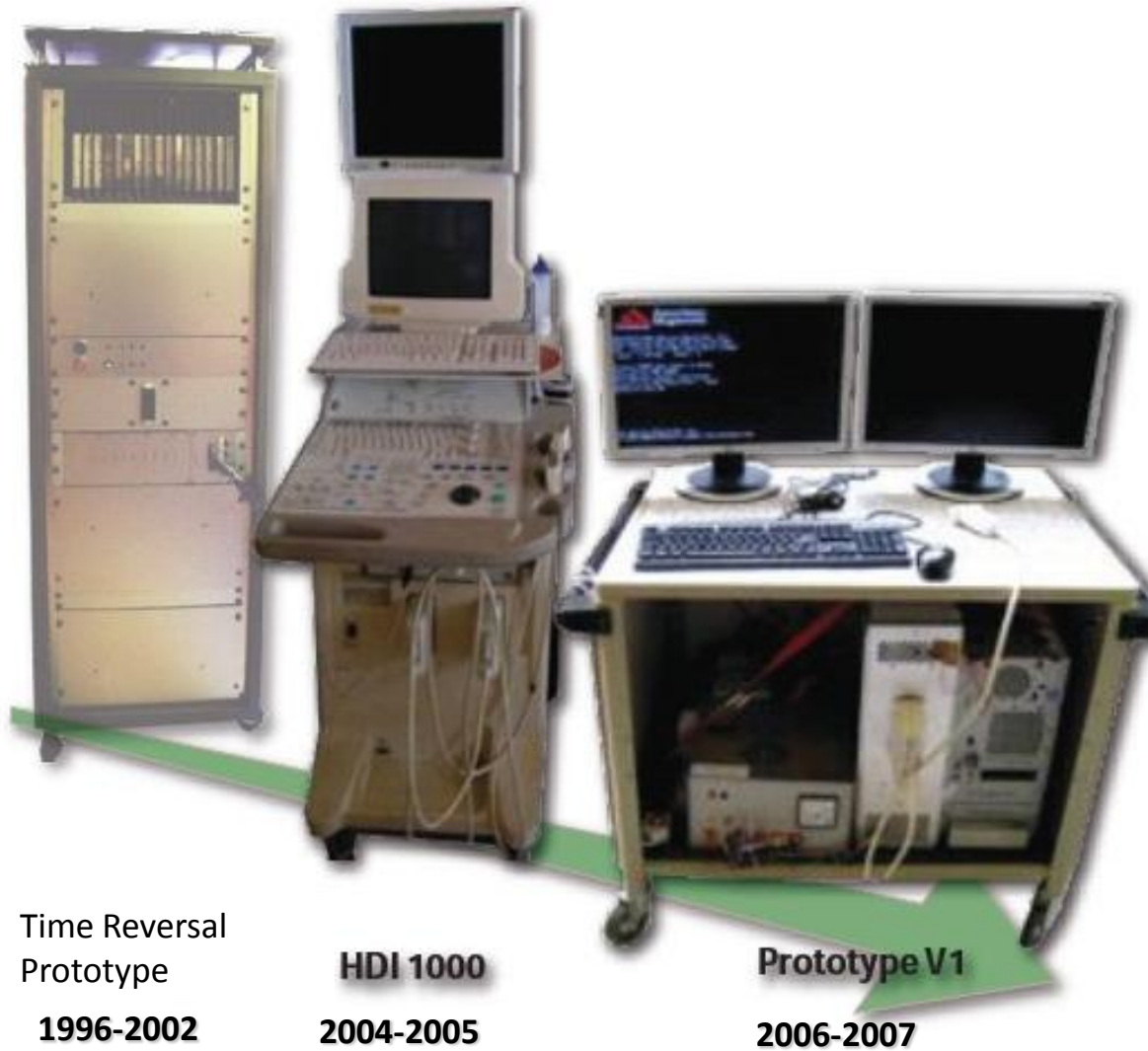
Shear wavelength : typically 10 mm

Spatial resolution on the shear modulus : 1 mm (λ_{US})



Multi-Wave Imaging allows to get the Contrast of One Wave with the Resolution of the Second Wave

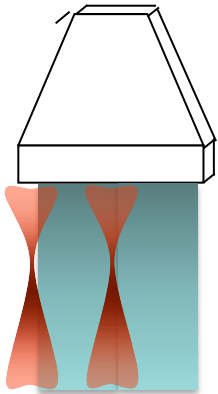
The Evolution of our Ultrafast Imaging Technology



Safety and Efficiency issues in Elastography

A Key difference between SSI and ARFI is **ULTRAFAST IMAGING**

SSI

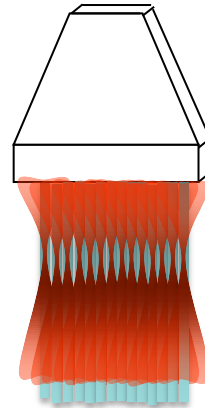


« Flash » Imaging
+
Limited nb of « push »



Real Time
Quantitative
No motion artefacts

ARFI

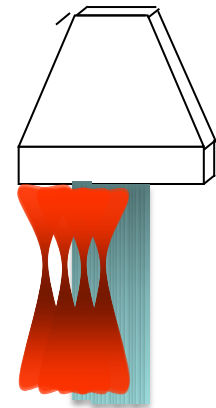


Imaging only at push location
+
High number of pushes



Qualitative

ARFI- SWS



Synthetic building
of «flash» sequence
+ repeated local «Push»

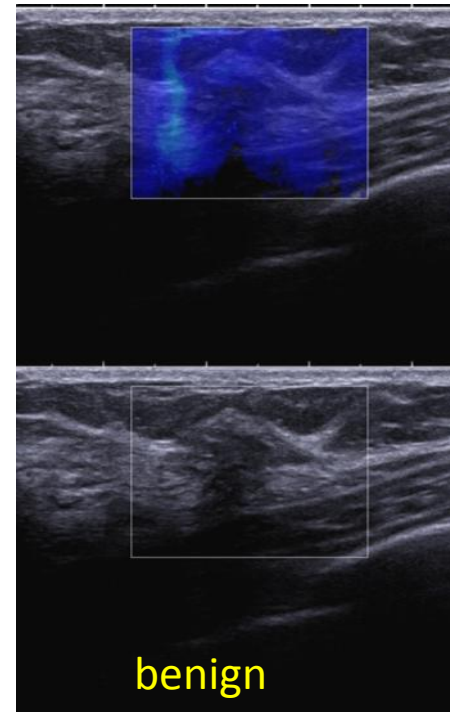
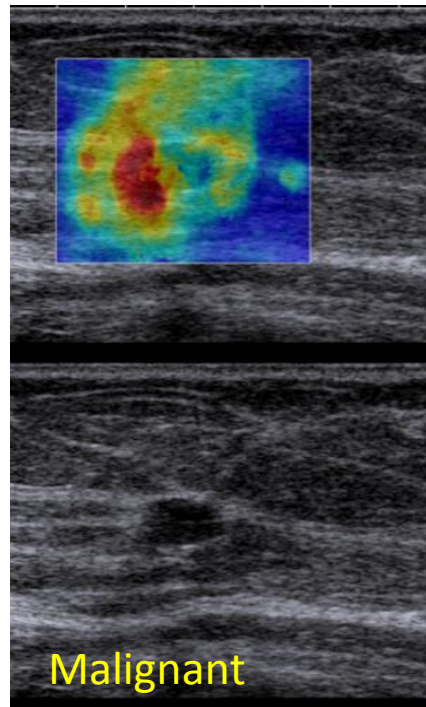
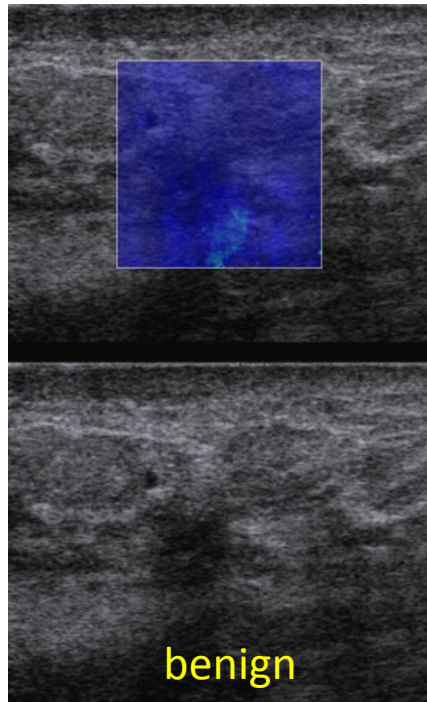


Quantitative
Not Real Time
Potential motion Artefacts

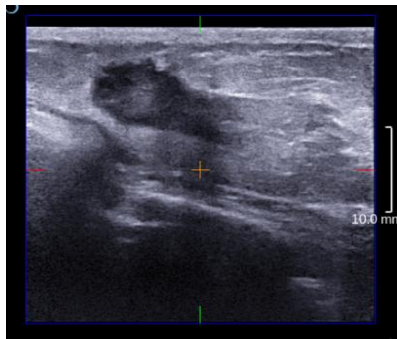
Medical applications

- Breast
- Thyroid
- Liver
- Kidney
- Muscle
- **Vascular**
- **Cardiac**
- Eye
- Prostate
- Monitoring HIFU

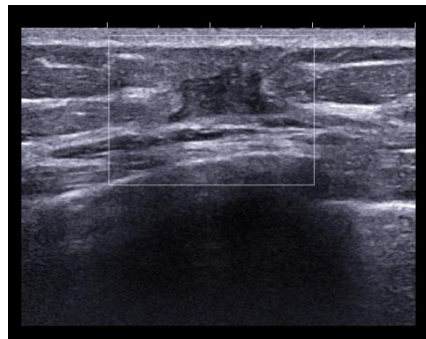
Diagnostic impact in breast :



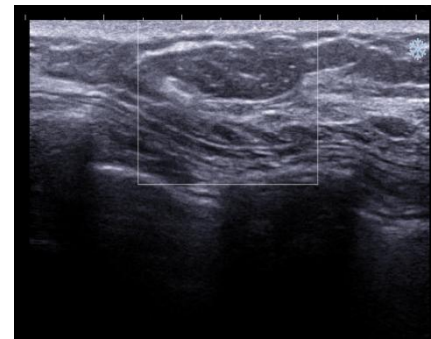
Breast Chemiotherapy



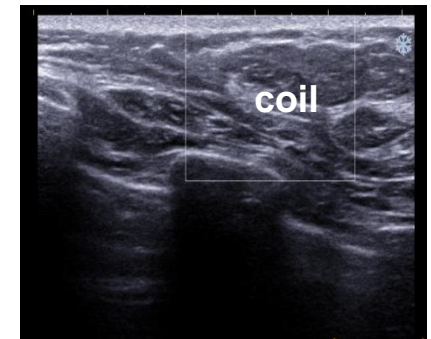
$\varnothing = 2.04$
cm



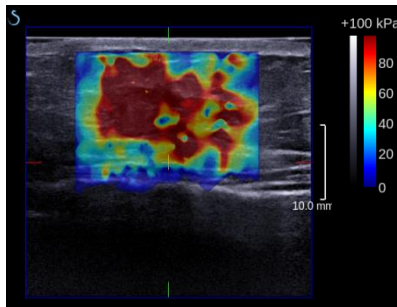
$\varnothing \approx 1.80$ cm



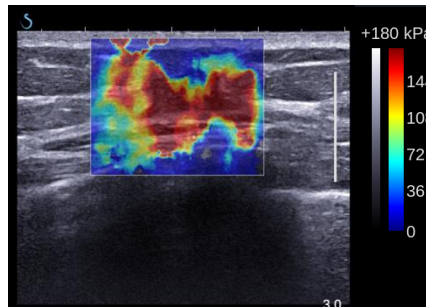
$\varnothing = 1.64$ cm



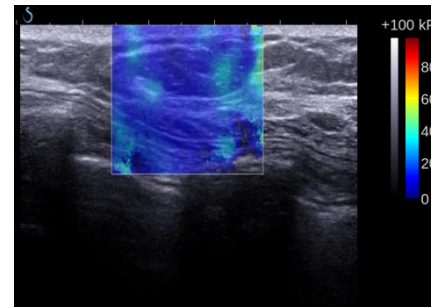
$\varnothing \approx 0.1$ cm



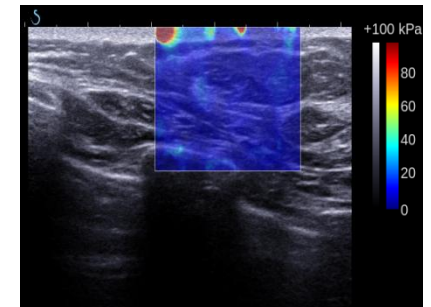
June/2011



July/2011



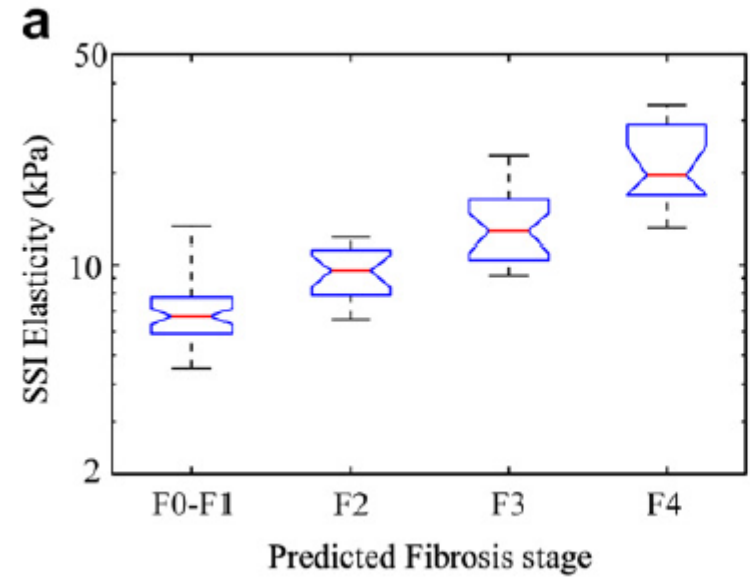
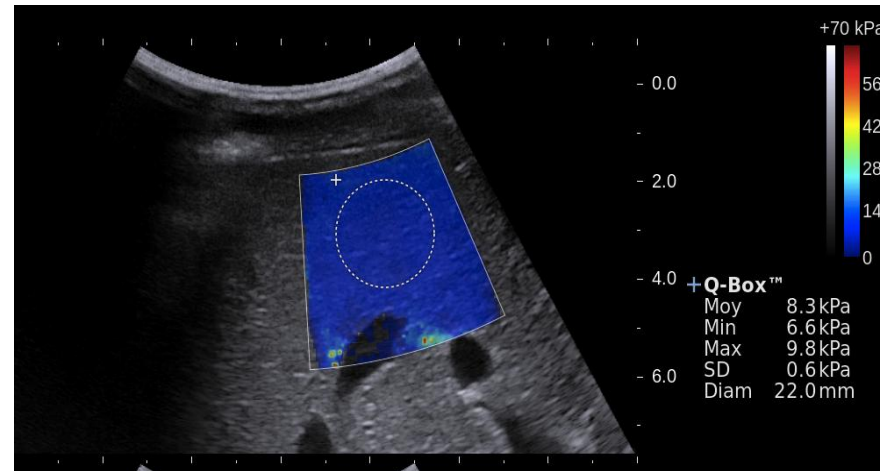
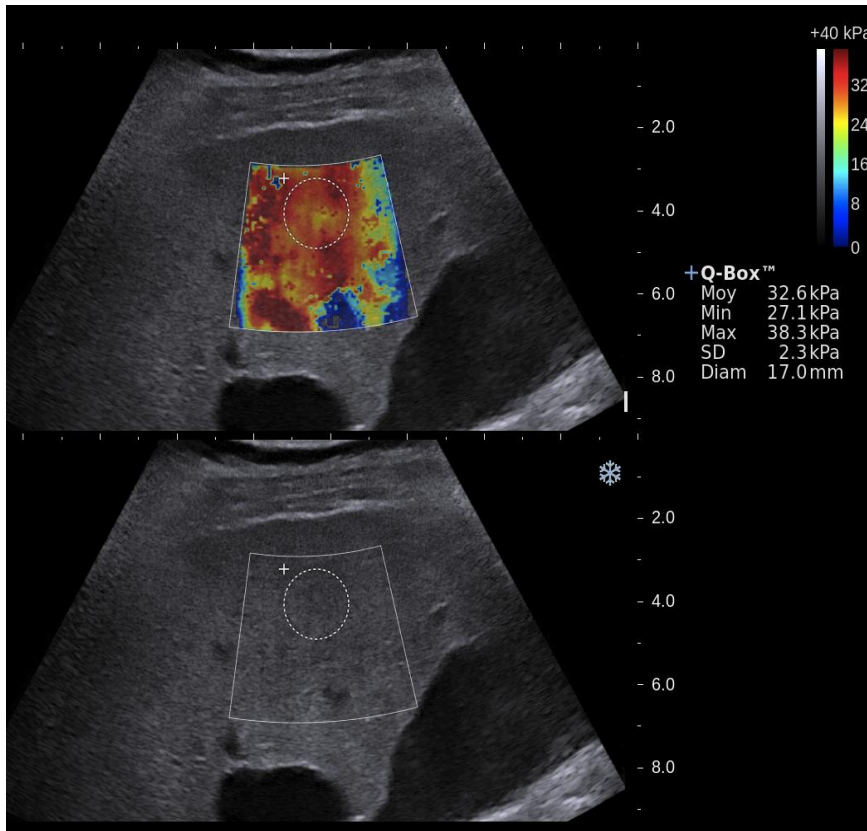
August/2011



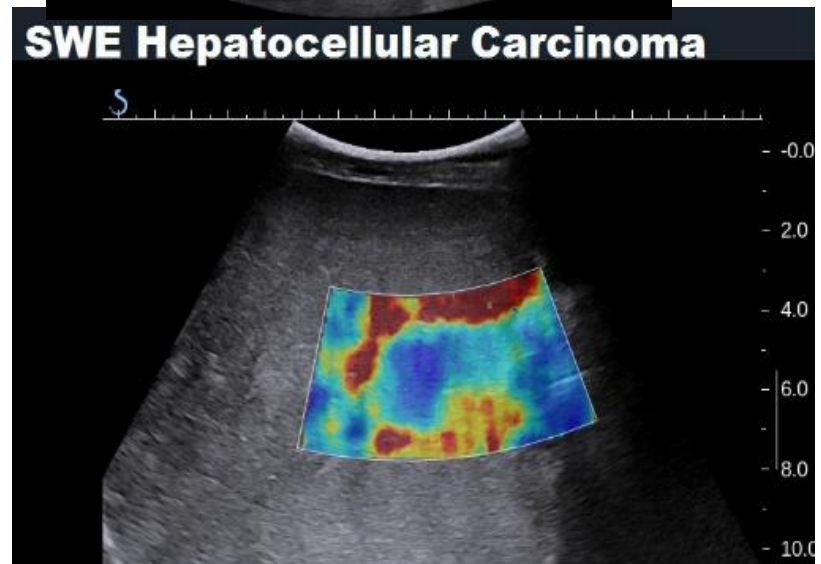
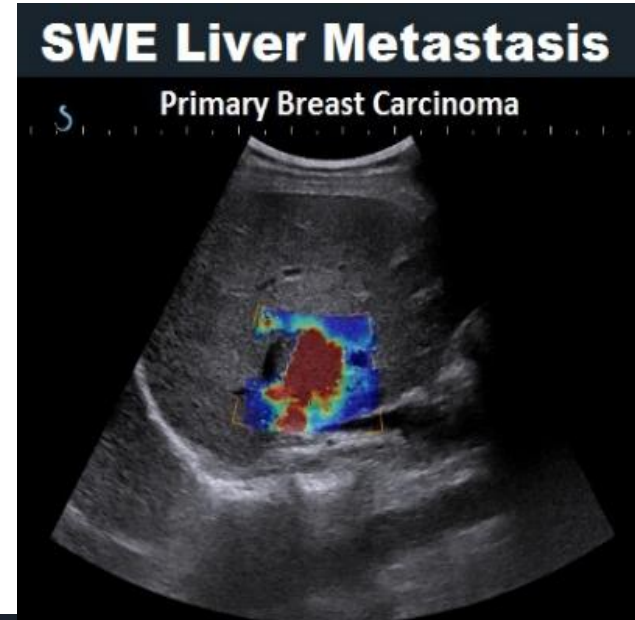
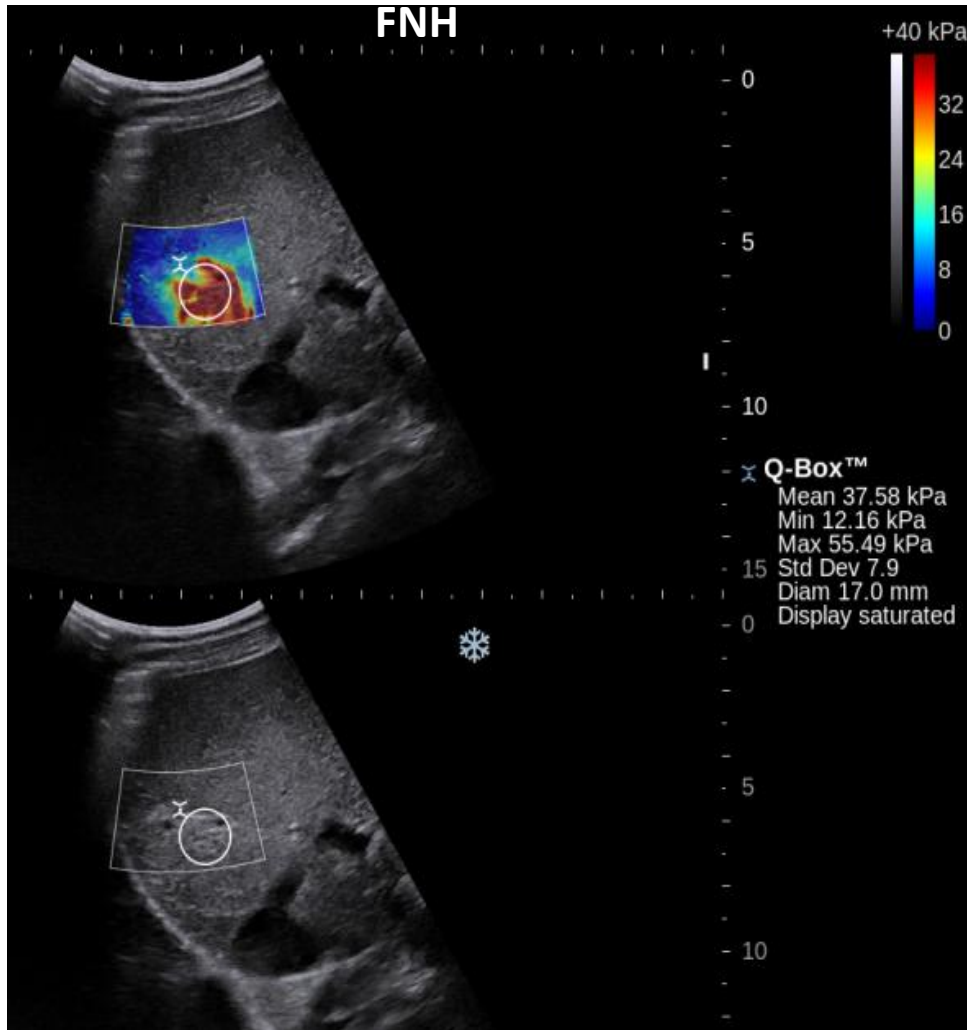
October/2011

(Collaboration A. Athanasiou, Curie Institute, Paris, France)

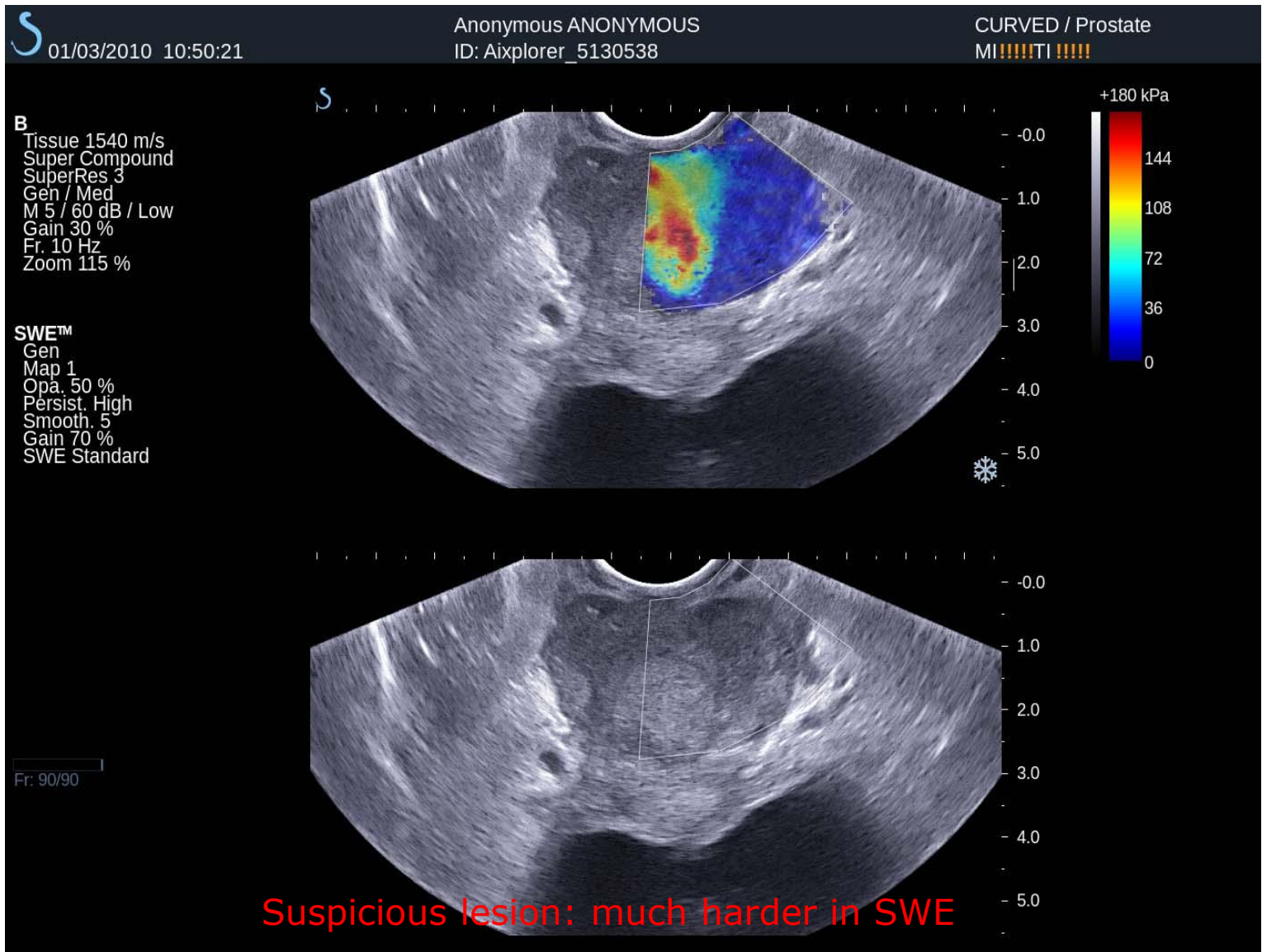
Liver : Fibrosis and Cirrhosis



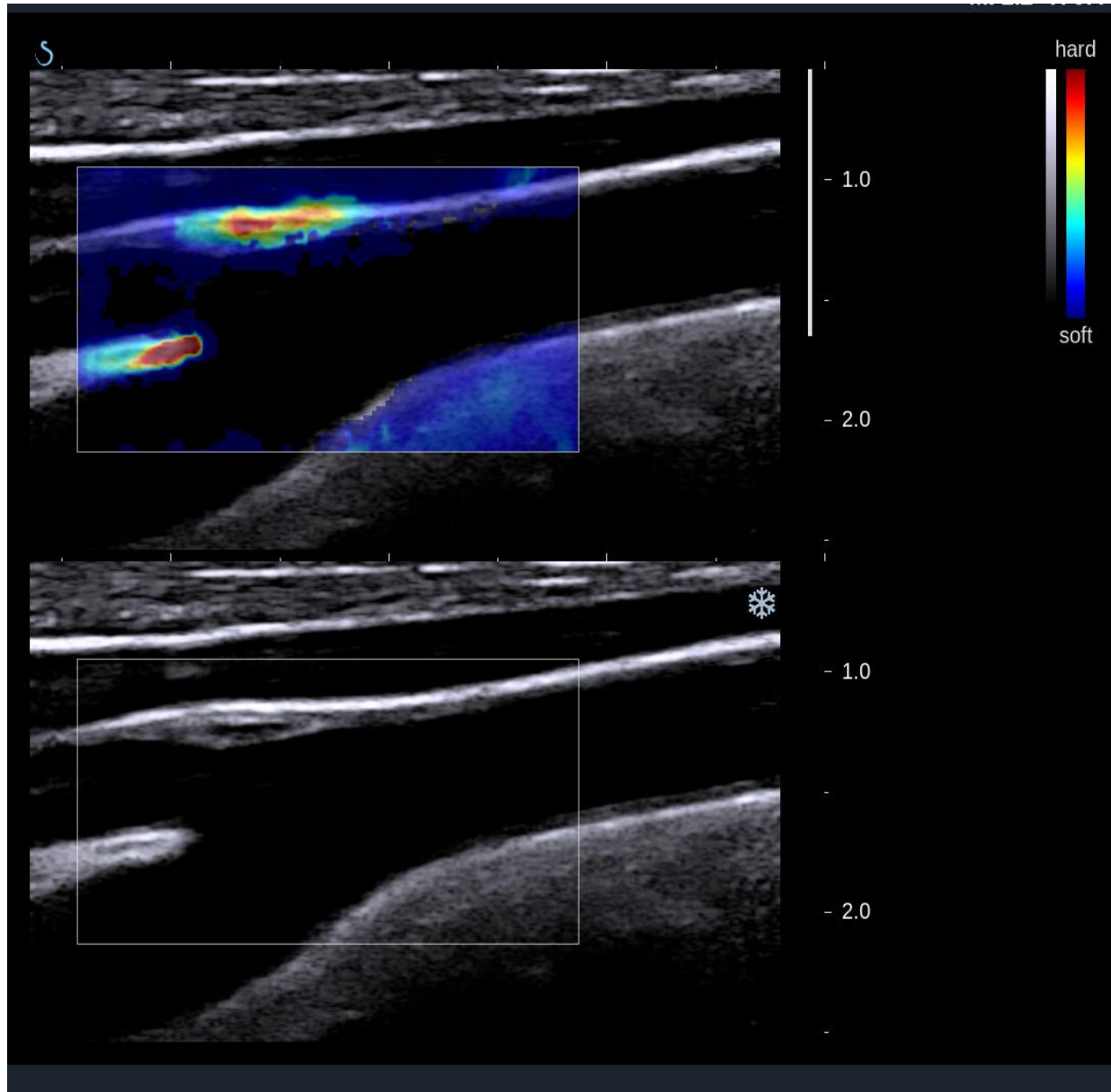
Focal lesions in Liver : examples



Prostate – multiwave imaging



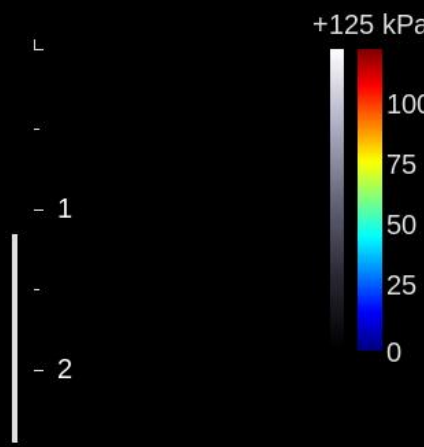
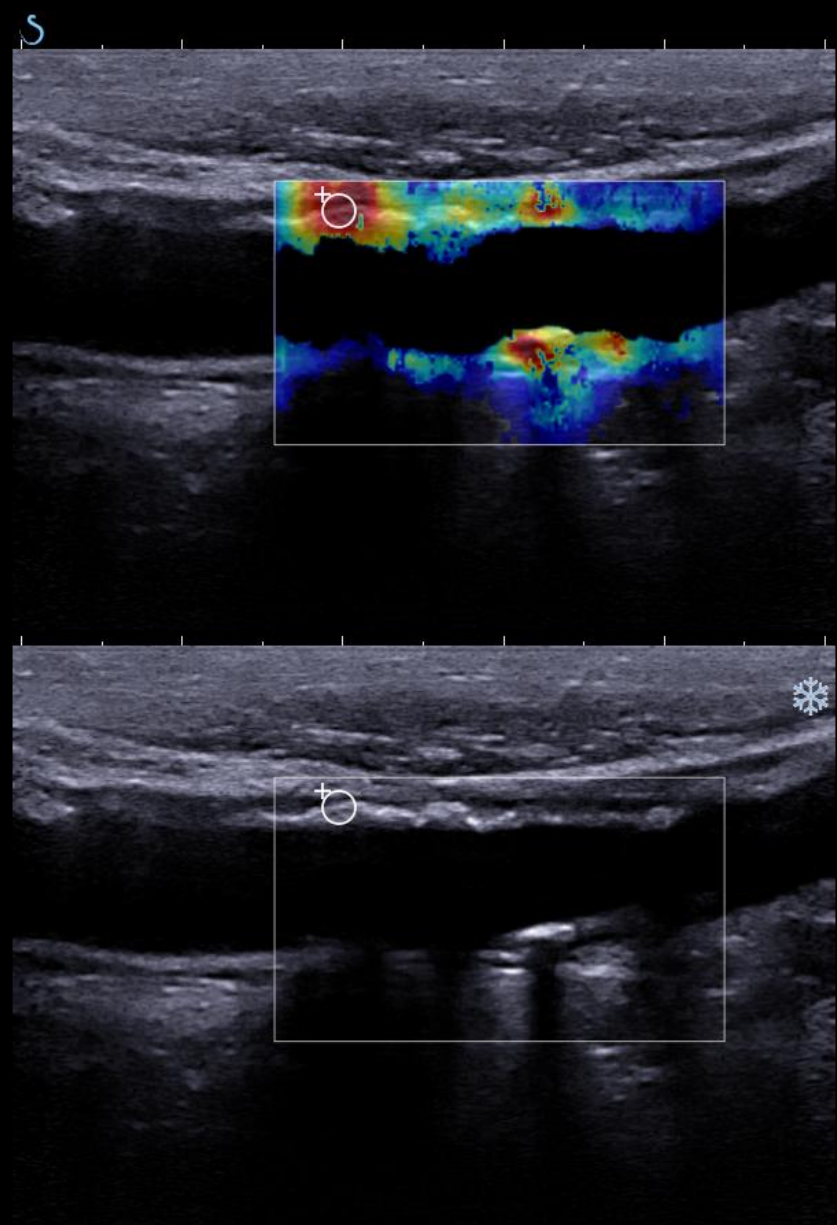
Carotid Plaque Stiffness



B
Pen/FR/H
M 5/67 dB/Low
T 1540 m/s
SR 6
G 40 %
Fr. 12 Hz

SWE™
Std/Med
M 1/High
S 5/O 50 %
G 70 %

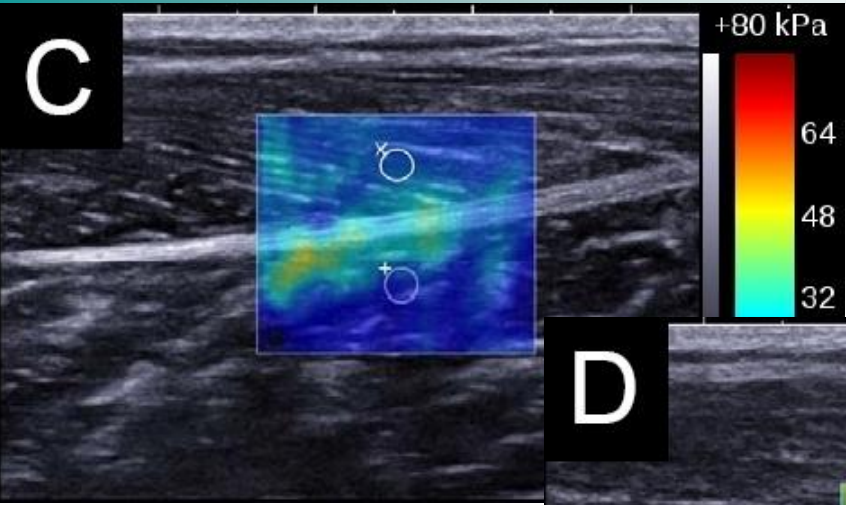
Z 100 %



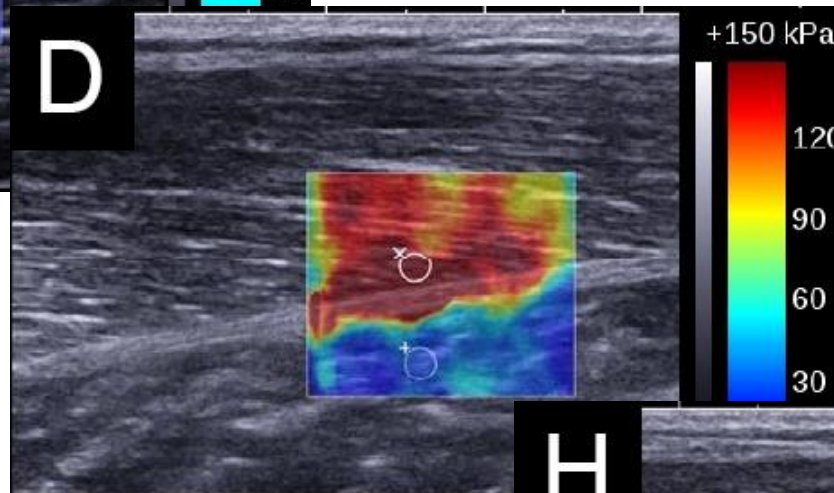
+ Mean 128.4 kPa
- Min 114.1 kPa
- Max 141.6 kPa
- SD 8.2 kPa
- Diam 2.0 mm
L Display saturated

Dynamics of Muscle Contraction

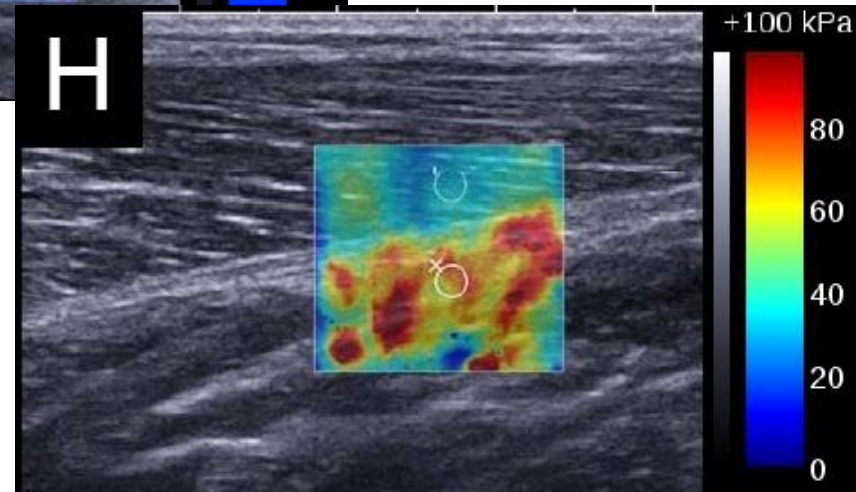
Coll. M. Shinohara, K. sabra,
Georgia Tech. University, Usa



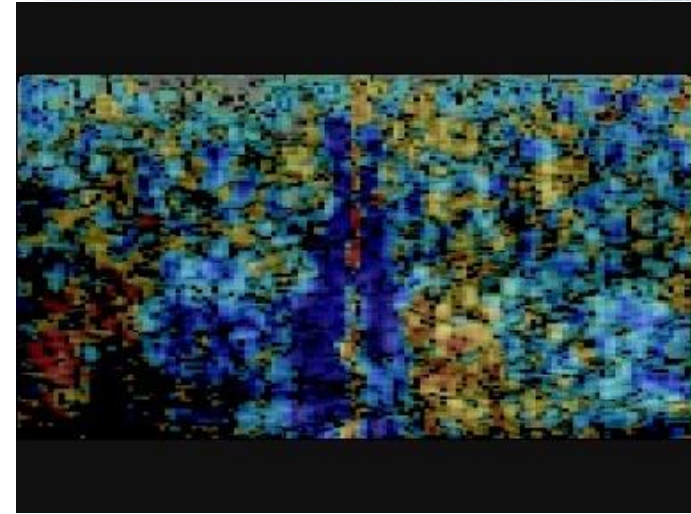
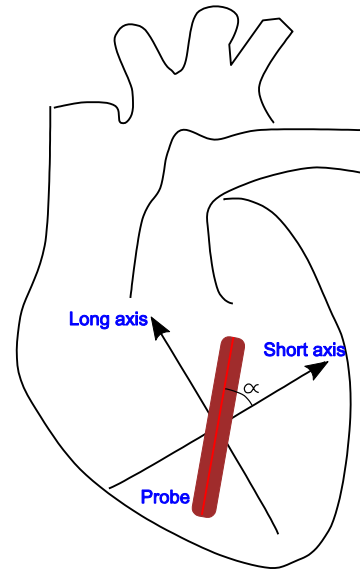
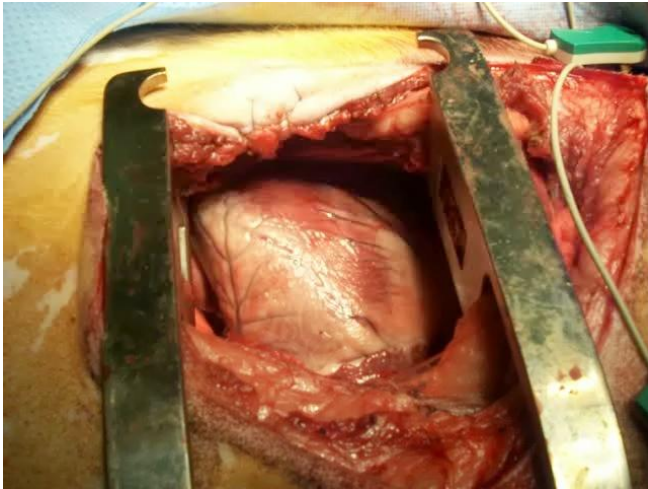
**Gastrocnemius
Contraction**



**Soleus
Contraction**

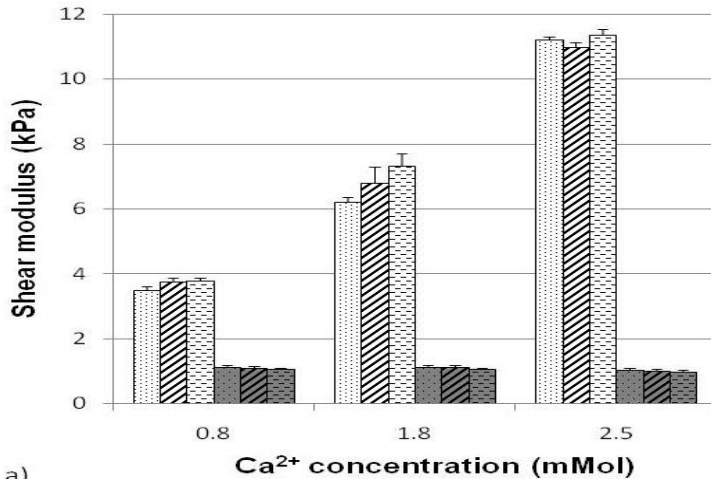


Real Time Elasticity Changes of *in vivo* Cardiac Muscle (Sheep Model)

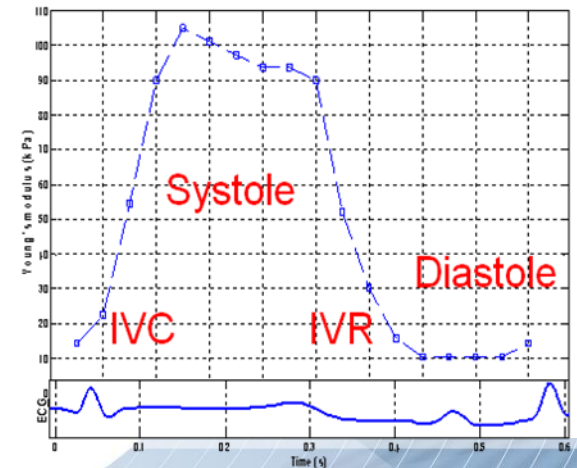


5000 fps

systole (0 μ l)
 systole (10 μ l)
 systole (25 μ l)
 diastole (0 μ l)
 diastole (10 μ l)
 diastole (25 μ l)



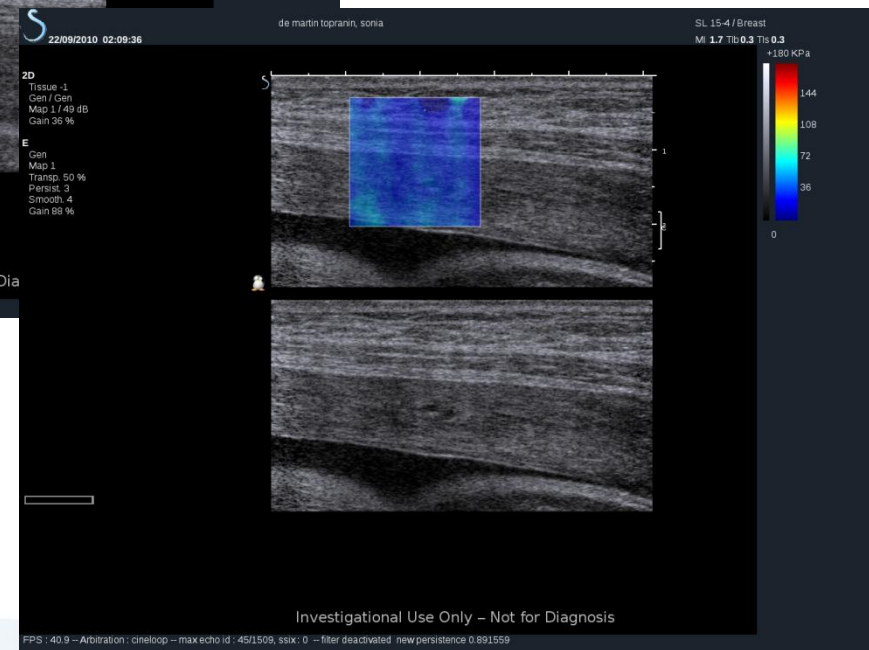
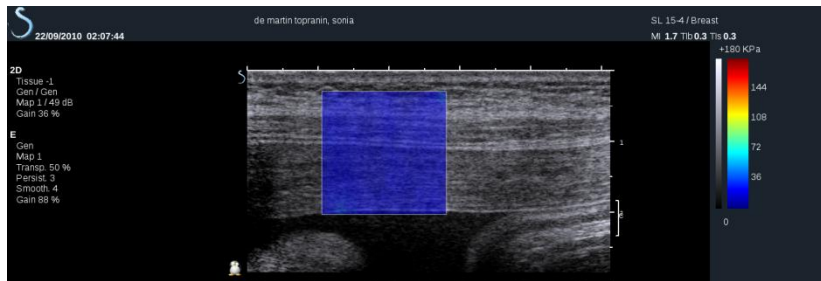
a)



Pernot M, Matteo P., Couade M., Crozatier B., Fischmeister R., Tanter M.
Journal of the American College of Cardiology, 2011

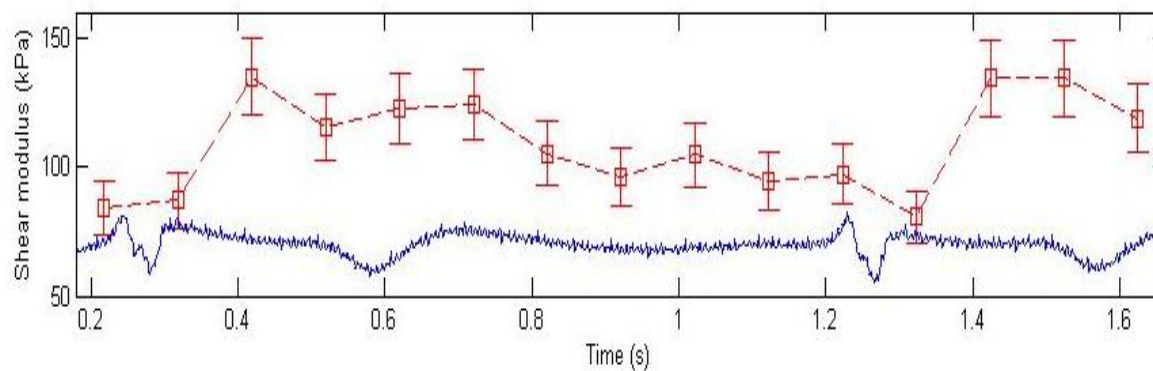
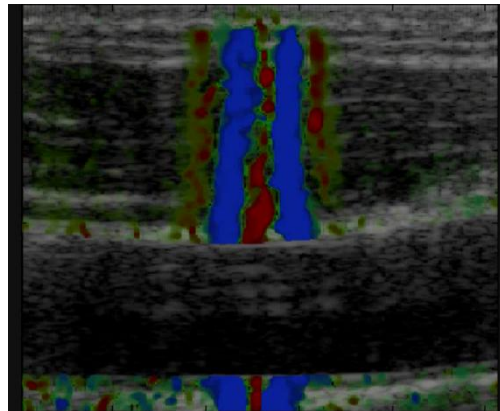
M. Couade, M. Pernot, P. Matteo, B. Crozatier, R. Fischmeister and M. Tanter
Ultr. Med. Biol., Oct. 2010

Quantitative Monitoring of Uterin Contraction during Pregnancy



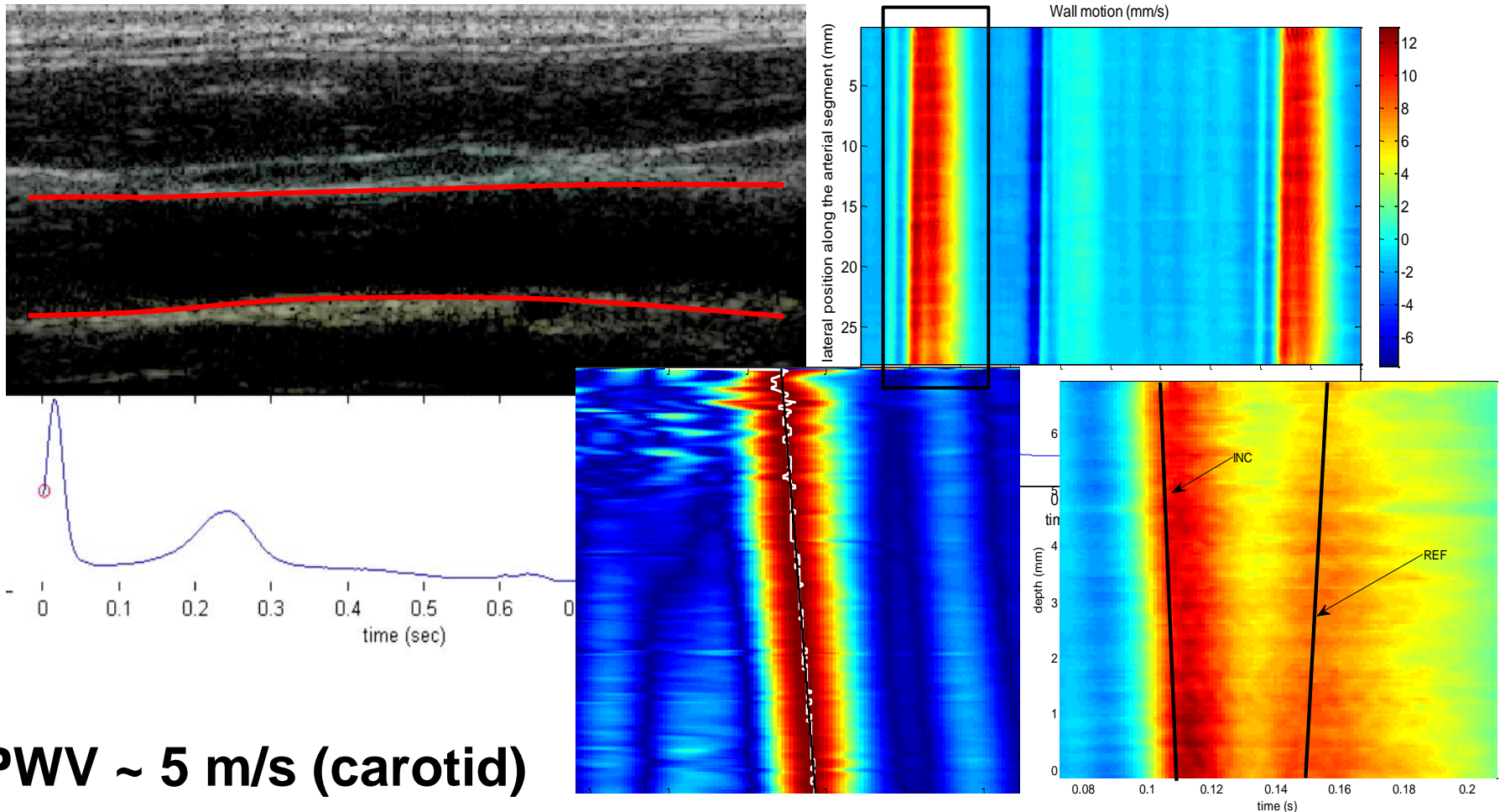
The arterial stiffness varies with blood pressure (diastole/systole) - Carotid

- 13 successive 20 ms experiment every 120 ms = 13 elasticity per cardiac cycle



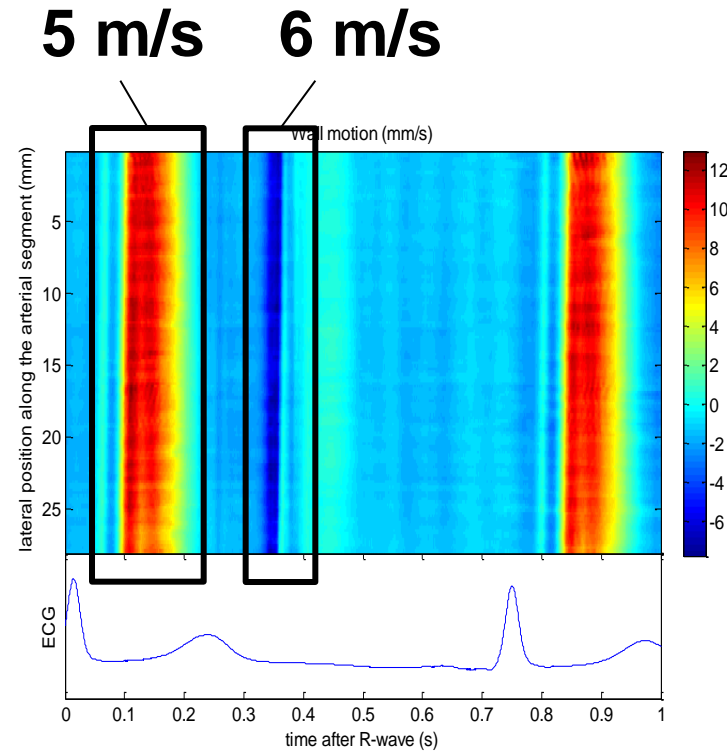
Ultrafast imaging of the pulse wave along the carotid

- Frame rate : 3.000 frames/second



PWV ~ 5 m/s (carotid)

Local estimation of PWV using ultrafast imaging

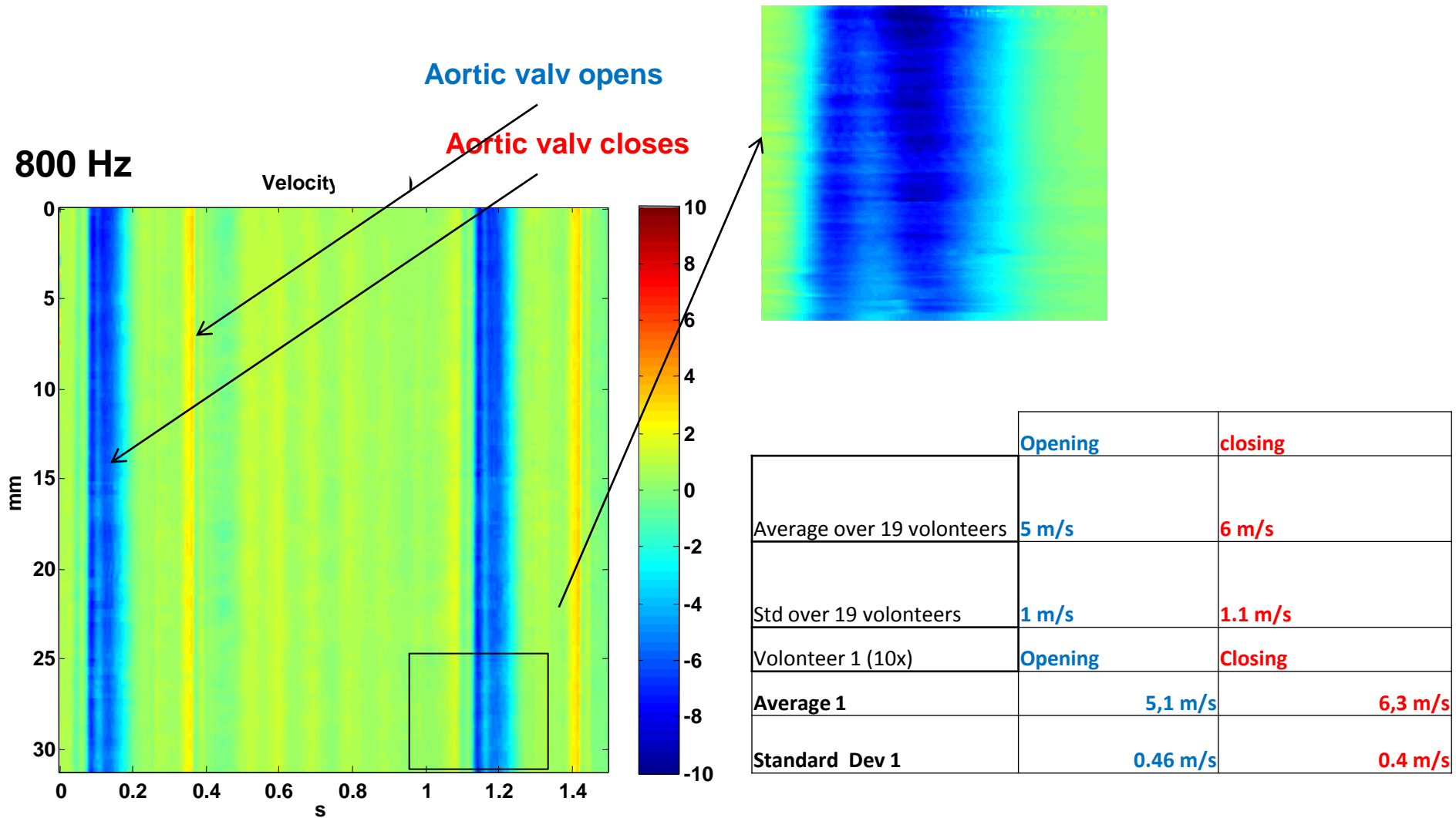


\neq propagation speed
=
 \neq elasticity

Two estimations per cardiac cycle

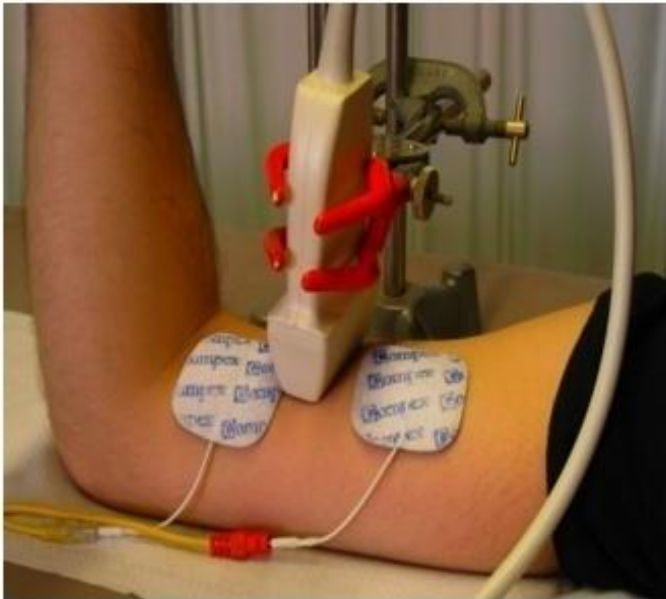
PWV measured by ultrafast imaging

PWV estimation using ultrafast scanner

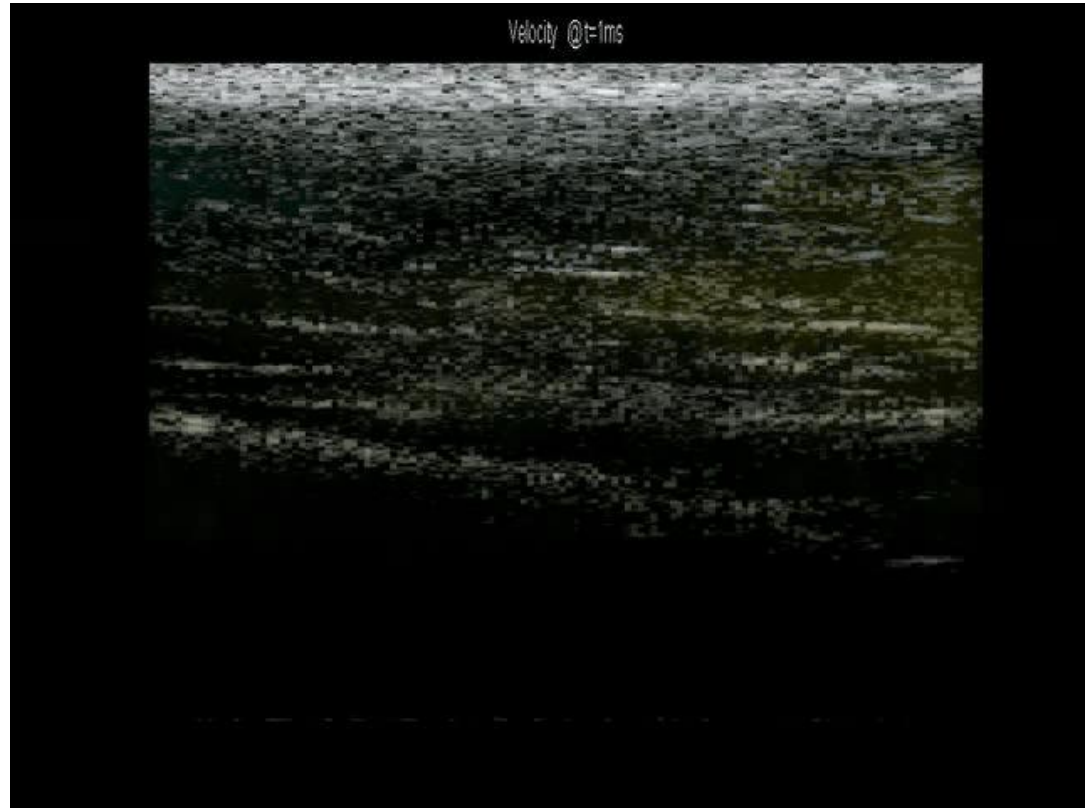


Ultrafast Imaging of Intrinsic waves

Ultrafast Ultrasonic Imaging of Muscle fibers activation



Our body is the ground of many transient phenomena at time scales of the order of milliseconds



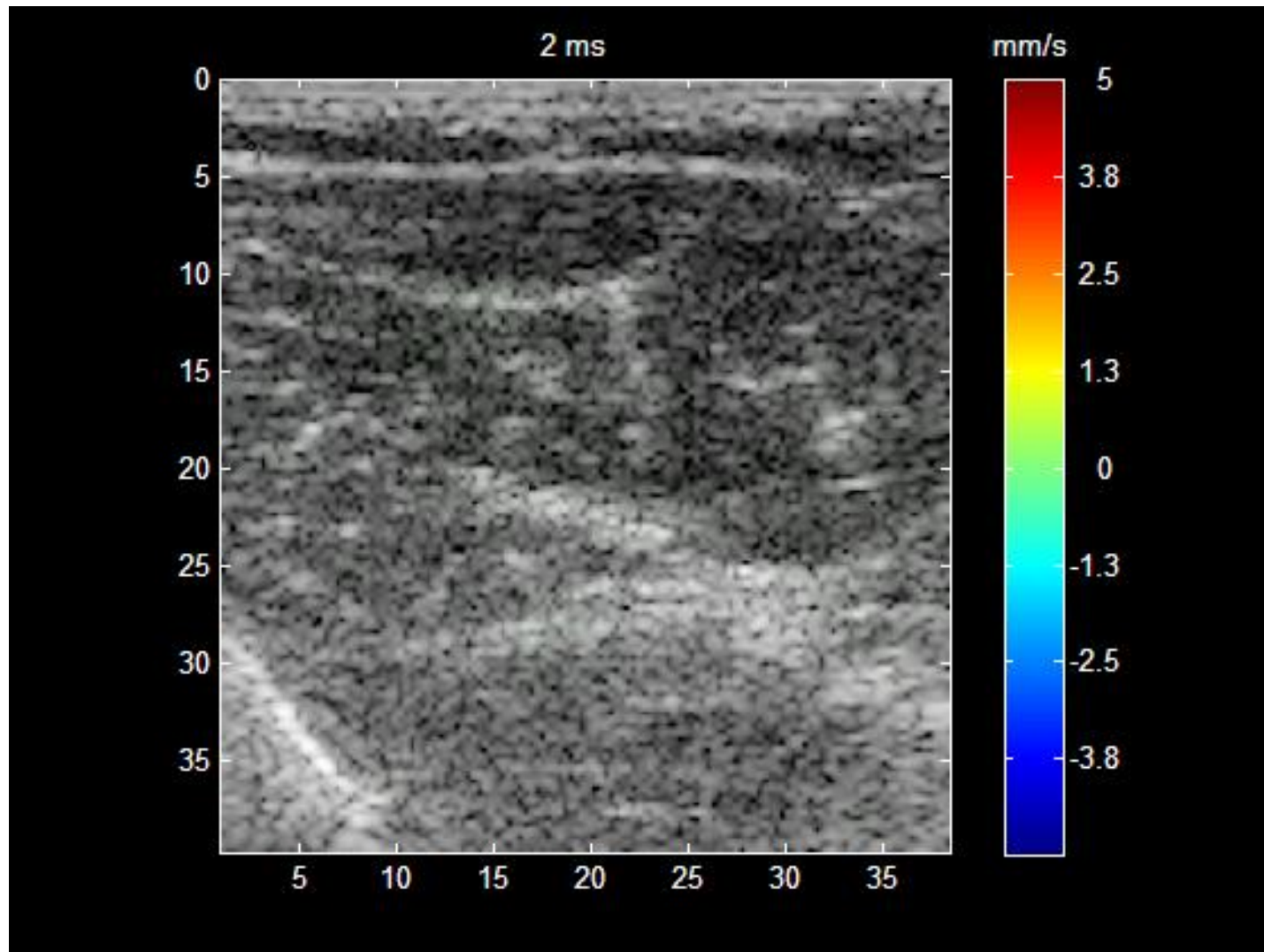
2000 images/s

Can we use mechanical vibrations where electromagnetic waves are limited due to large wavelengths (cardiology, epilepsy,...) ?

Deffieux, T.; Gennisson, J.-L.; Tanter, M.; Fink, M. Nordez, A.
'Ultrafast imaging of in vivo muscle contraction using ultrasound', *Applied Physics Letters* 89(18), 2006

Deffieux T, Gennisson JL, Tanter M, et al. IEEE TRANSACTIONS ON ULTRASONICS, 55 (10), Pages: 2177-2190, OCT 2008

Ultrafast Localization of activated muscle fiber bundles



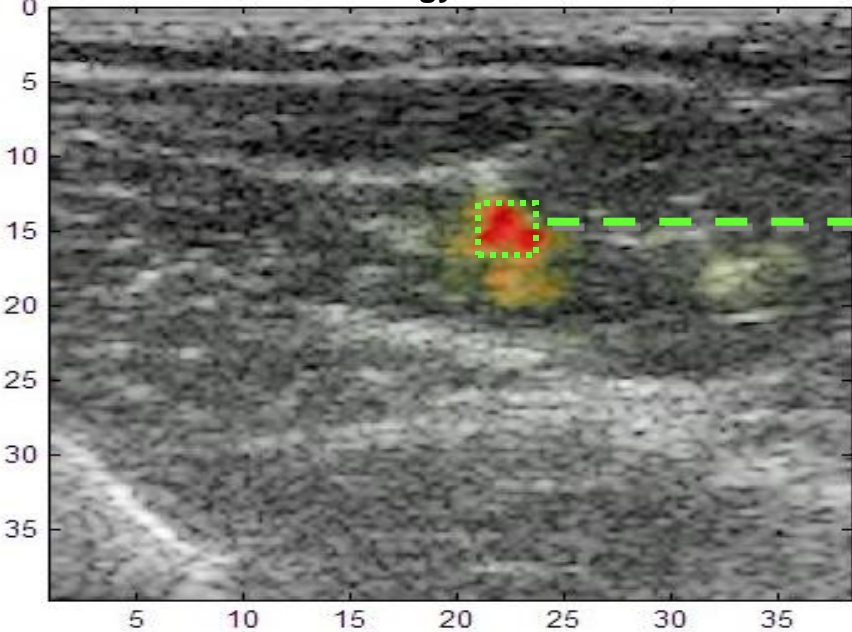
Deffieux, T.; Gennisson, J.-L.; Tanter, M.; Fink, M. Nordez, A.

'Ultrafast imaging of in vivo muscle contraction using ultrasound', *Applied Physics Letters* 89(18), 2006

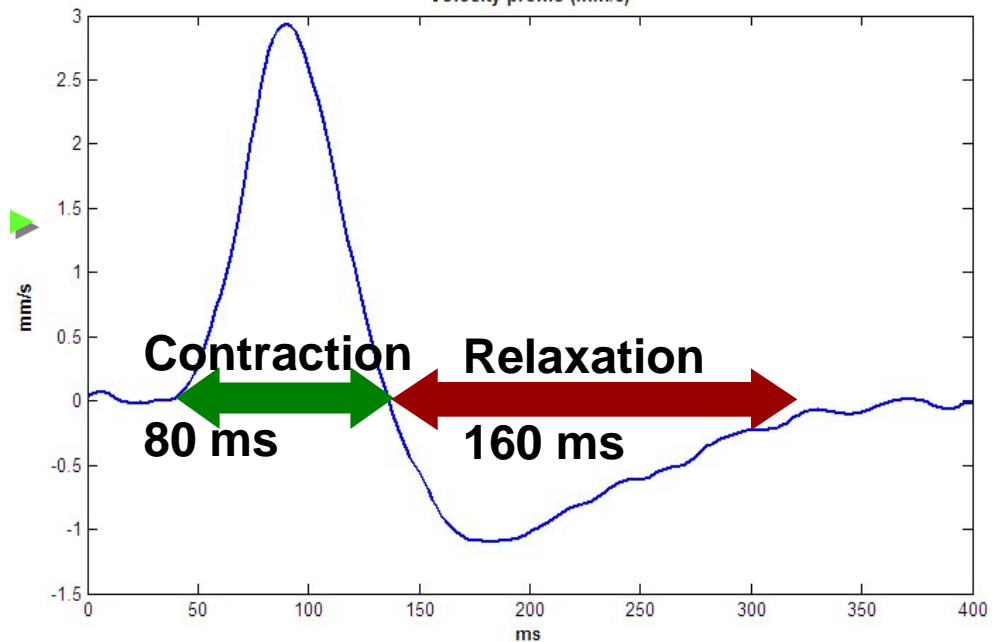
Deffieux T, Gennisson JL, Tanter M, et al. IEEE TRANSACTIONS ON ULTRASONICS, 55 (10), Pages: 2177-2190, OCT 2008

Localization and time profile of contraction

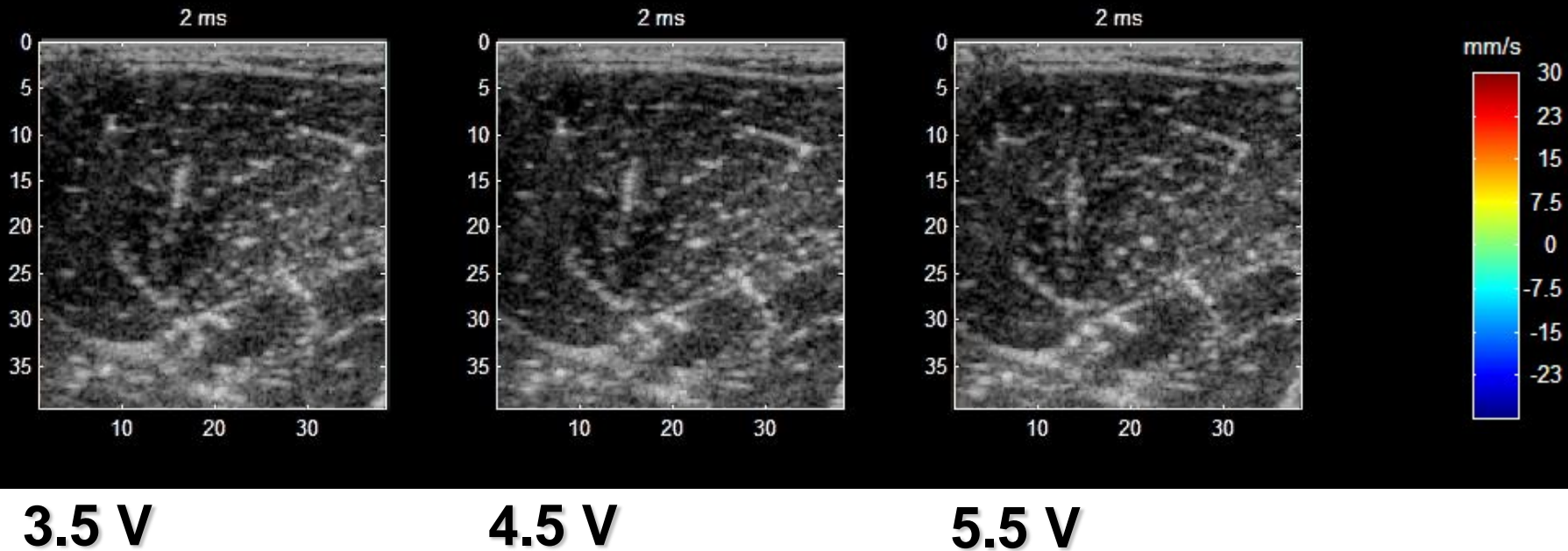
Kinetic energy



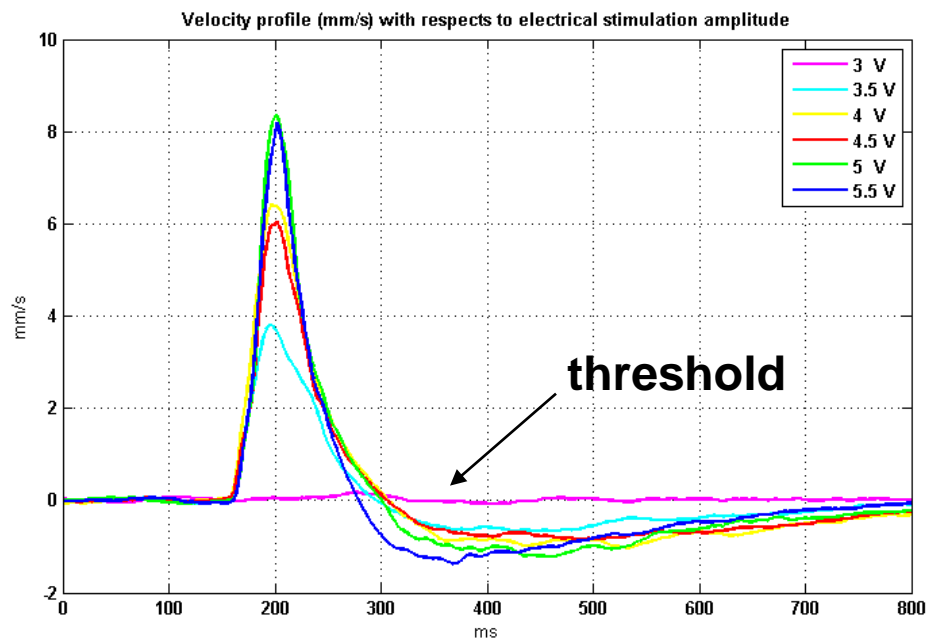
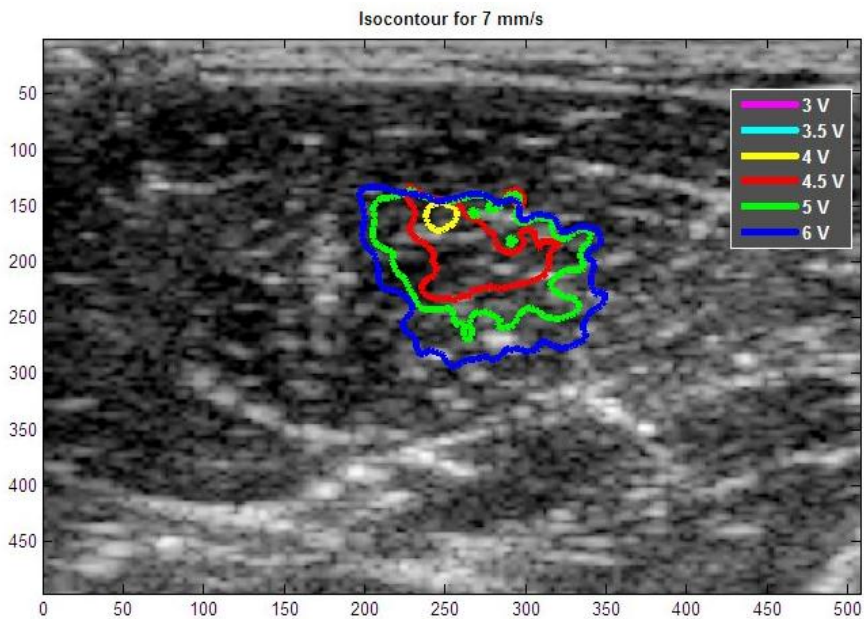
Velocity profile (mm/s)



Effect of electro stimulation amplitude on the contraction



Effect of electro stimulation amplitude on the contraction



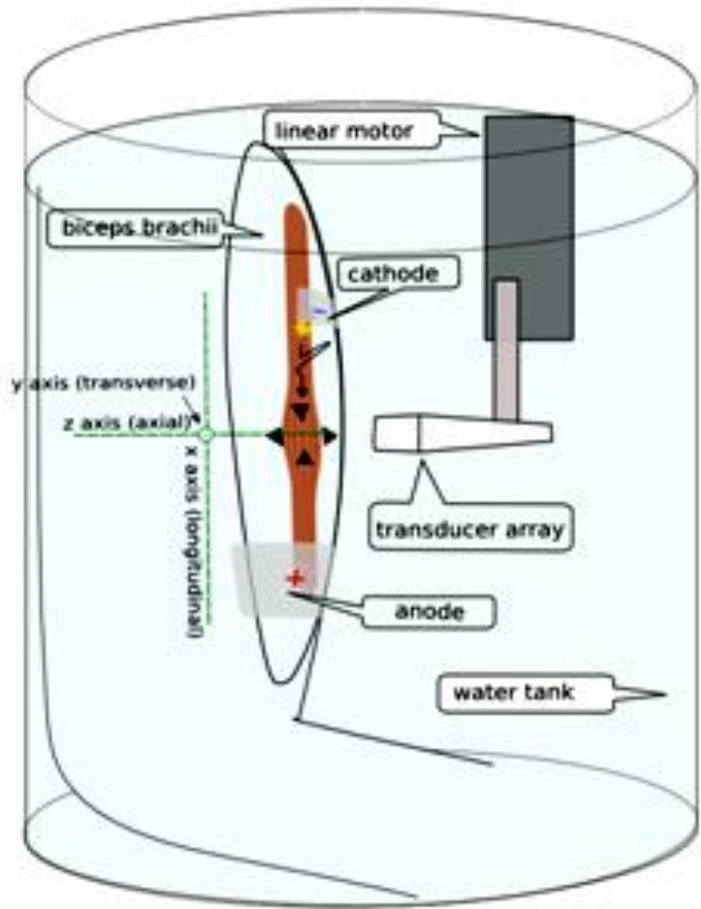
Deffieux, T.; Gennisson, J.-L.; Tanter, M.; Fink, M. Nordez, A.

'Ultrafast imaging of in vivo muscle contraction using ultrasound', *Applied Physics Letters* 89(18), 2006

Deffieux T, Gennisson JL, Tanter M, et al. IEEE TRANSACTIONS ON ULTRASONICS, 55 (10), Pages: 2177-2190, OCT 2008

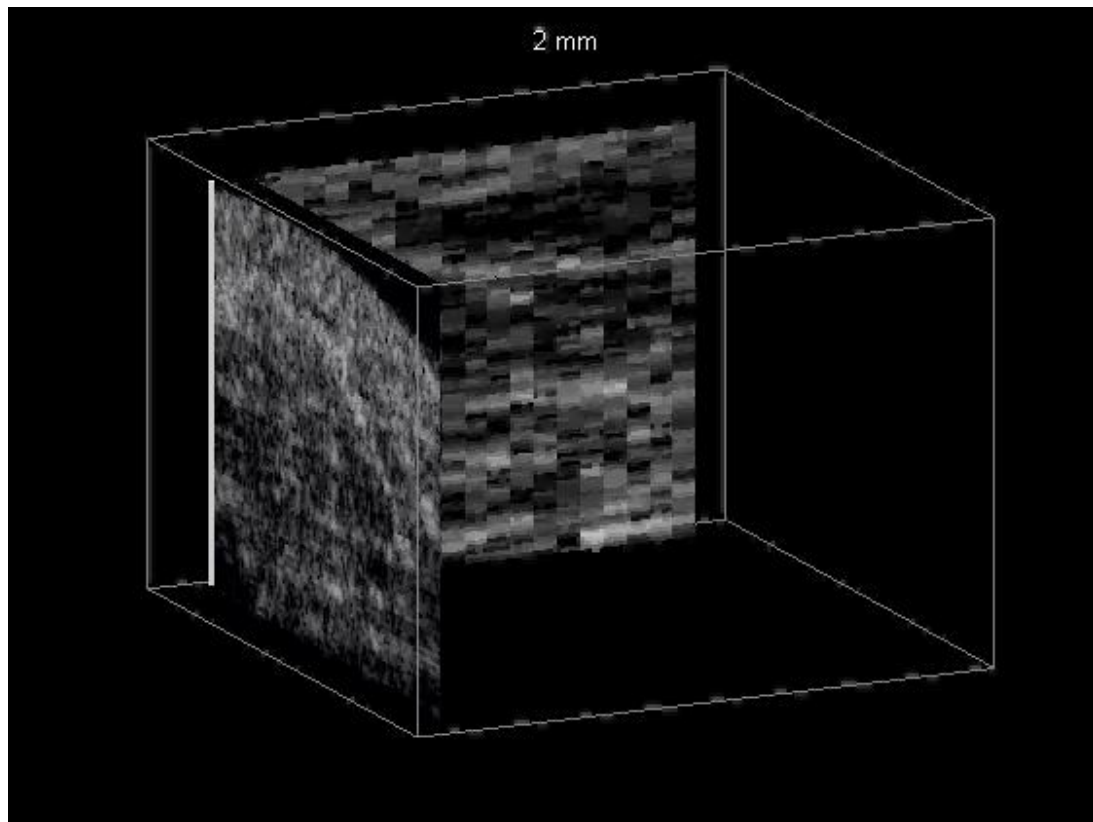
3D Ultrafast imaging of muscle electrostimulation

3D linear Scan with triggered acquisition/electrostimulation



22 translations with a 2 mm step

3D Scan volume : 35x35x44 mm³



Electromechanical waves in the heart

Myocardial rapid velocity distribution, Kanai, H; Koiwa, Y
ULTRASOUND IN MEDICINE AND BIOLOGY, 27(4), 481-498, 2001

First ultrasonic imaging
of mechanical Waves

Left ventricular transmural systolic function by high-sensitivity velocity measurement "phased-tracking method" across the septum in doxorubicin cardiomyopathy, Koiwa, Y; Kanai, H; et al.
ULTRASOUND IN MEDICINE AND BIOLOGY, 28, 11-12, 1395-1403, 2002

Electromechanical imaging of the myocardium at normal and pathological states
Pernot, M; Konofagou, IEEE International Ultrasonics Symposium Location: Rotterdam, 2005

First US imaging of
Electro- mechanical
Waves (ECG Gated)

ECG-gated, mechanical and electromechanical wave imaging of cardiovascular tissues in vivo
Pernot, Mathieu; Fujikura, Kana; Fung-Kee-Fung, Simon D.; et al., ULTRASOUND IN MEDICINE AND BIOLOGY, 33 (7), 1075-1085, 2007

Noninvasive electromechanical wave imaging and conduction velocity estimation in vivo
Konofagou, Elisa; Luo, Jianwen; Saluja, Deepak; et al. IEEE ULTRASONICS SYMPOSIUM, 969-972, 2007

Ultrafast imaging of the heart using circular wave synthetic imaging with phased arrays
Couade M., Hagege, A.-A. ; Fink, M. IEEE Ultrasonics Symposium, pp 515-518, 2009.

First ultrafast imaging
of single heartbeat

H. Kanai: "Propagation of Vibration Caused by Electrical Excitation in the Normal Human Heart"
Ultrasound in Medicine & Biology Vol. 35, No. 6, pp. 936-948 (June 2009)

Electromechanical Wave Imaging for Noninvasive Mapping of the 3D Electrical Activation Sequence in vivo, Provost, Jean; Lee, Wei-Ning; Fujikura, Kana; et al., CIRCULATION, 122(21), 2010

Physiologic Cardiovascular Strain and Intrinsic Wave Imaging, Konofagou, Elisa; Lee, Wei-Ning; Luo, Jianwen; et al., ANNUAL REVIEW OF BIOMEDICAL ENGINEERING, VOL 13 Book Series: Annual Review of Biomedical Engineering, 13,477-505, 2011

ECG Gated US imaging
Of Electromechanical
waves

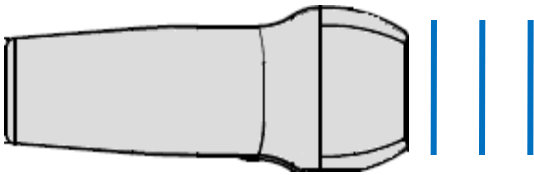
Imaging the electromechanical activity of the heart in vivo,
Provost, Jean; Lee, Wei-Ning; Fujikura, Kana; et al., P.N.A.S., 108(21), 2011

Single-heartbeat electromechanical wave imaging using temporally unequipped acquisition sequences,
Provost, Jean; Thiebaut, Stephane; Luo, Jianwen; et al., Phys. Med. Biol., 57(4), 2012

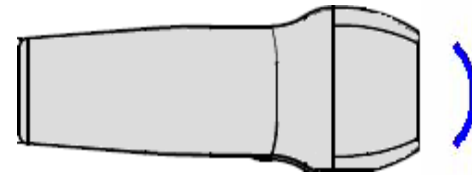
Ultrafast imaging of
single heartbeat

Use of circular waves to increase field of view

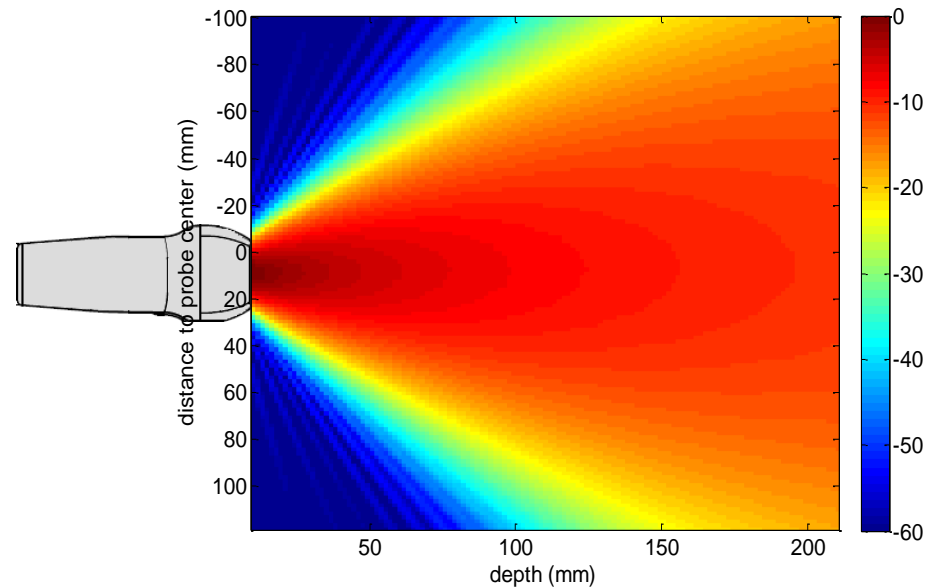
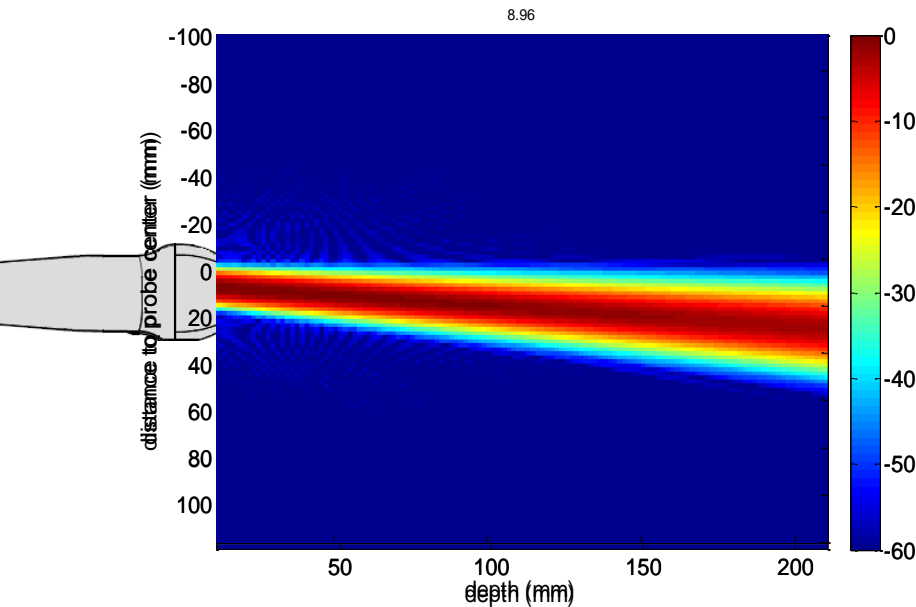
Flat transmit



- **Circular transmit**



Andresen et al. UFFC 2006 Symposium

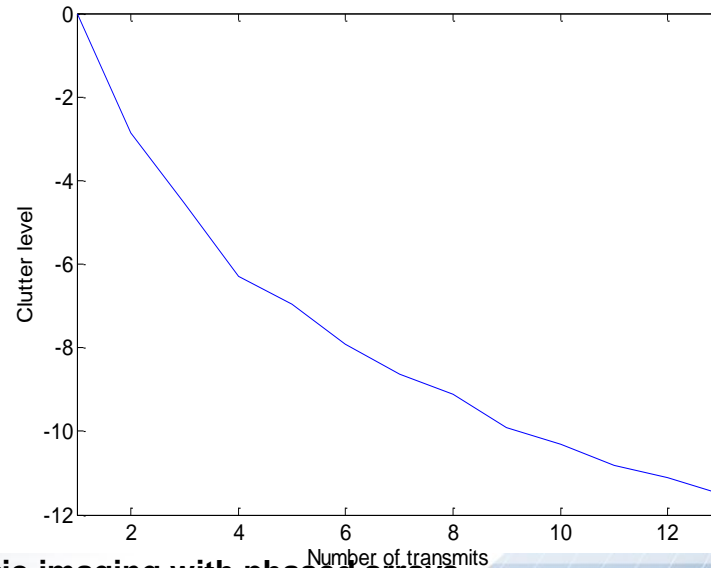
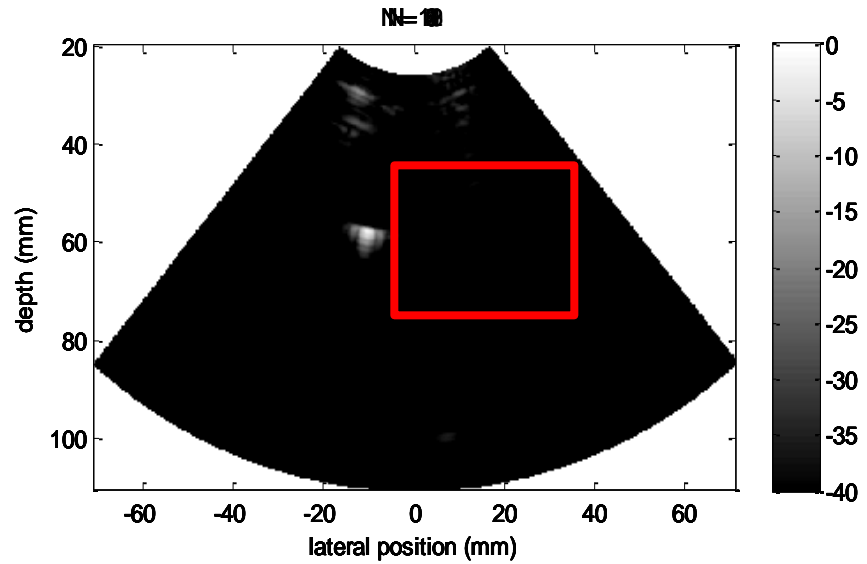
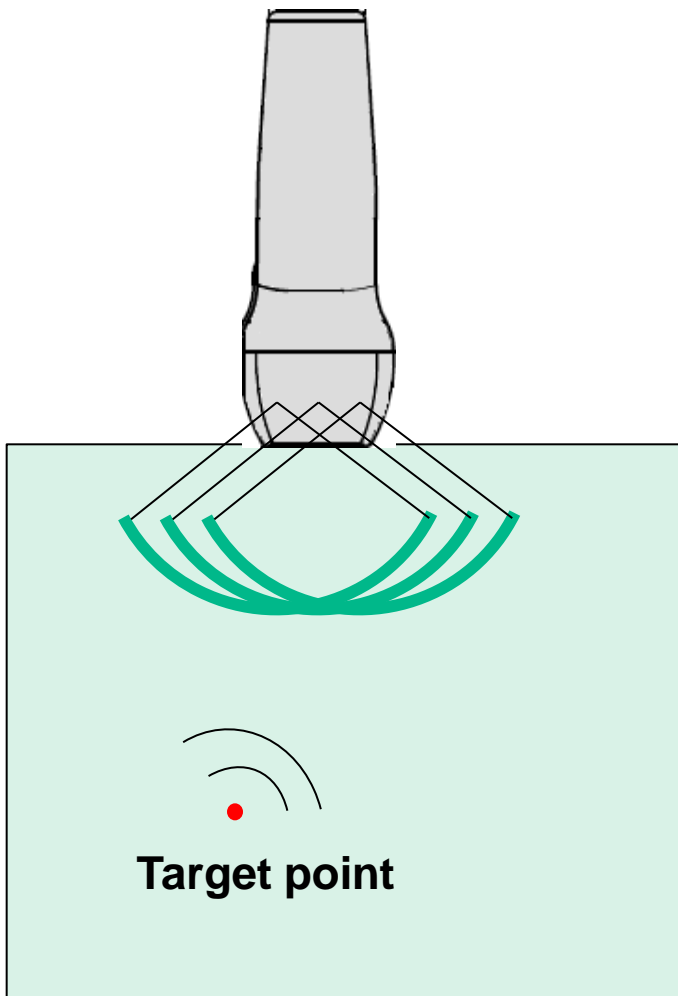


Ultrafast imaging of the heart using circular wave synthetic imaging with phased arrays

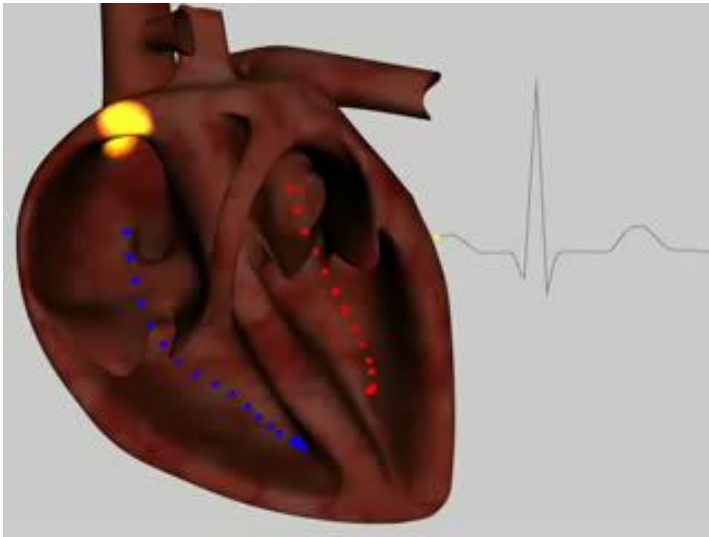
Couade M., Hagege, A.-A. ; Fink, M. IEEE Ultrasonics Symposium, pp 515-518, 2009.

Papadacci C., Pernot M., et al. IEEE IUS, Dresden, 2012

Synthetic imaging with circular waves



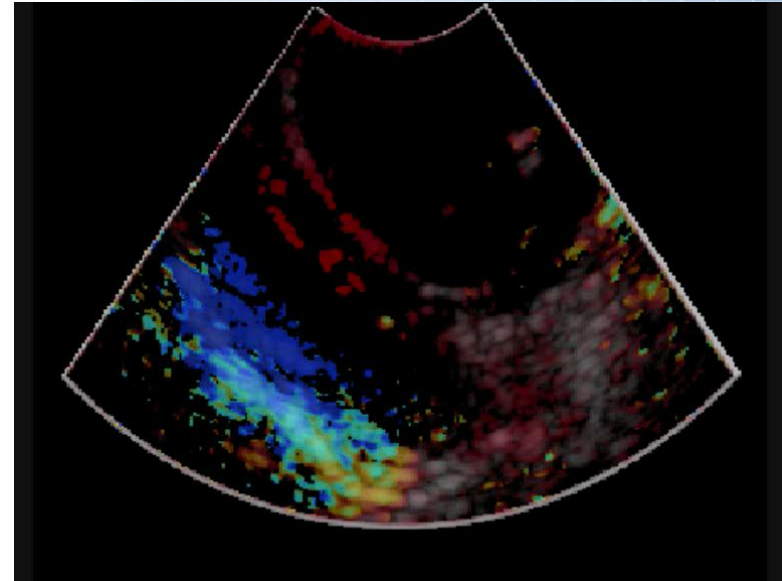
Ultrafast Imaging of Heart Transient Vibrations



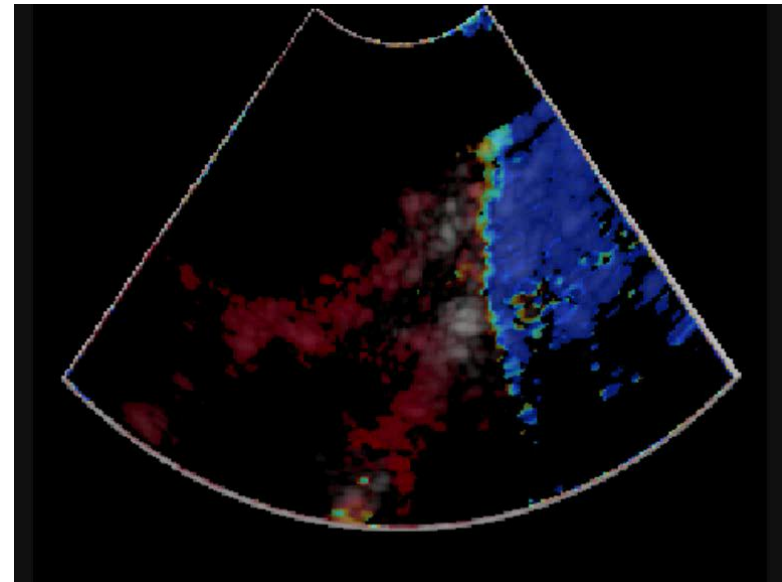
Hiroshi Kanai: "Propagation of Vibration Caused by Electrical Excitation in the Normal Human Heart" *Ultrasound in Medicine & Biology* Vol. 35, No. 6, pp. 936-948 (June 2009)

**Ultrafast Imaging of *in vivo* heart potentials
(Wide field of view during a single cardiac cycle)**

**in vivo Sheep experiments
Phased Array, $f_c = 3.3$ MHz
Field of View 8 cm
1600 frames per second**

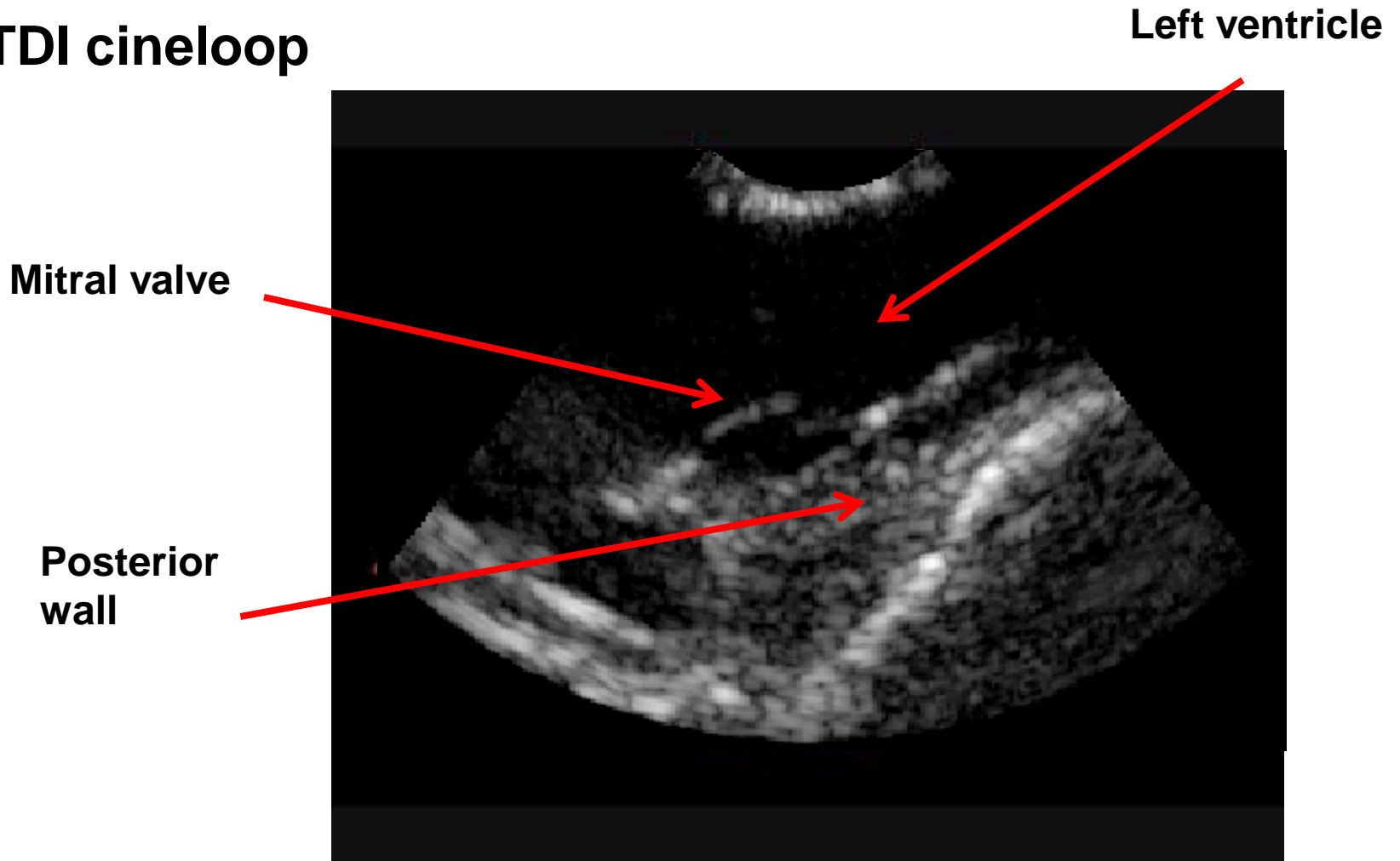


Short Axis



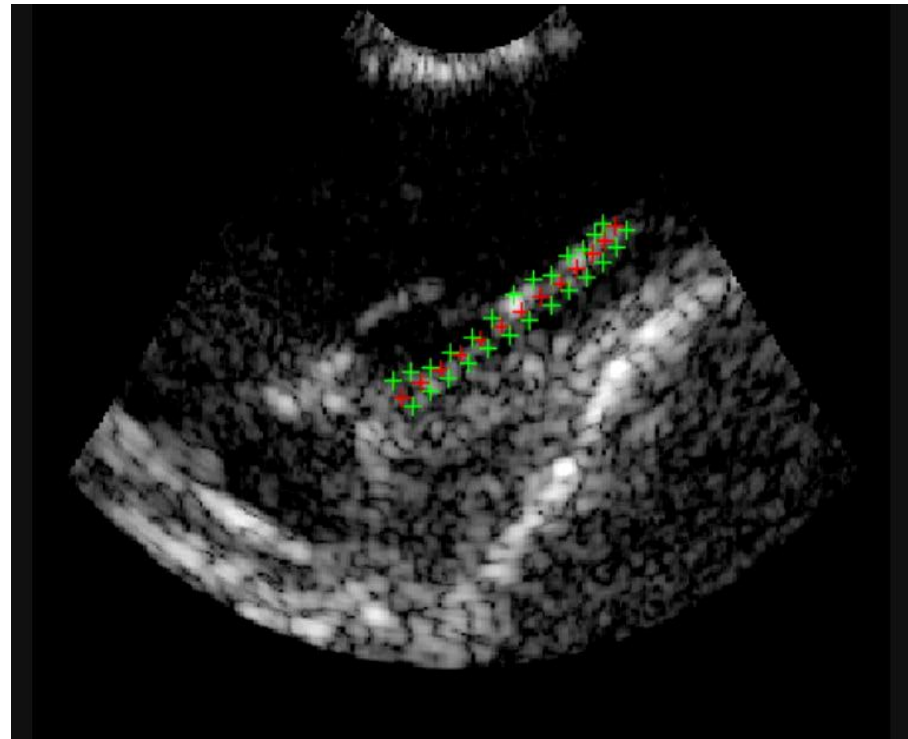
Long Axis

- **TDI cineloop**

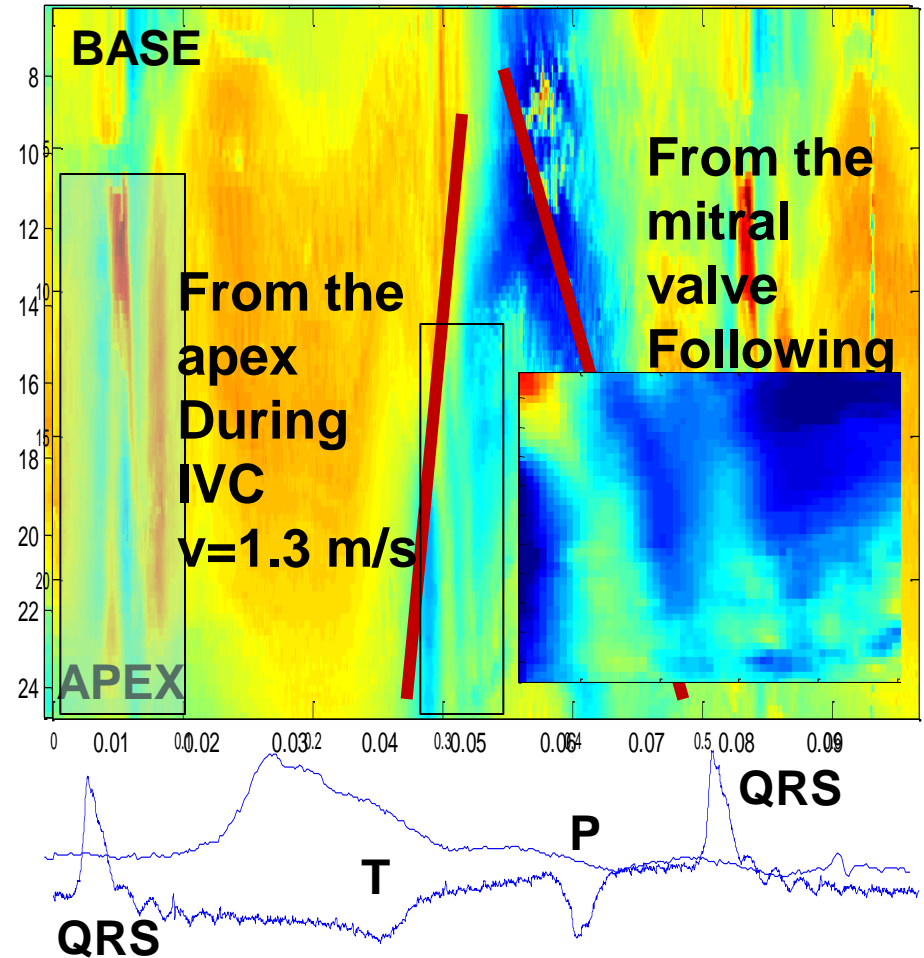


Wall tracking with 2D speckle tracking combined with TDI

Wall tracking

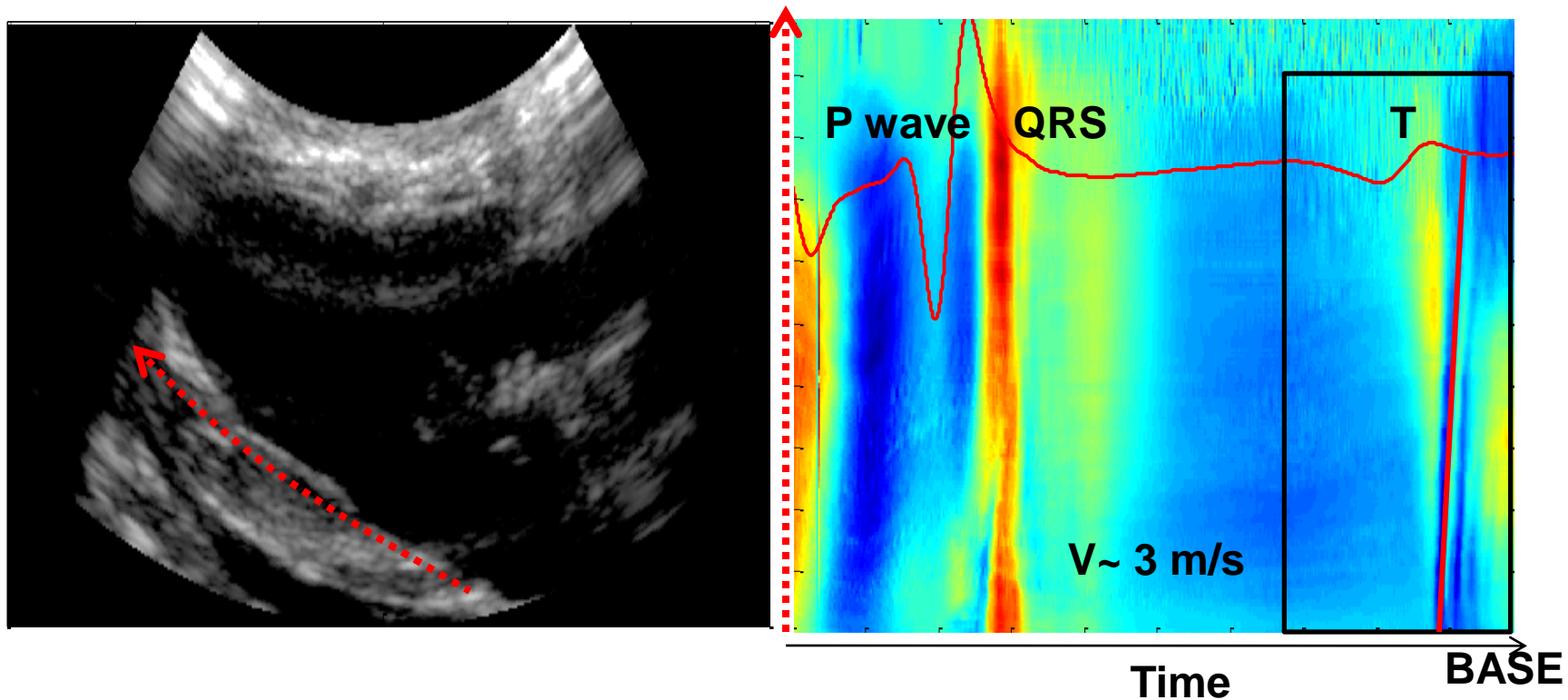


TDI signal along the tracked wall



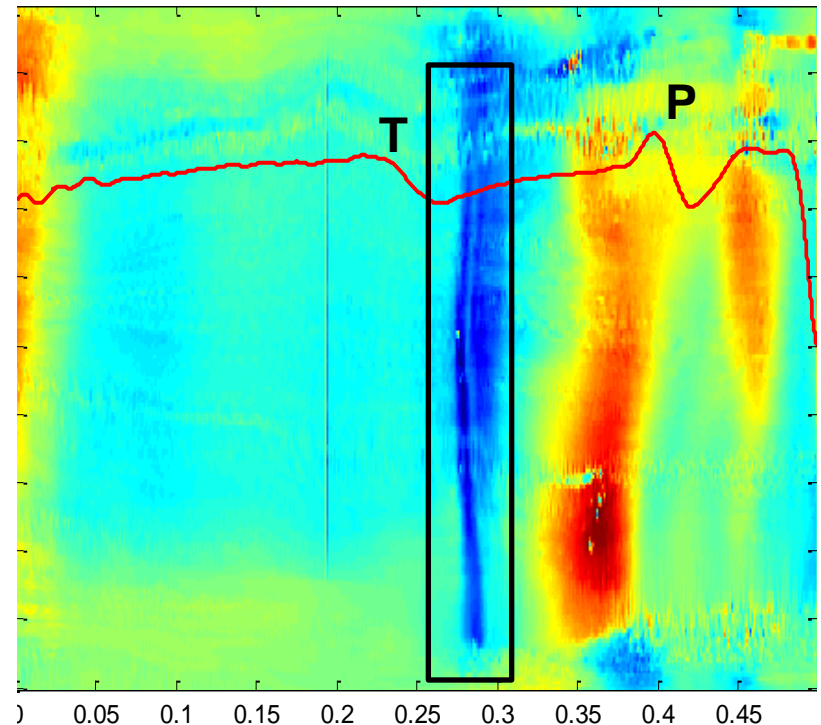
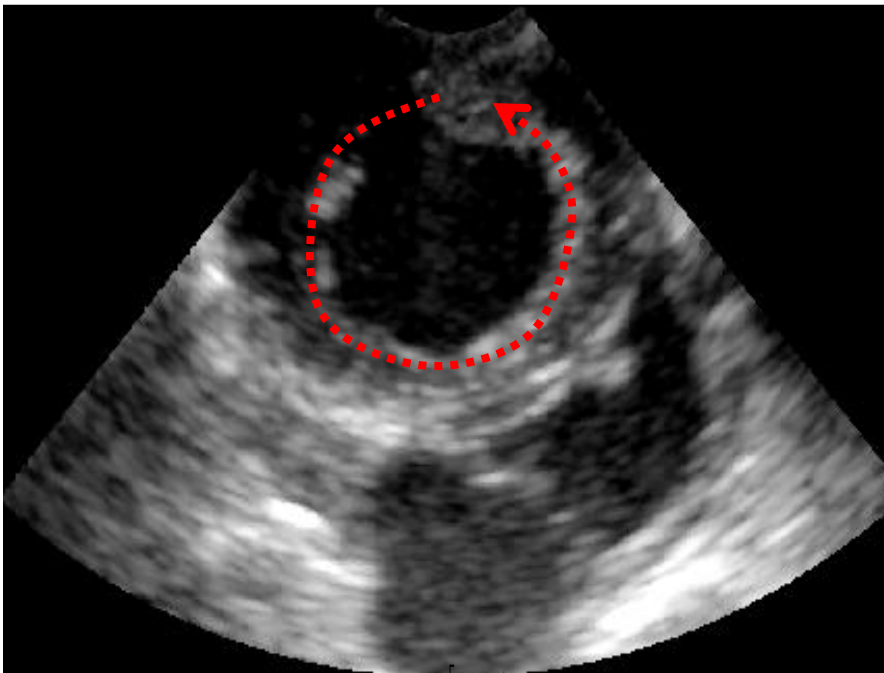
Aortic valve closure

- Long Axis View, signal along the septum
- FR = 1600 Hz, 800 frames



Aortic valve closure

- FR = 1600 Hz, 800 frames
- Propagation of the heart sound from the aortic valve (short axis view)

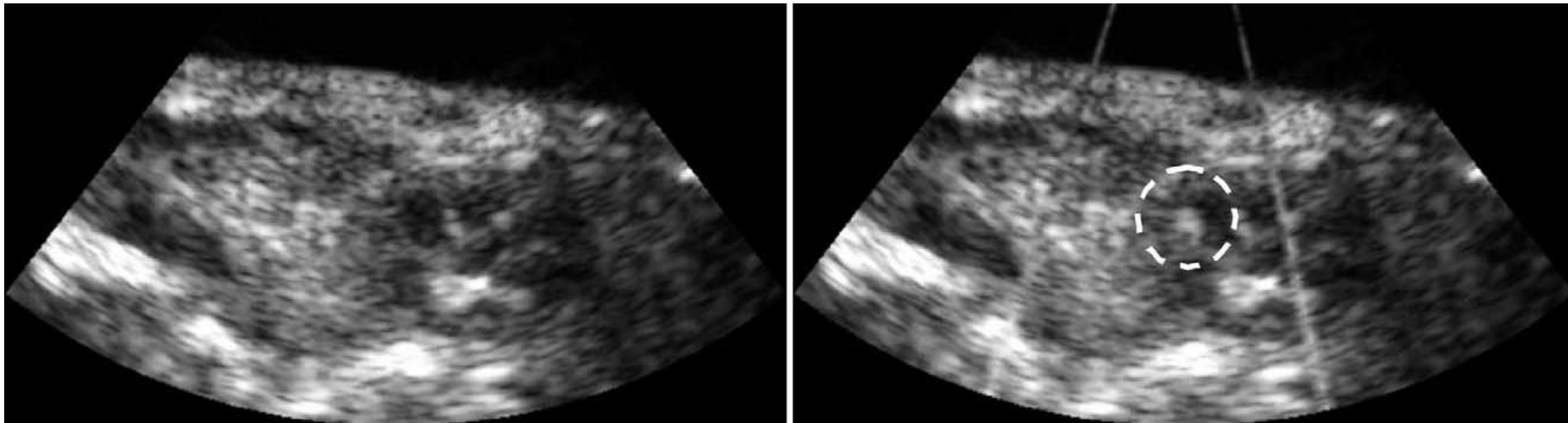


Ultrafast Imaging of Acoustic Cavitation

Active detection of cavitation events in HIFU treatments

> **Bubbles as scatterers**

Conventional B-mode imaging :hyperechogenic region in the treated region



Acoustically induced bubbles

Roberts, WW; Hall, TL; Ives, K; et al. Journal of Urology, 175 (2): 734-738, 2006

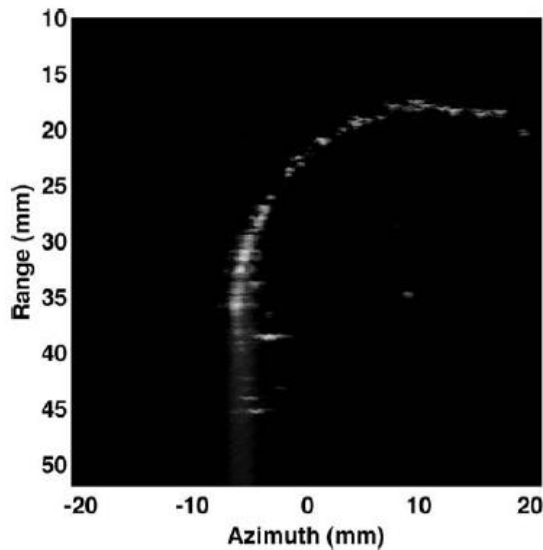
(+) localization of the bubbles

(-) only large number of bubbles can be detected (bubble clouds)

Passive detection and localization of cavitation events in HIFU

> Detection of the acoustic emission of the cavitation events

Passive imaging in saline solution (520-kHz CW),



B-scan

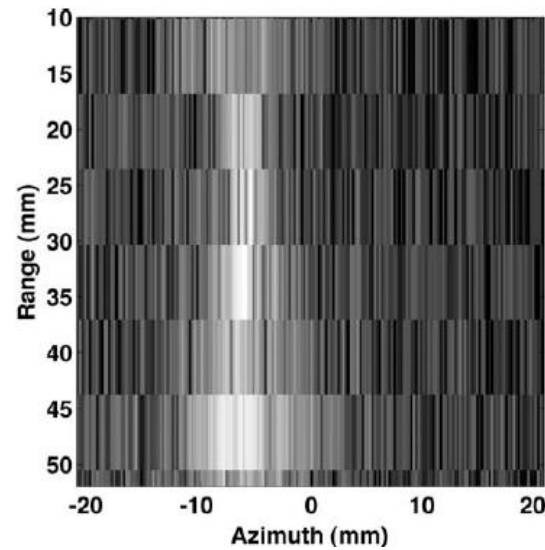
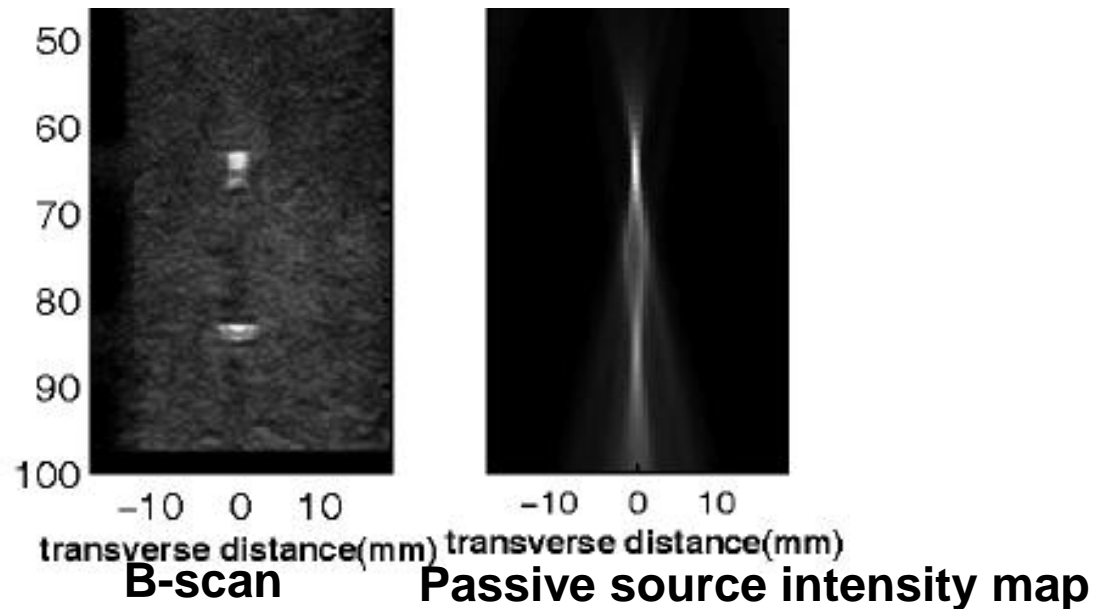


**Image formed from
passive recording**

Passive detection and localization of cavitation events in HIFU

> Detection of the acoustic emission of the cavitation events

Passive mapping of two disjoint cavitation regions produced by insonifying an agar phantom with two talc suspensions



Passive Spatial Mapping of Inertial Cavitation During HIFU Exposure

M. Gyongy and C. Coussios IEEE TRANSACTIONS ON BIOMEDICAL ENGINEERING, 2010

(+) localization of the cavitation events

(-) poor axial resolution

*Why to study acoustic cavitation
using ultrafast ultrasound imaging ?*

In Vivo mapping of single cavitation events generated with **high amplitude short** ultrasonic excitation of tissue

- For monitoring early stages of **therapeutic applications** :
 - cavitation-enhanced heating
 - histotripsy
 - > *location of the first bubbles leading to the initial cloud*
- For evaluating the nucleation threshold in vivo (investigate safety in **diagnostic applications**)

Impact of Ultrafast Imaging in cavitation detection imaging

Potential in Therapeutic Ultrasound (HIFU, Histotripsy, RF ablation)

Active Imaging with an ultrasonic array

- Not sensitive to single cavitation events (bubble clouds)

Improvement for single event detection : *subtraction of a reference image+ ultrafast imaging technique (9KHz imaging rate)*

Passive imaging with an ultrasonic array

Farny, CH; Holt, RG; Roy, RA, UMB , 35 (4): 603-615 APR 2009

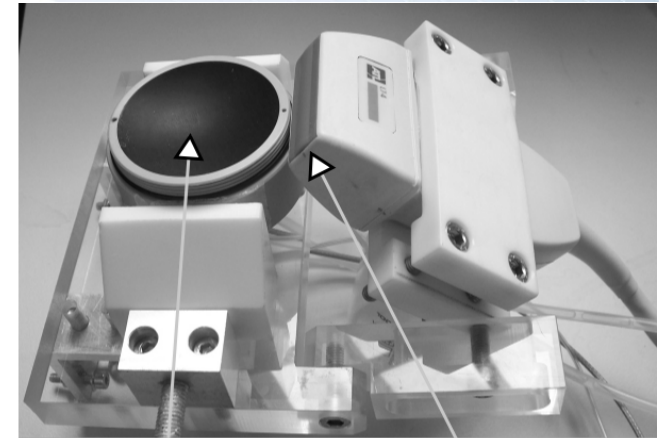
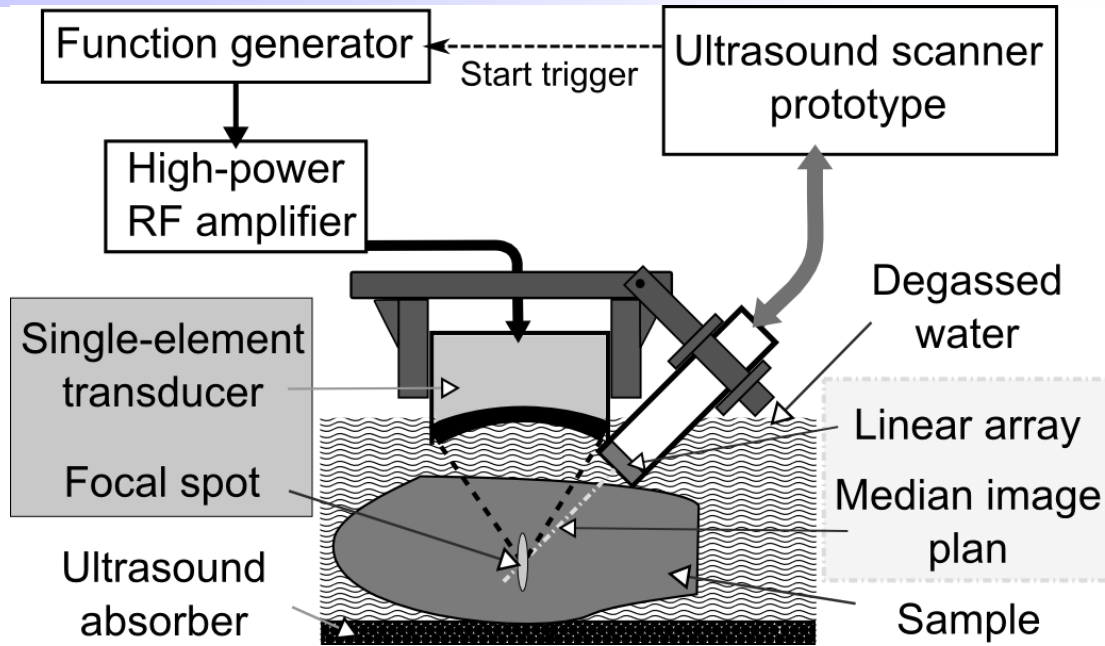
Salgaonkar, VA; Datta, S; Holland, CK; et al, JASA 126 (6): 3071-3083 DEC 2009

Gyongy, M; Coussios, CC IEEE TBME, 57 (1): 48-56 JAN 2010

> no time origin, localization submitted to diffraction limit (both in lateral and axial dimension)

Improvement for single event detection : *synchronized detection (no integration in time: improved axial resolution)*

Ultrafast Cavitation Imaging



Single-element transducer

Linear array

HIFU single element transducer (Imasonic, France)

660kHz central frequency

Focal distance: 45 mm, $f\#=1$

driven by: function generator +
300W or 5kW amplifier

Standard ultrasound imaging linear array (L7-4, Phillips)

128 transducers, pitch 0.3 mm,
bandwidth: 4-7MHz

driven by: SuperSonic prototype
programmable channels both in receive
(64 channels) and transmit (128
channels)

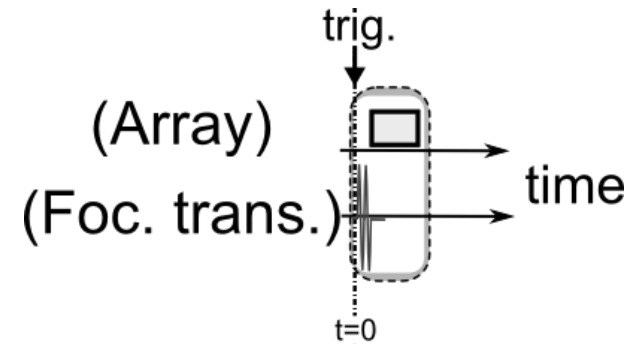
Passive Imaging In vitro experiment: gelatin phantom

Phantom : 5% (w/v) gelatin gel > free of scatterer

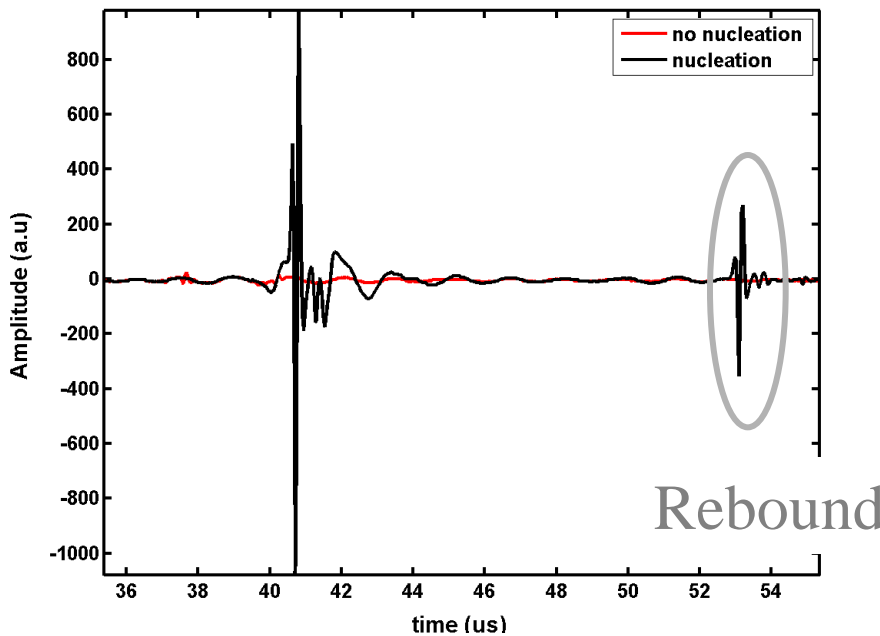
High amplitude excitation : 2cy. @ 660 kHz,
- 6.4 MPa negative peak

Synchronization with the emission:

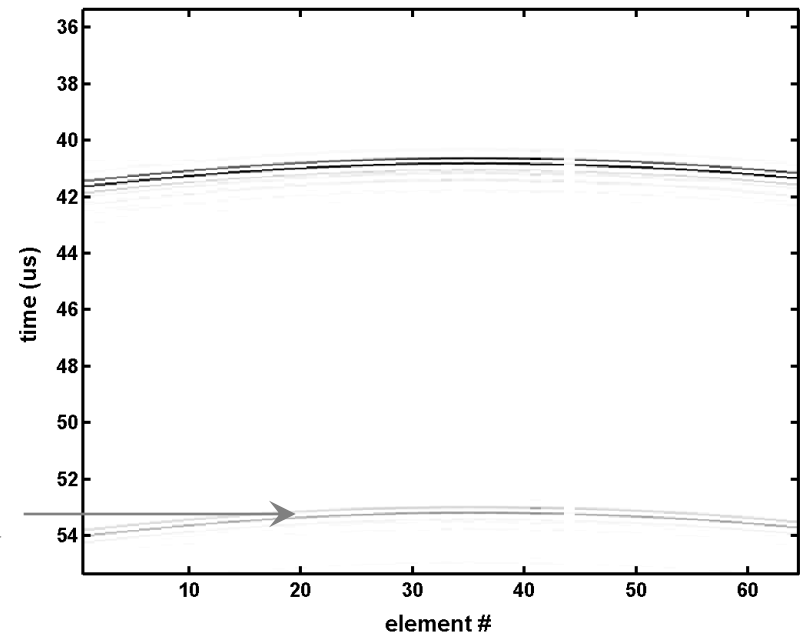
passive recording starts 22 μ s after the transmit



First case: one nucleated bubble

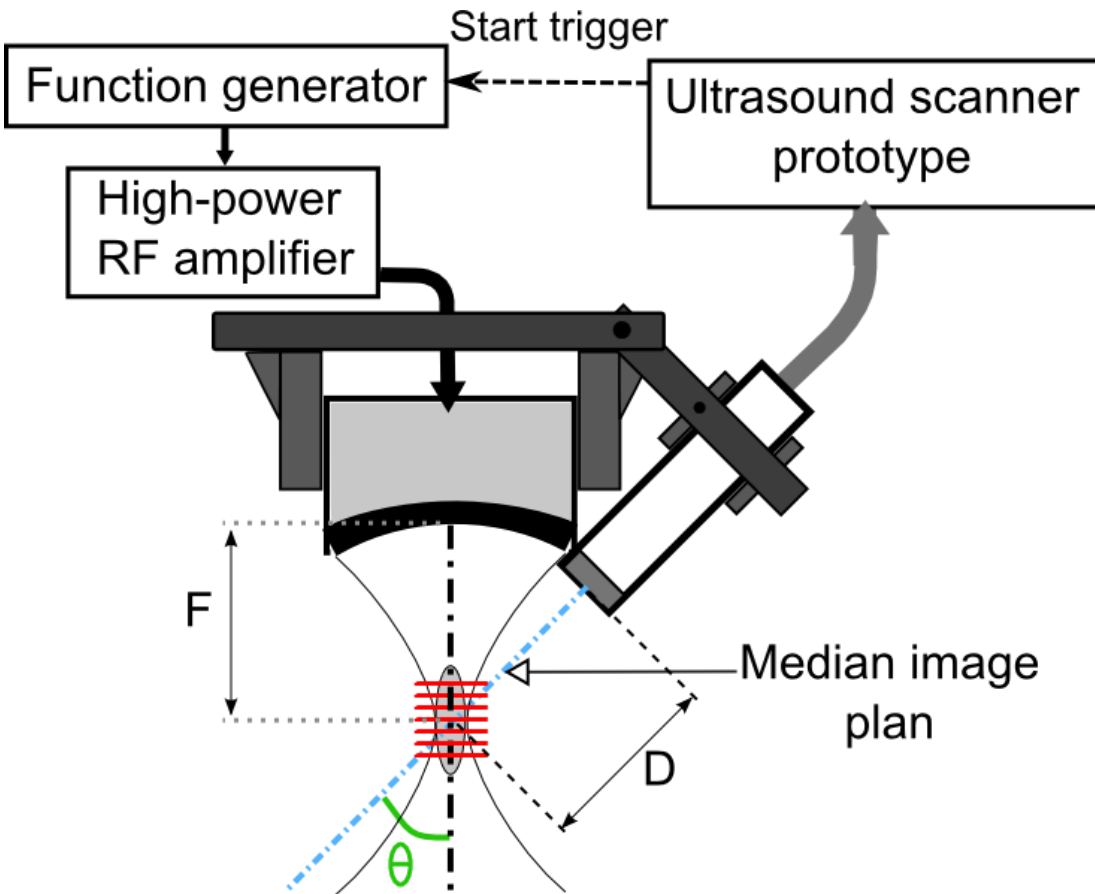


RF data on the element # 32



High frequency wave-front

Ultrafast Passive receive beamforming



Model for beamforming :

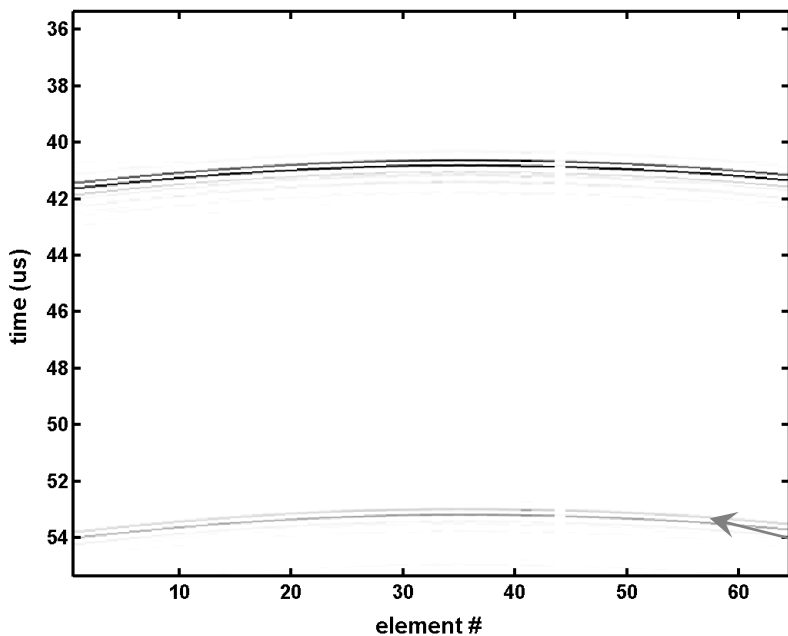
Geometry:

- ✓ D measured by imaging actively an hydrophone tip at focal point
- ✓ θ set equal to 45°

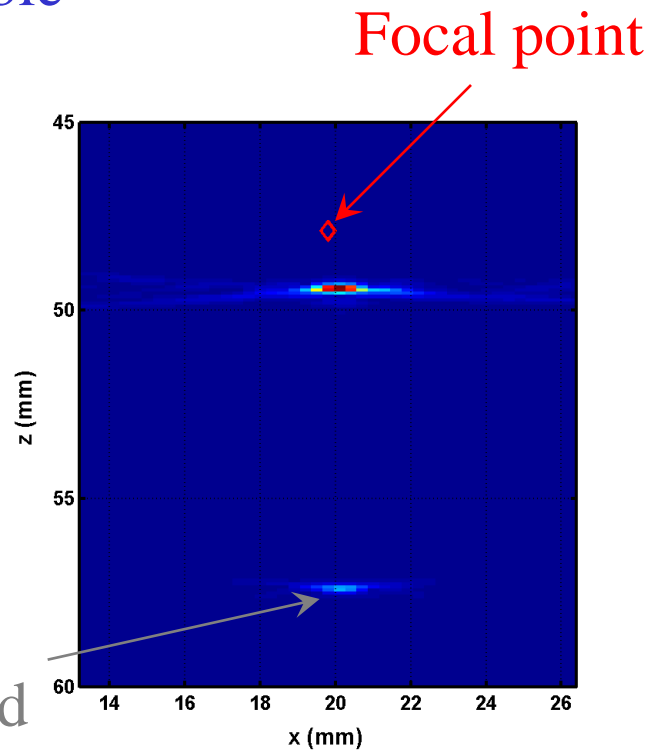
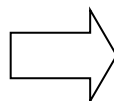
Wave propagation:

- ✓ plane wave-front in the focal spot of the single element
- ✓ immediate response of nuclei

First case: one nucleated bubble

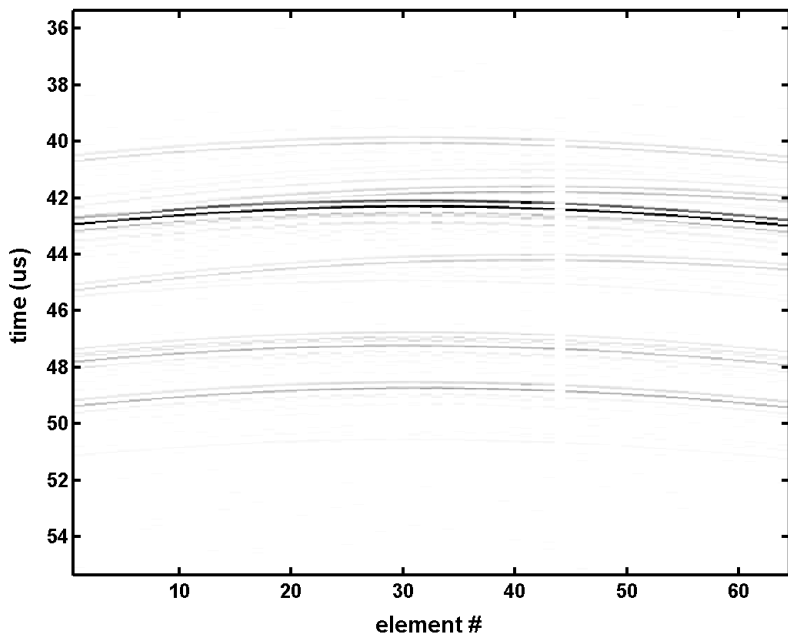


High frequency wave-front

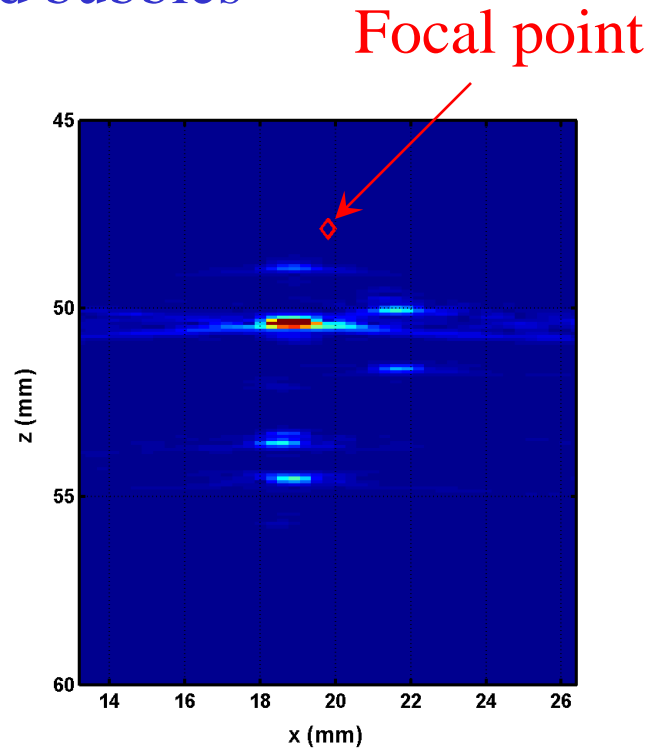
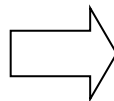


Beamformed RF data

Second case: several nucleated bubbles



High frequency wave-front



Beamformed RF data

Questions : How many bubbles ? How accurate are the locations ?

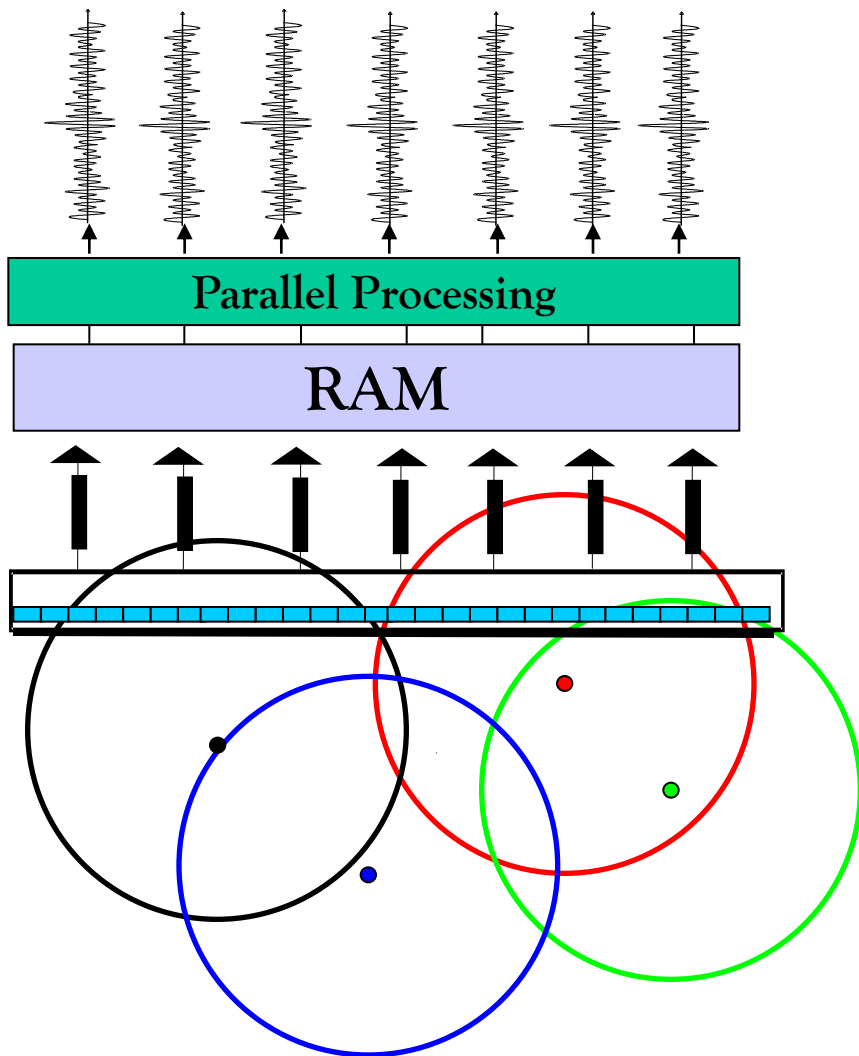
Standard Active Cavitation Detection (ACD)

B-mode imaging : maximum frame rate 100Hz > possible dissolution of bubble before the 1st image

Improvement for single event detection : *ultra-fast imaging up to 9kHz*

Standard Active Cavitation Detection (ACD)

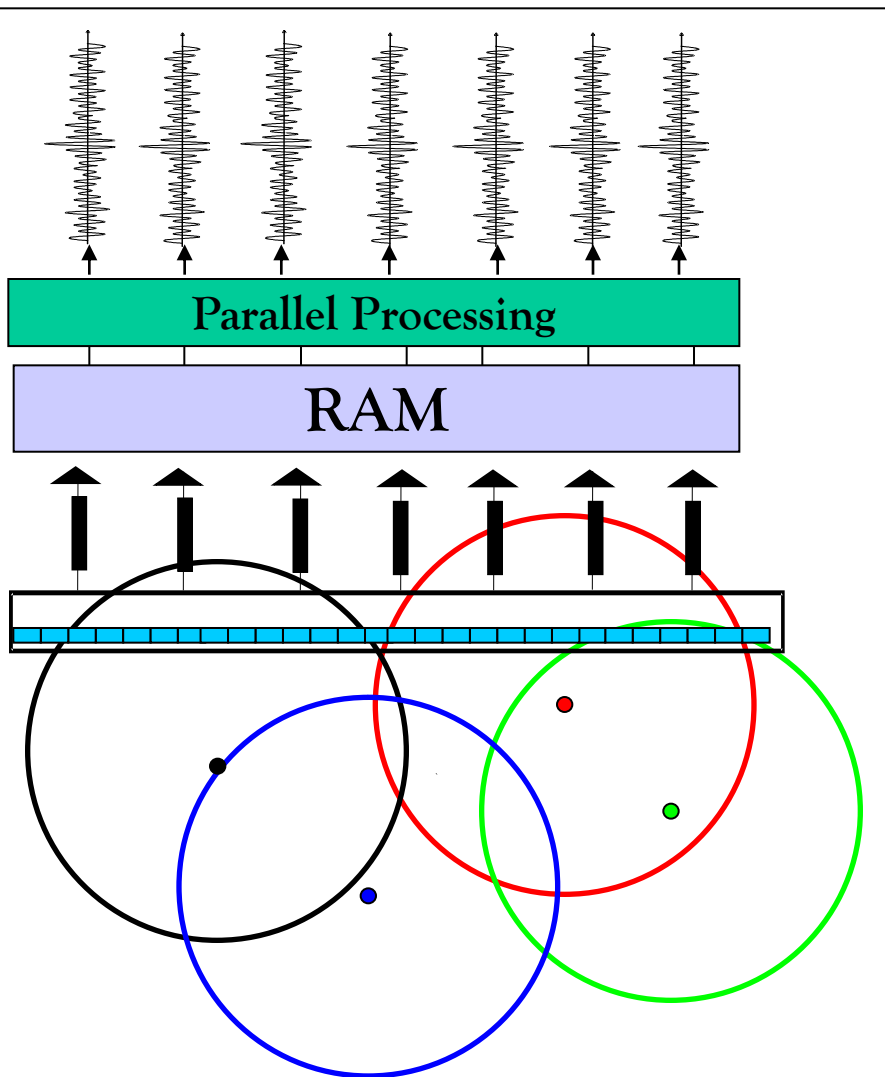
B-mode imaging : maximum frame rate 100Hz > possible dissolution of bubble before the 1st image



Improvement for single event detection :
ultra-fast imaging up to 9 kHz here

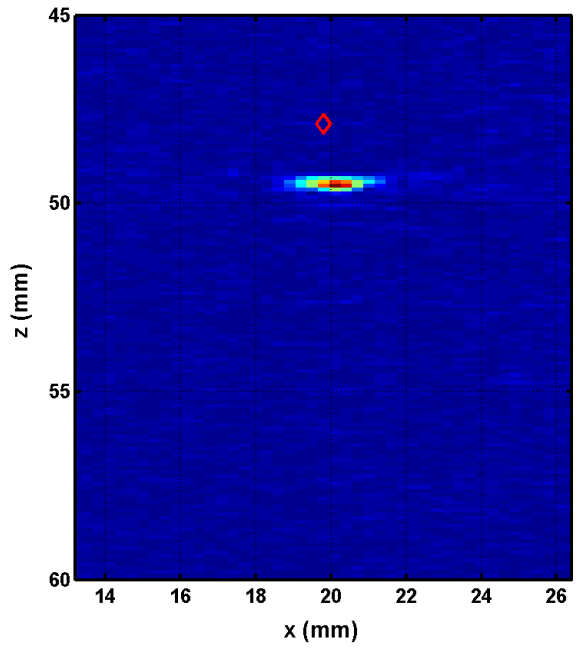
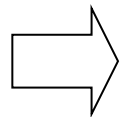
Standard Active Cavitation Detection (ACD)

B-mode imaging : maximum frame rate 100Hz > possible dissolution of bubble before the 1st image



Improvement for single event detection :
ultra-fast imaging up to 9 kHz here

Plane wave : 1 cy. , 6MHz

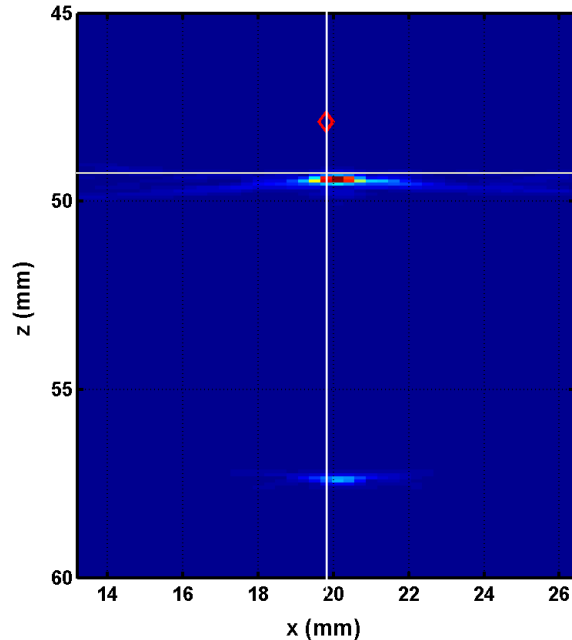


330 μ s after the high amplitude excitation

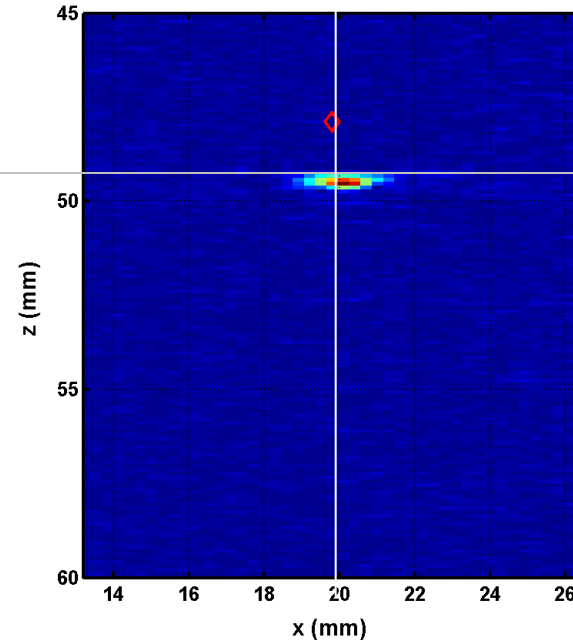
Comparison passive and active detection

First case : one nucleated bubble

Passive image



Active image



330 μ s after the high amplitude excitation

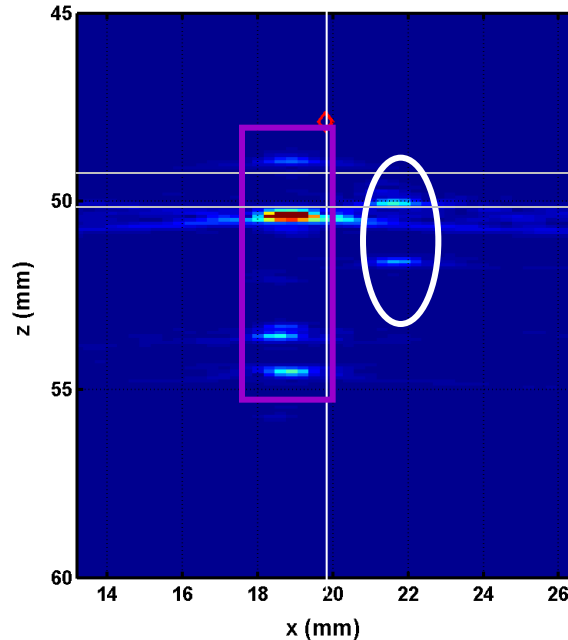


Good spatial agreement between active and passive imaging

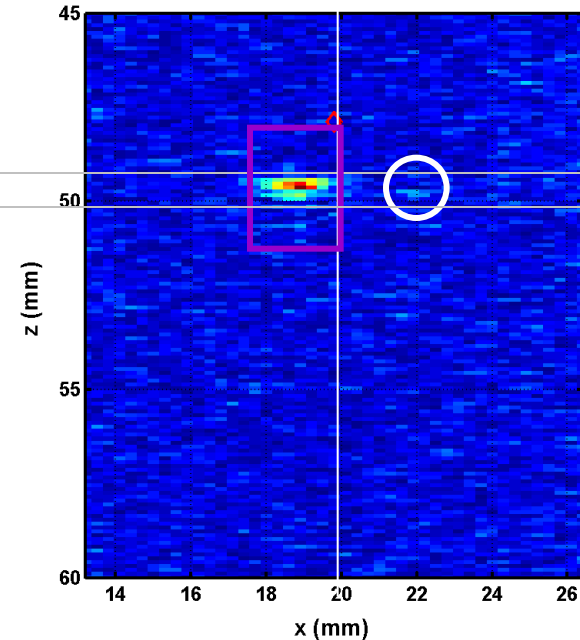
Comparison passive and active detection

Second case : several nucleated bubbles

Passive image



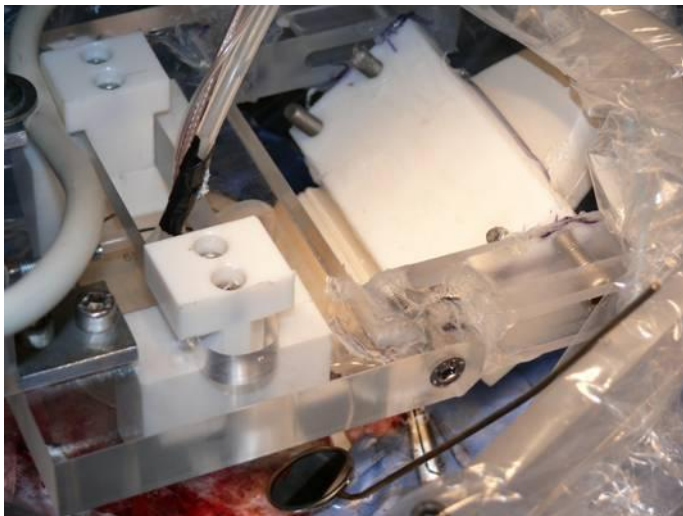
Active image



- ⇒ Only 2 bubbles in the active image and 1mm axial agreement :
- the assumptions for passive beamforming are not exact
 - complex passive signature of nucleating bubble (rebound, collapse...)

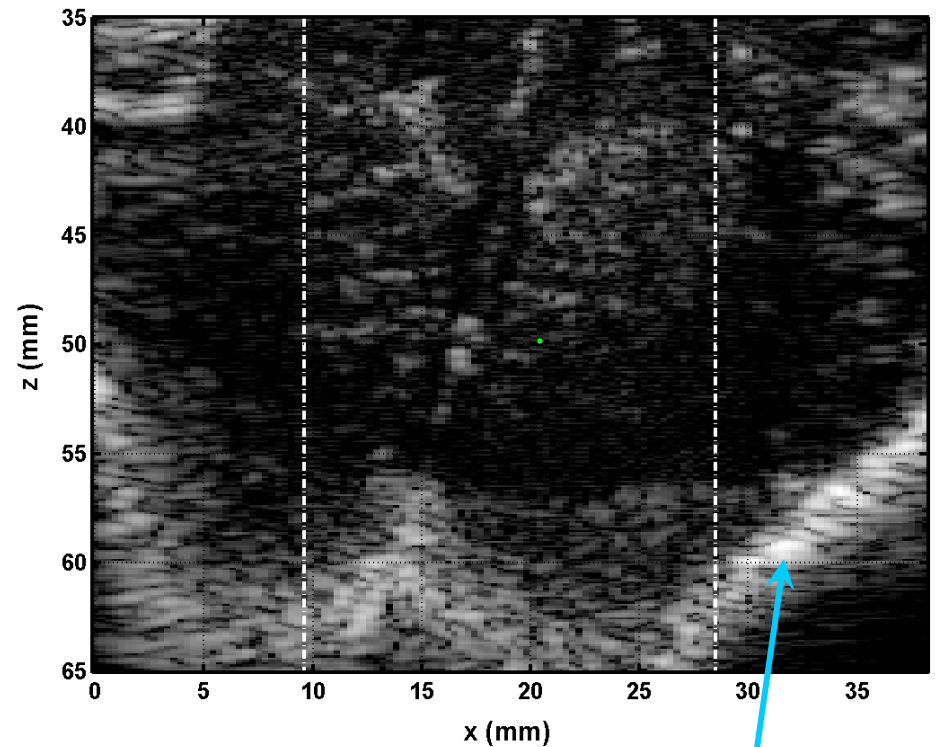
> Passive images more complex, but qualitative agreement

In vivo experiments on sheep brain



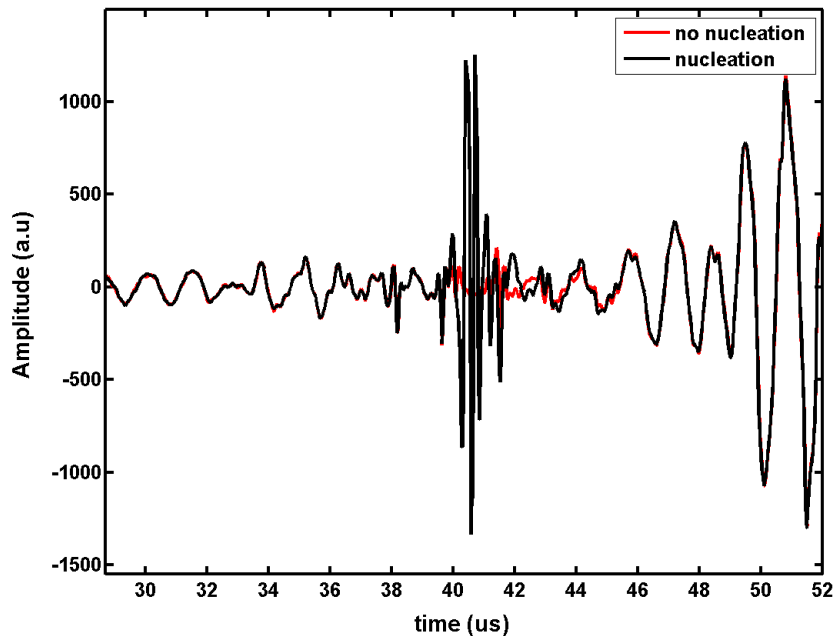
Ultrafast Imaging is key for *In vivo* determination of the acoustic cavitation threshold

Bmode image

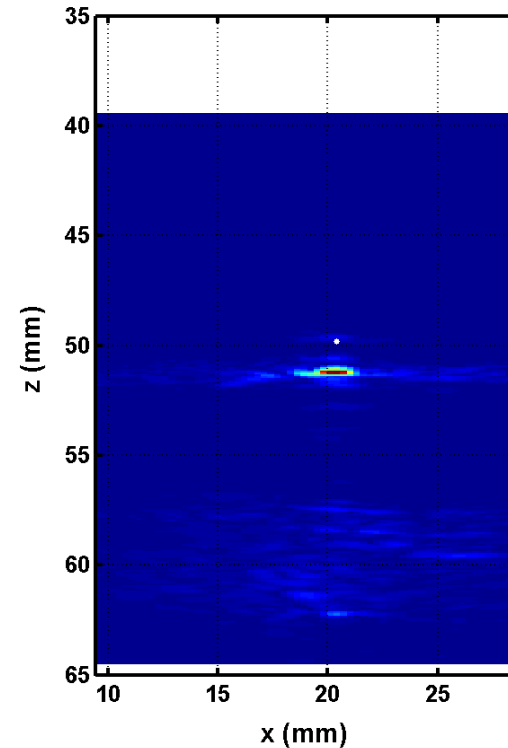


In vivo experiments on sheep brain

High amplitude excitation : 2cy. @ 660 kHz,
up to - 20 MPa negative peak pressure



RF data on the element # 32

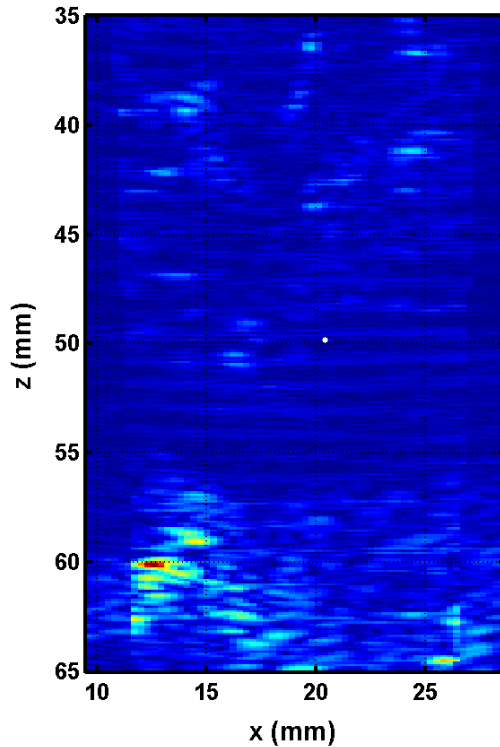


Passive image

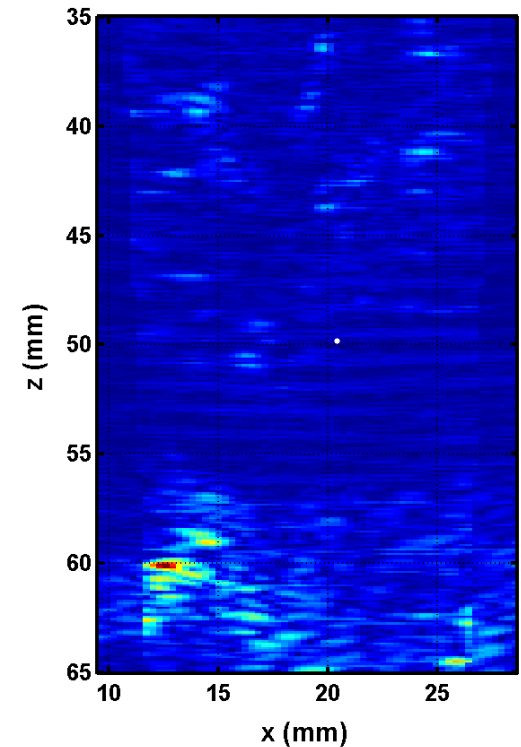
In vivo experiments on sheep brain

Active images 550 μ s after the high amplitude excitation

No nucleation

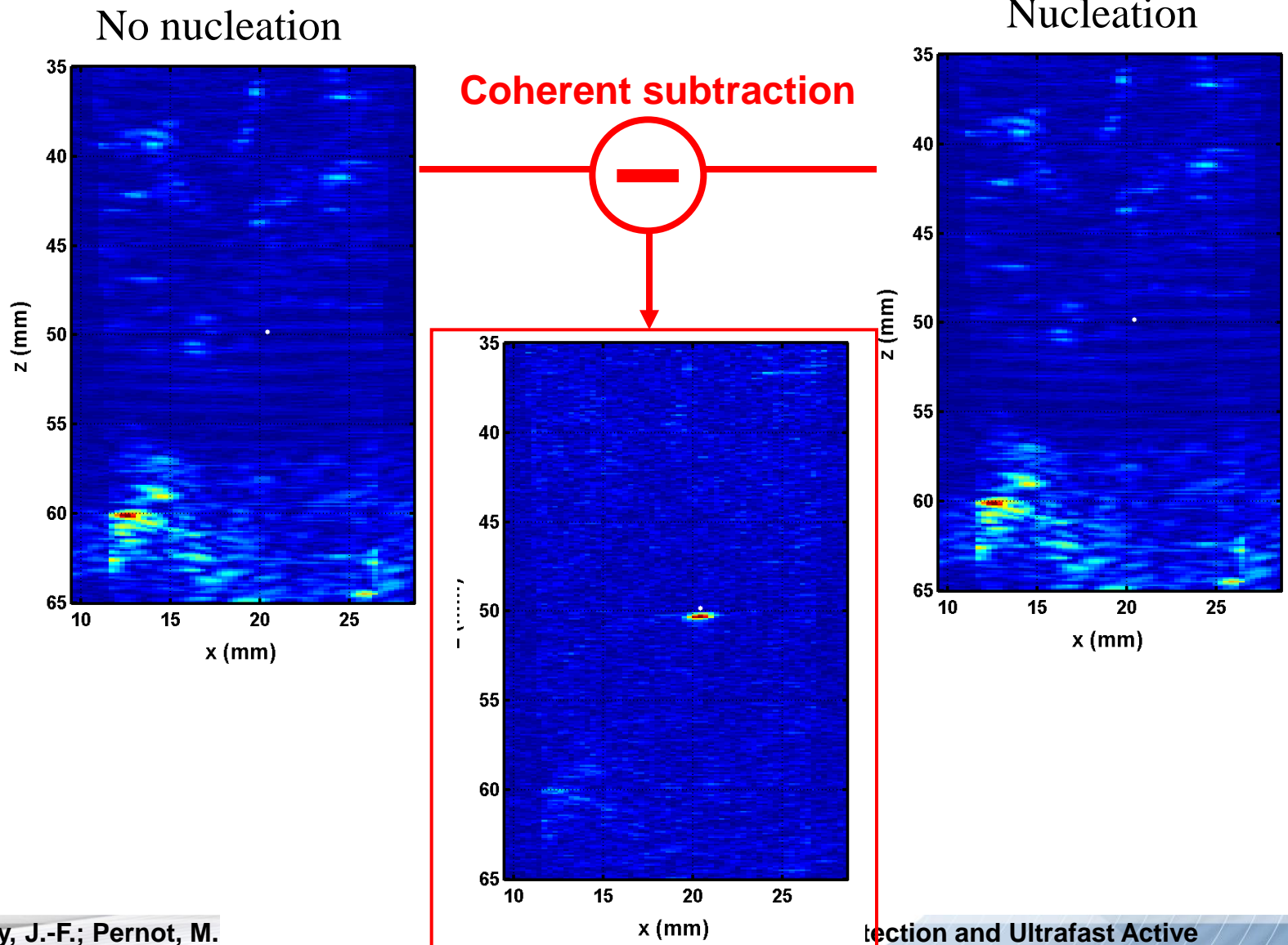


Nucleation



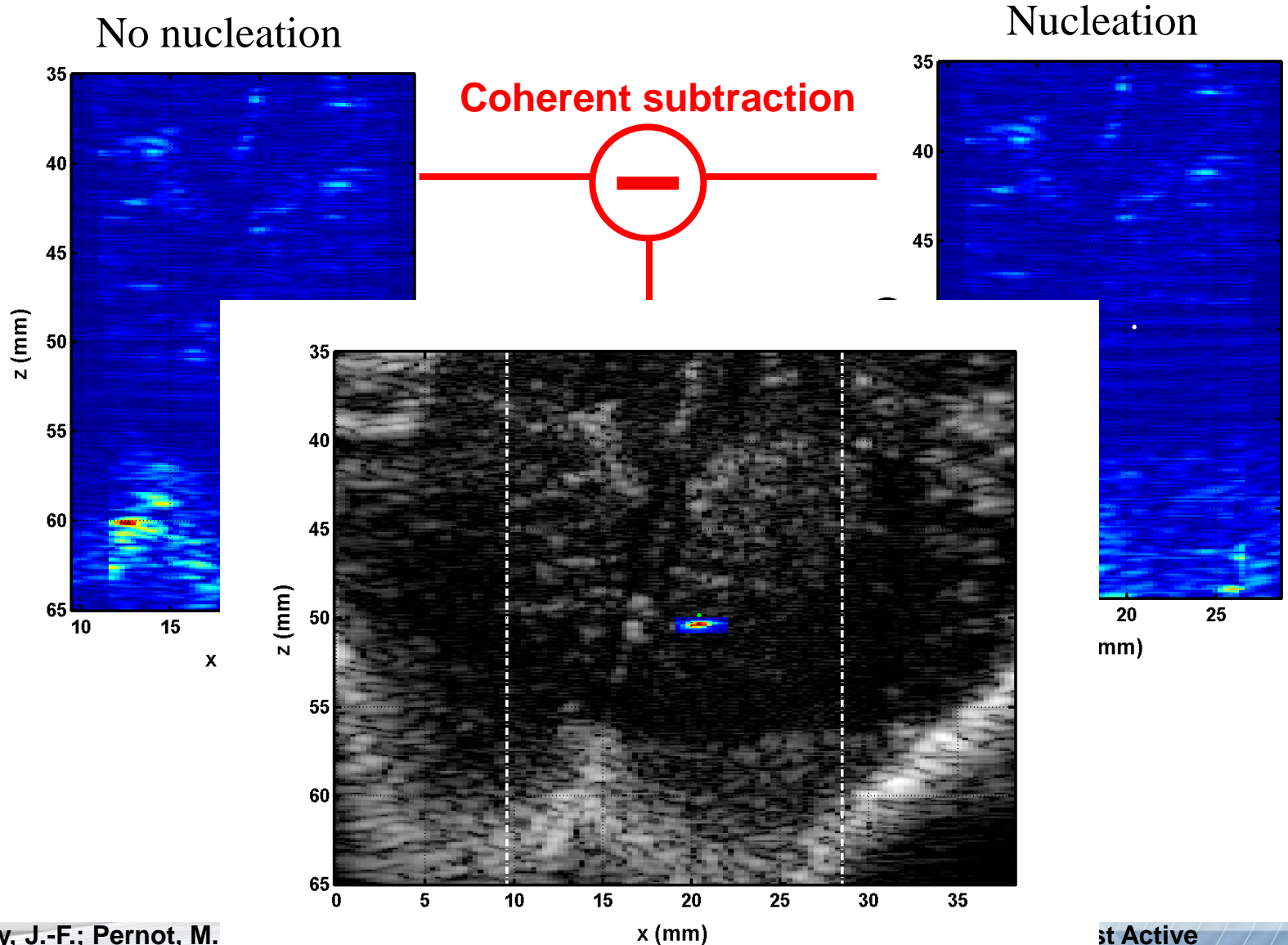
In vivo experiments on sheep brain

Active images 550 μ s after the high amplitude excitation



In vivo experiments on sheep brain

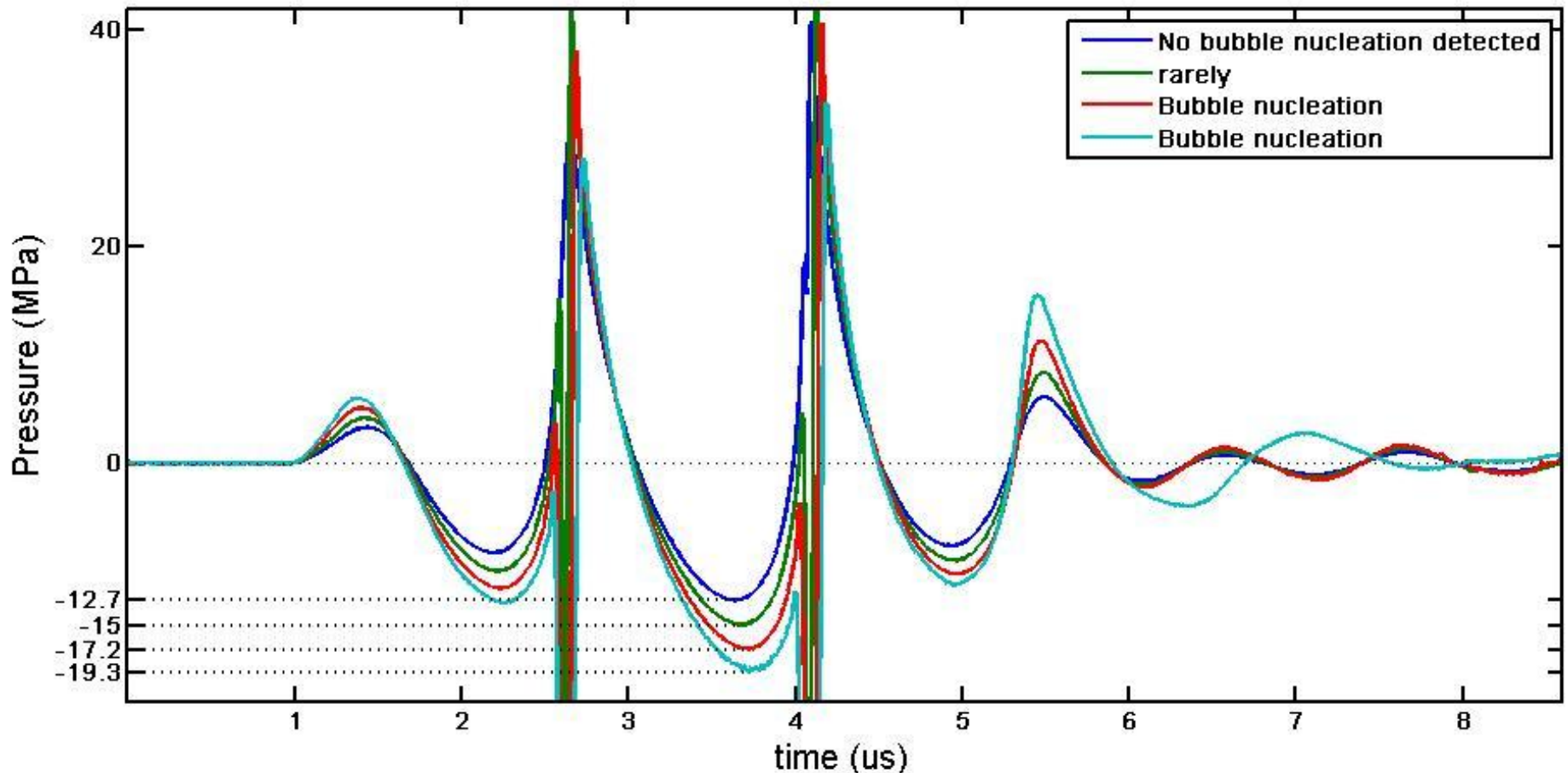
Active images 550 μ s after the high amplitude excitation



In vivo estimation of the cavitation threshold sheep brain

Statistical study on 4 sheeps: 100 different sonications in the brain
Experiments still ongoing

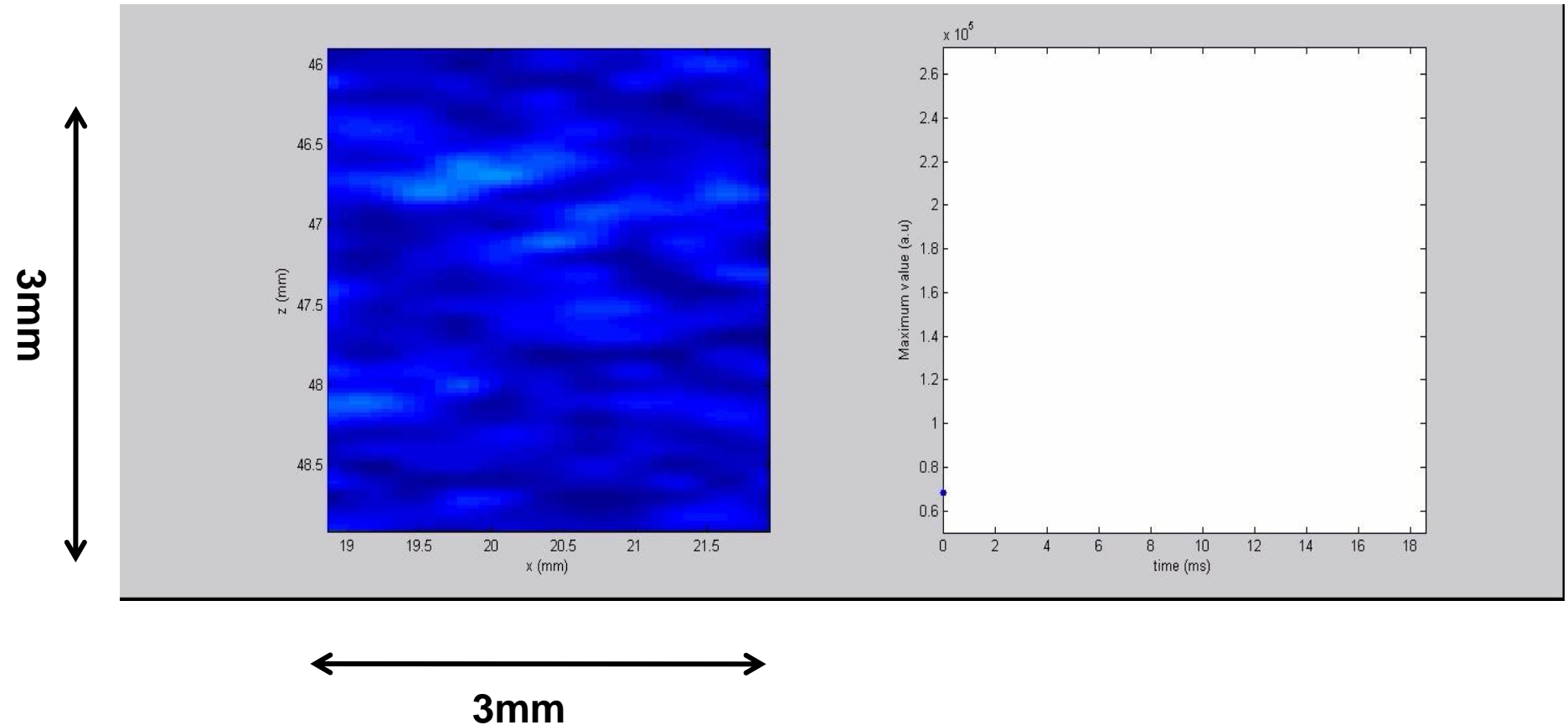
Cavitation threshold : between -15MPa and -17.2MPa (660kHz)



Calibration of the 600kHz transducer with an heterodyne interferometer

Ultrafast Imaging of bubble dynamics

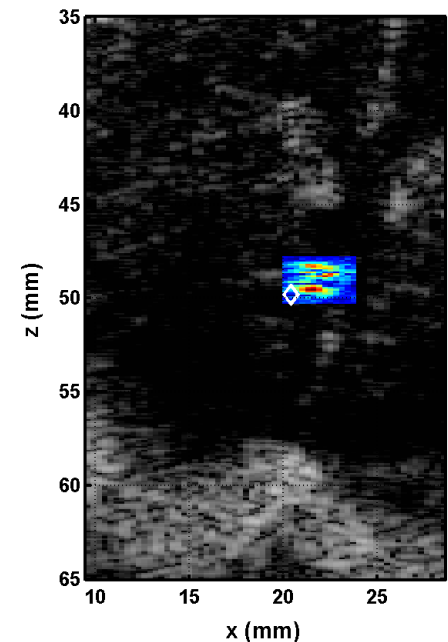
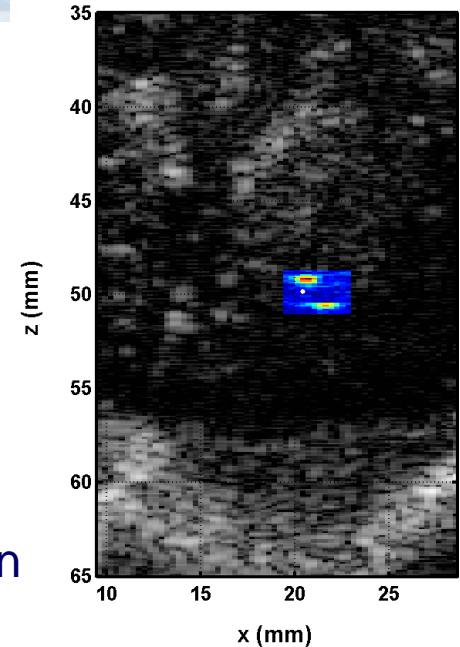
Use of the high imaging frame rate to follow the bubble dynamics



Summary - Ultrafast Imaging of Acoustic Cavitation

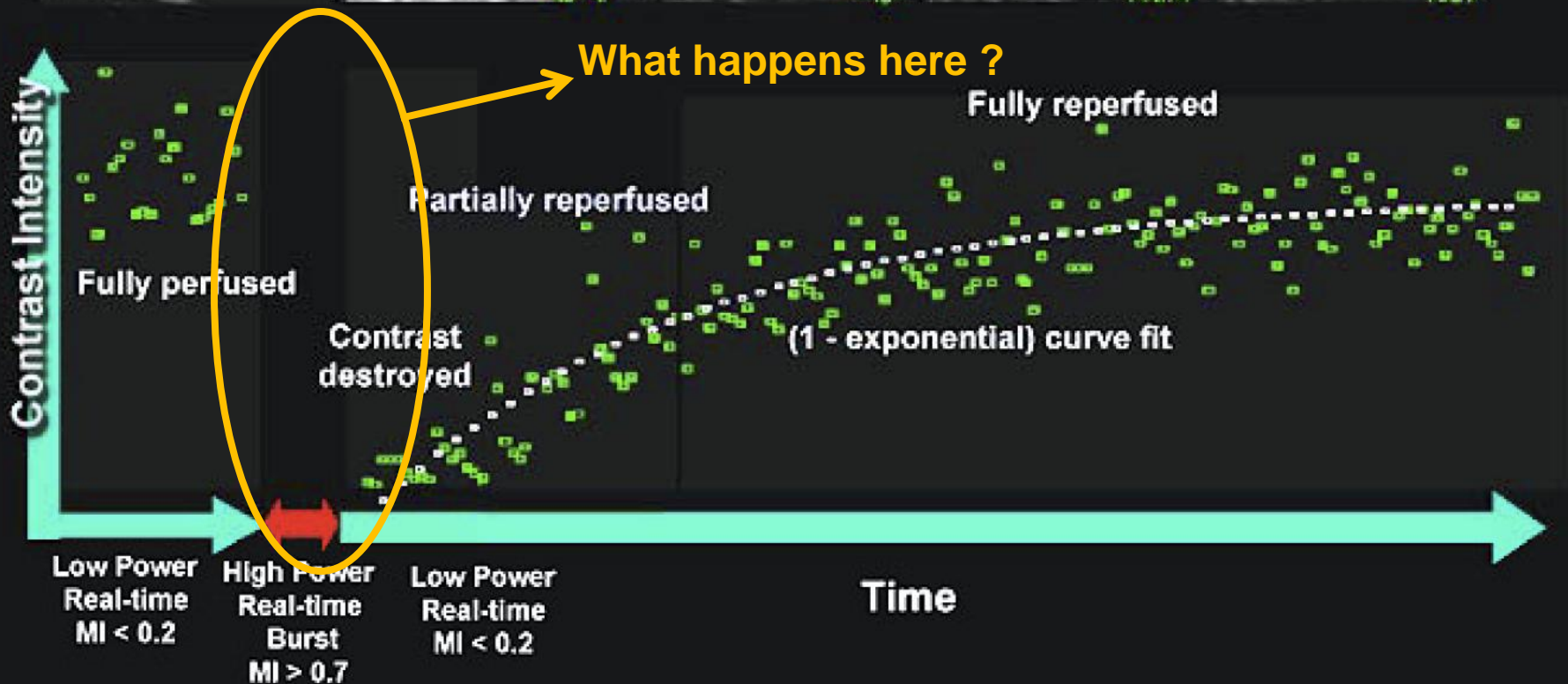
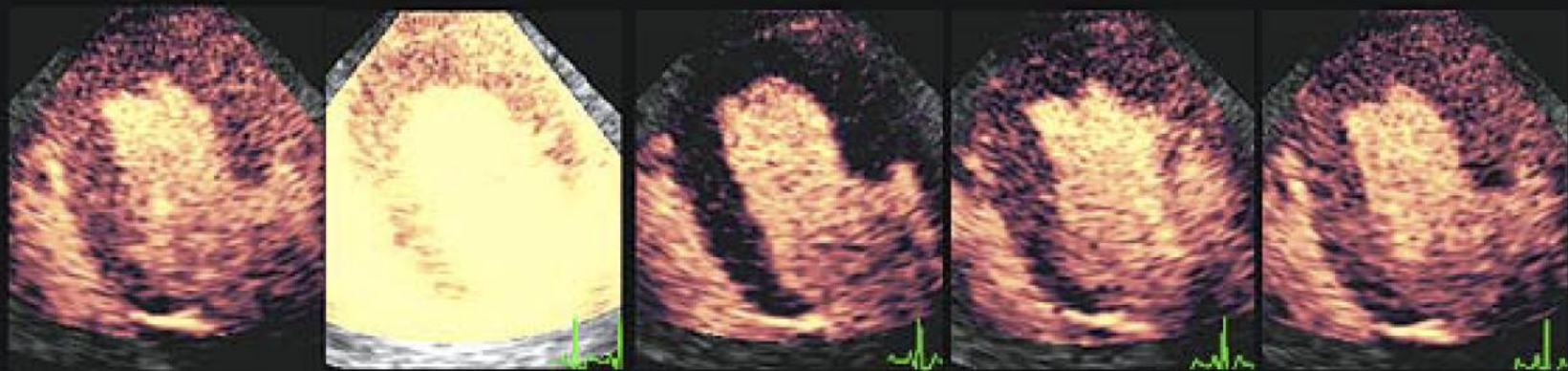
- Single bubble nucleation events were detected and localized passively and actively with an axial resolution of less than 0.3 mm
- Active detection is performed even in scattering media
- Small number of events can be separated
- Combination of passive and active detection provides information on the nucleation event and the induced bubbles
Cavitation threshold in vivo in brain: between -15MPa and -17.2MPa (660kHz) (still ongoing)
- Active high frame rate :
 - reach PRF in the kHz range > step by step formation a bubble cloud
 - follow the dynamics of the induced bubble

Applications : study the nuclei population *in vivo* and monitor the initiation phase of bubble cloud formation for cavitation therapies

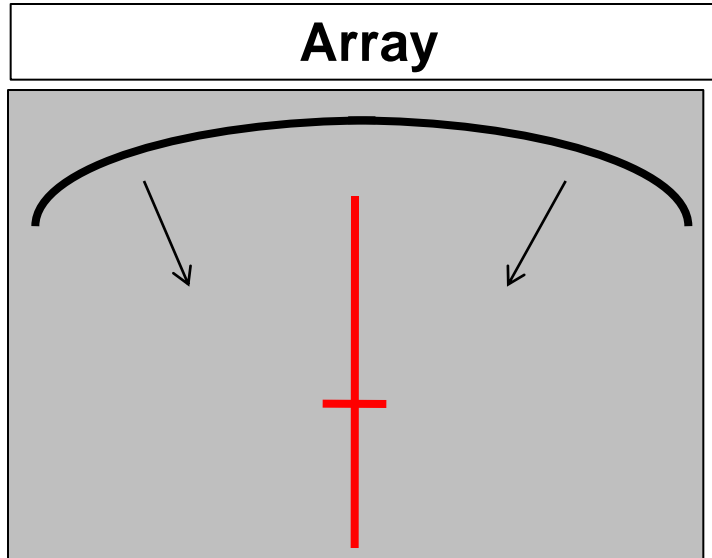


Ultrafast Imaging of contrast agents disruption

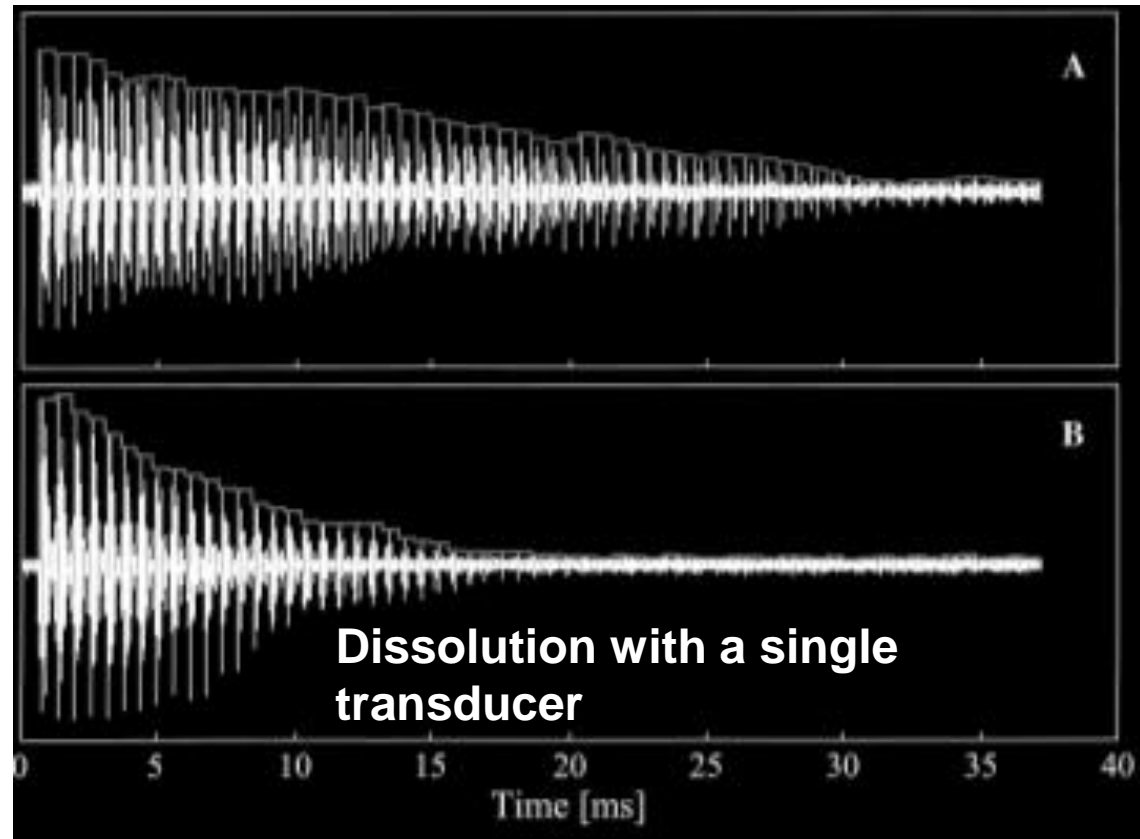
Context – Conventional ultrasonic imaging of Blood Perfusion



Conventional imaging is too slow to image dissolution over an entire image

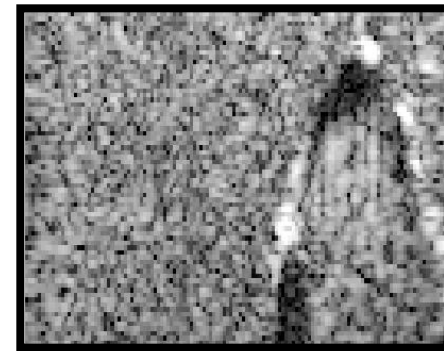
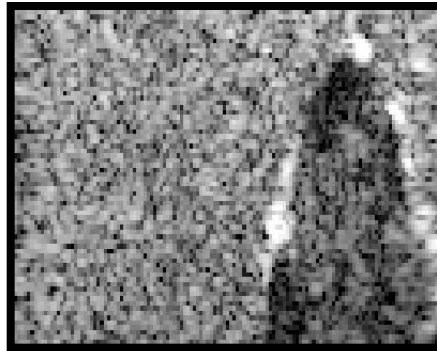
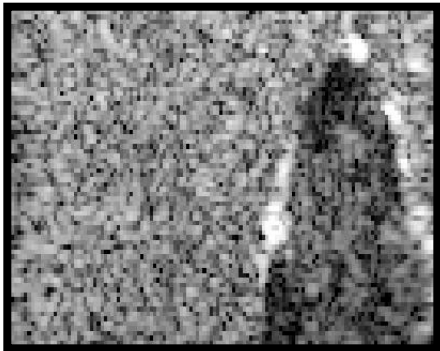
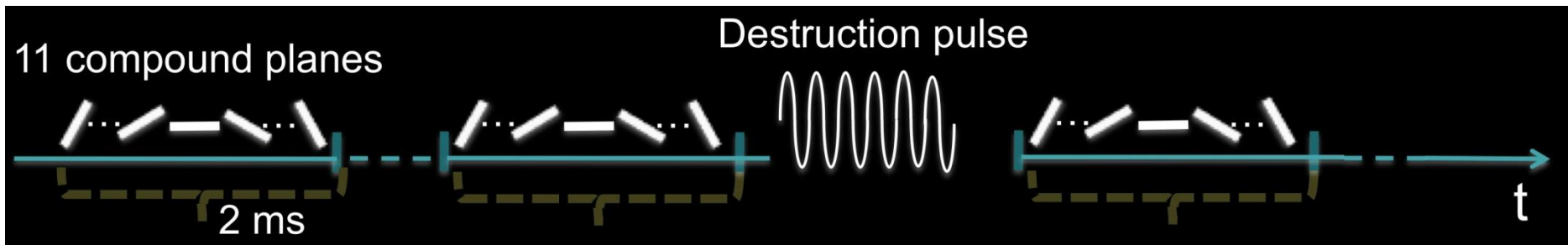


**Single Imaging line
At ultrafast frame rate**

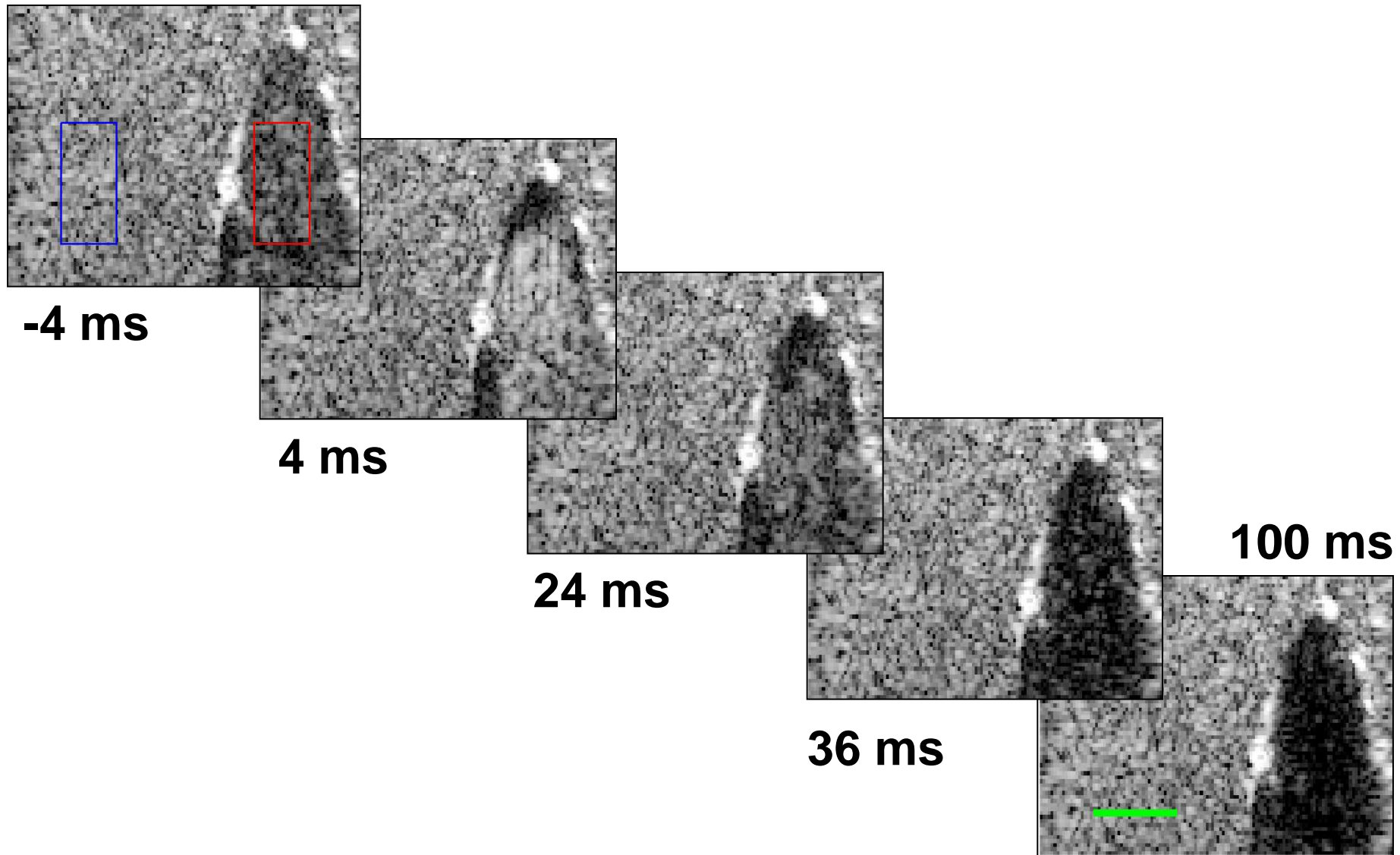


Plane wave compounding increases SNR and reduces frame rate to 500 Hz

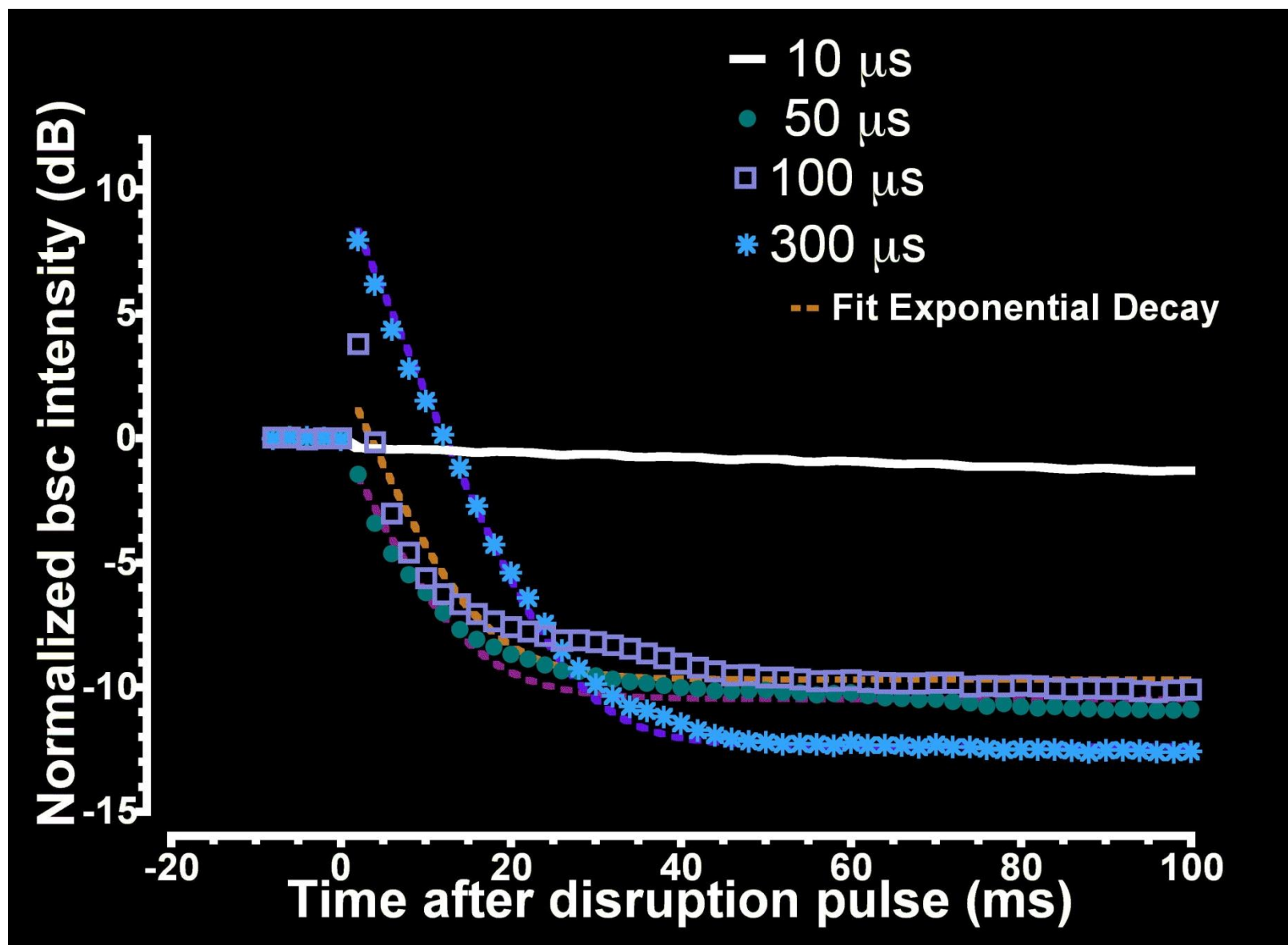
Pulse sequence used for contrast agents dissolution imaging



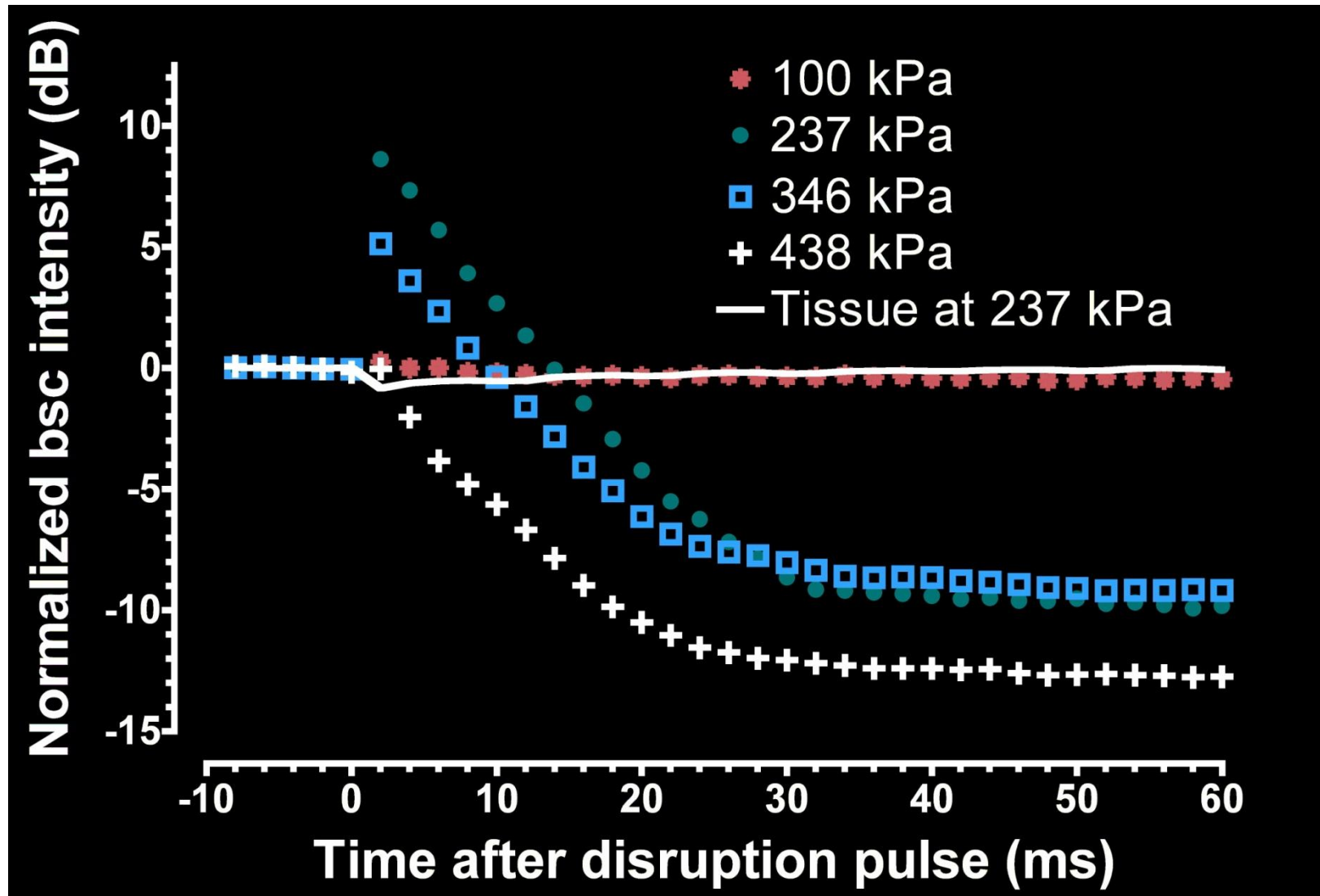
The process of dissolution in the wall-less vessel is observable over 100 ms



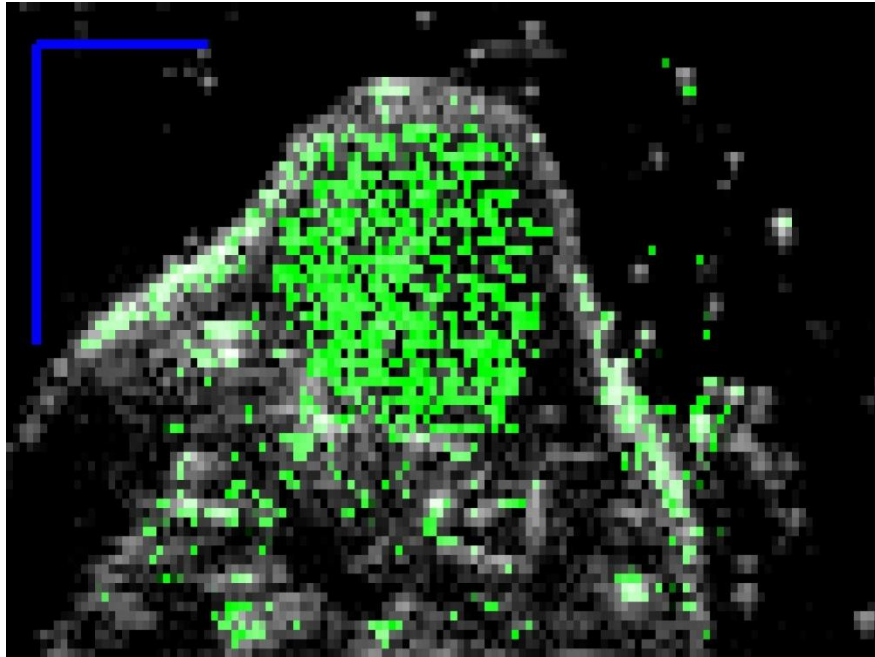
The dissolution curves in 2D are similar to those measured with single transducers



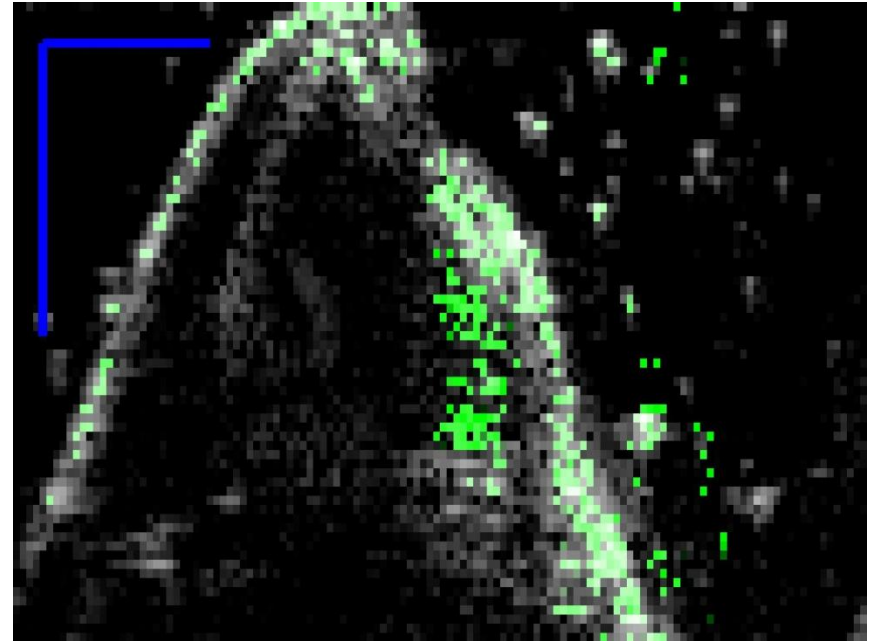
The dissolution curves depends on disruption pulse length and amplitude



Distinguishing bound and unbound microbubbles is a challenge in molecular imaging with ultrasound



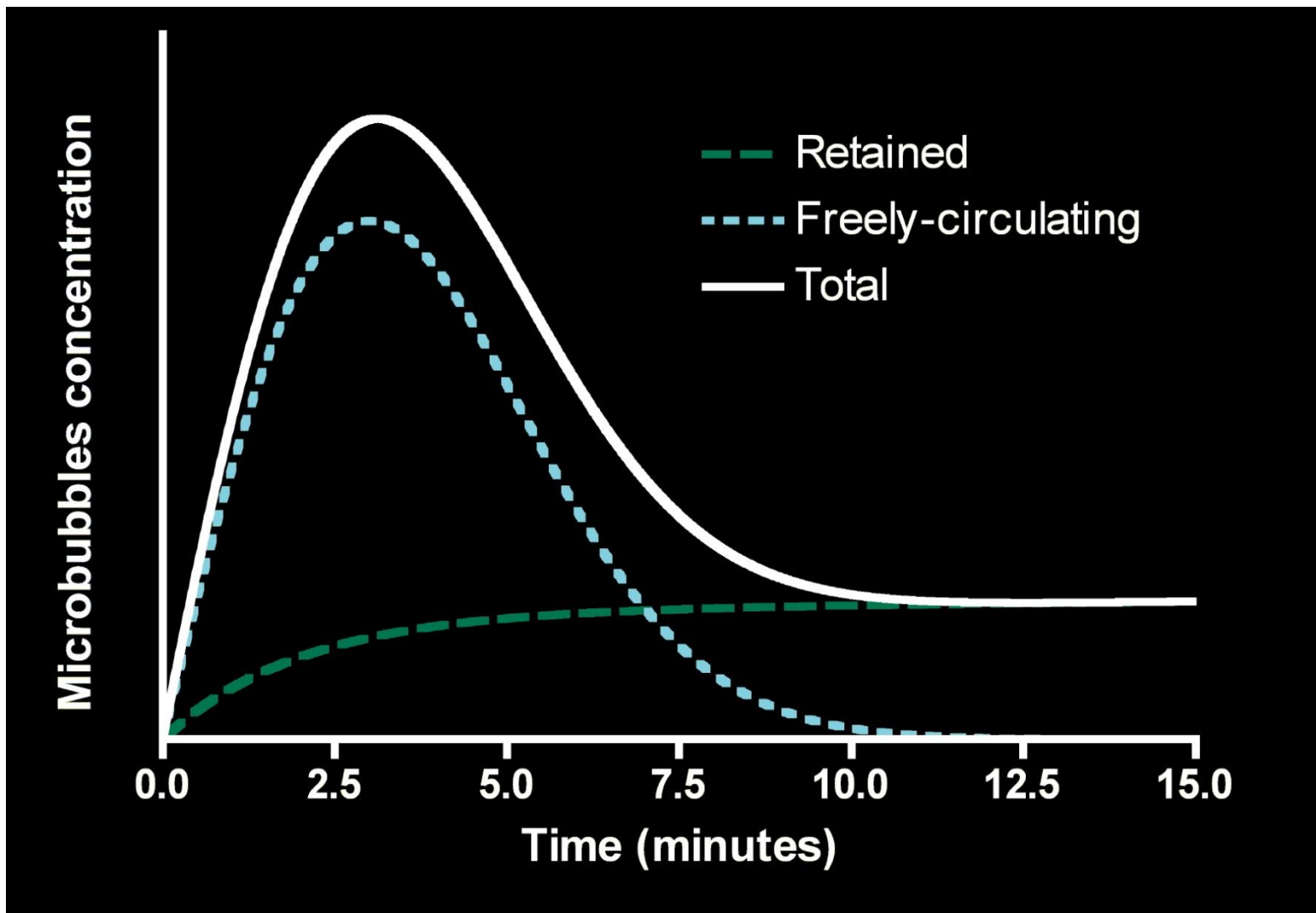
**Tumor-targeted
Microbubbles**



**Control
microbubbles**

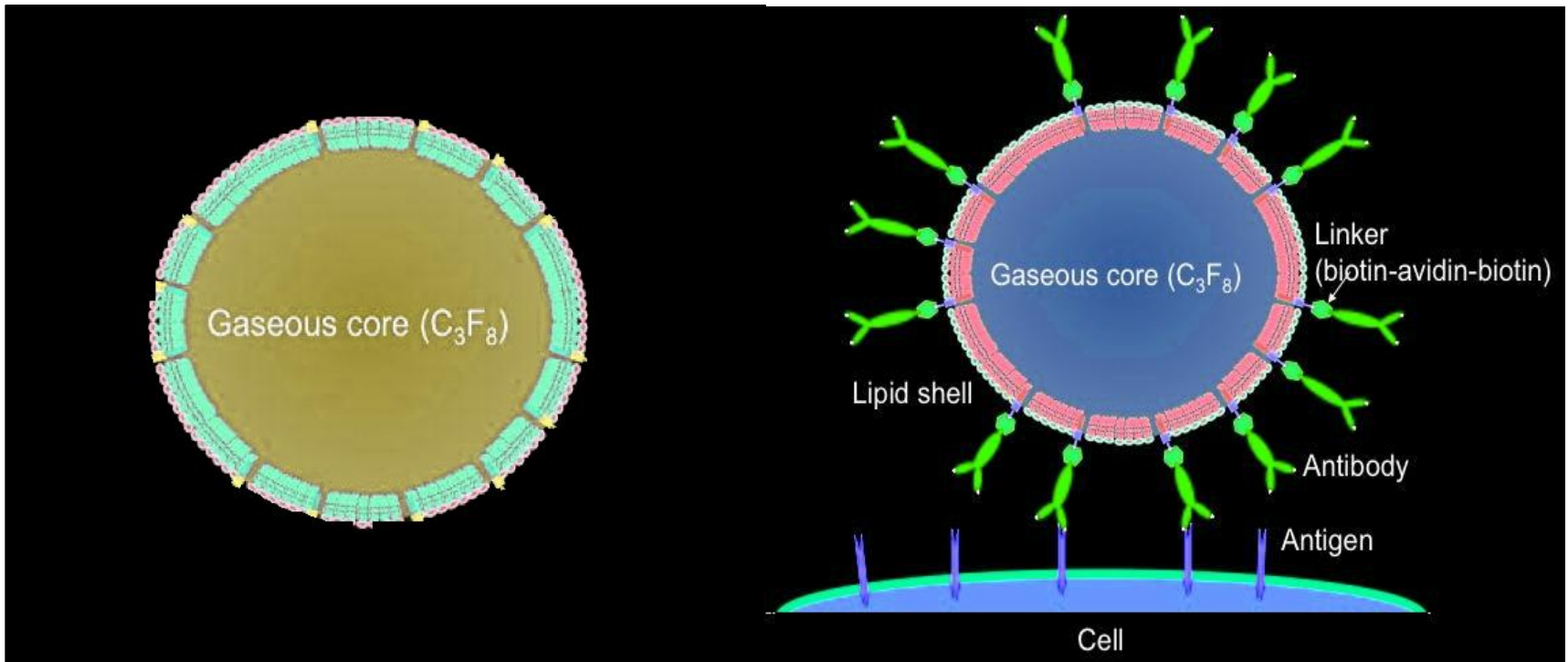
(StBx Shiga Toxin)

Bound and unbound microbubbles are distinguished through their clearance time in the tumor



The physical environment affects the acoustic response of microbubbles

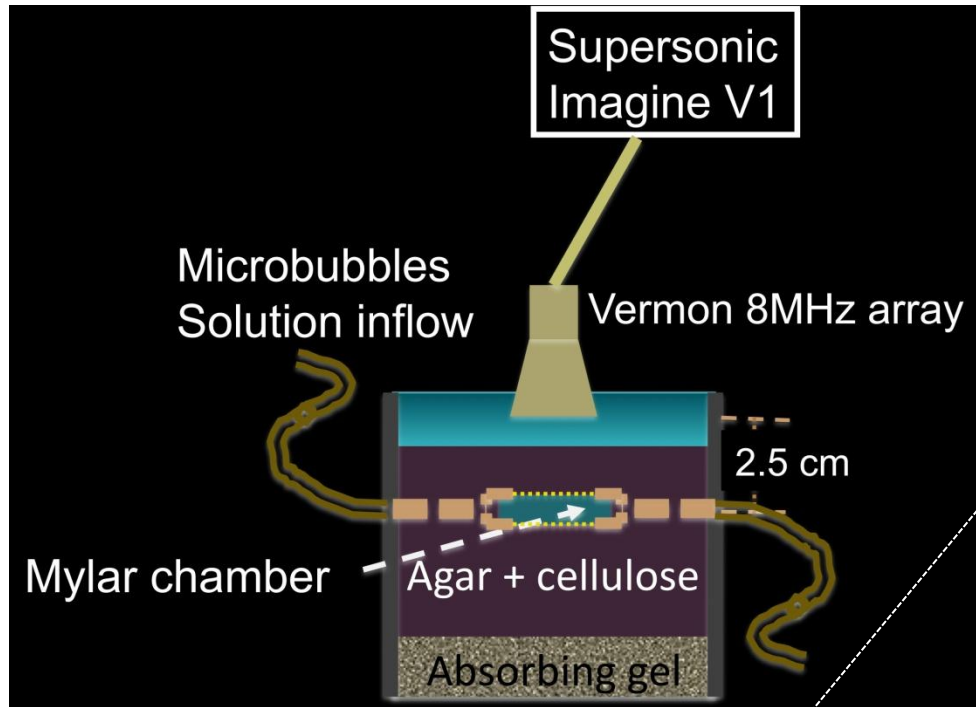
Hypothesis: The dissolution time after disruption changes in the “bound state”.



Free Bubbles

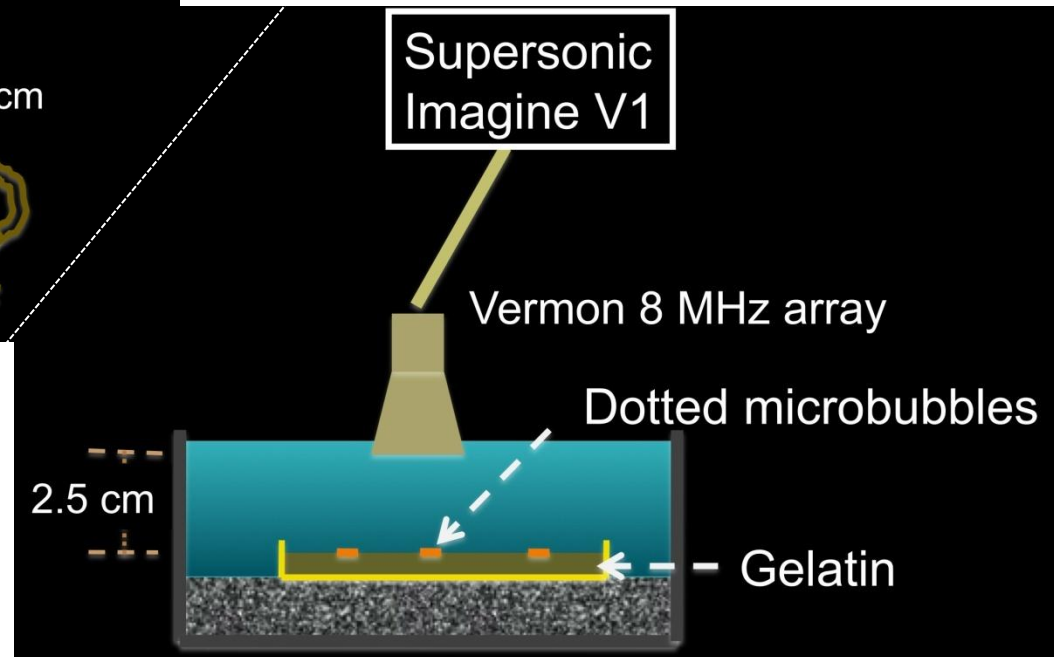
Targeted microbubbles

Dissolution imaging is performed with an elastography apparatus on two parallel setup

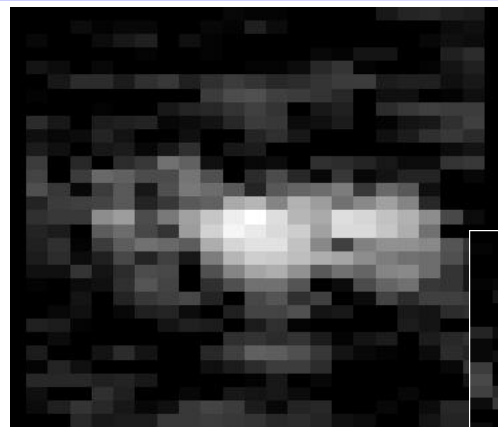


Flowing setup

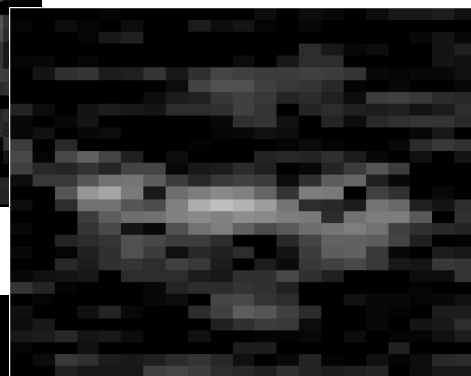
Bound setup



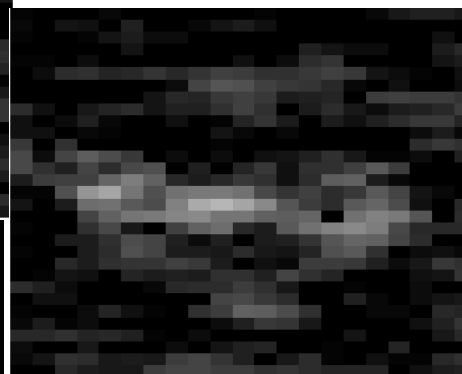
The process of dissolution is also observable on a dot of targeted microbubbles



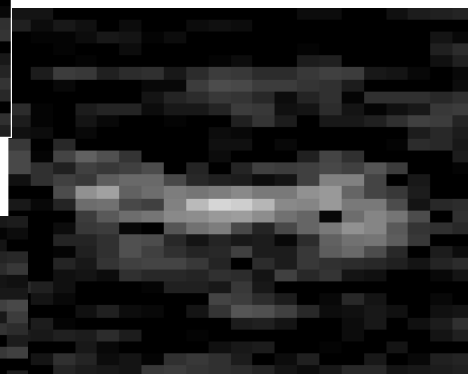
-4 ms



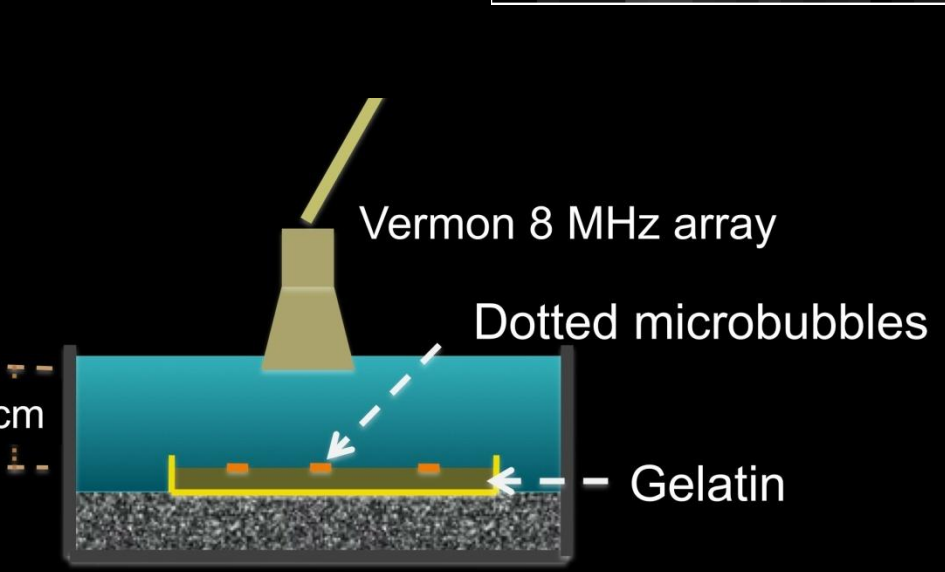
24 ms



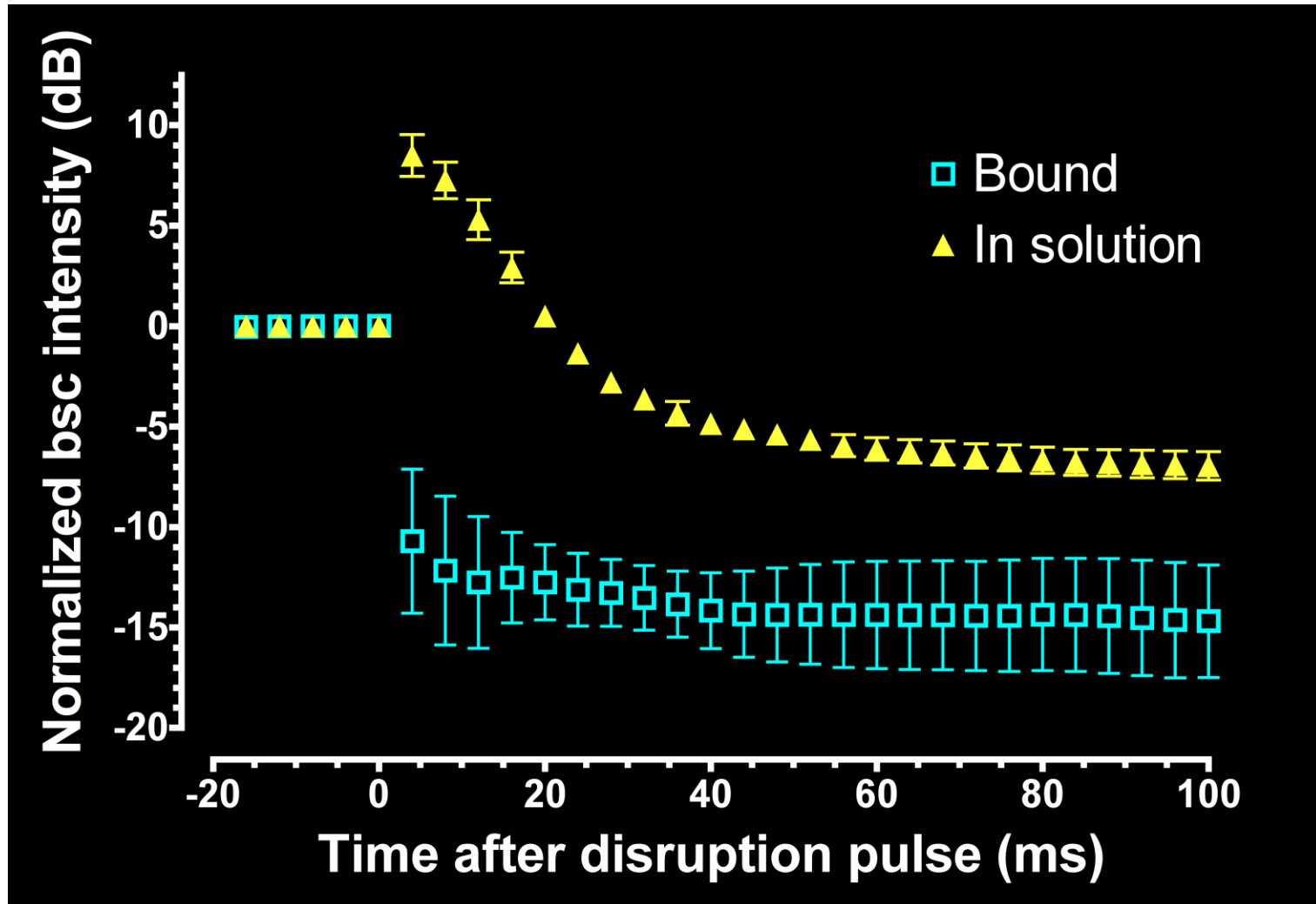
36 ms



100 ms



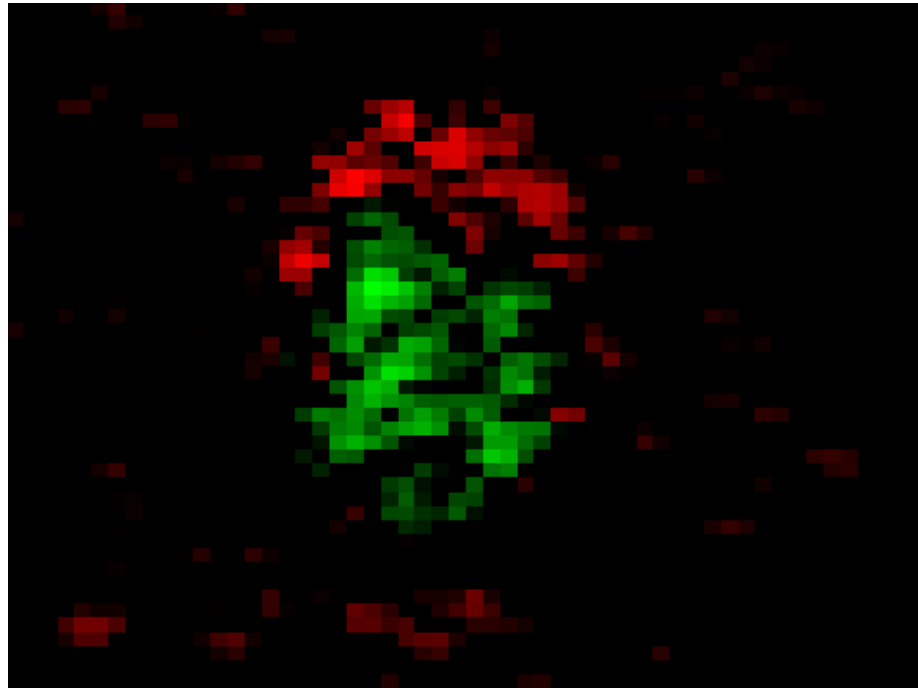
Targeted microbubbles dissolve faster than freely moving microbubbles.



Couture, O.; Bannouf, S.; Montaldo, G.; Aubry, J.-F.; Fink, M. & Tanter, M. (2009), 'Ultrafast Imaging of Ultrasound Contrast Agents', *Ultrasound In Medicine and Biology* 35(11), 1908--1916.

Couture, O.; Dransart, E.; Dehay, S.; Nemati, F.; Decaudin, D.; Johannes, L. & Tanter, M. (2011), 'Tumor Delivery of Ultrasound Contrast Agents Using Shiga Toxin B Subunit', *Molecular Imaging* 10(2), 135--143.

Impact of ultrafast imaging for contrast agents imaging



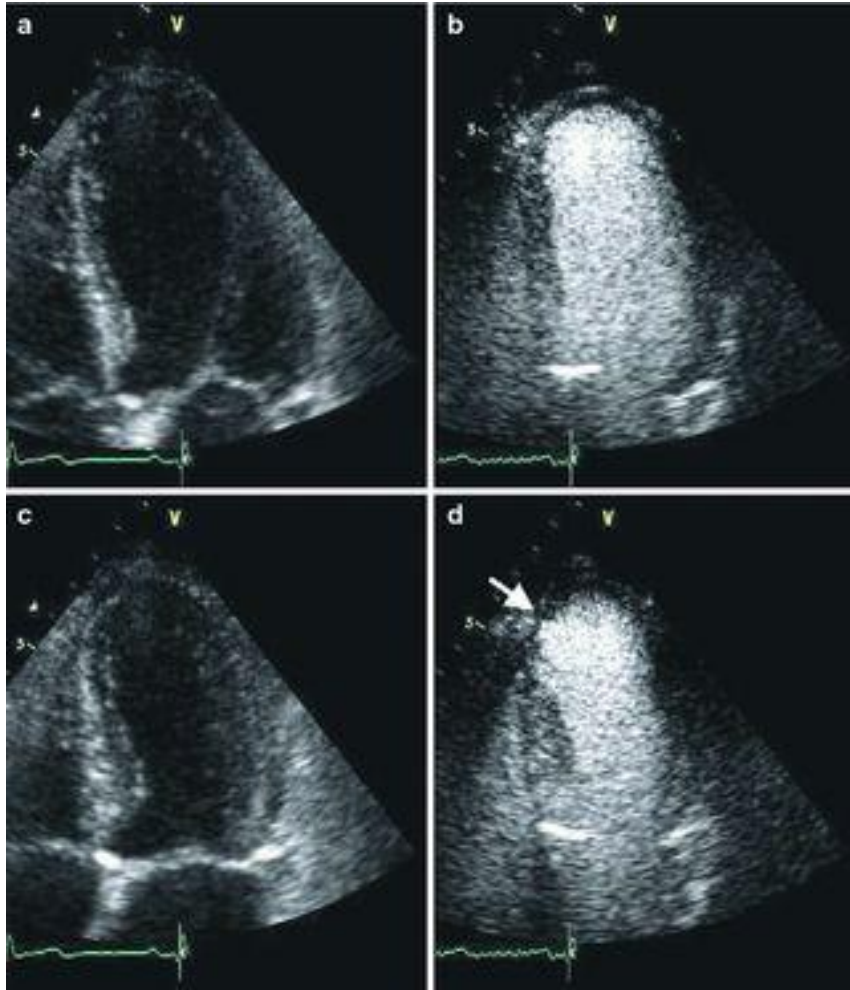
- Differentiate bound from unspecific microbubbles
- Fast events are dependent on the geometry of the environment
- Pulses schemes (PI, AM, ...) can be applied to entire frames
- Frame rate accelerates with calculations capacity

Couture, O.; Bannouf, S.; Montaldo, G.; Aubry, J.-F.; Fink, M. & Tanter, M. (2009), 'Ultrafast Imaging of Ultrasound Contrast Agents', *Ultrasound In Medicine and Biology* 35(11), 1908--1916.

Couture, O.; Dransart, E.; Dehay, S.; Nemat, F.; Decaudin, D.; Johannes, L. & Tanter, M. (2011), 'Tumor Delivery of Ultrasound Contrast Agents Using Shiga Toxin B Subunit', *Molecular Imaging* 10(2), 135--143.

Ultrafast Contrast Imaging

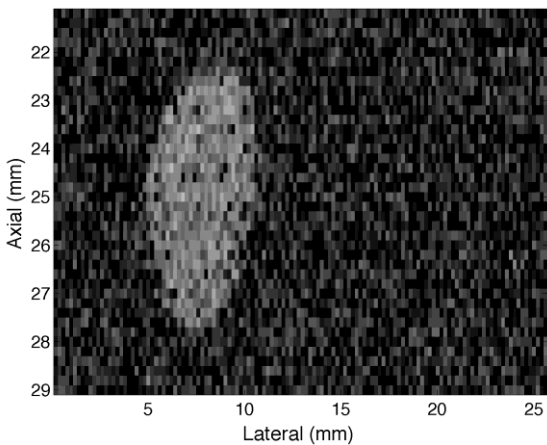
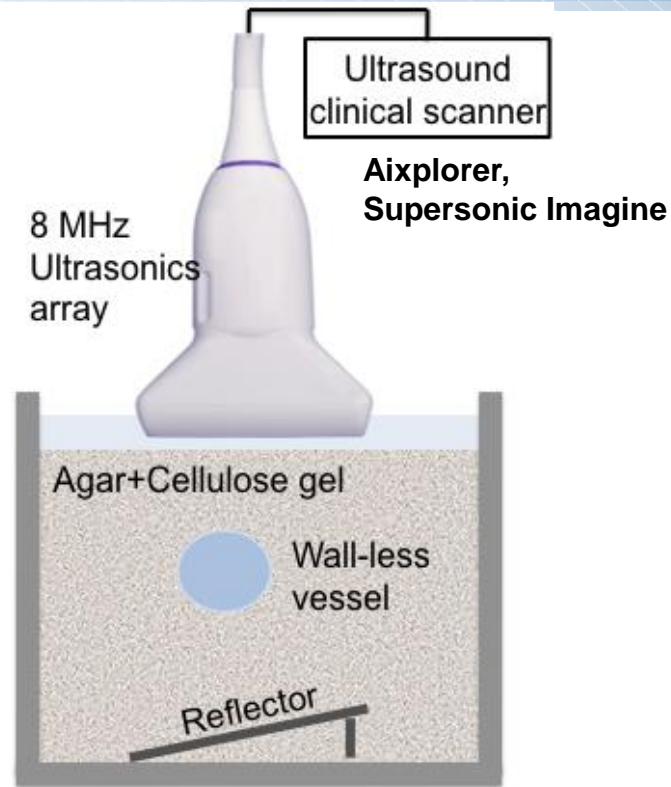
Microbubbles are used to image vascularization and measure perfusion



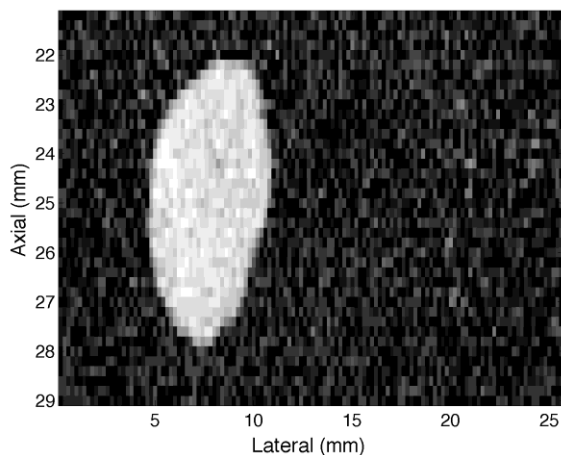
Ultrafast Contrast Plane Wave Imaging produces a much better contrast

Different Contrast schemes

Pulse	1	2	3	Linear comb.	Non-linear
Linear					—
Pulse-Inversion				—	
Amplitude Modulation				—	
Contrast Pulse Sequencing				—	



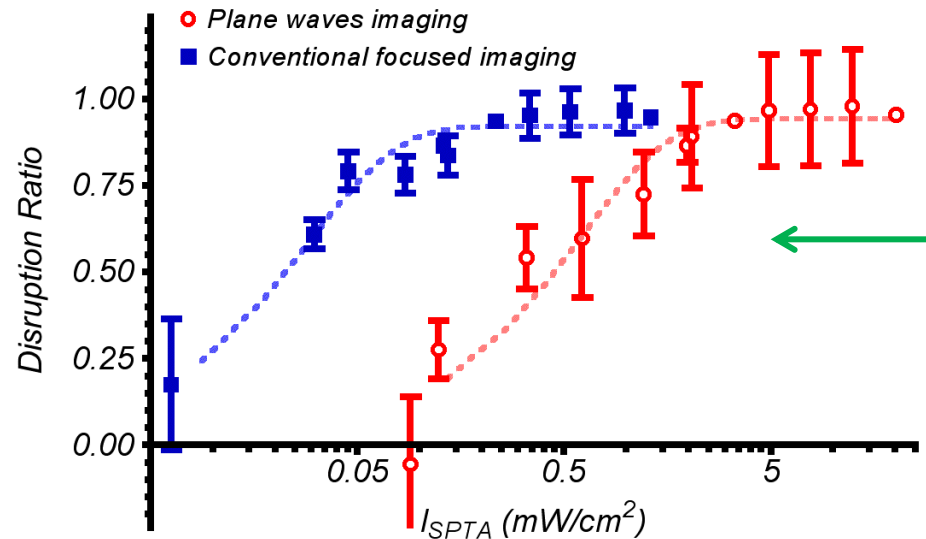
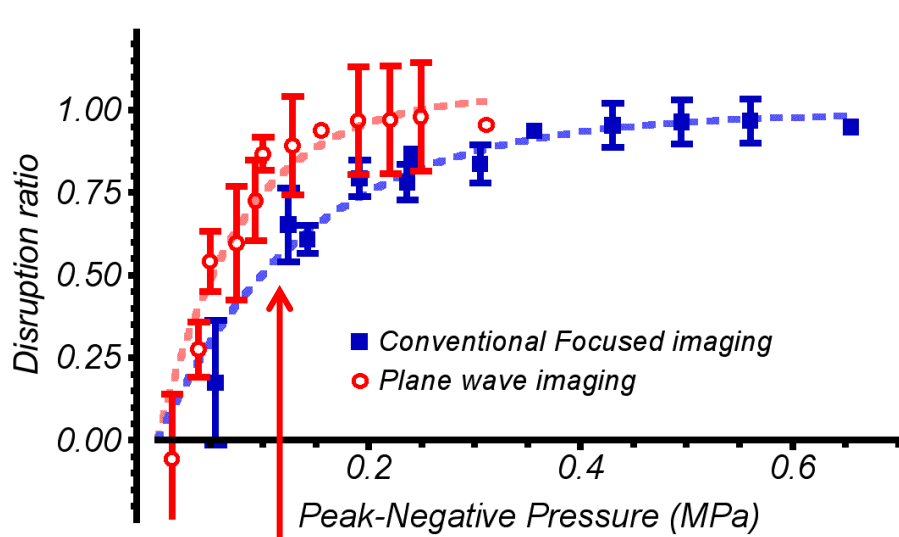
Conventional focused CPS



Plane Wave CPS

Images obtained for a similar disruption ratio of microbubbles (25 % disruption after 100 images or focused: 55 kPa peak-negative pressure and Plane waves = 40 kPa).

Ultrafast Contrast Plane Wave Imaging spreads the acoustic intensity in time



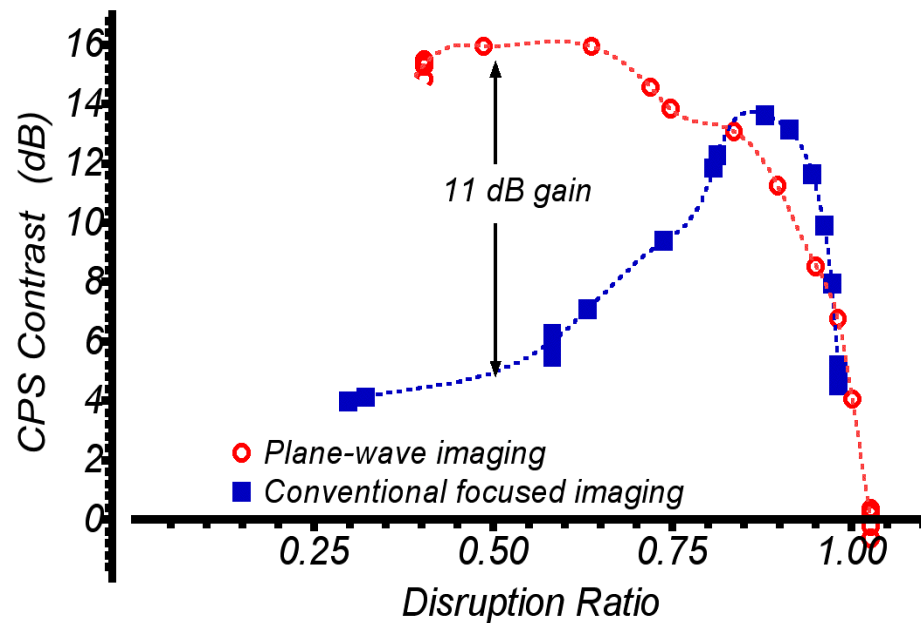
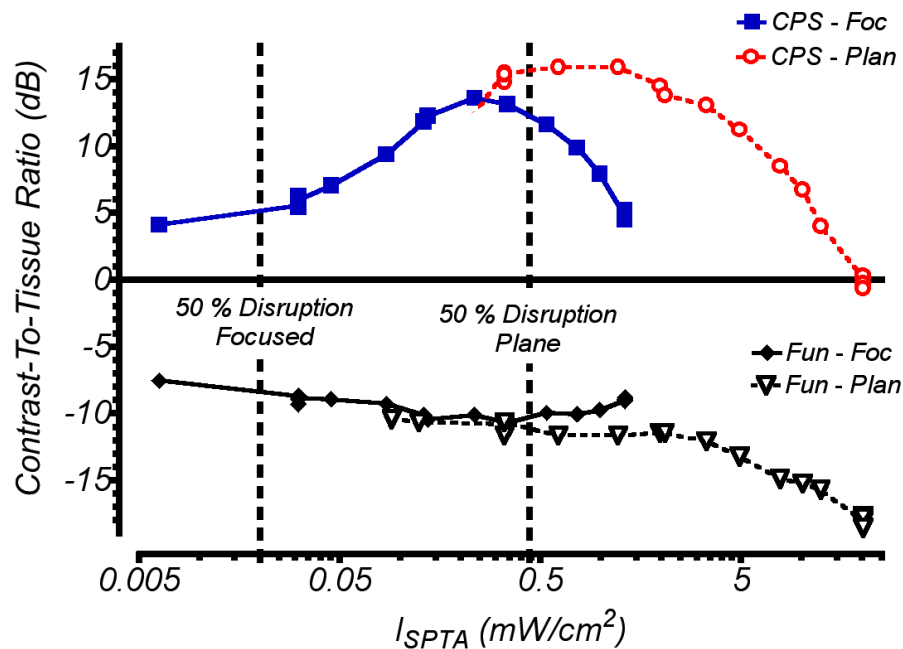
Disruption ratio obtained after 100 images. The ratio is calculated from the intensity of the microbubble echo before and after the full sequence. In plane-wave imaging, each pixel is insonified 121 times rather than a single time in focused imaging.

Hence, at the same peak-negative pressure, plane-wave imaging disrupts slightly more bubbles.

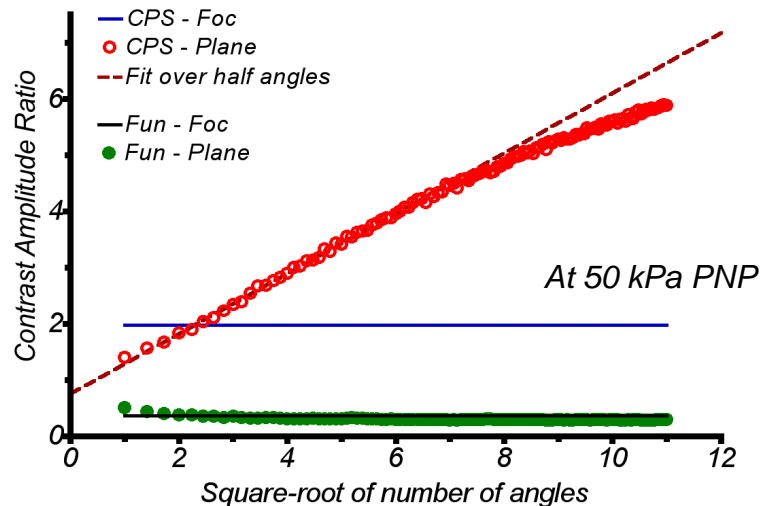
But Plane-wave imaging spread the energy over more pulses at lower pressure. Microbubbles being sensitive to the peak-negative pressure, rather than the total energy, the 50% disruption point is only observed at **0.47 mW/cm²** for plane-wave imaging as compared to **0.02 mW/cm²** for focused pulses.

Less acoustic energy can be emitted with focused pulses before microbubbles disruption occurs.

Ultrafast Contrast Imaging keeps a high CTR while preserving bubbles

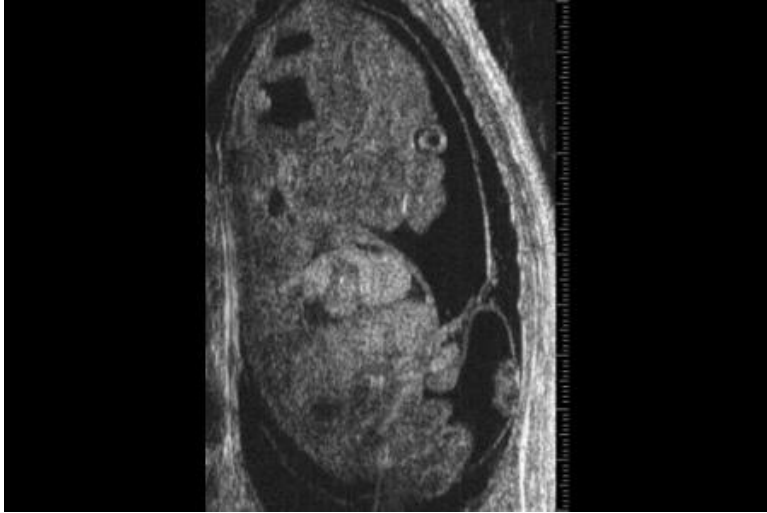


$$\frac{CTR_{PlaneWave}}{CTR_{Focused}} \sim \sqrt{N_{angles}}$$



Ultrafast Ultrasound for Contrast Superresolution Imaging

Ultrasound imaging is still limited by the trade-off between resolution and penetration

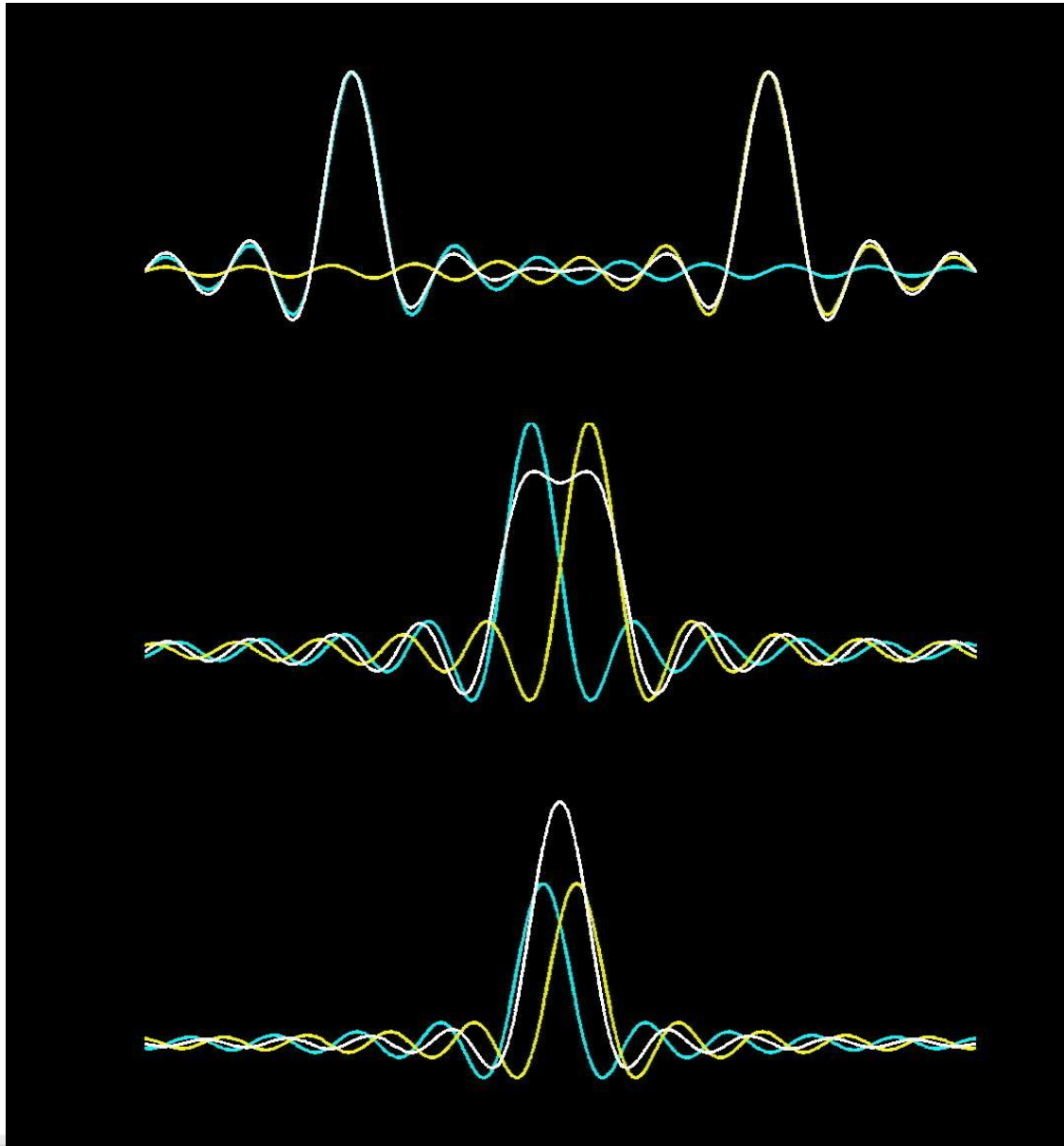


Mouse embryo at 40 MHz
Penetration \approx 1 cm



Human foetus at 5 MHz
Penetration \approx 10 cm

Imaging resolution is limited by the wavelength

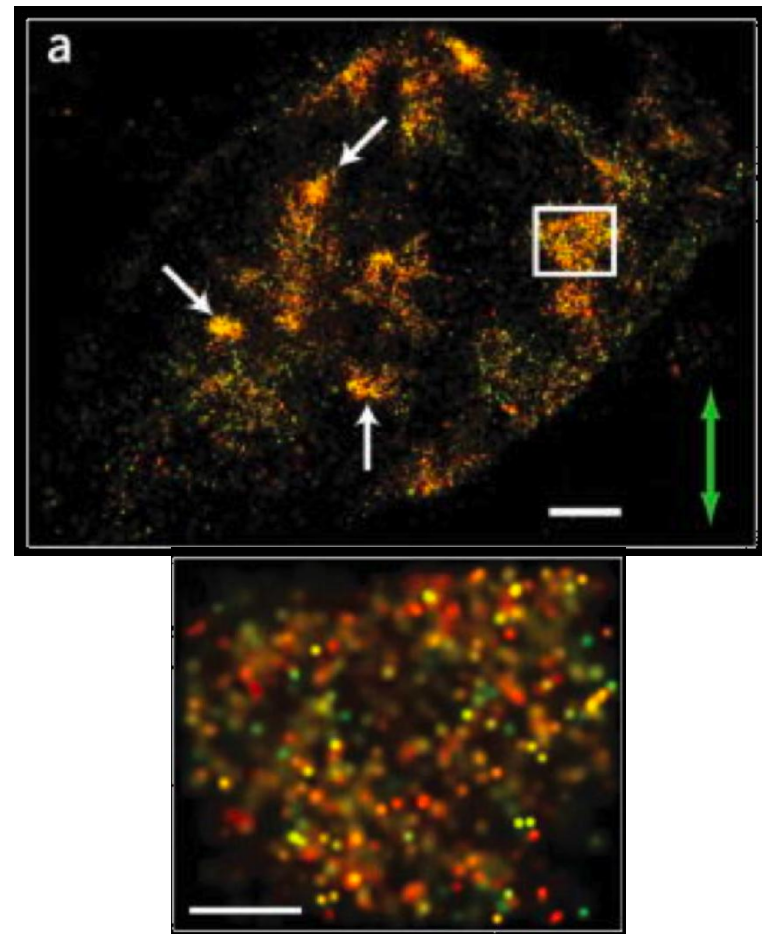
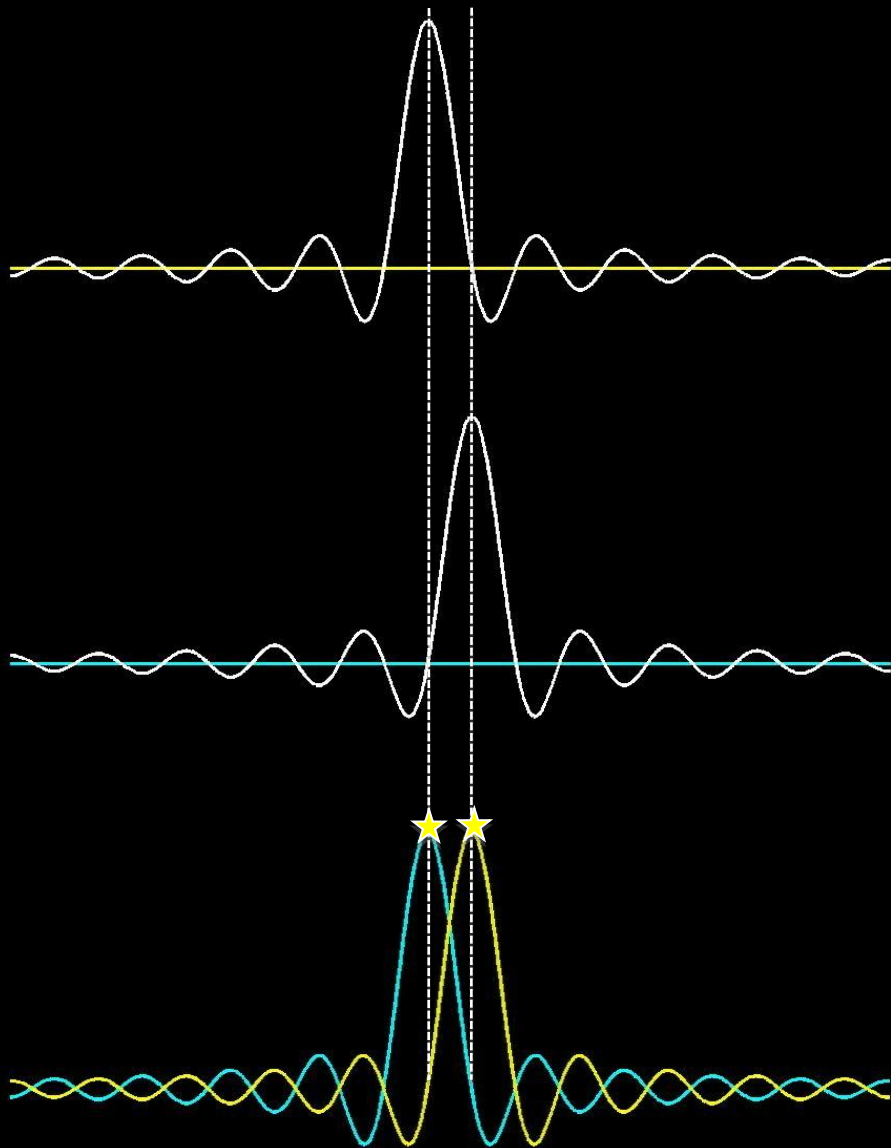


**Two distincts
sources**

Rayleigh criterion

**Two indistinguishable
sources**

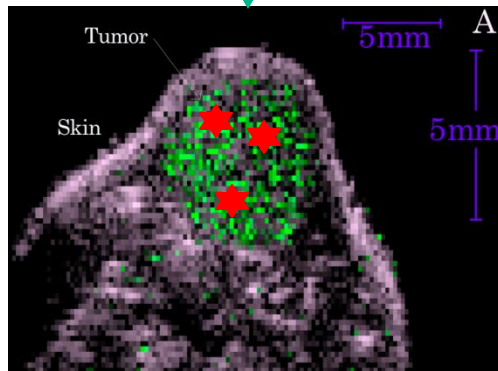
Sources become distinguishable when they are activated separately



**P-FPALM image of a fixed fibroblast
(scale bar = 1 μm).**

Gould et al. Nat Methods 2008. (Hess group)

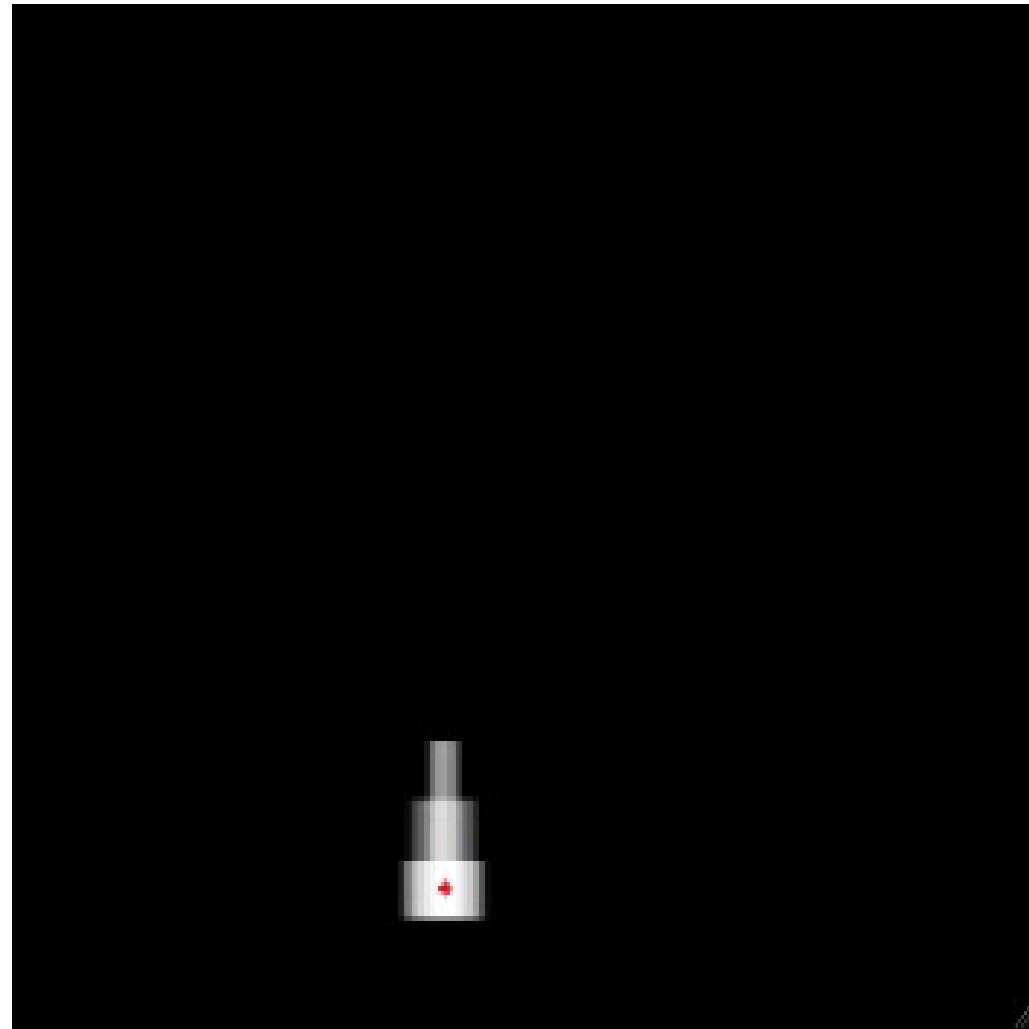
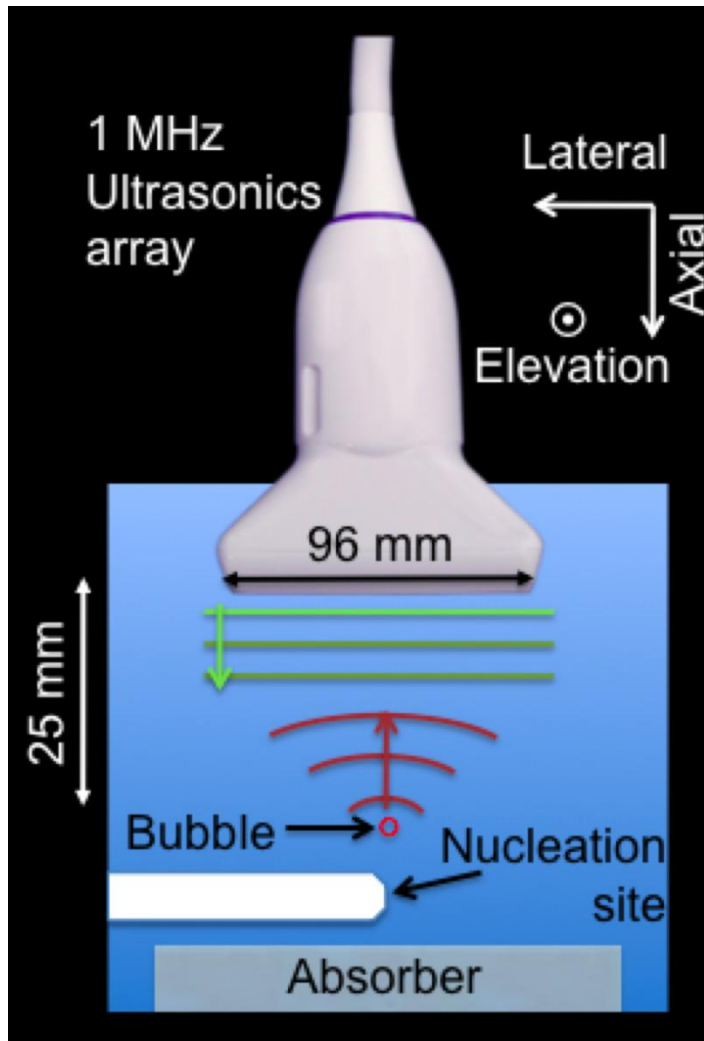
Ultrafast (plane-wave) imaging shows distinct events in-vivo



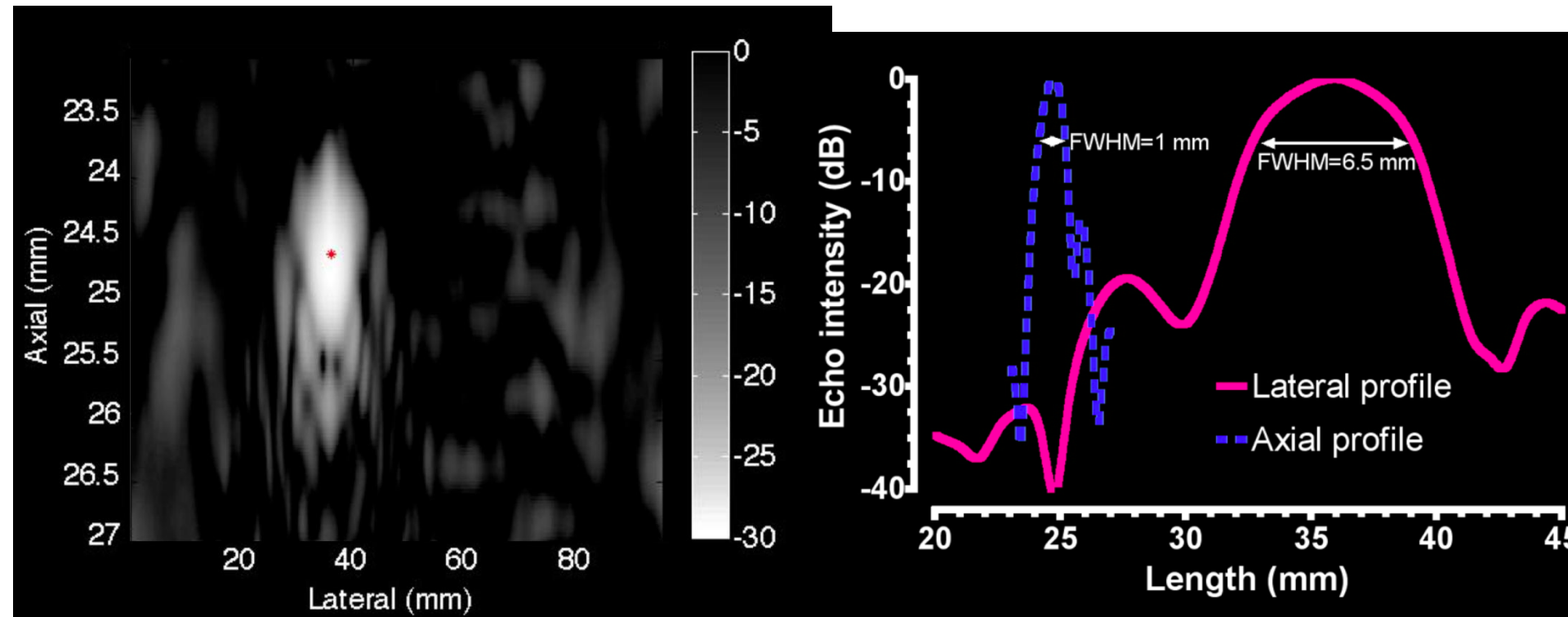
Frame Rate: 5000 kHz



A bubble is an ideal punctual source



A punctual source defines the classical resolution limit after the beamforming process



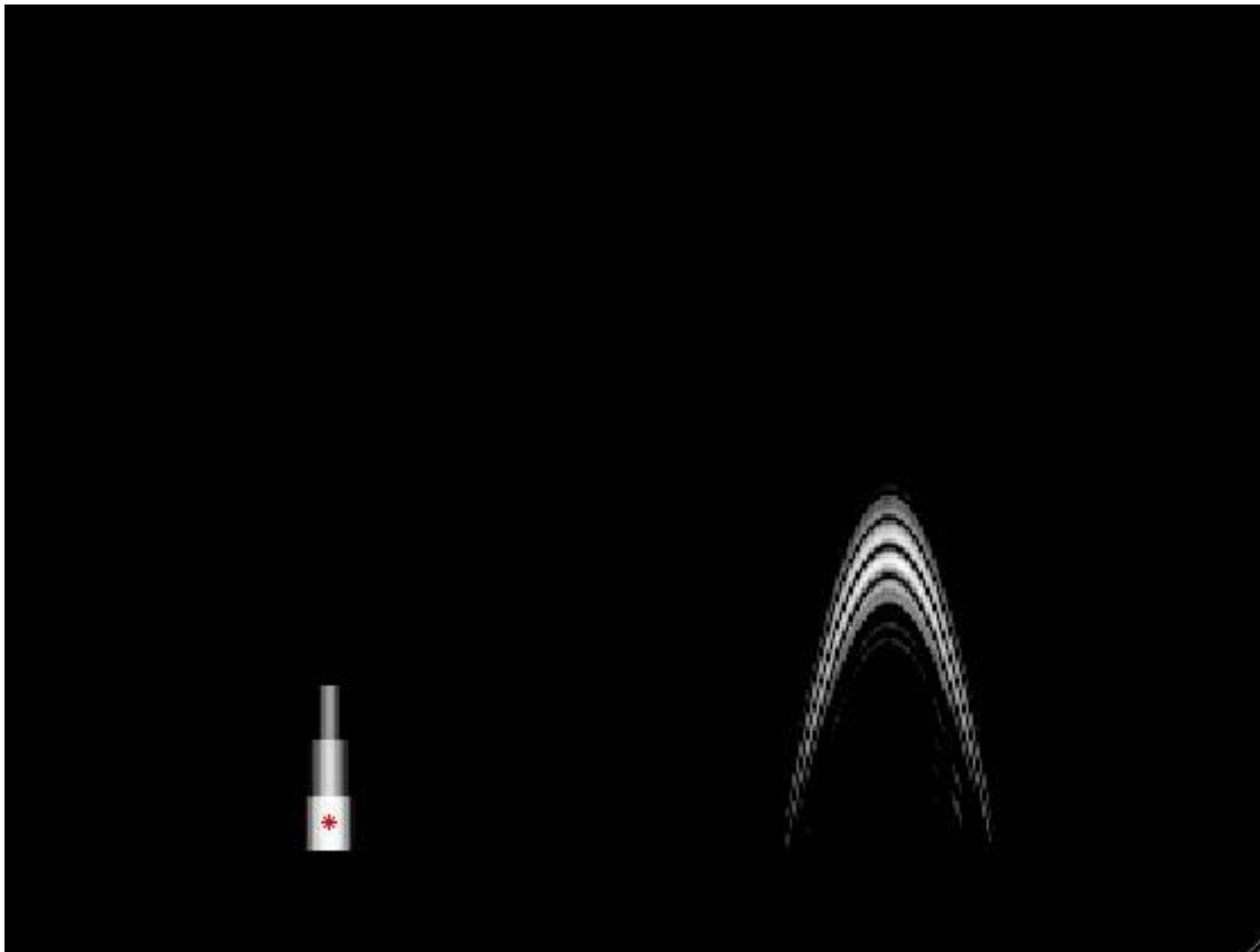
A punctual source generates a parabola on the RF signals (Bscan)

Lateral (elements)

Lateral (elements)

Depth (axial)

Time (axial)

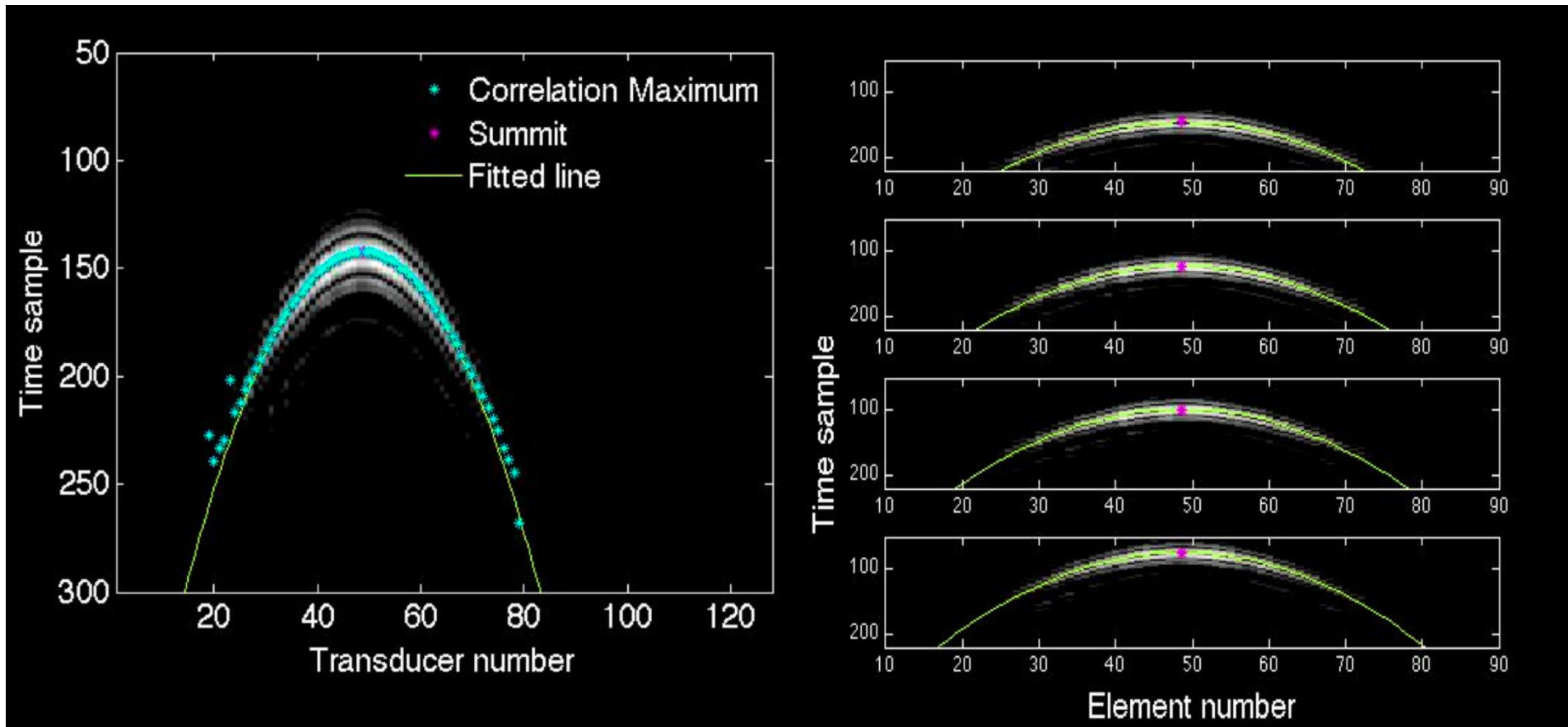


Beamformed Image

Raw Data

Fitting the arrival times parabola localizes the bubble

$$delay = \frac{\sqrt{depth_of_bubble^2 + (x - lateral_position)^2}}{speed_of_sound}$$

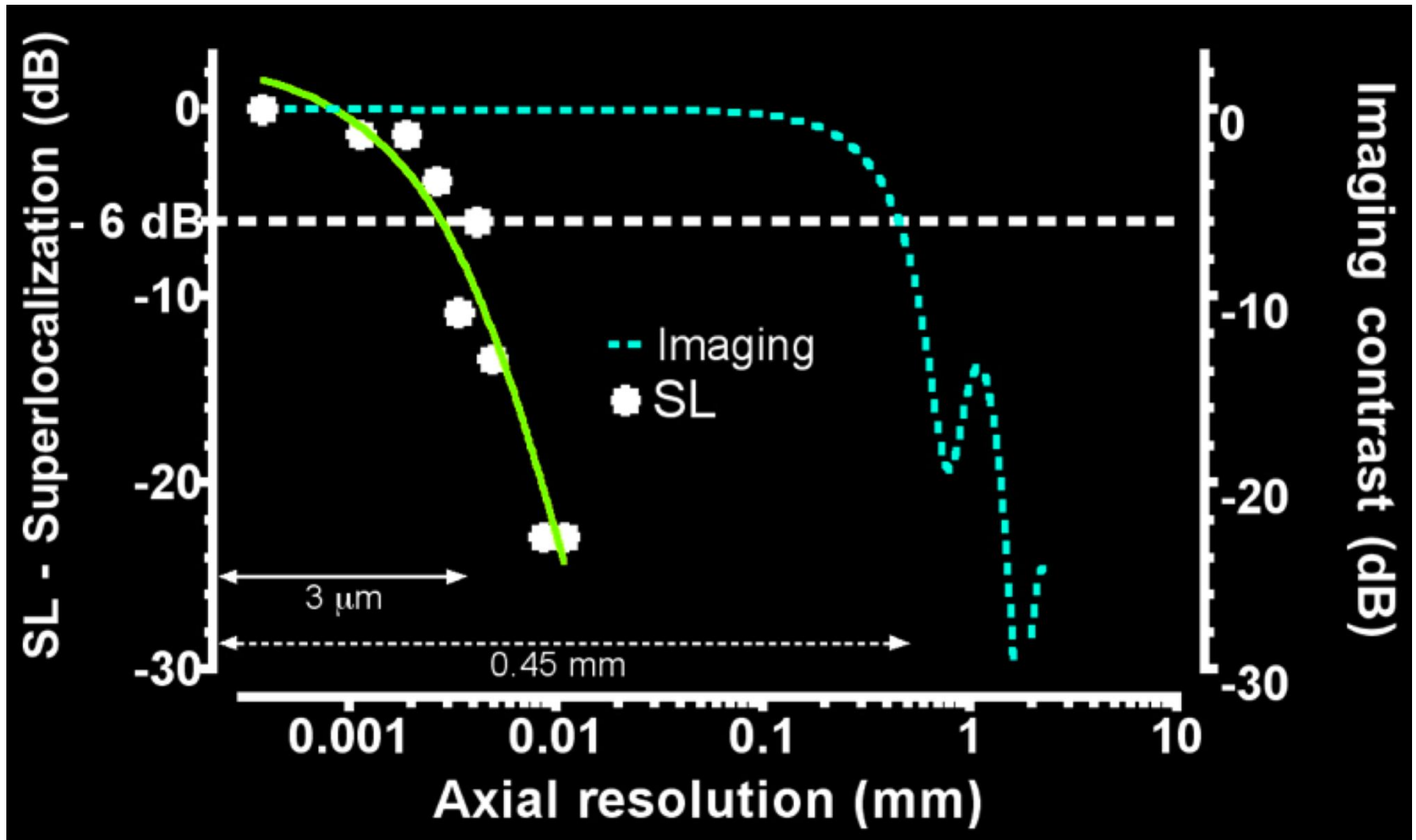


Spatial Localization precision is much better than conventional imaging


'Ultrasound Contrast Plane Wave Imaging'

O. Couture, M. Fink, M. Tanter, IEEE Trans. Ultr. Ferr. Freq. Ctrl., in press, 2012

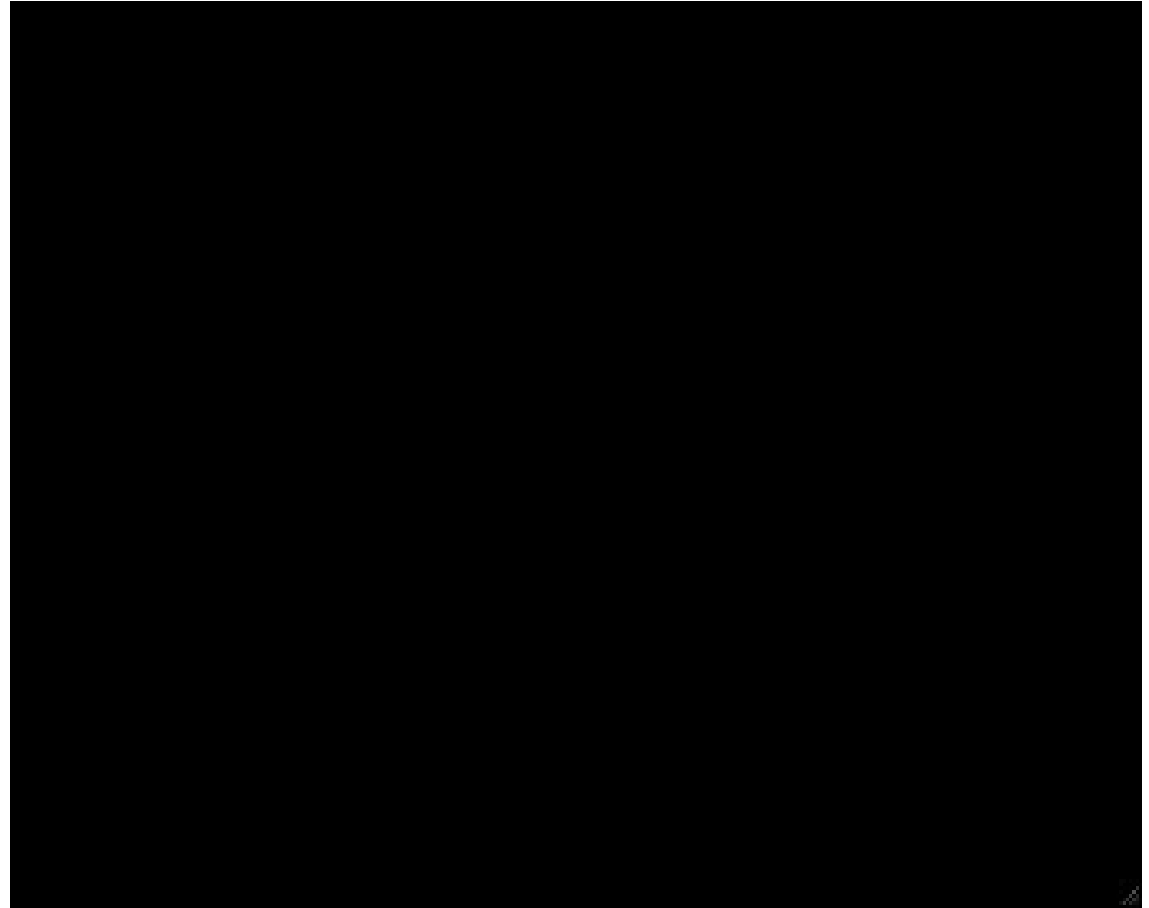
Axial "resolution" goes from 1 mm to 6 μm



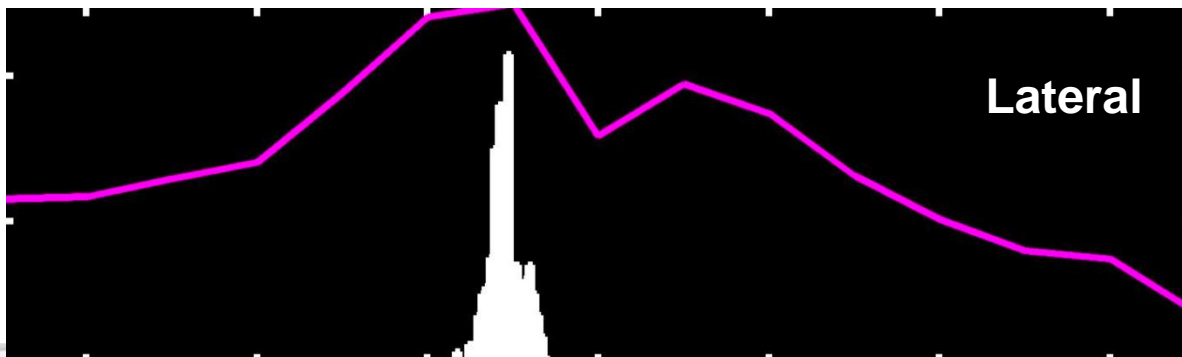
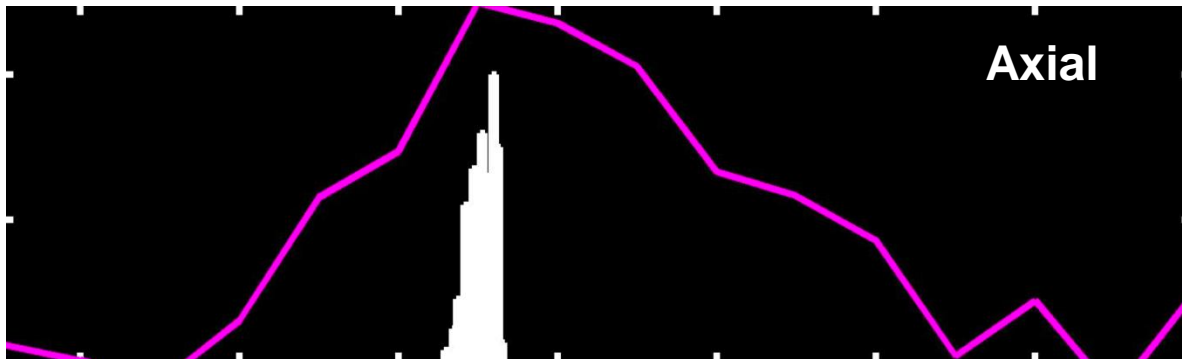
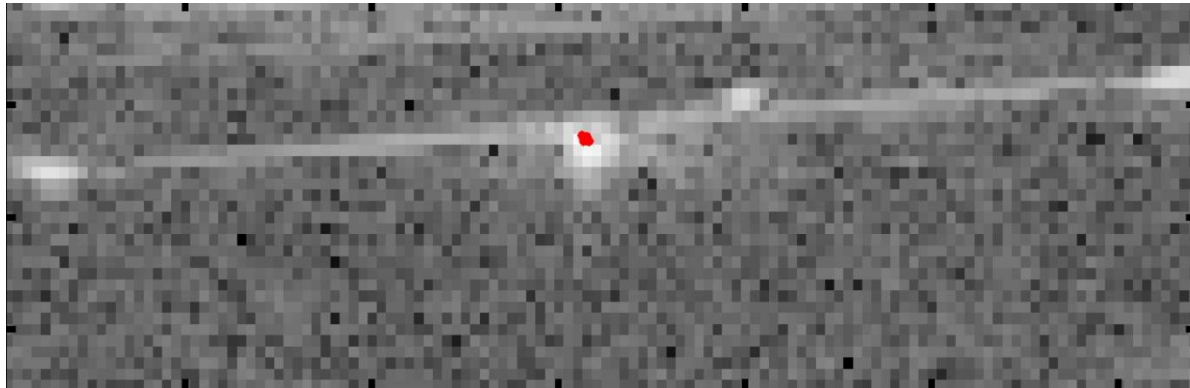
Microbubble ultrasound super-localization imaging (MUSLI) improves resolution 100-fold

			
		EXP.	Simulation
1.5 MHz	$\lambda / 2$	6 μm	4.5 μm
AXIAL	500 μm		
LATERAL		40 μm	11 μm

Experimental proof of concept in 2D with microchannels



MUSLI can resolve a microchannel carrying microbubbles

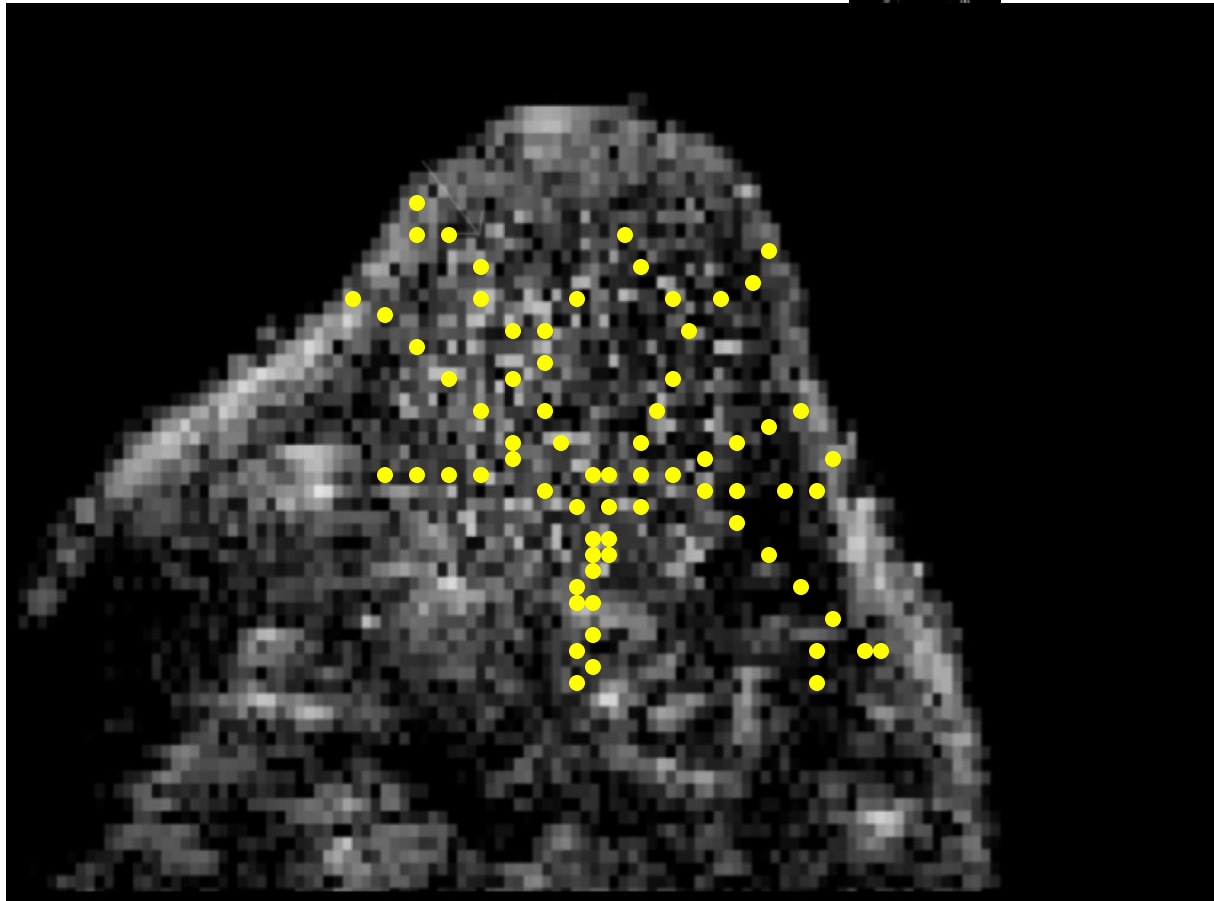


Microbubbles ultrasound super-localization imaging could resolve capillaries at low frequencies

$\lambda / 2 = 500 \mu\text{m}$



$= 6 \mu\text{m}$

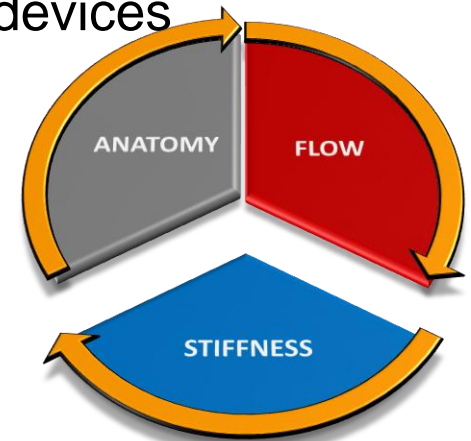


Ultrafast Doppler Imaging

SWE

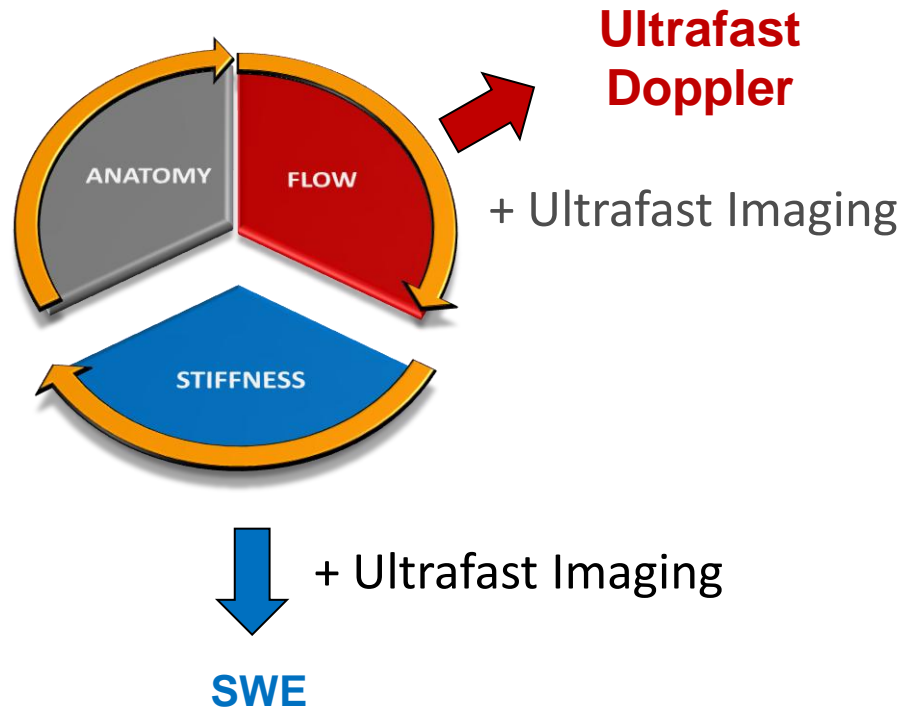
- ShearWave Elastography (SWE) provides an additional information to the user: tissue stiffness
- SWE completes the information circle of ultrasound devices

✓	B-mode	→	ANATOMY	(1970s – 1980s)
✓	Doppler	→	FLOW	(1980s – 1990s)
✓	Elastography	→	STIFFNESS	(2000s – 2010s)



- SWE has key advantages compared to other elastography techniques
 - Automated stress generation
 - Quantitative imaging (2D/3D)
 - Real time

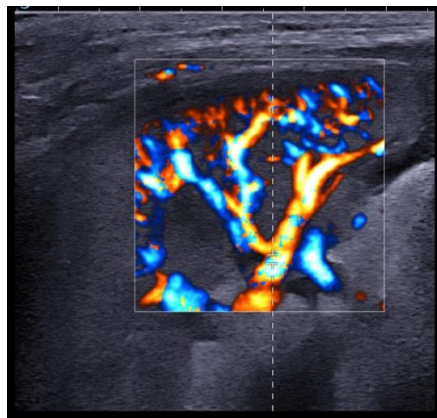
Can we reinvent conventional ultrasound modes with an Ultrafast imaging system ?



Doppler imaging today: two separate modes

1) Color Flow Imaging

- Real time imaging of flow
- Display the mean velocity per pixel in a color coded representation
- Used for detection of flow or localization of flow abnormalities

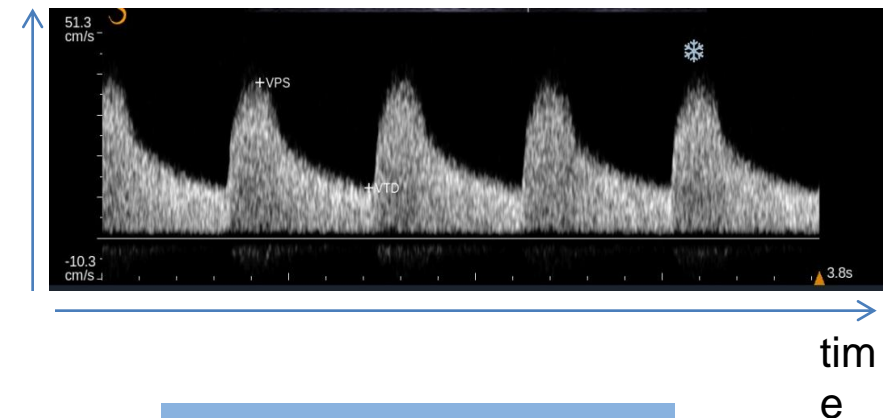


Imaging

2) Spectral Doppler

- Full quantification of flow velocity per Fourier analysis
- Available at on given location

velocities

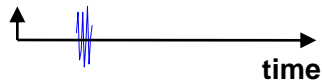
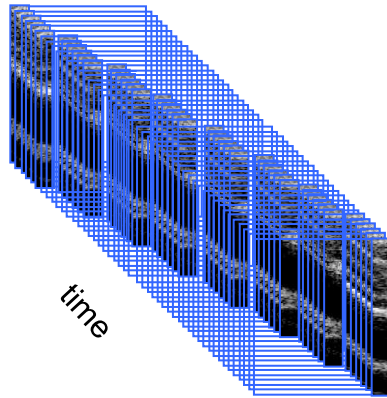


Quantification

AND

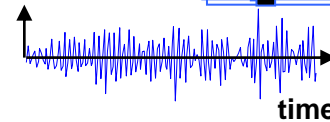
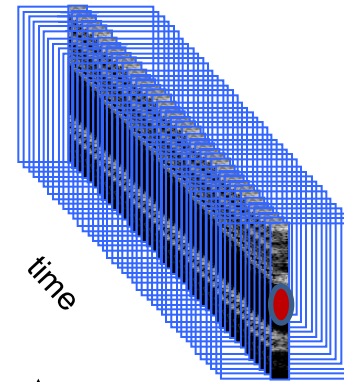
Conventional vs Ultrafast Doppler sequences

- Conventional CFI



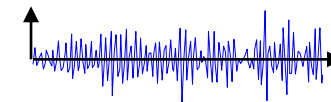
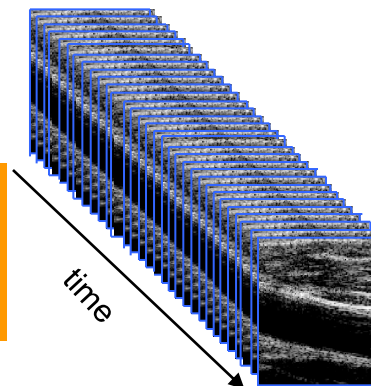
Only 10 points per pixel
Mean Velocity estimation

- Conventional PW



50- 150 points per pixel
at a given sample volume

• Ultrafast Doppler

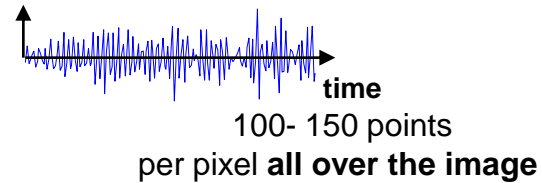
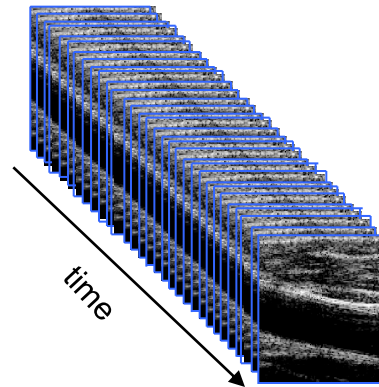


50- 150 points
per pixel **all over the image**

Ultrafast allow gathering of complete Doppler information for all pixels

Leveraging Ultrafast Doppler Data

- Ultrafast Doppler

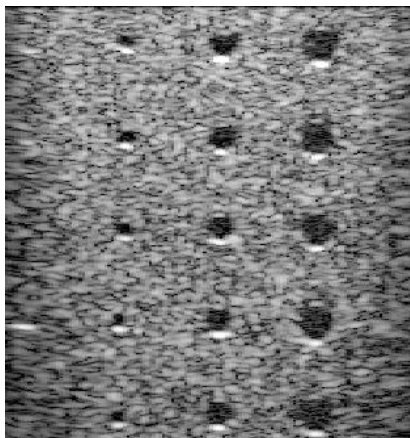


- 1) Increase color flow imaging performances
 - + Sensitivity: improve slow flow detection
 - + Frame rate: finer flow dynamics analysis
 - + Consistency: All pixels shown are synchroneous.
- 2) Quantification => PW (spectral analysis) everywhere

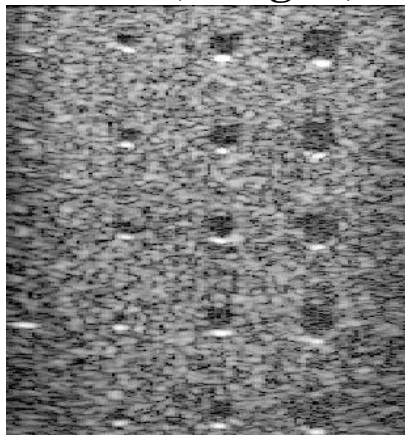
A Trade-off between Speed and Sensitivity

FASTER

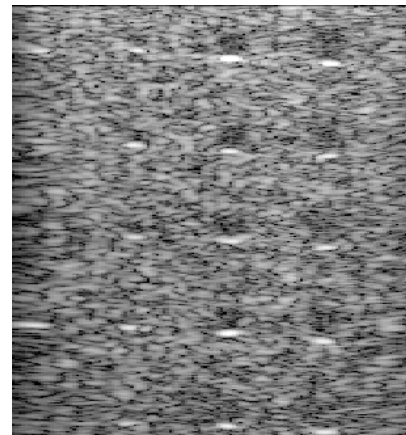
1kHz (17 angles)



3 kHz (5 angles)

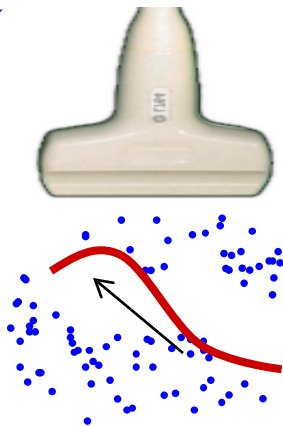


18 kHz (1 angle)



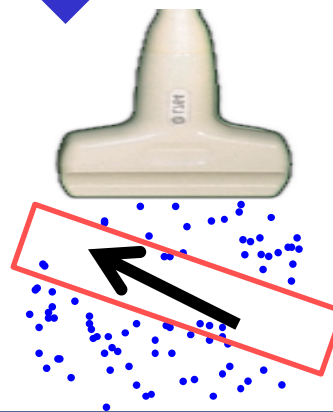
Application 2:
Small vessels

Slow flow ~mm/s
SENSITIVITY

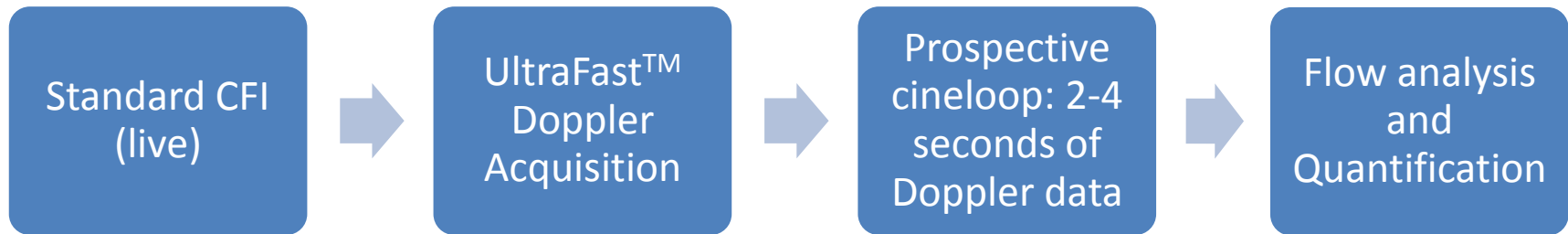


Application 1:
Carotid Artery

Rapid flow >10cm/s
ULTRAFAST

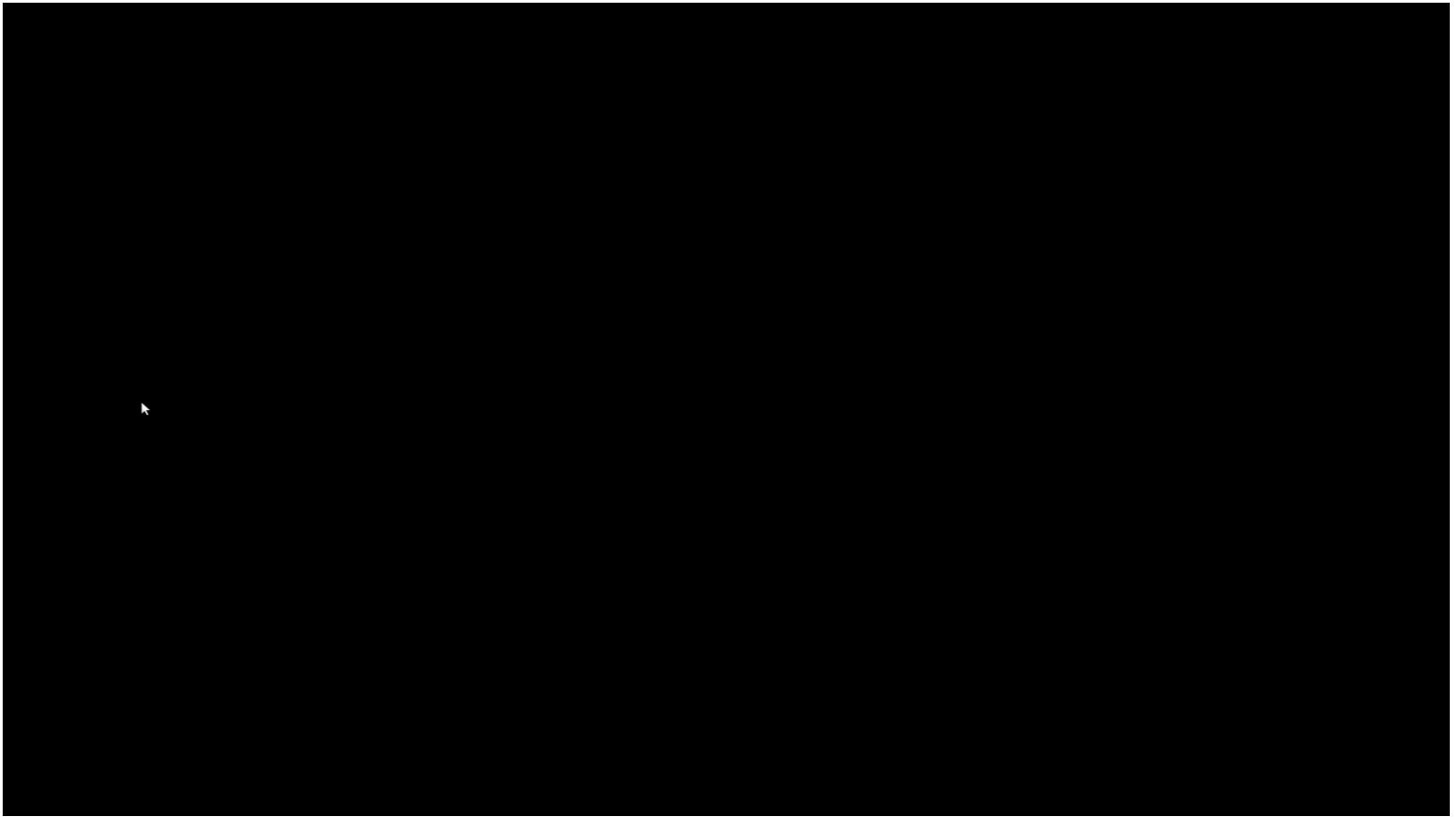


Ultrafast Doppler mode presentation Workflow



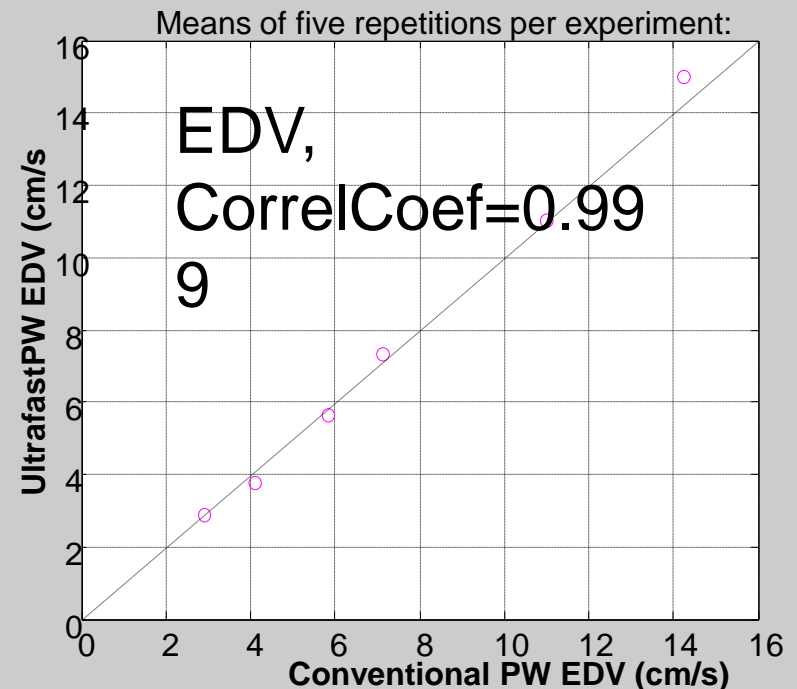
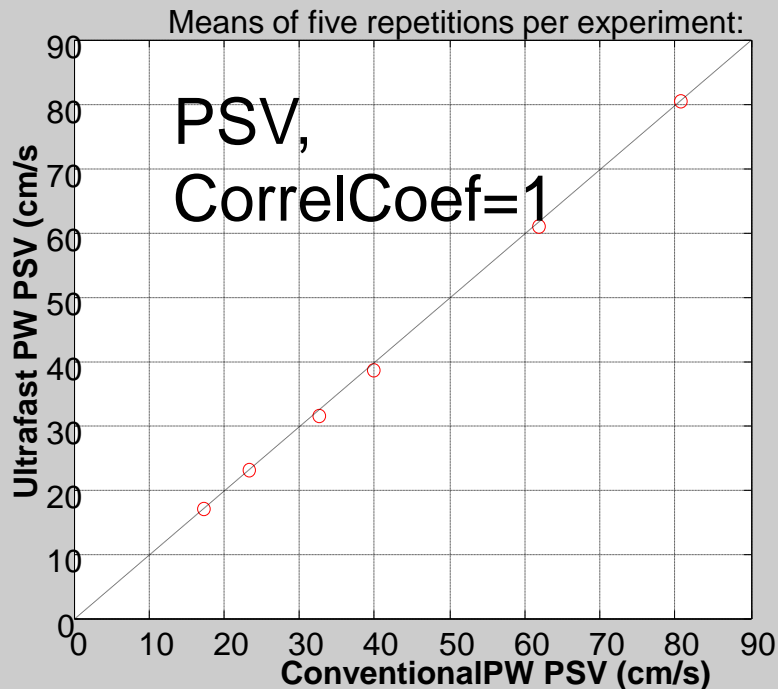
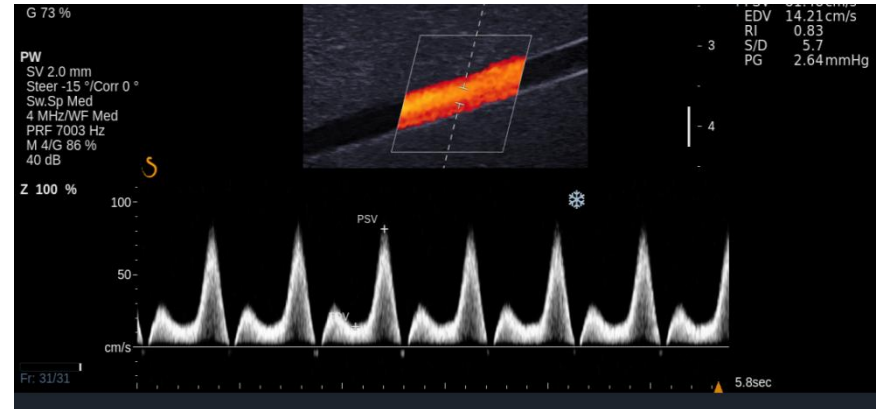
Bercoff, J.; Montaldo, G.; Loupas, T.; Savery, D.; Meziere, F.; Fink, M. & Tanter, M. (2011), 'Ultrafast Compound Doppler Imaging: Providing Full Blood Flow Characterization', *Ieee Trans. Ultr. Ferr. Frq. Ctrl*, 58(1)

Ultrafast Doppler: Full Retrospective analysis

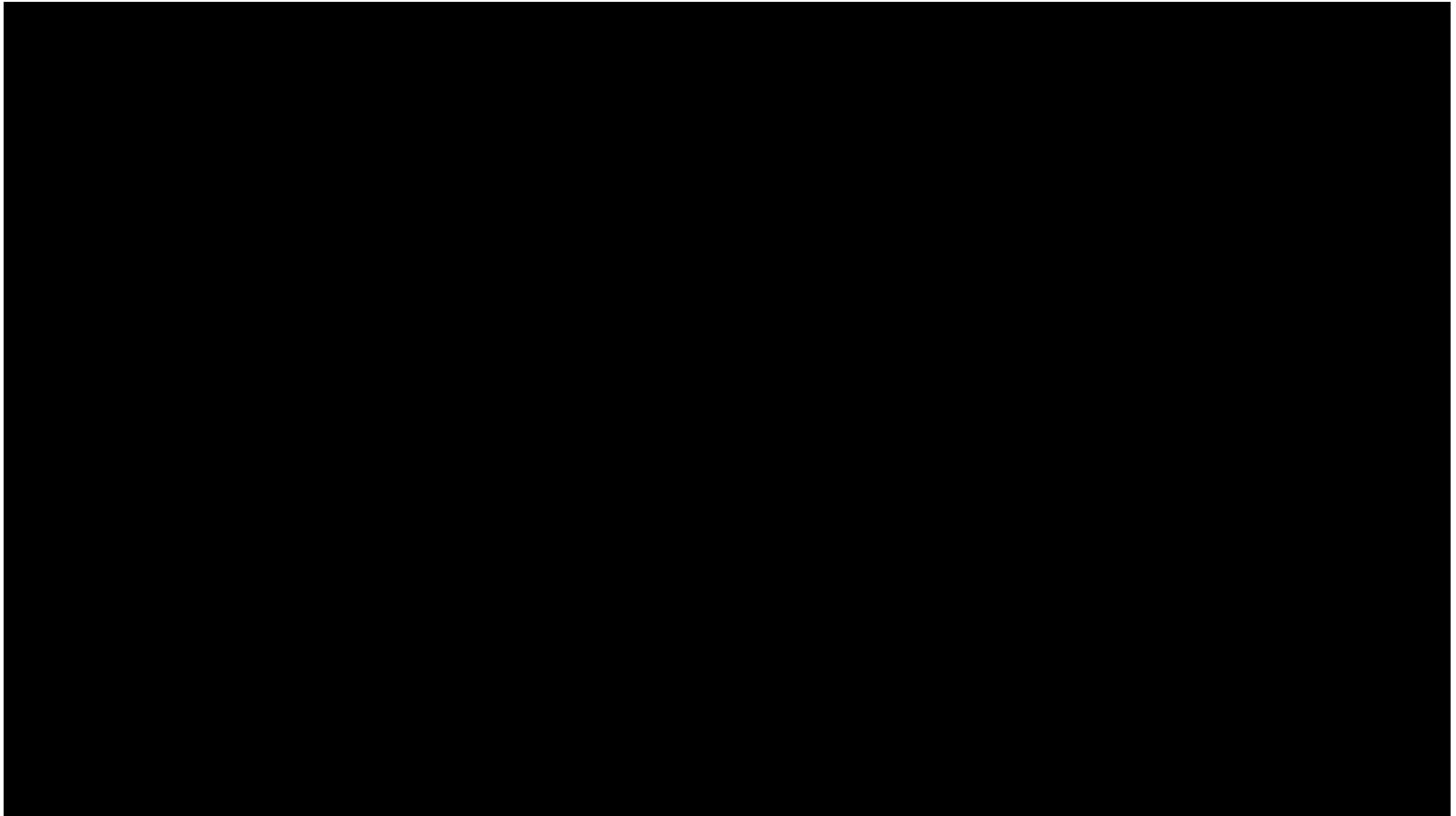


Ultrafast Doppler: Quantitative Validation

- Ultrafast PW vs Conventional PW

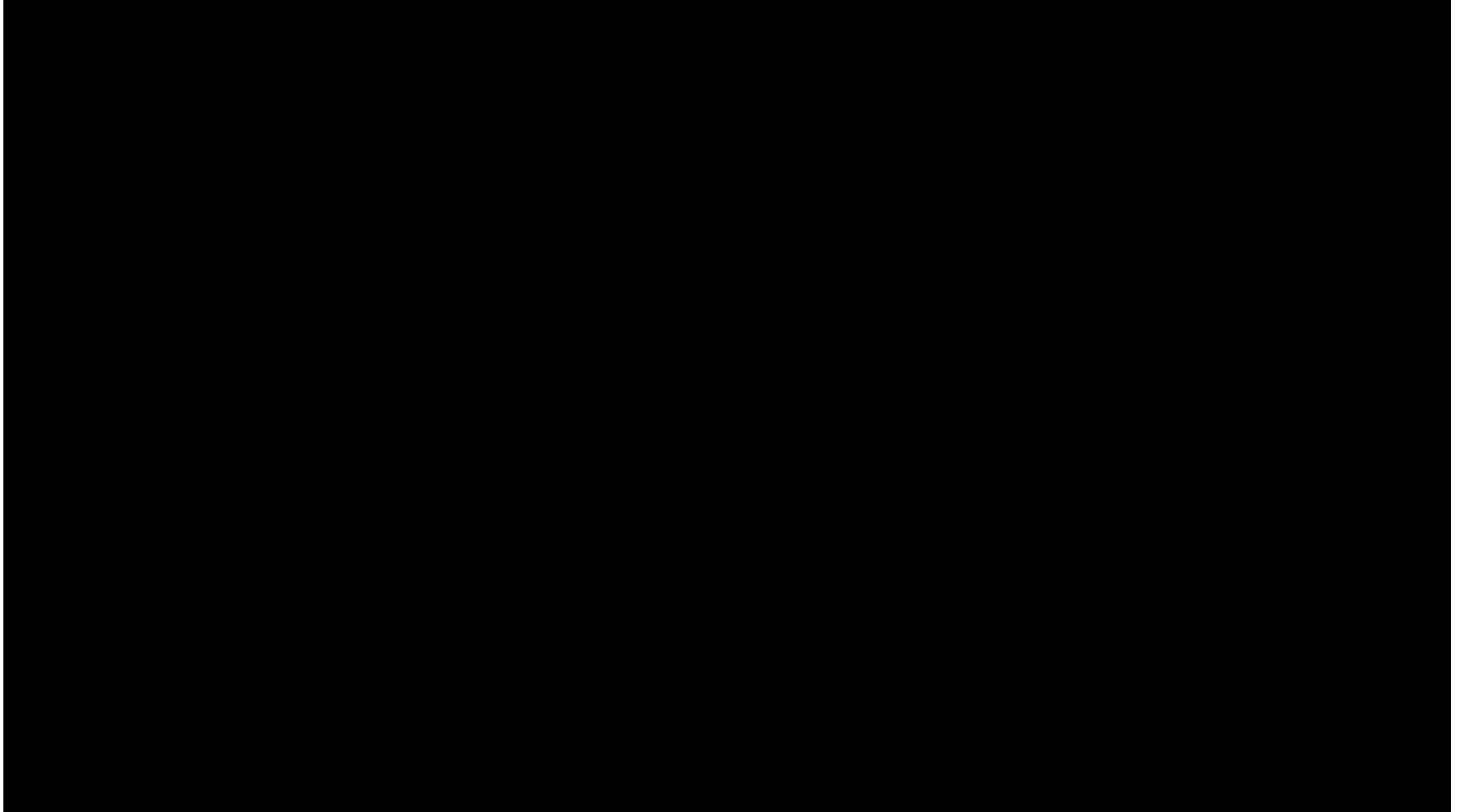


Example



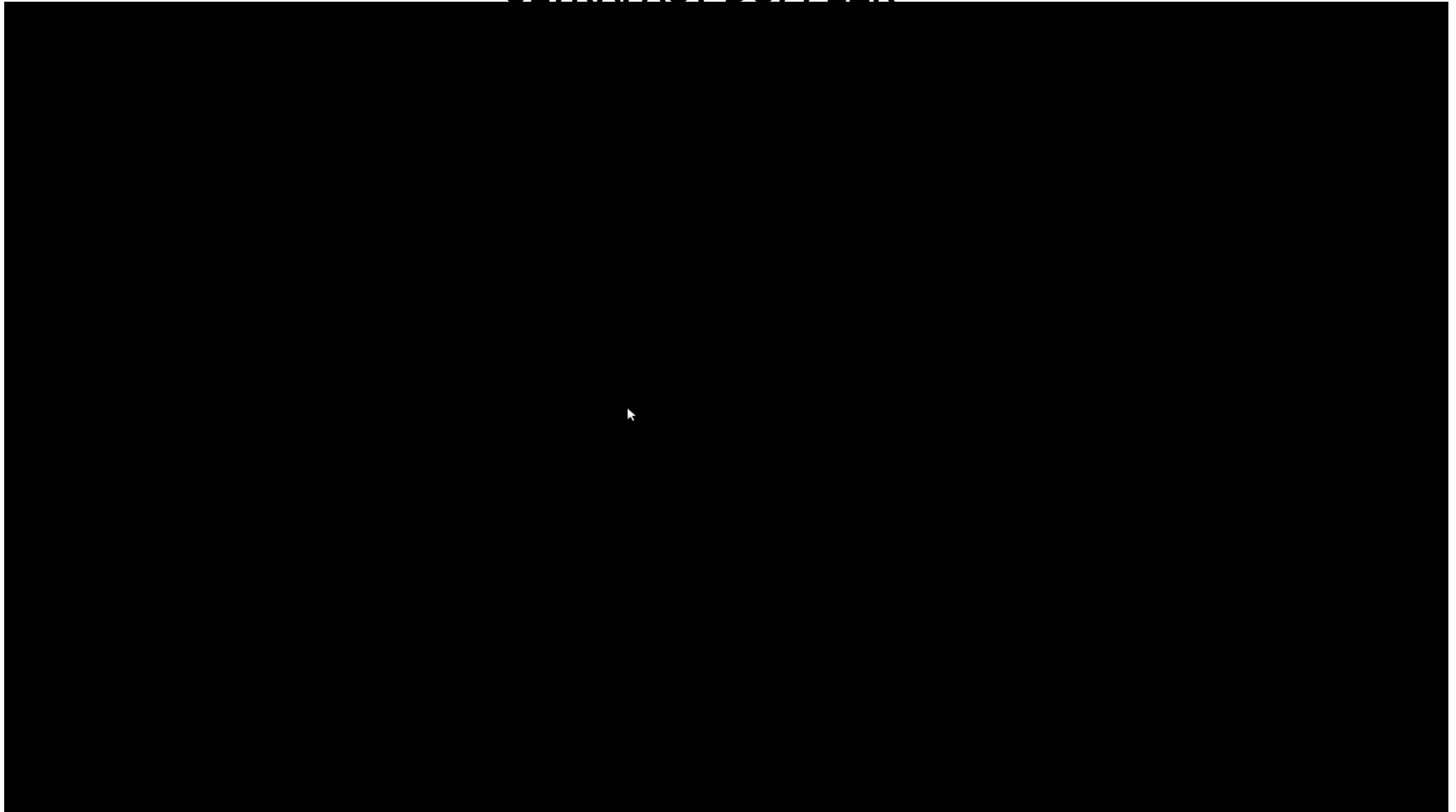
Improving visualisation of hemodynamics

STANDARD CFI

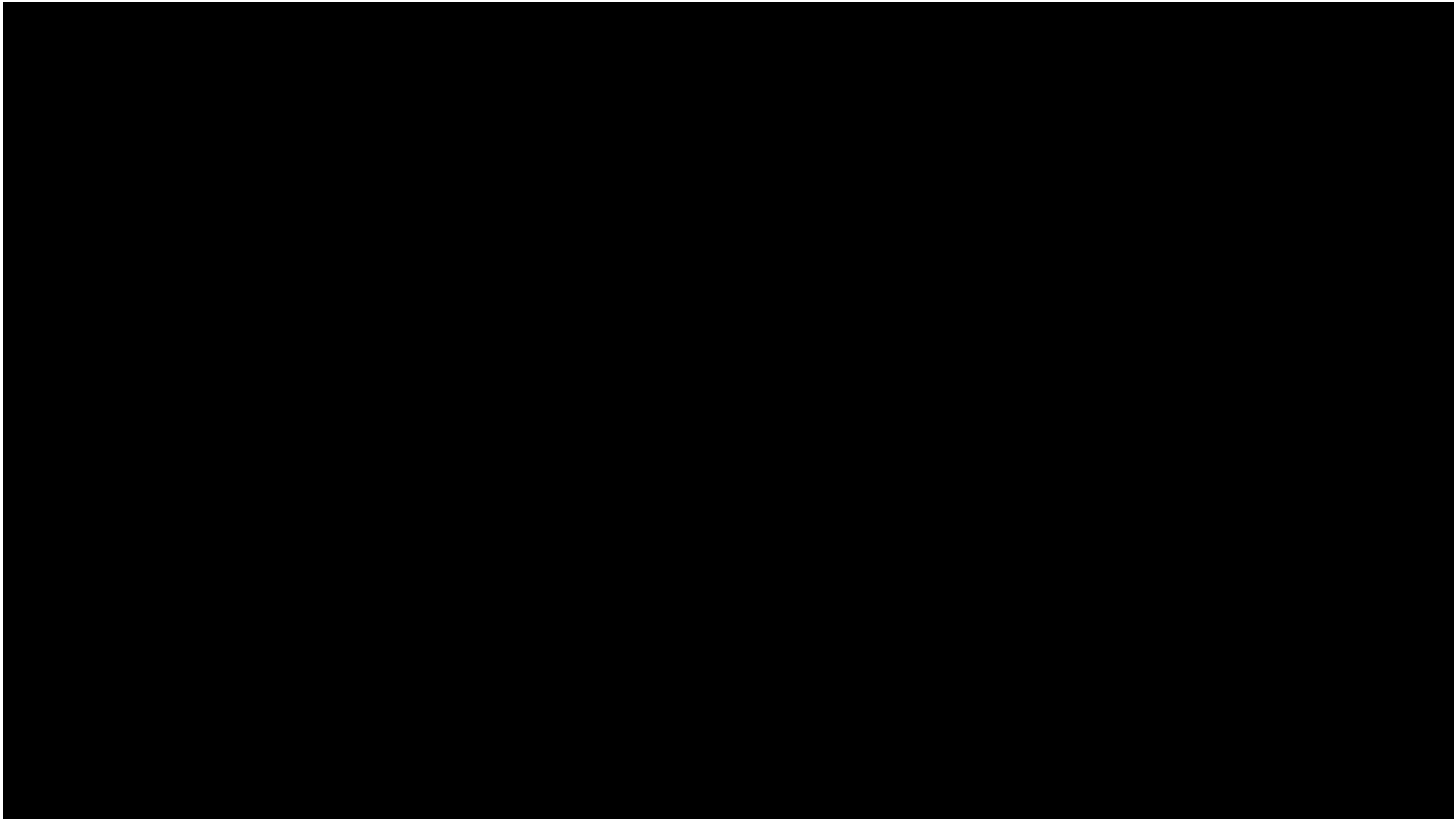


Improving visualisation of hemodynamics

ULTRAFAST DOPPLER



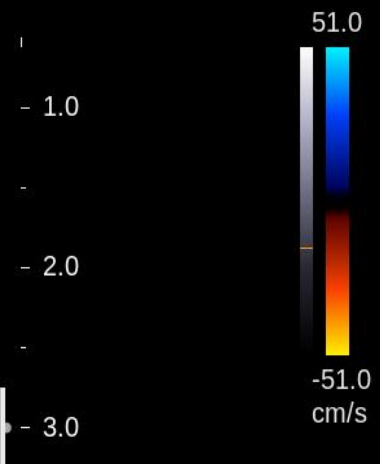
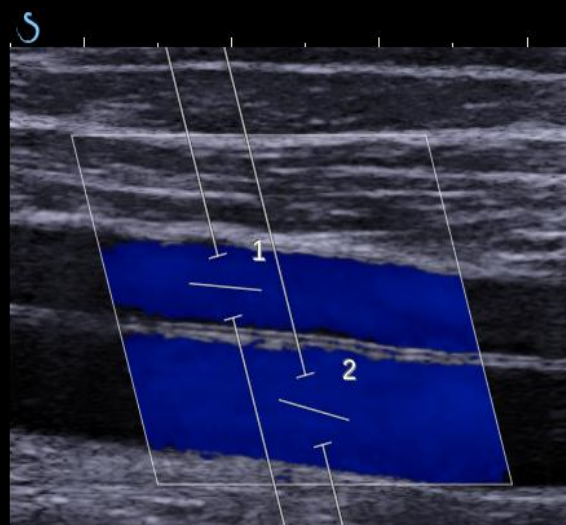
Full flow Characterization





B

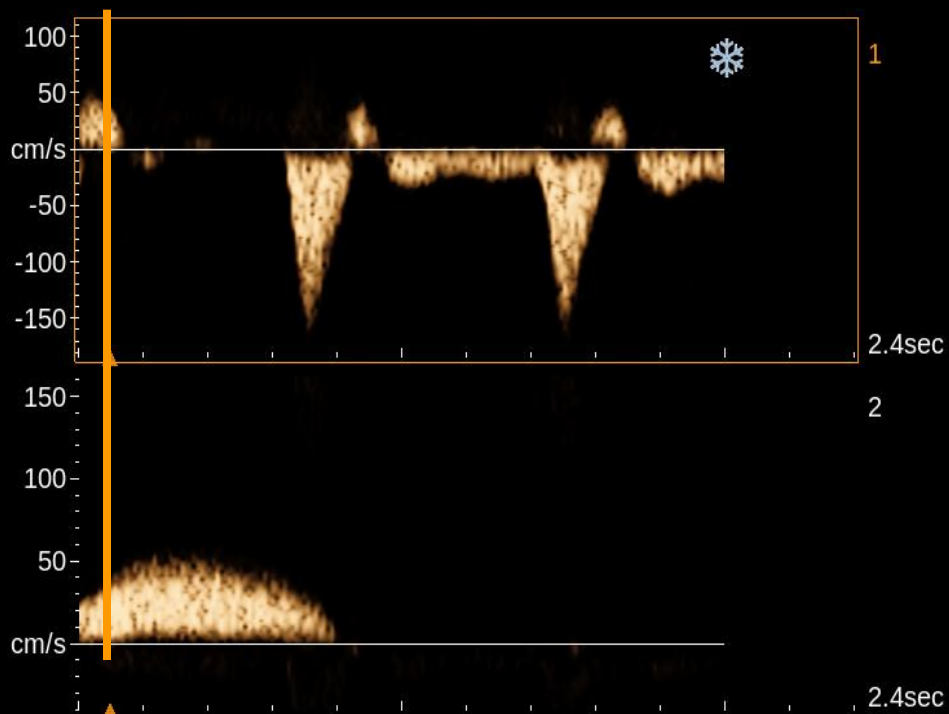
Gen/Med/H
M 6/67 dB/Low
T 1540 m/s
SC/SR 5
G 29 %
Fr. 83 Hz



CFI

Pen/HD
Off/WF Low
M 7/P. Med
Scale 51 cm/s
S 1
G 80 %

Z 150 %





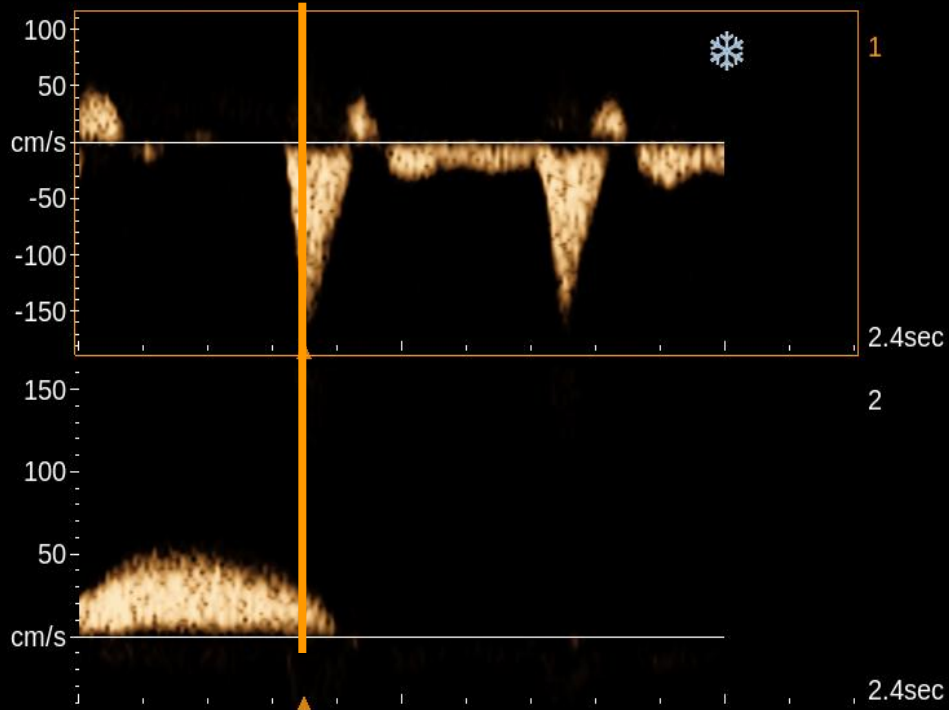
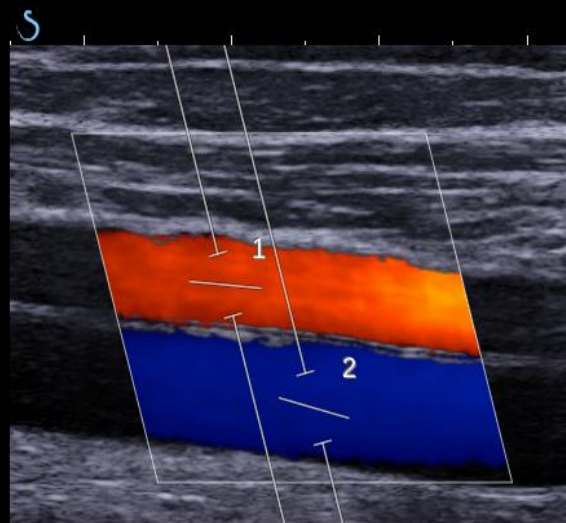
B

Gen/Med/H
M 6/67 dB/Low
T 1540 m/s
SC/SR 5
G 29 %
Fr. 83 Hz

CFI

Pen/HD
Off/WF Low
M 7/P. Med
Scale 51 cm/s
S 1
G 80 %

Z 150 %





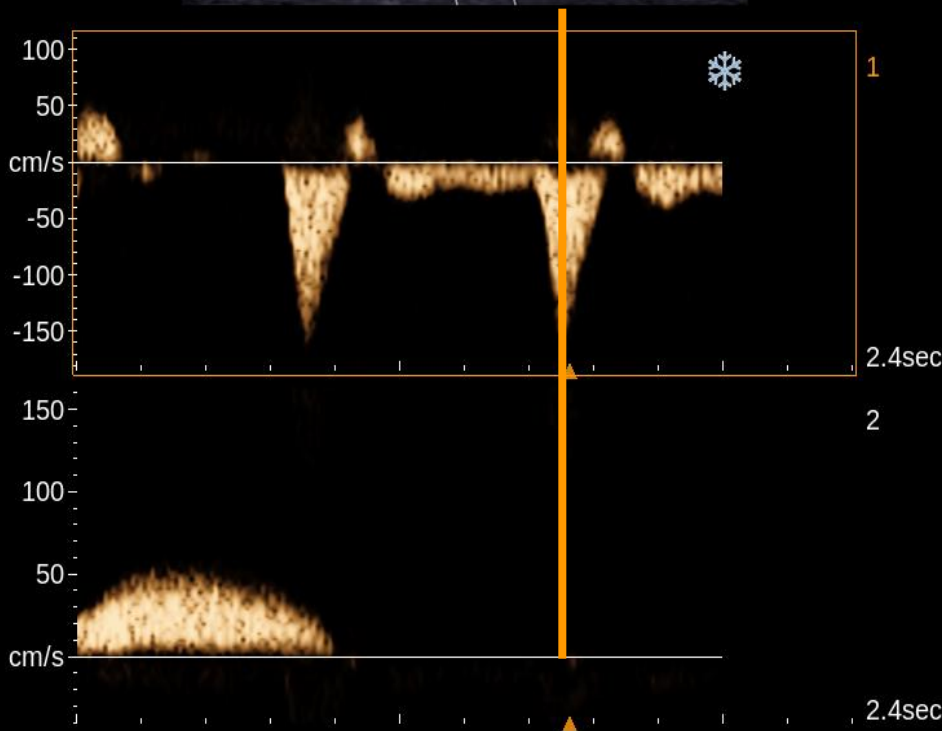
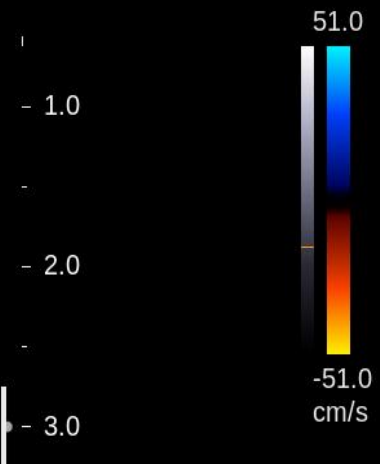
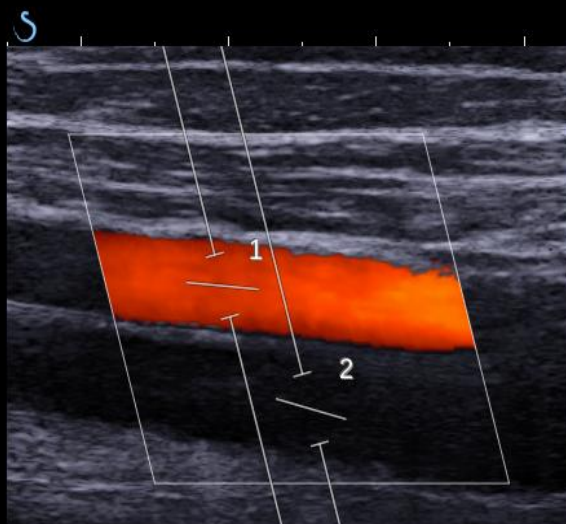
B

Gen/Med/H
M 6/67 dB/Low
T 1540 m/s
SC/SR 5
G 29 %
Fr. 83 Hz

CFI

Pen/HD
Off/WF Low
M 7/P. Med
Scale 51 cm/s
S 1
G 80 %

Z 150 %



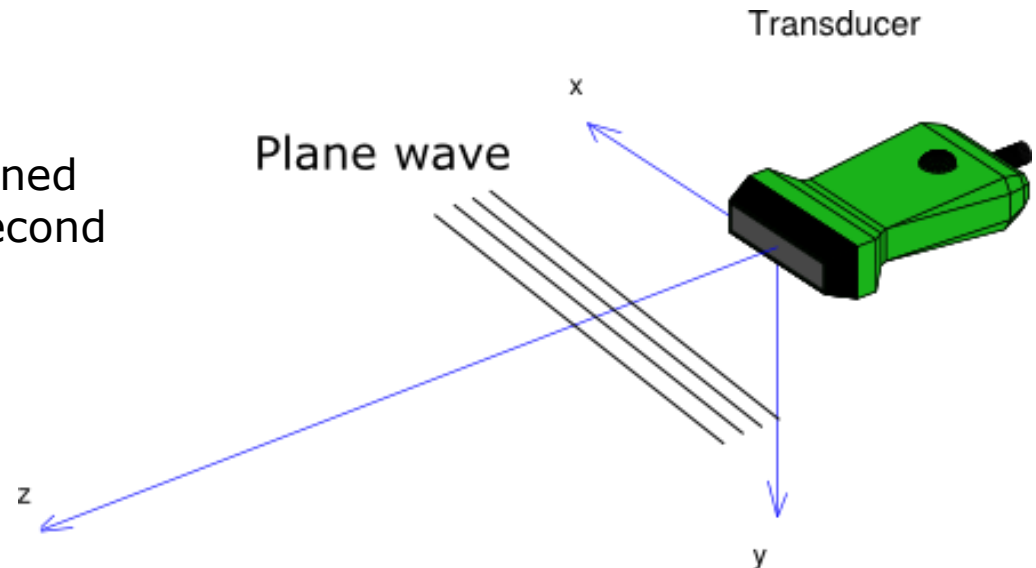
Ultrafast Vector Doppler Imaging

Courtesy of Jørgen Arendt Jensen

**Center for Fast Ultrasound Imaging
Department of Electrical Engineering
Technical University of Denmark**

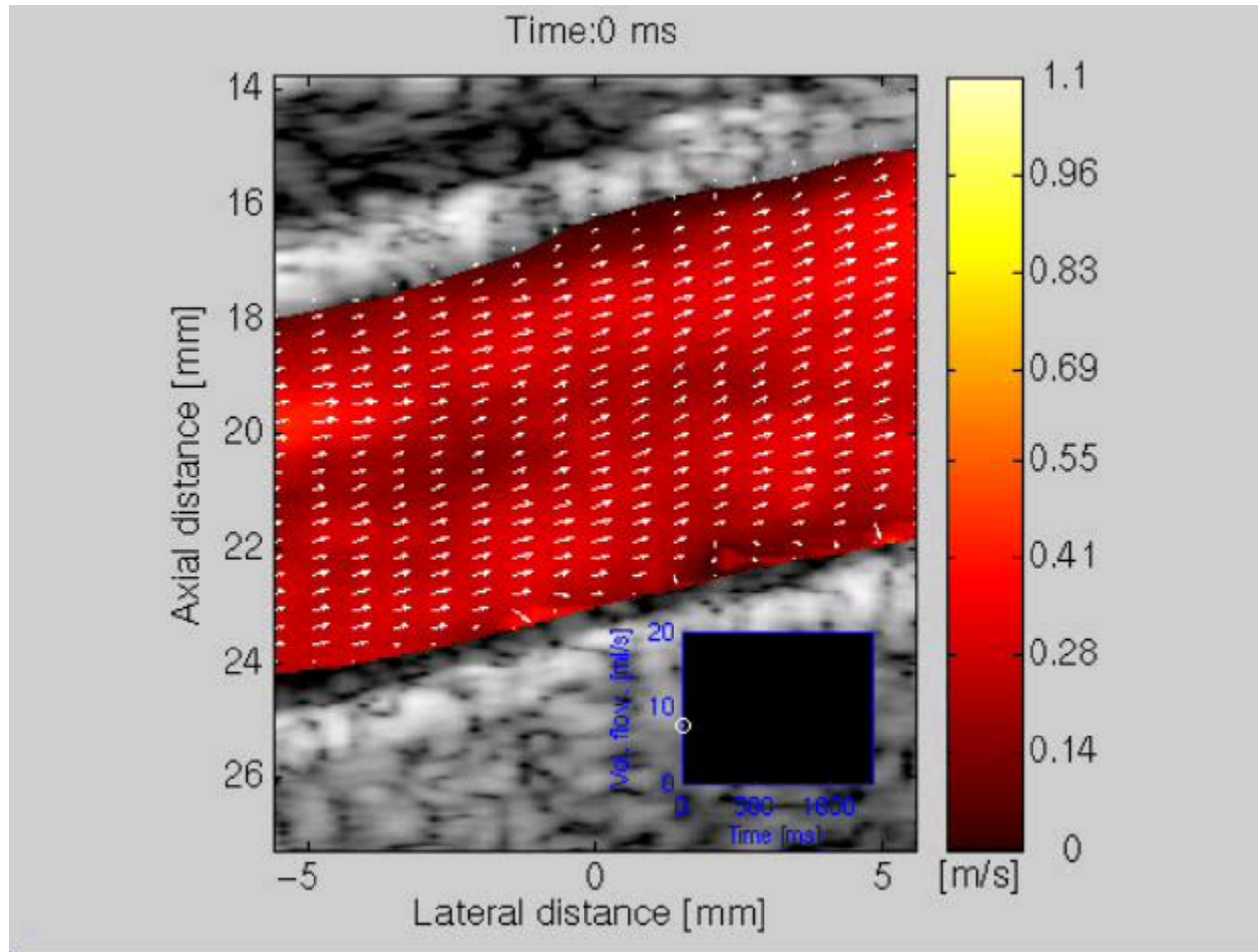
Fast plane wave imaging

- Single plane wave emitted
- Full image reconstructed from single emission
- Very fast imaging can be attained with thousand of image per second
- Flow imaging with excellent temporal resolution
- Vector flow imaging possible
- Implemented on the RASMUS experimental scanner
- Frame rate of more than 100 Hz



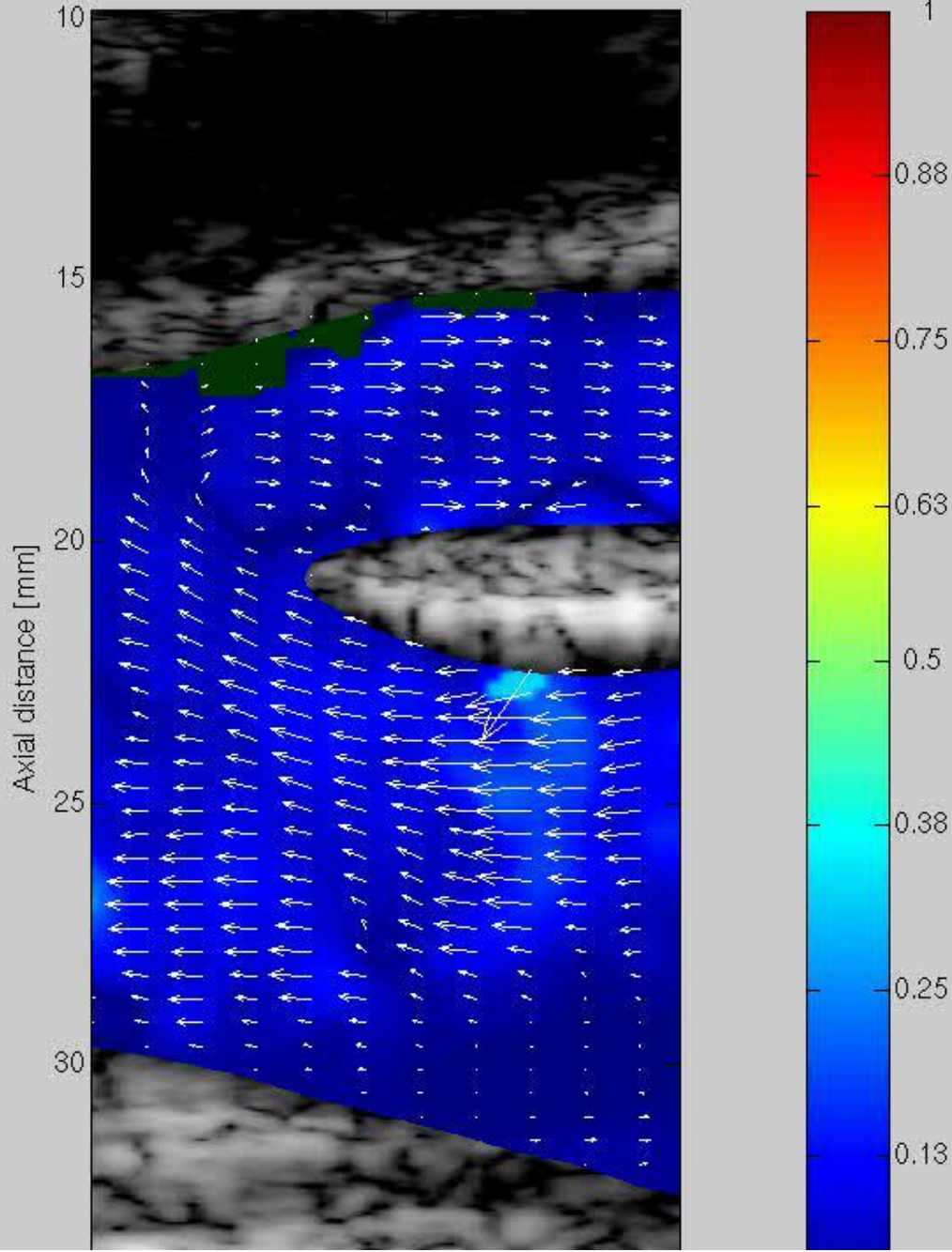
Udesen et al: 'High Frame-Rate Blood Vector Velocity Imaging Using Plane Waves: Simulations and Preliminary Experiments', IEEE UFFC, vol 55, no. 8, pp. 1729-1743, 2008.

Frame rate : 100 Hz, Common carotid artery



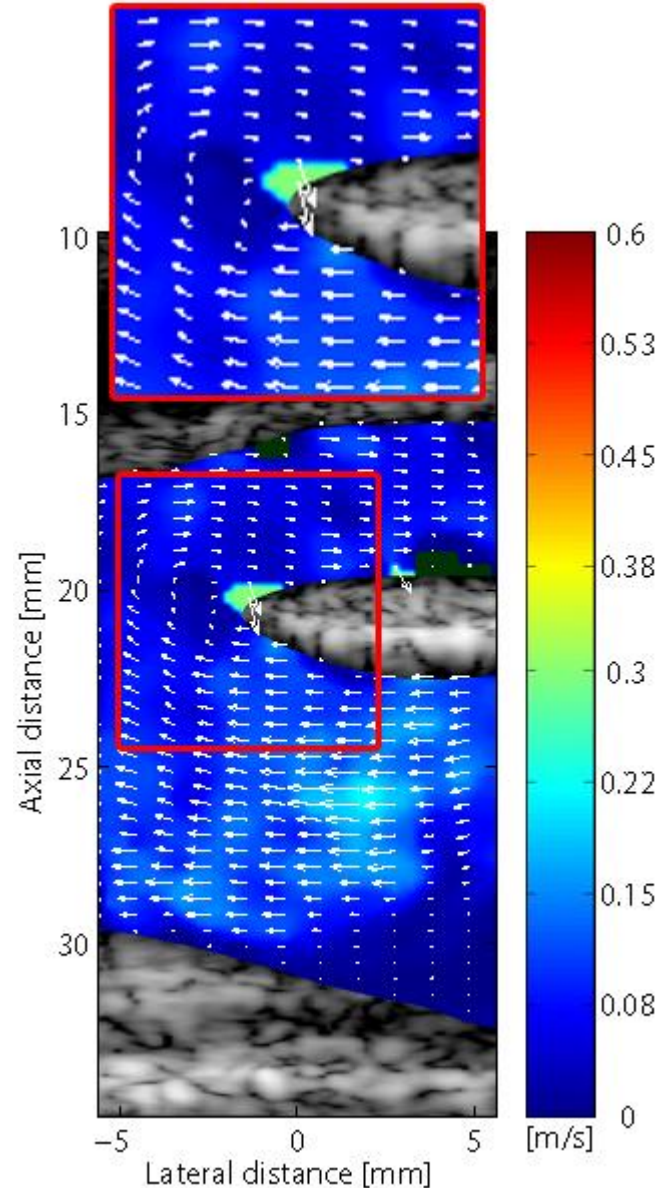
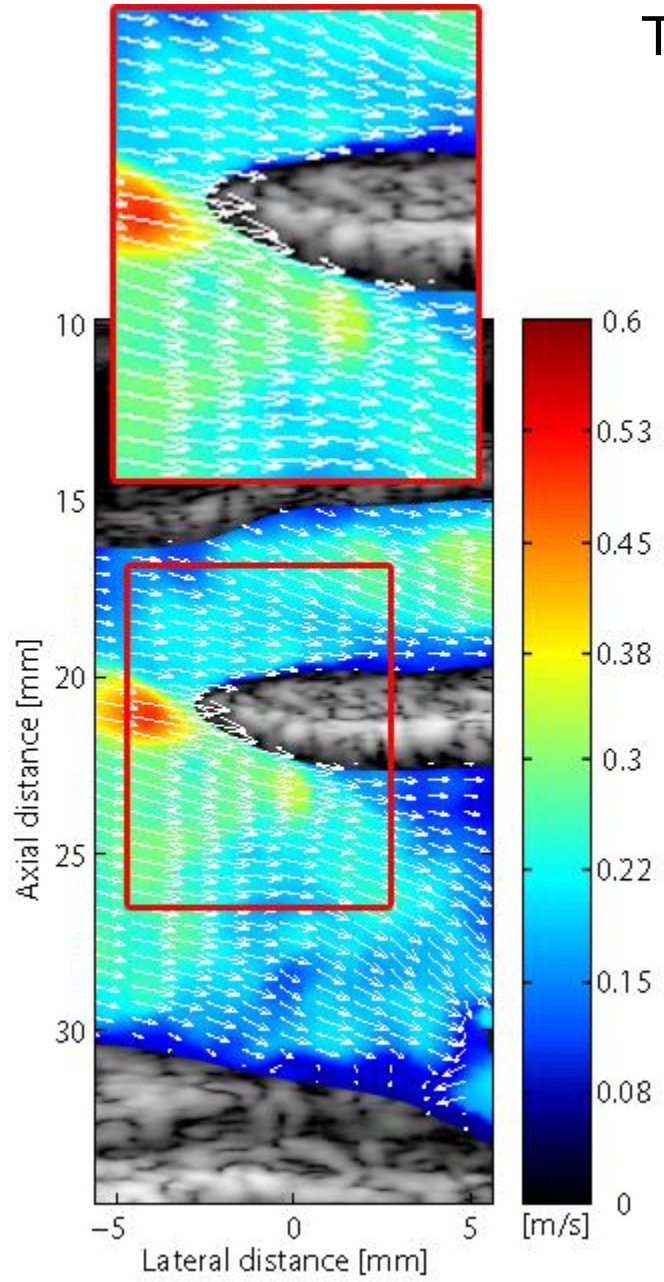
From Hansen et al: *In-vivo Examples of Flow Patterns With The Fast Vector Velocity Ultrasound Method* *Ultraschall in der Medizin*, vol 30, no. 5, pp. 471-477, 2009

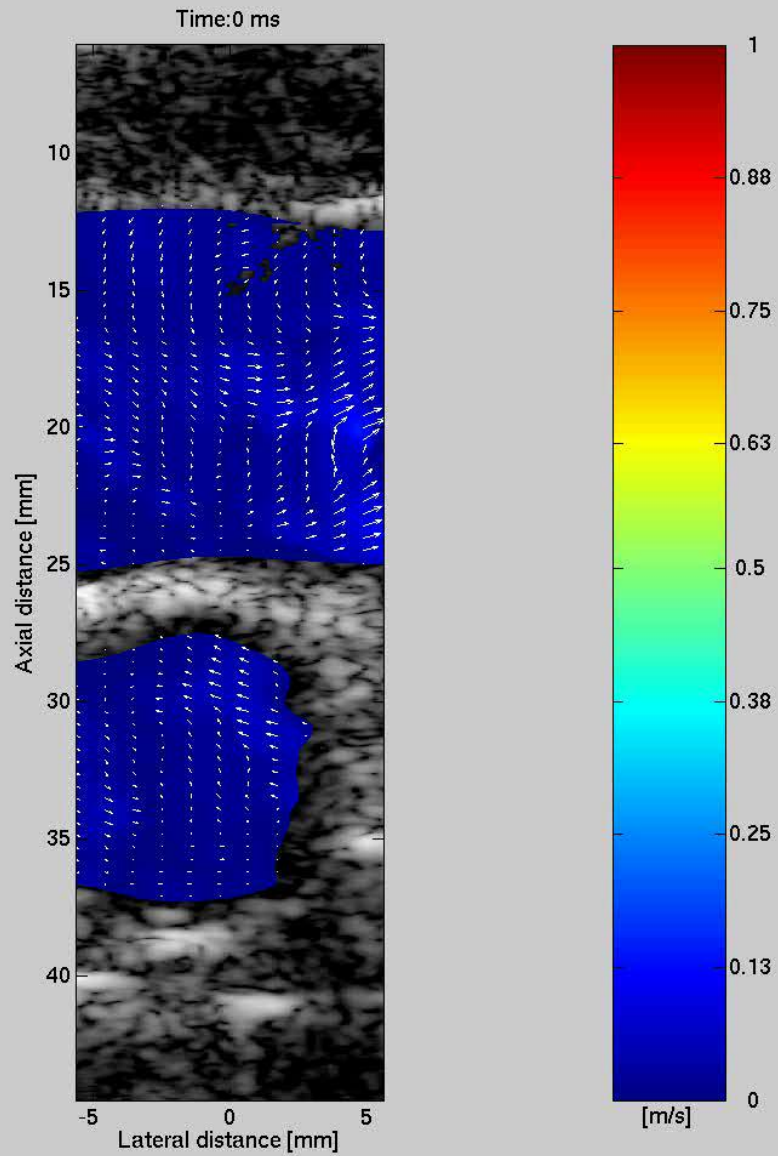
Echo min:37 Echo max:37 Time:0 ms



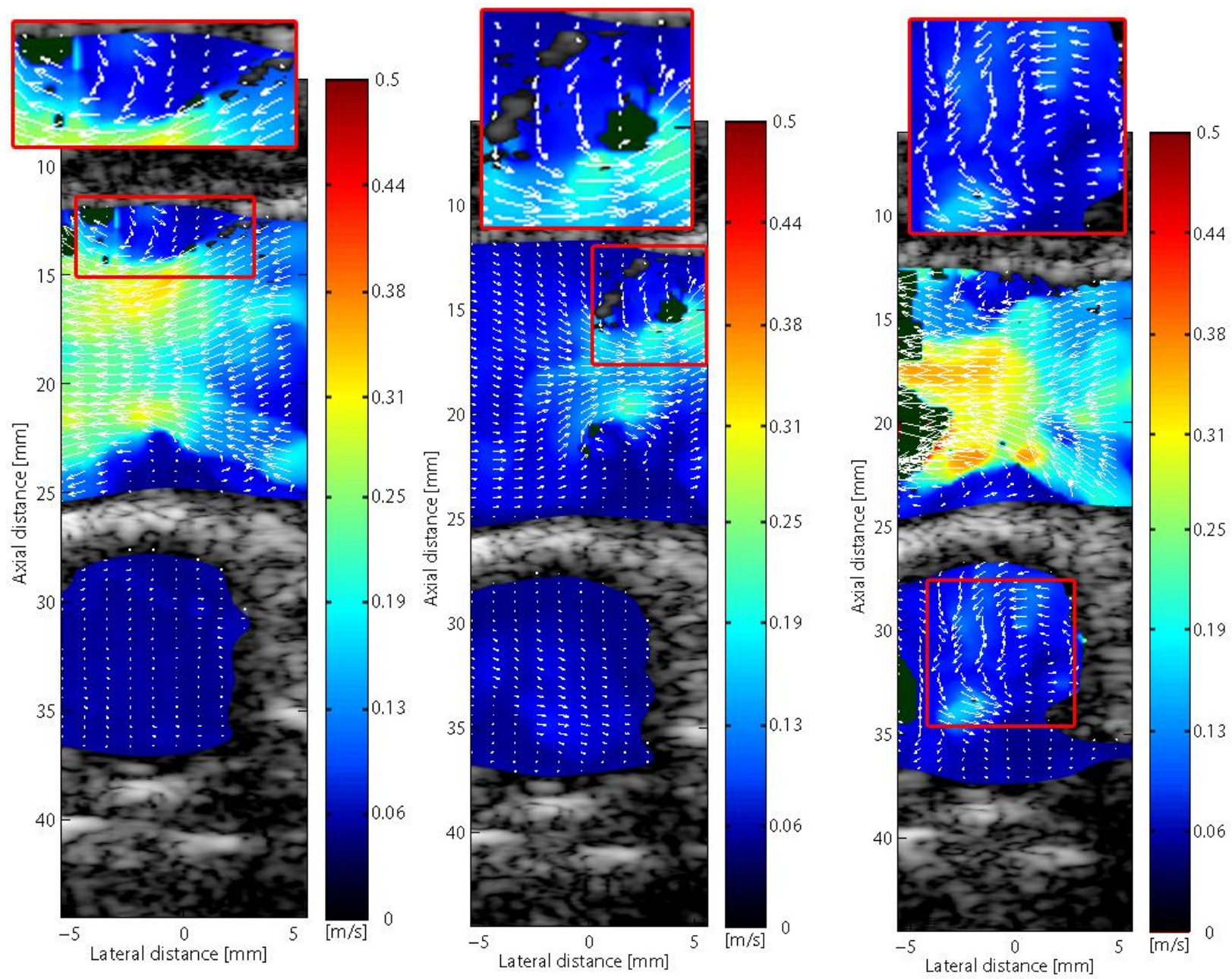
Truncus
brachiocephalic
a, a. subclavia
and
a. carotis com.

Truncus brachiocephalica



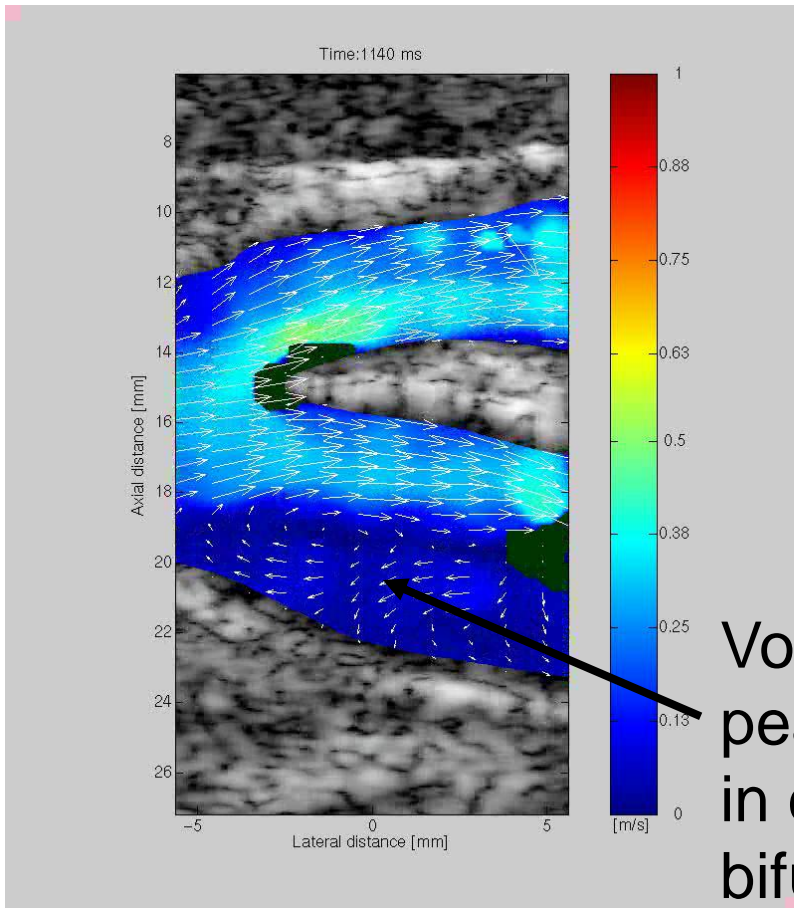


The jugular vein and carotid artery

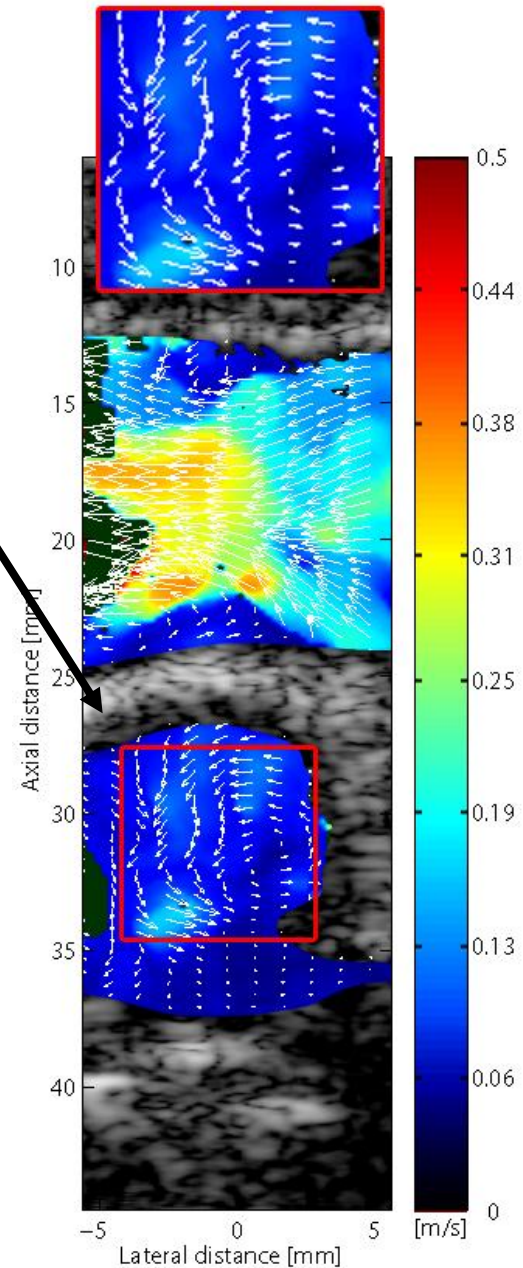


3D flow

Rotational flow in the carotid artery



Vortices after peak systole in carotid bifurcation



A more complex case : the Myocardium

Ultrafast Doppler Imaging of small flows in a fast moving organ ?

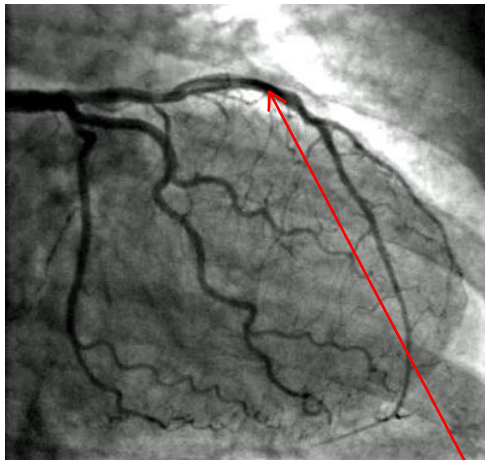
Myocardial Blood Flow Dynamics

Intramyocardial Blood Flow Dynamics

-> Early diagnosis of cardio-vascular diseases

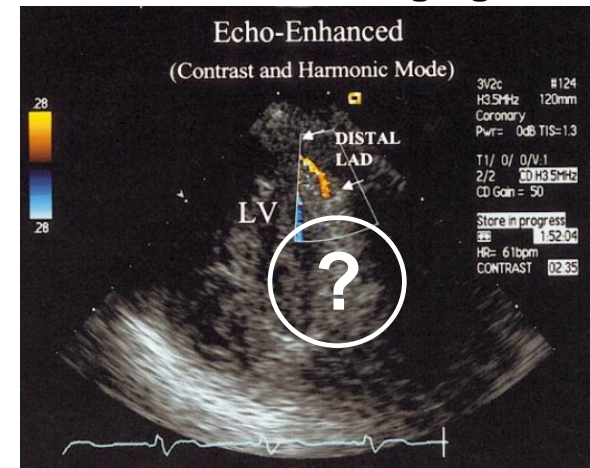
State of the Art

X ray coronarography



**Left Anterior Descending
Coronary Artery
(LAD)**

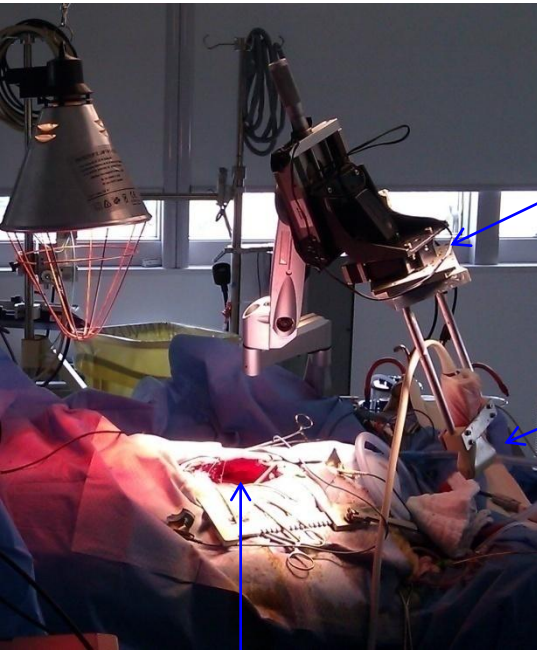
Ultrasound imaging



C. Caiati, Circulation (1999)

Ultrafast Imaging of the myocardium : Experimental Set-Up

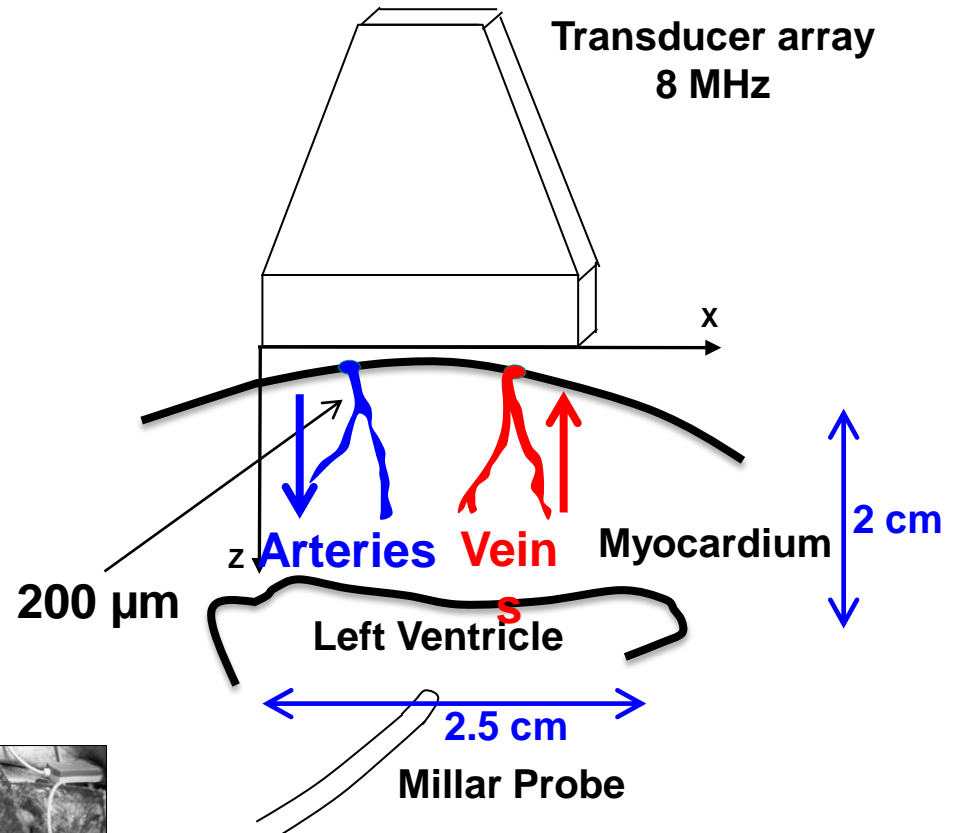
Results obtained on 5 sheeps



Metallic Arm

Acoustic probe

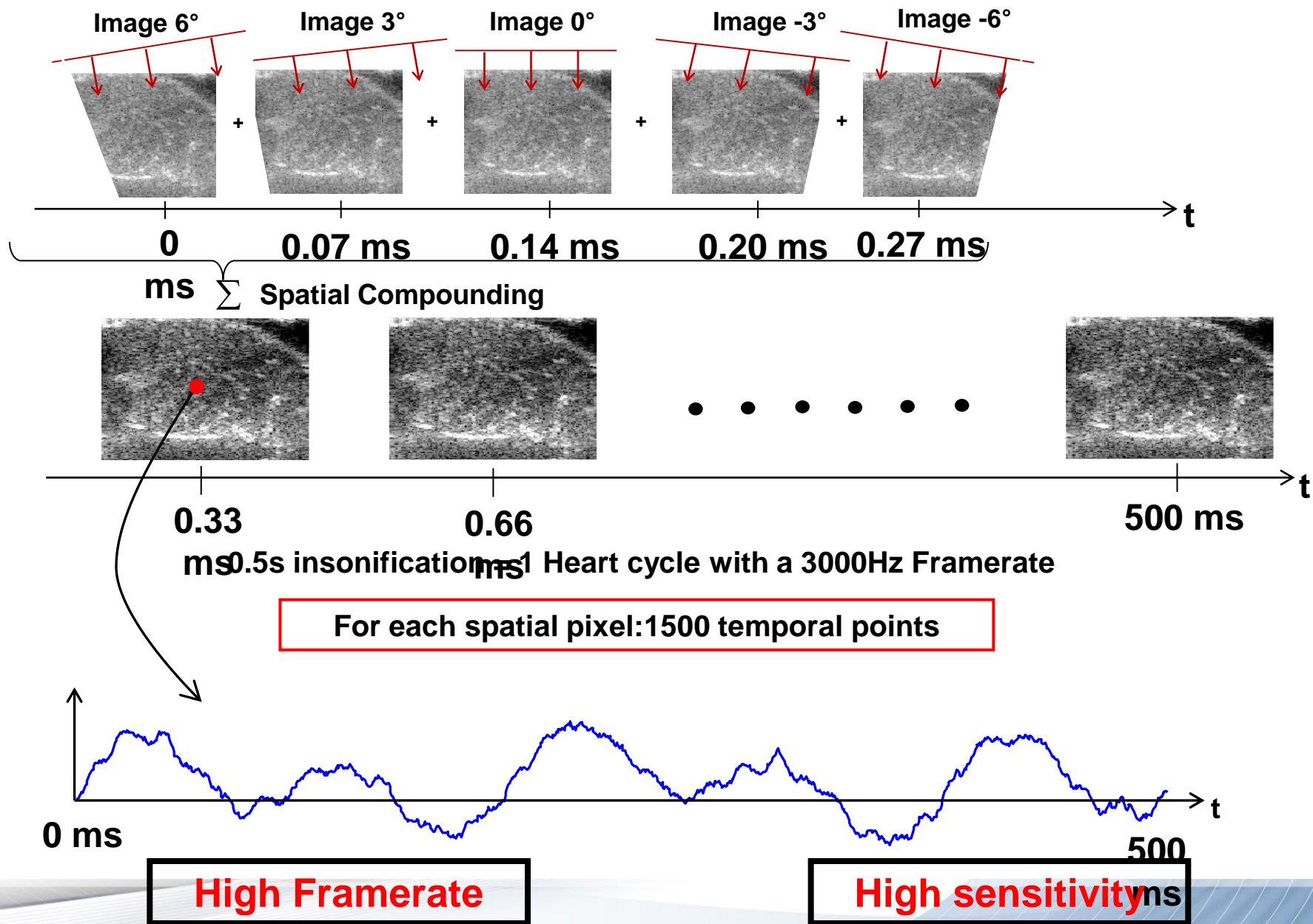
Chest Cavity



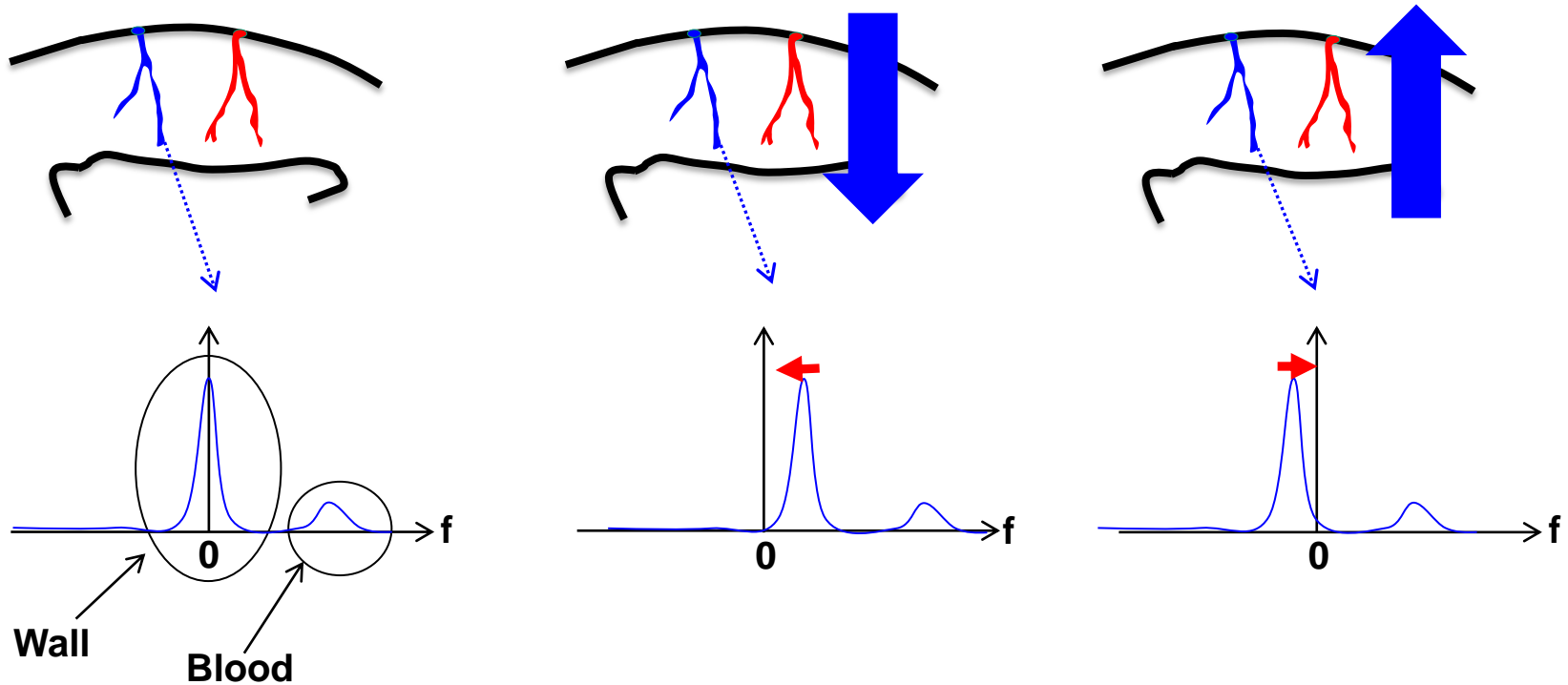
$V_{\text{Tissue}} \sim \text{cm/s}$

Ultrafast Acquisition

Ultrafast Imaging of the myocardium : acquisition sequence



Fast tissue Motion = additional Frequency Modulation



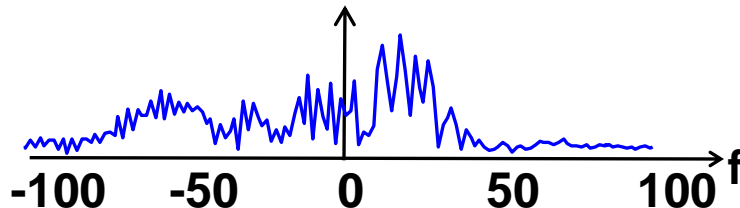
Solution = Frequency Demodulation

Ultrafast Imaging of the myocardium : demodulation process

In-Phase Quadrature Data
Temporal signal of a spatial pixel

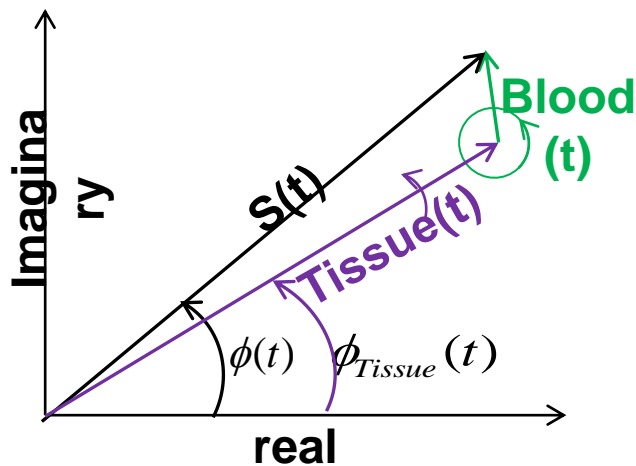
$$s(t) = A(t)e^{j\phi(t)}$$

$$FFT\{s(t)\} = FFT\{A(t)\} \otimes FFT\{e^{j\phi(t)}\}$$



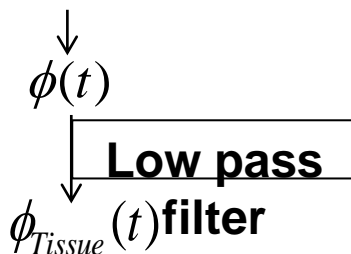
$$Arg\{s(t)\} = \phi(t) \longrightarrow \cancel{s_{dem}(t) = s(t)e^{-j\phi(t)} = A(t)}$$

$$s_{dem}(t) = s(t)e^{-j\phi_{Tissue}(t)}$$

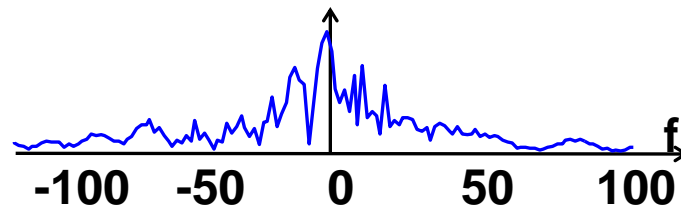


$$\phi(t) = \phi_{Tissue}(t) + \phi_{HF}(t)$$

Tissue and blood signal



$$FFT\{s_{dem}(t)\}$$

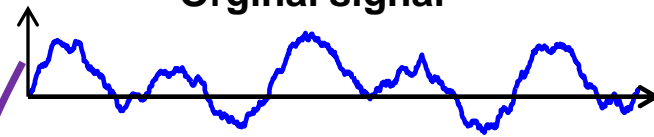


Signed Power Doppler: discriminate arteries and Veins

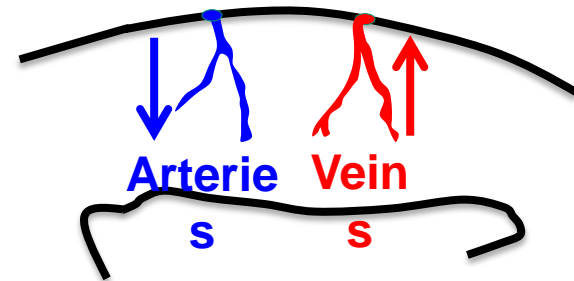
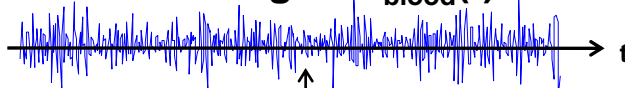
Demodulation

Wall Filtering

Original signal

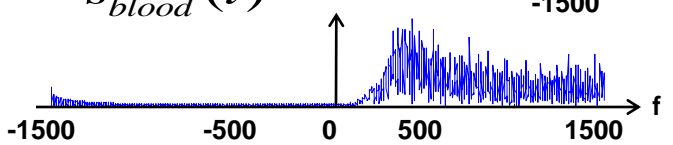


Blood signal $s_{\text{blood}}(t)$



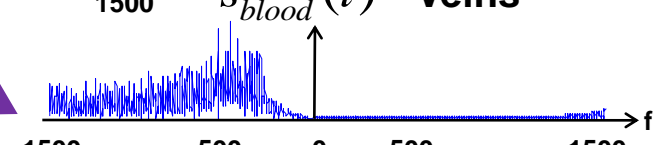
$S_{\text{blood}}^{\text{down}}(t)$

Arteries



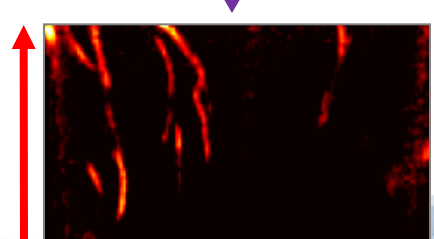
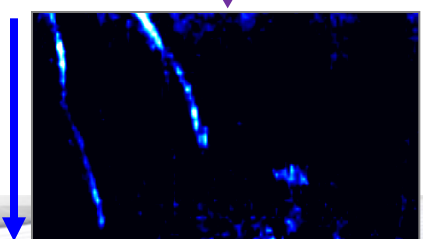
$S_{\text{blood}}^{\text{up}}(t)$

Veins

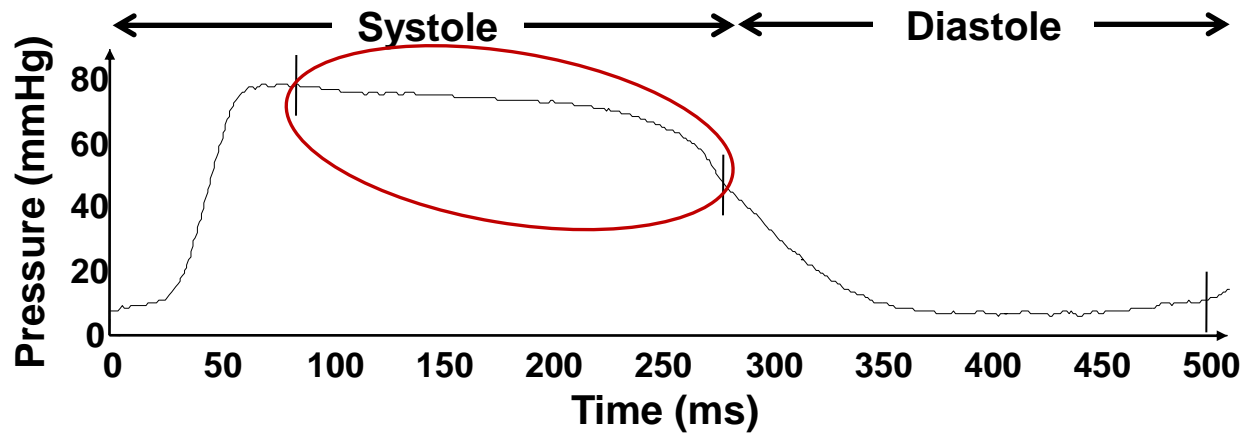


$$I_{\text{blood}}^{\text{down}}(t) = \frac{1}{T} \int_t^{t+T} |s_{\text{blood}}^{\text{down}}(\tau)|^2 d\tau$$

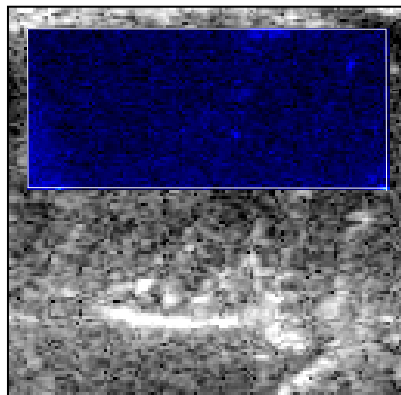
$$I_{\text{blood}}^{\text{up}}(t) = \frac{1}{T} \int_t^{t+T} |s_{\text{blood}}^{\text{up}}(\tau)|^2 d\tau$$



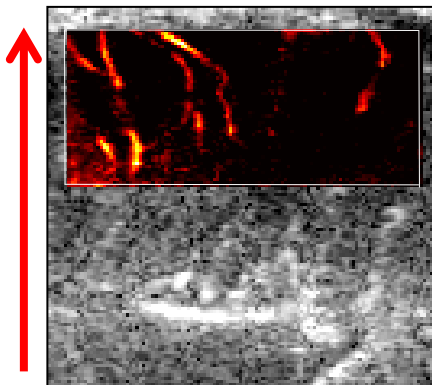
Ultrafast Imaging of the myocardium : systole ejection



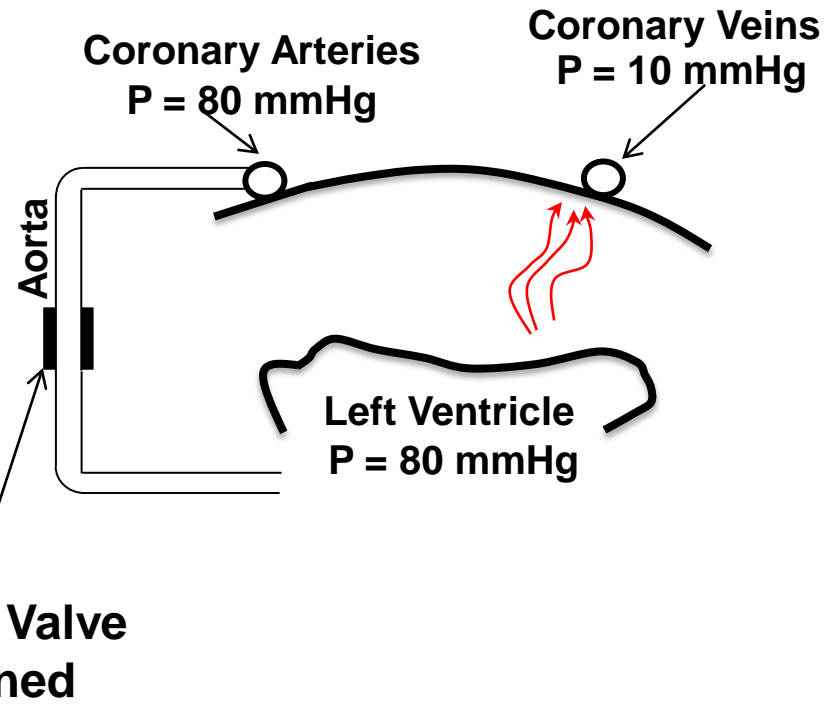
Signed Power Doppler



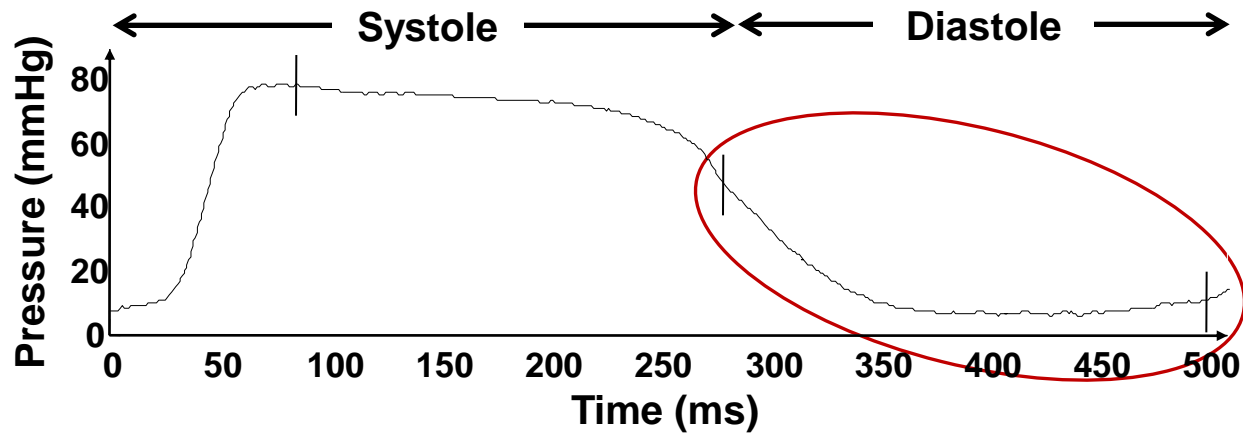
Arteries



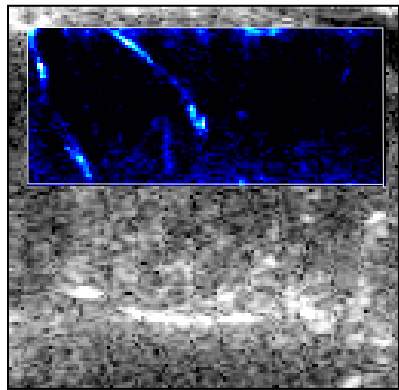
Veins



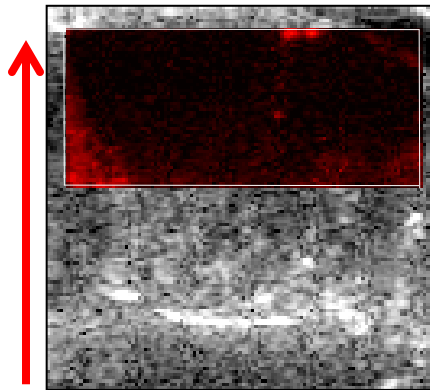
Ultrafast Imaging of the myocardium : Diastole



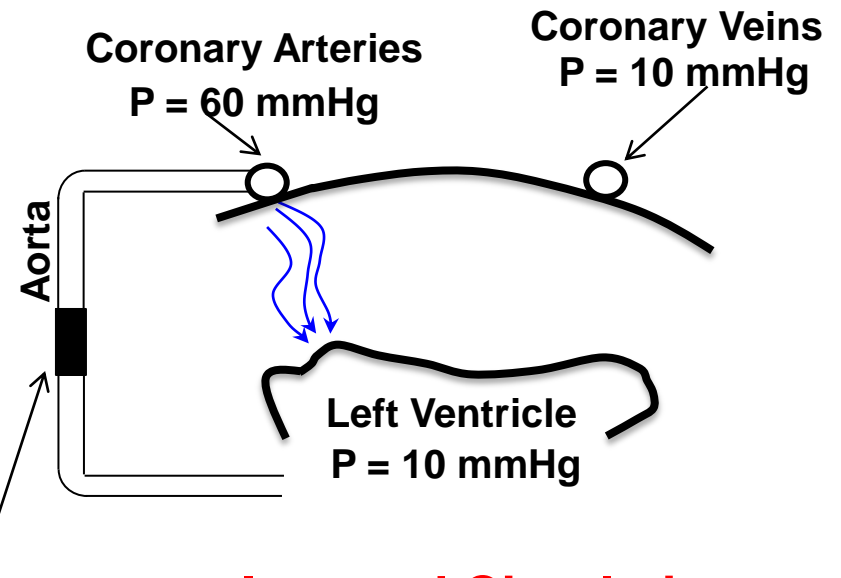
Signed Power Doppler



Arteries



Veins

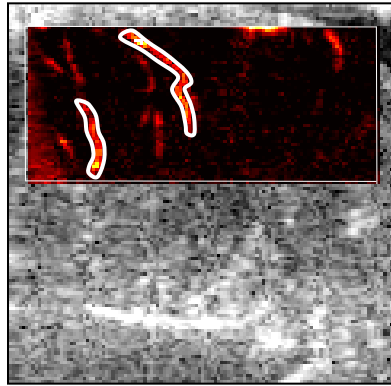


Aortic Valve closed

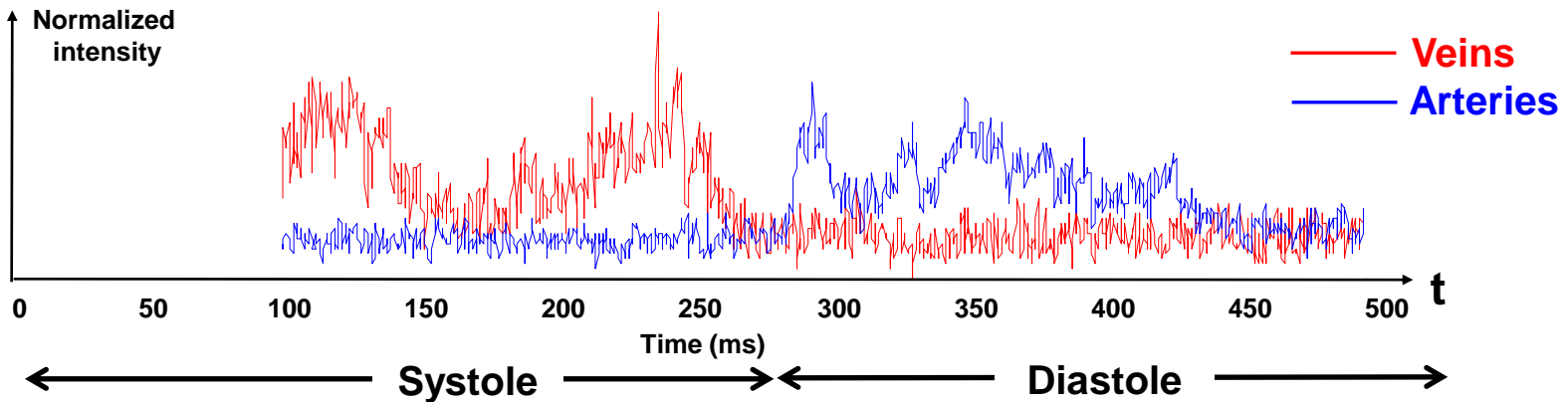
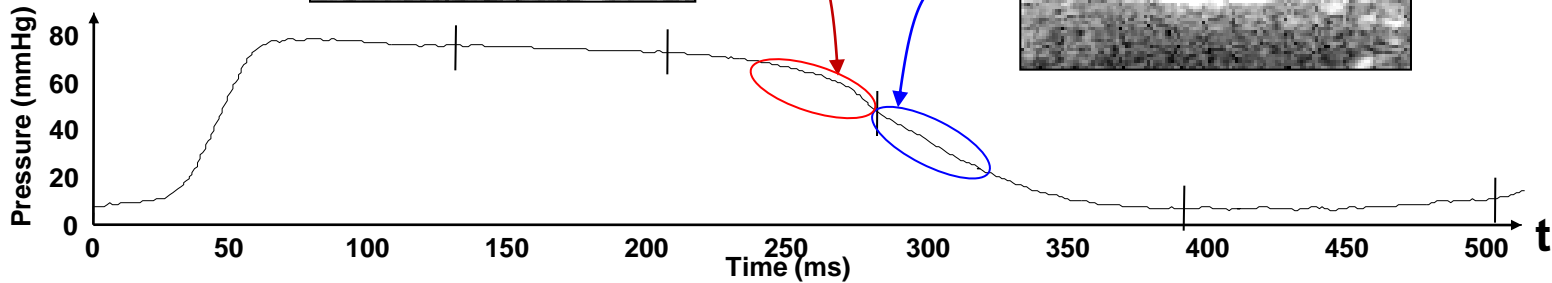
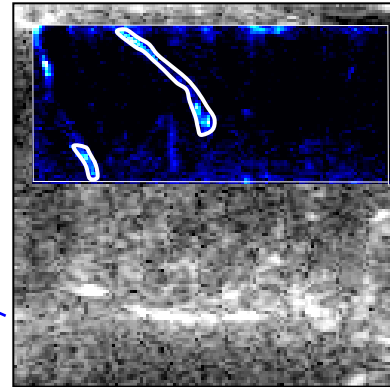
Inverted Circulation

Transition between Arterial and Venous Flow

End of Systole (Venous Flow)



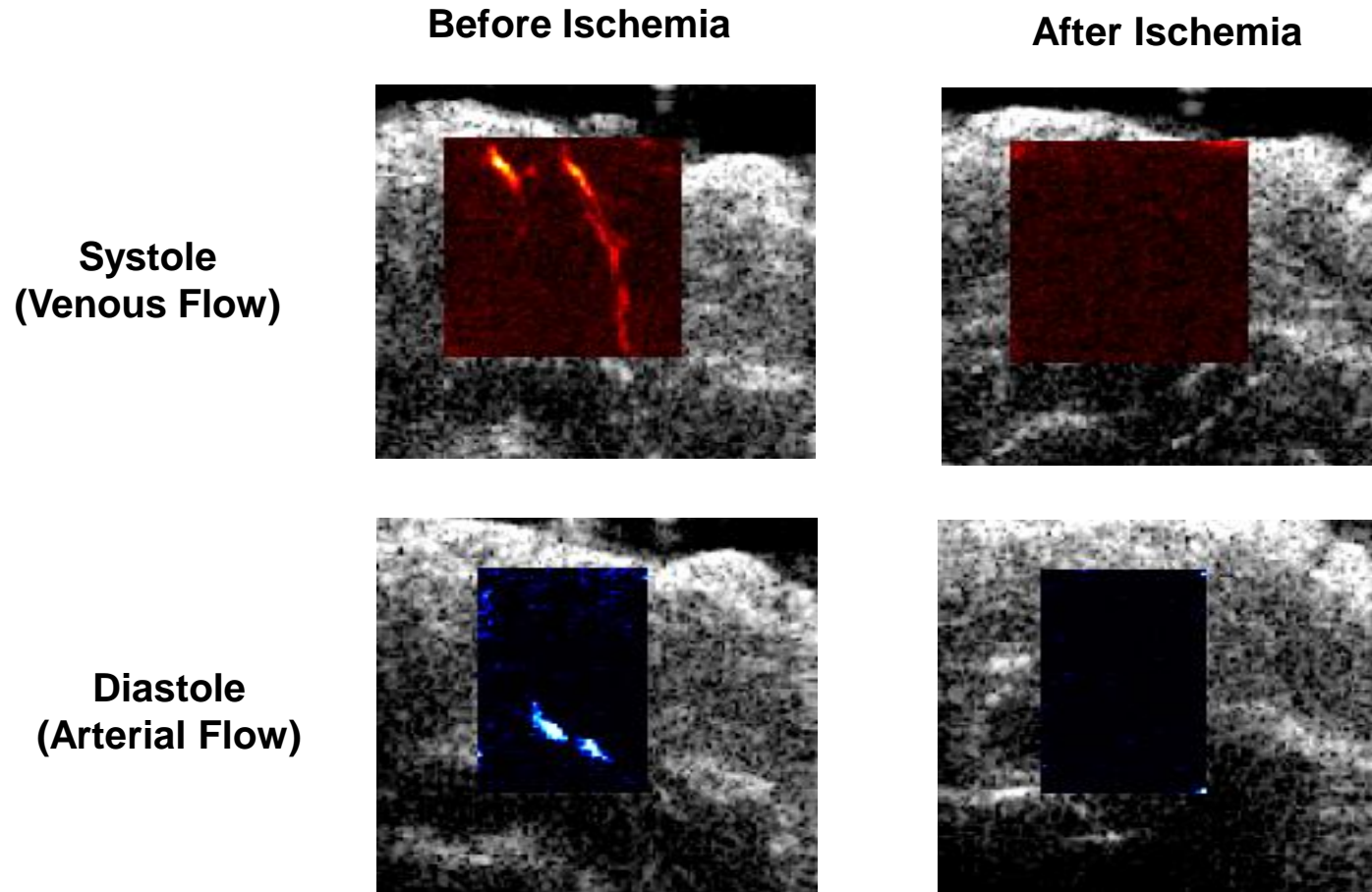
Beginning of Diastole (Arterial Flow)



Phase Opposition Waveform

Ultrafast Imaging of the myocardium : ischemia

Occlusion of two main epicardial coronary arteries upstream the imaging plane

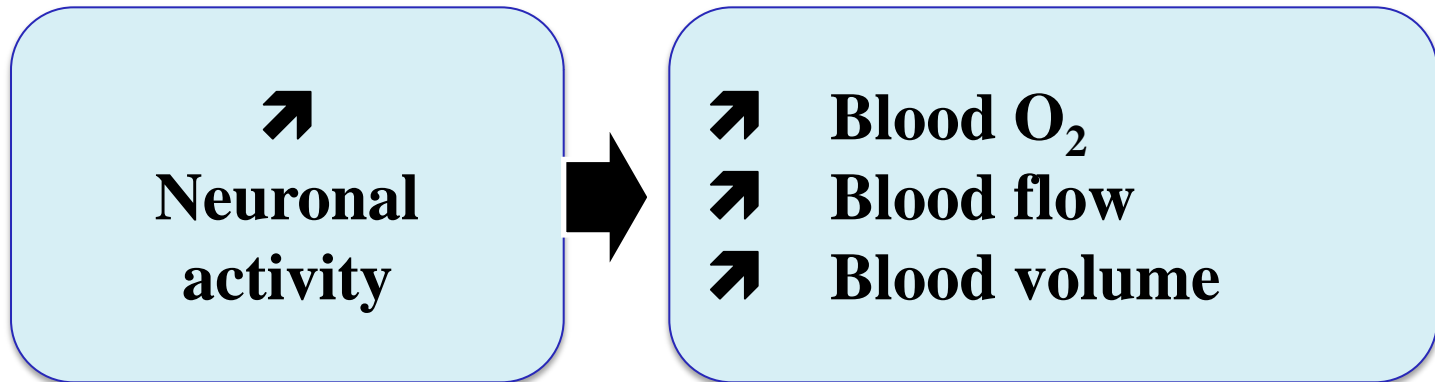


Ultrafast Doppler for *f*Ultrasound :

Functional Ultrasound Imaging of brain Activity

How to image the brain in action?

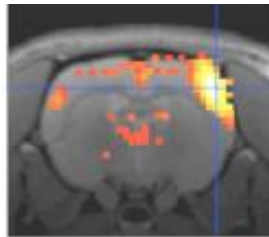
Neurovascular coupling



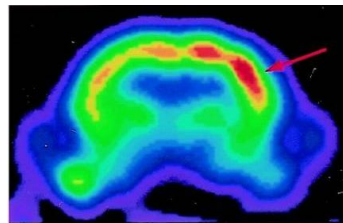
Blood changes → Indirect image of brain activation

Functional imaging techniques

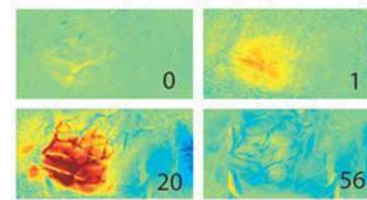
fMRI



PET



Optical
imaging



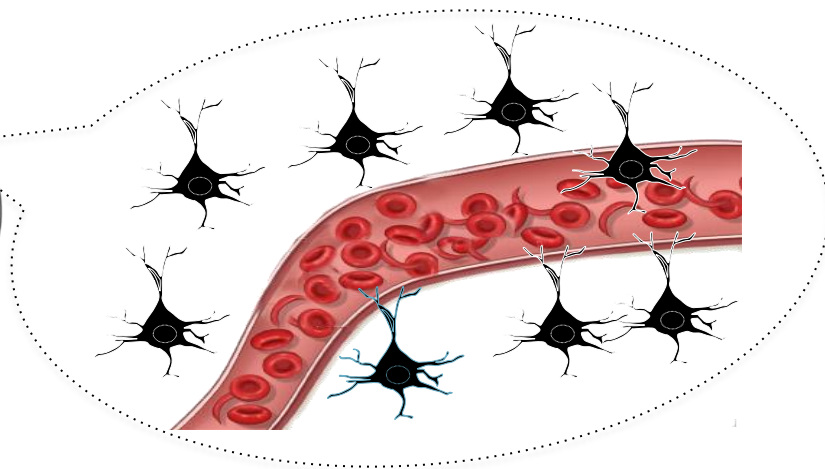
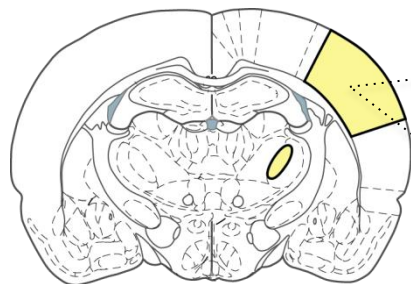
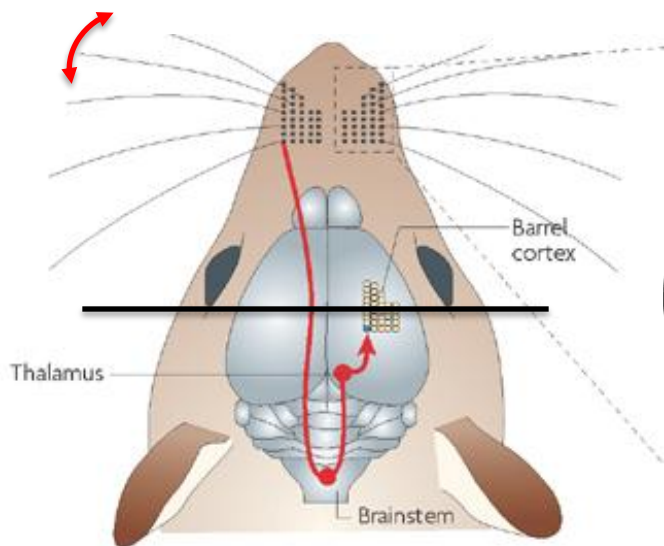
Doppler
ultrasound

?

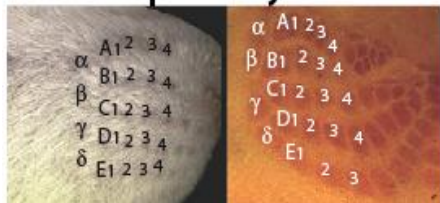
Penetration	✓✓	✓✓	✗	
Spatial resolution	✓	✗	✓✓	
Temporal resolution	✗	✗	✓✓	
Sensitivity (SNR)	✗	✓	✓	

Functional ultrasound (fUS) overcomes the poor sensitivity of Doppler ultrasound

A classical model of brain activation: whisker stimulation



whisker pad **layer 4 cortex**



Stimulus

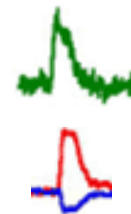


Neurons



electrical potential

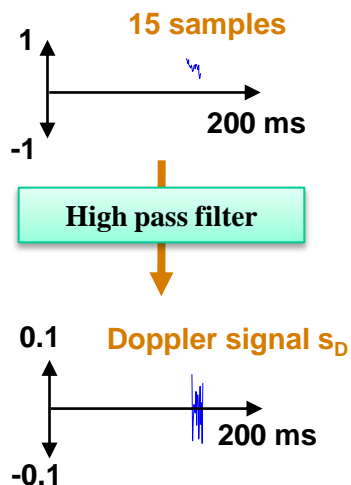
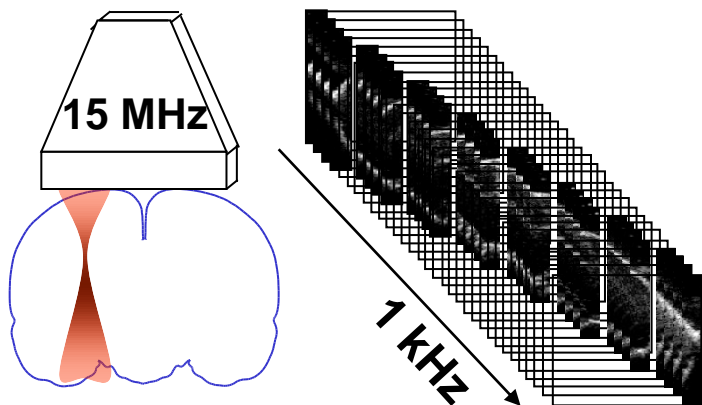
Microvessels



blood flow and volume
blood O₂

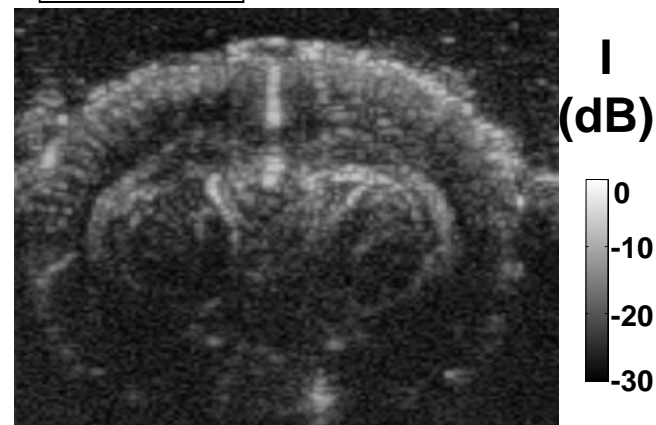
The concept of μ Doppler based on Ultrafast Imaging

Conventional Doppler

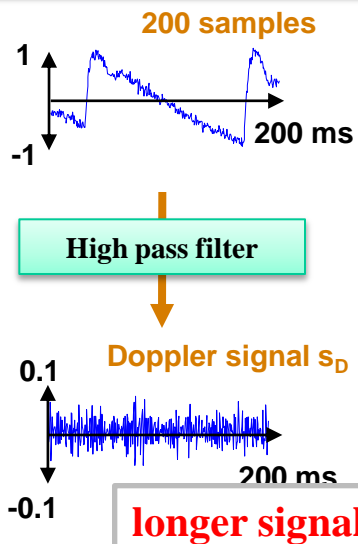
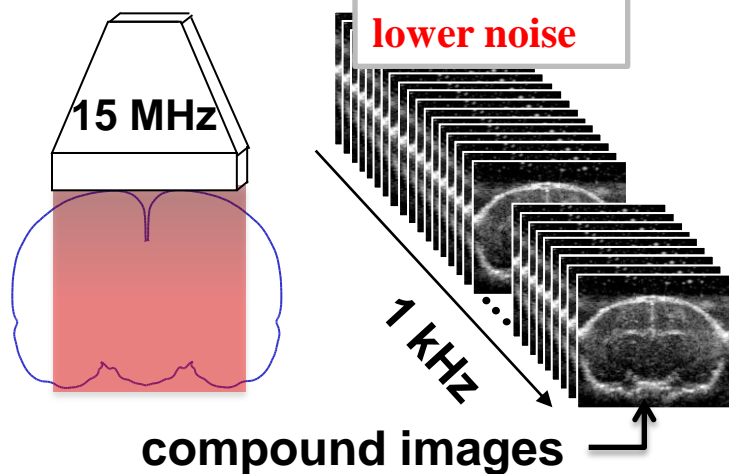


$$I = \int s_D^2(t) dt$$

Power Doppler

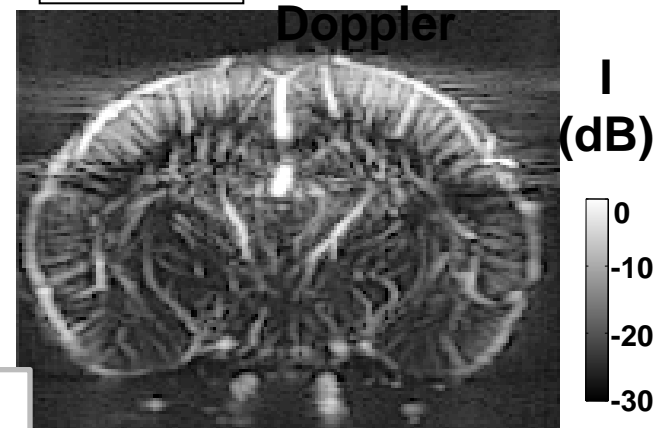


μ Doppler



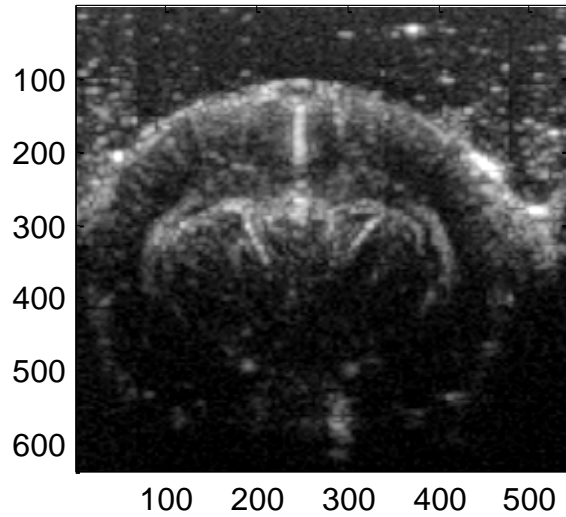
$$I = \int s_D^2(t) dt$$

Power Doppler

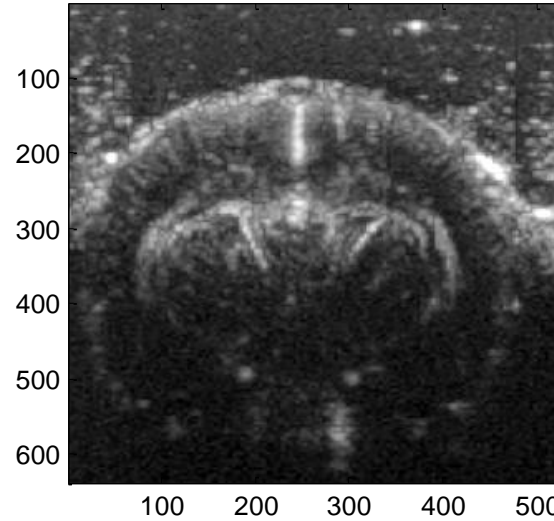


Impact of the number of time samples on Ultrafast Doppler sensitivity

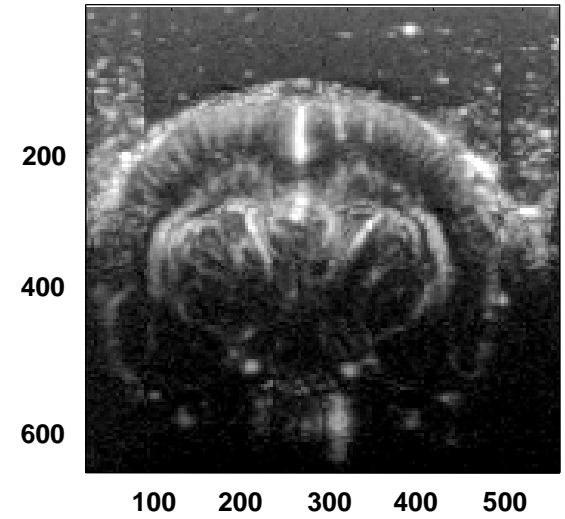
15 focused



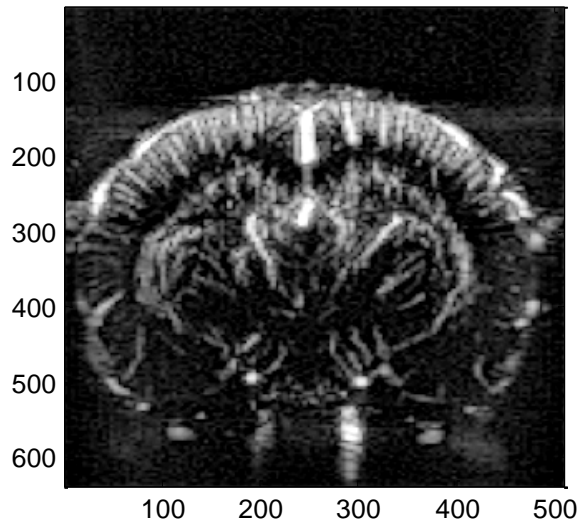
20 focused



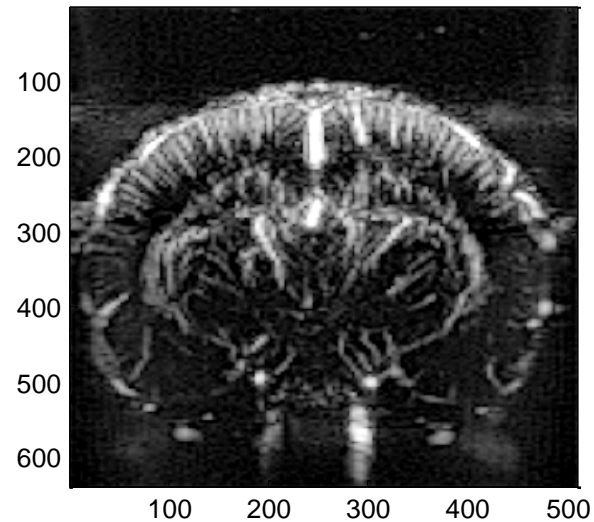
53 focused



200 compound

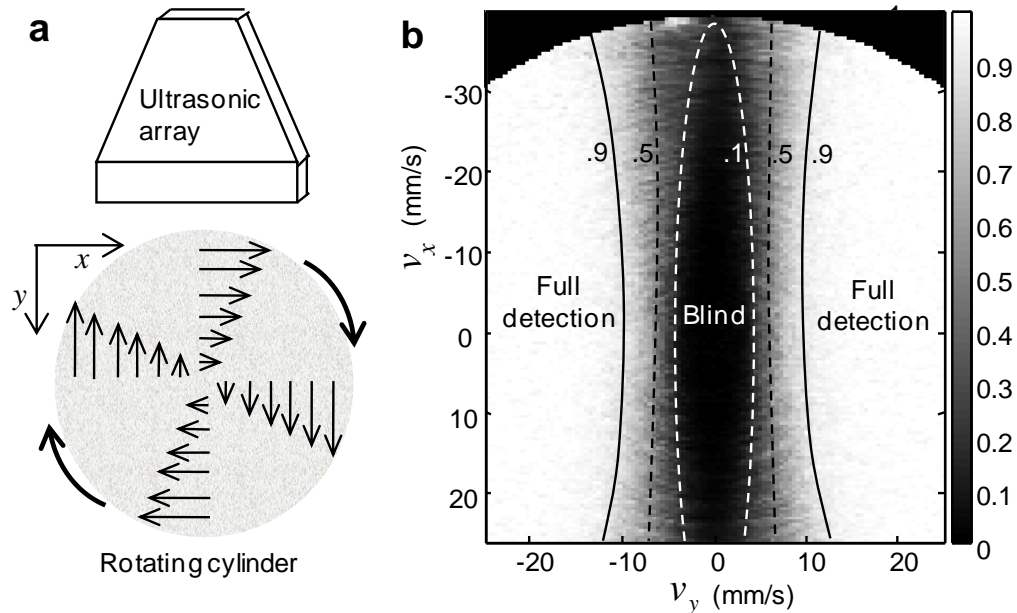


400 compound



What is really measured by I ?

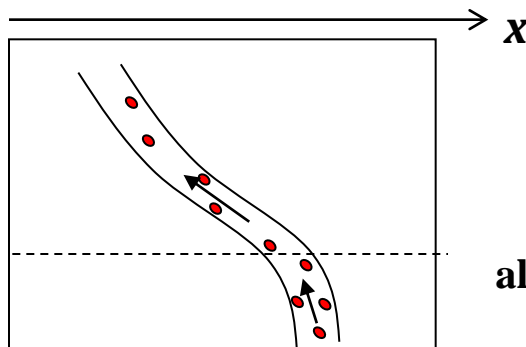
- 1/ I is proportional to the number of scatterers (red blood cells) in the voxel
- 2/ Only a range of velocity is detected
 - Doppler frequencies > cutoff frequency (70 Hz)
- 3/ The effect of the vessel angle can be neglected



I measures the volume of blood flowing at a velocity higher than 4 mm/s (vessels >30 μm) in the voxel

What is the sensitivity of Power Doppler Imaging?

$$I_{Doppler} = \int s^2(t) dt$$

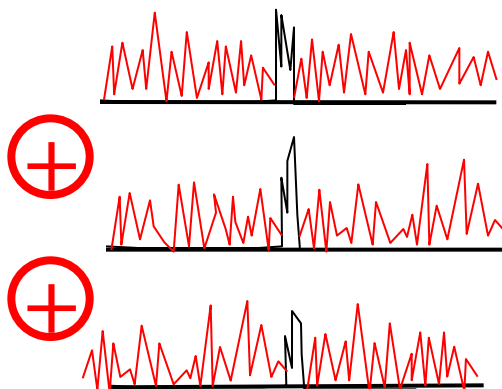
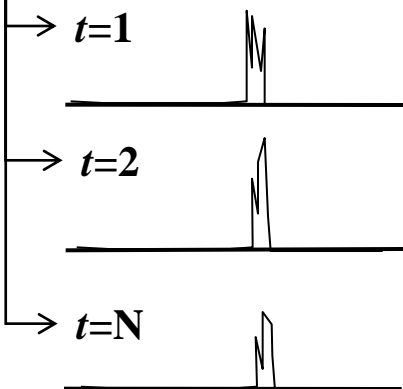


$I_{Doppler}$
along a line ?

$s^2(x, t)$

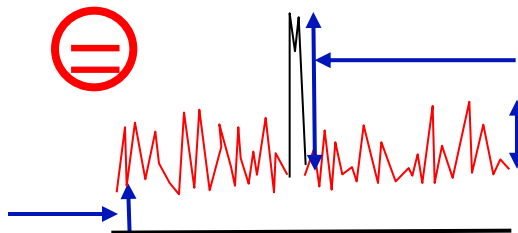
Ideal case: no noise

Real case: a noise is added



$$I_{\min} = \frac{I_{noise}}{\sqrt{\frac{N_{Frames}}{2} - 1}}$$

Offset due to noise
(no influence)



Blood intensity

Noise variance
reduced by the
number of frames

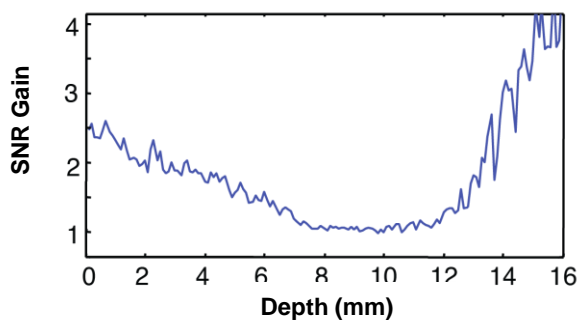
Detectability condition

Blood intensity > noise
variance

Theoretical Sensitivity Gain : Conventional/ Ultrafast Doppler

Sensitivity Gain

$$\frac{S_{\mu\text{Doppler}}}{S_{\text{focalisé}}}$$



$$\frac{SNR^{compound}(z_{foc}, n_{angles})}{SNR^{focalisé}(z_{foc})} = \frac{\sqrt{n_{angles}} z_{foc} \lambda}{D}$$

$$\frac{S_{\mu\text{Doppler}}}{S_{\text{focalisé}}} = \frac{I_{\eta}^{focalisé}}{I_{\eta}^{\mu\text{Doppler}}} \frac{\left(\sqrt{n_{eff}^{\mu\text{Doppler}}/2} - 1\right)}{\left(\sqrt{n_{eff}^{focalisé}}/2 - 1\right)}$$

J. Bercoff, G. Montaldo, T. Loupas, D. Savery, F. Meziere, M. Fink, M. Tanter
'Ultrafast Compound Doppler Imaging', *IEEE UFFC*, 58(1), 134–147, 2011

E. Macé, G. Montaldo, I. Cohen, M. Baulac, M. Fink, M. Tanter
Functional Ultrasonic Imaging of Brain Activity, *Nature Methods*,
July 2011

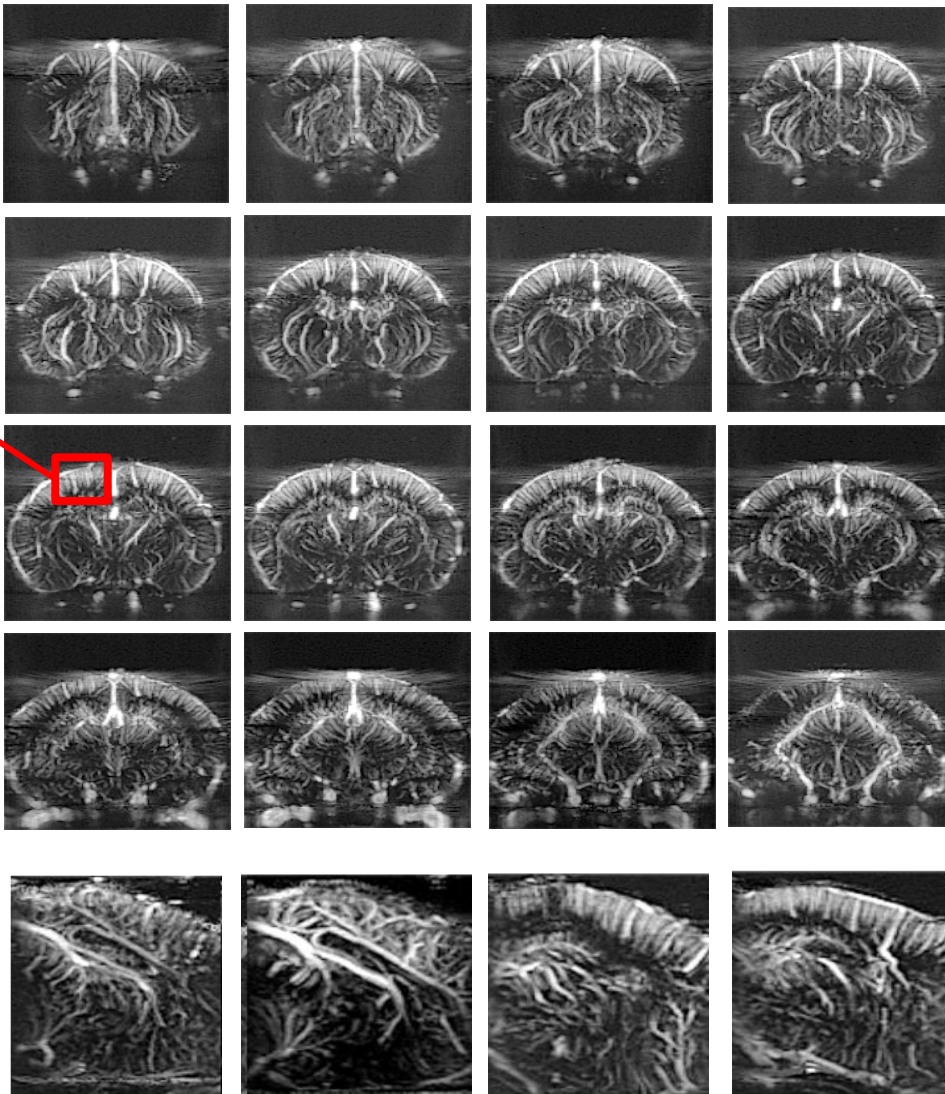
$$\frac{S_{\mu\text{Doppler}}}{S_{\text{focalisé}}}(z) \sim N_{angles} \sqrt{\frac{n_{eff}^{\mu\text{Doppler}}}{n_{eff}^{focalisé}}}$$

Functional ultrasound imaging of the brain: theory and basic principles.

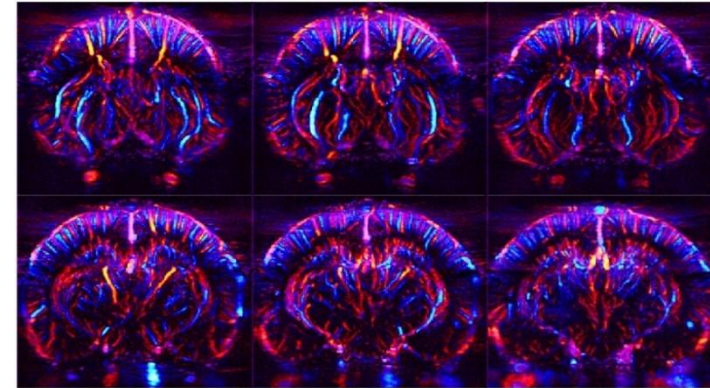
E. Mace, G. Montaldo, B.-F. Osmanski, I. Cohen, M. Fink, M. Tanter IEEE UFFC, *under review*

3D μ Doppler Scan of rat Cerebral Blood Flow

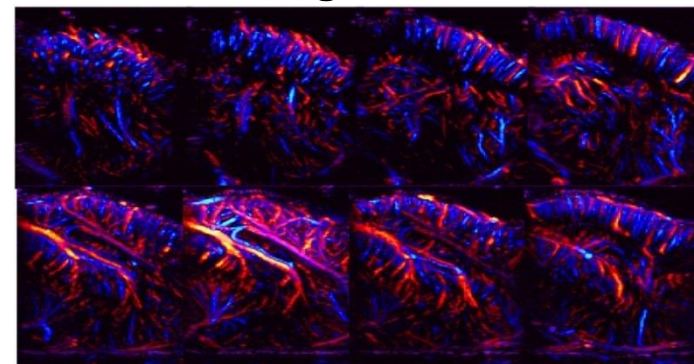
Local
Cerebral
blood
volume



Coronal

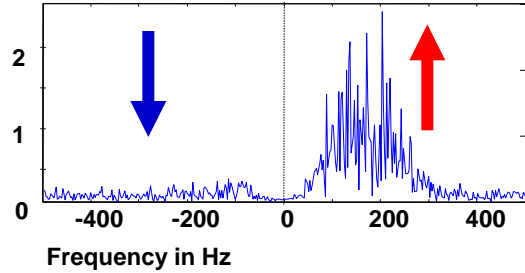


Sagittal

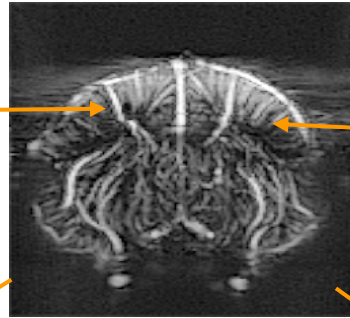
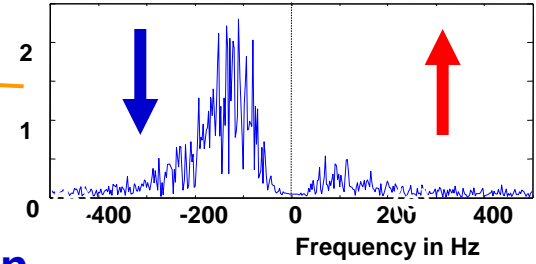


Mapping the direction of the flow

Positive frequency = flow goes up

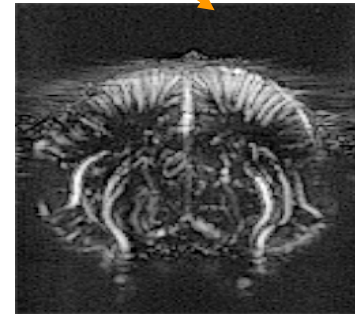
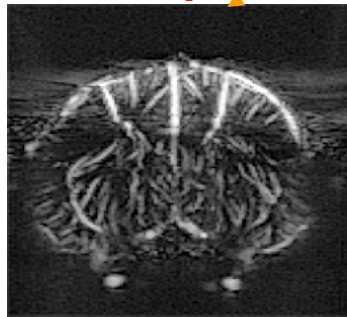


Negative = flow goes down

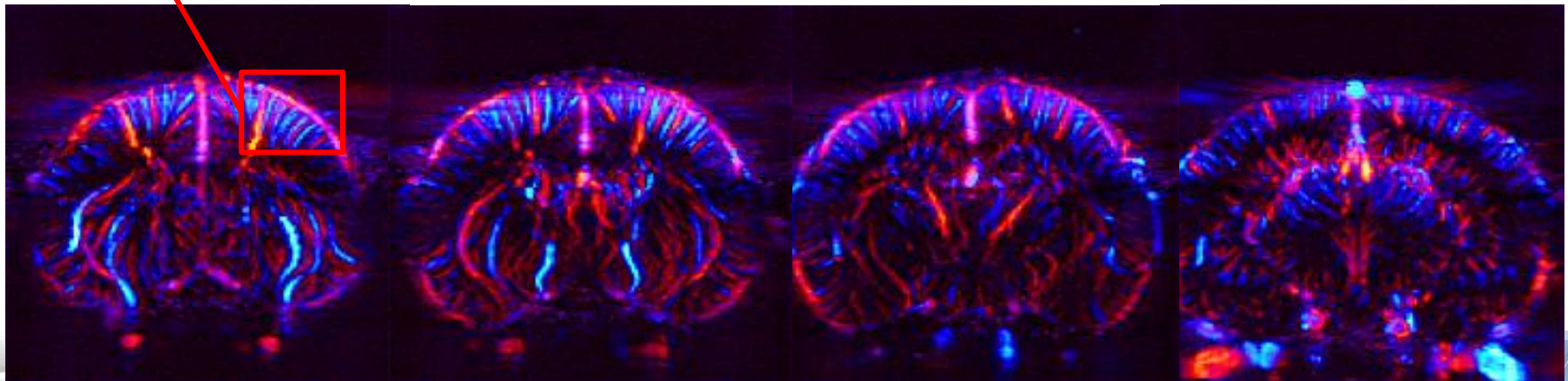
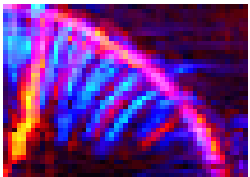
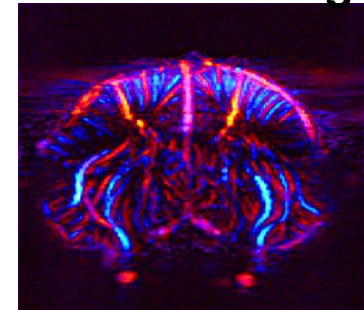


up

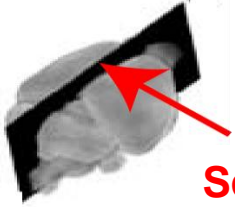
down



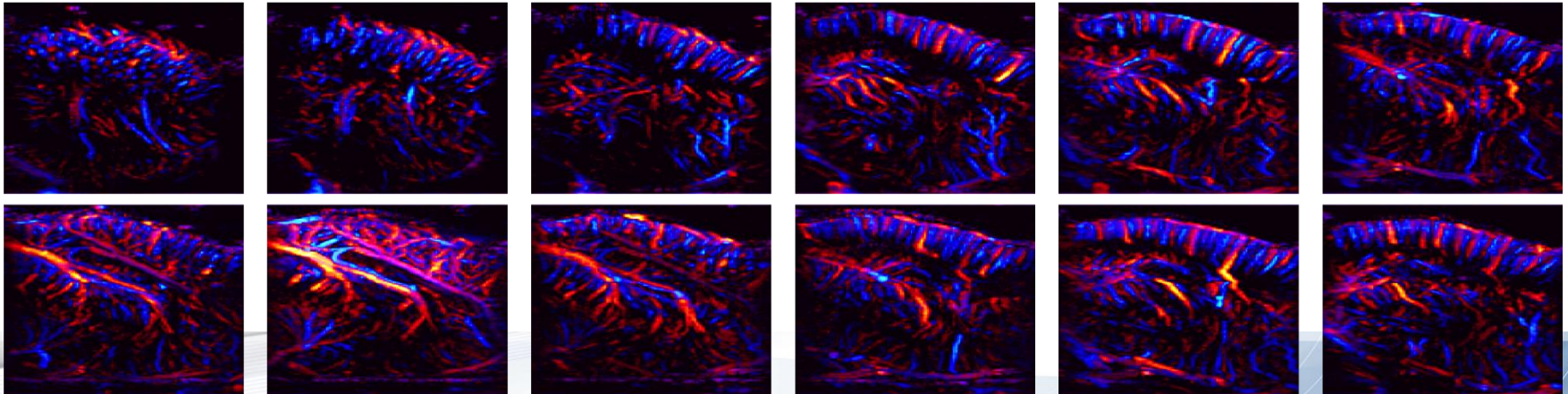
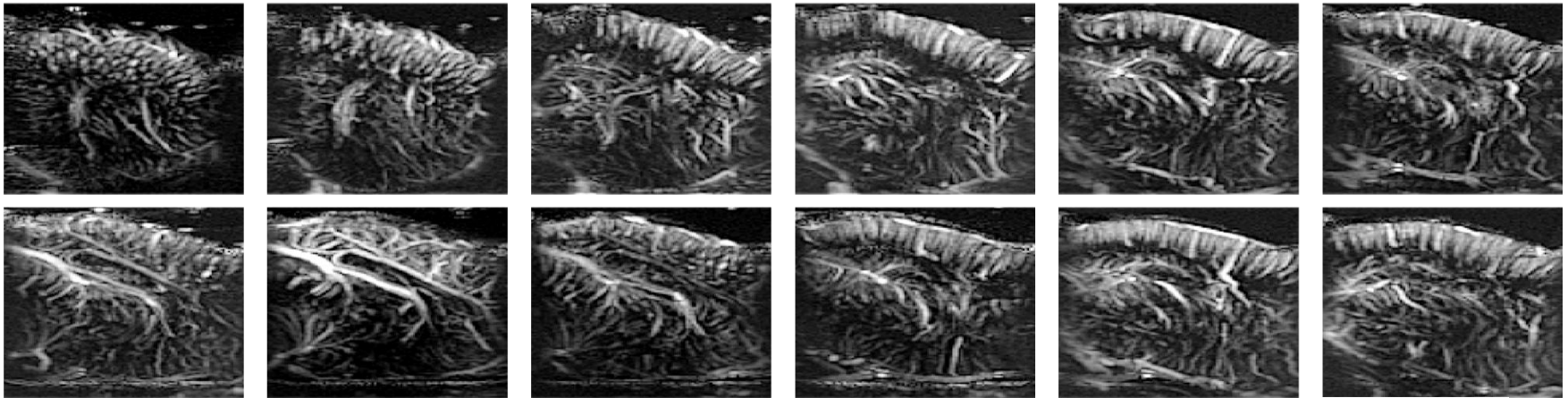
Color coding



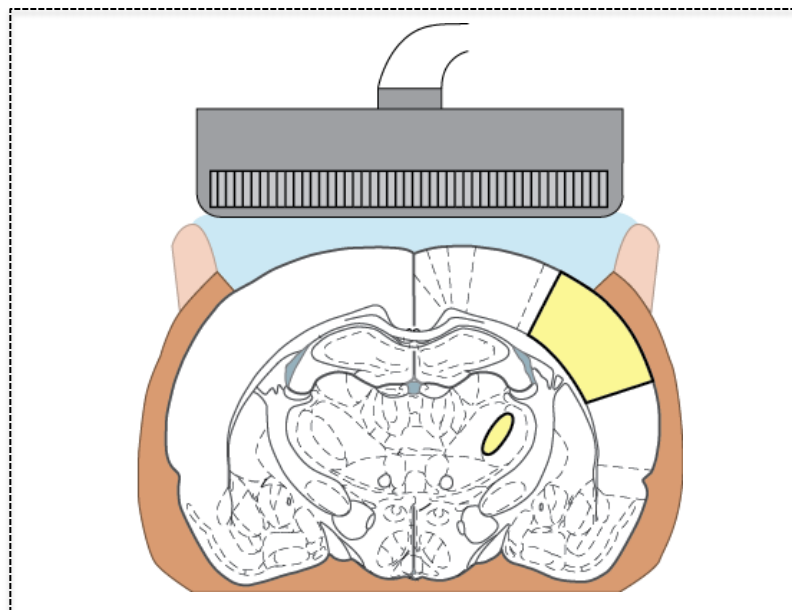
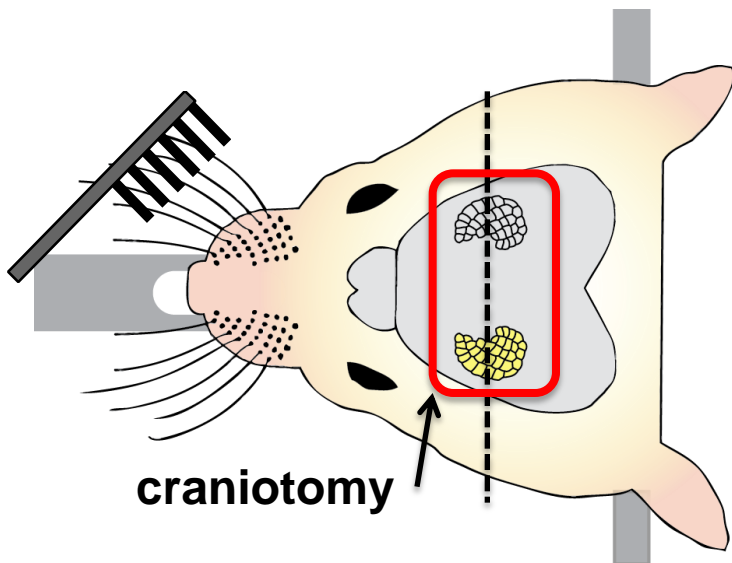
3D μ Doppler Scan of rat CBV : Sagittal orientation



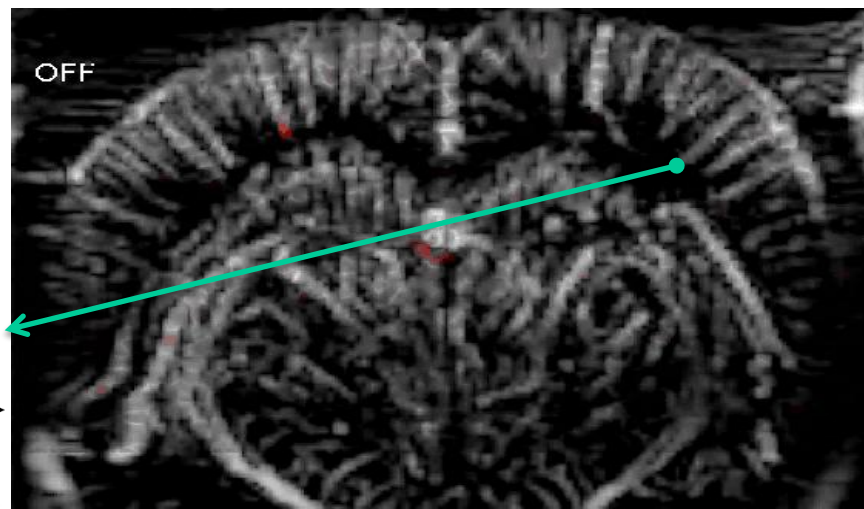
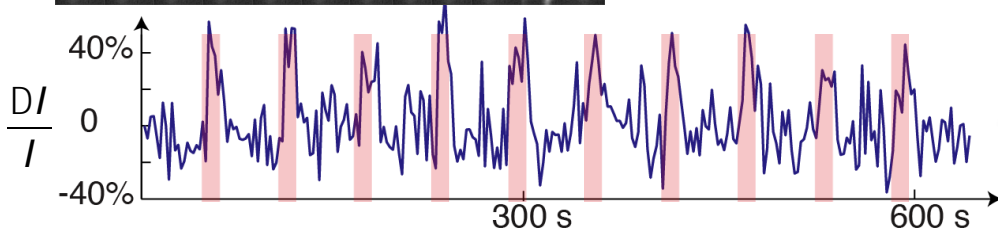
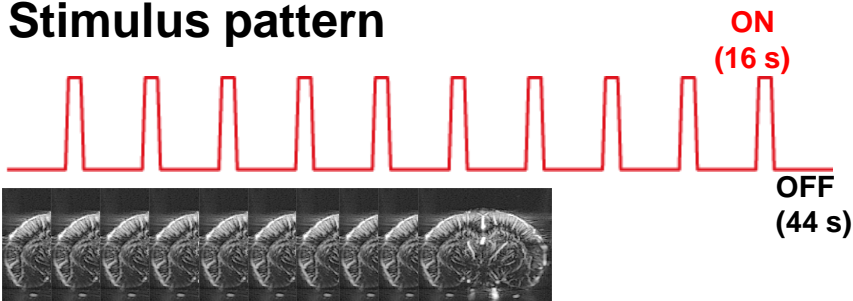
Scan orientation



in-vivo validation



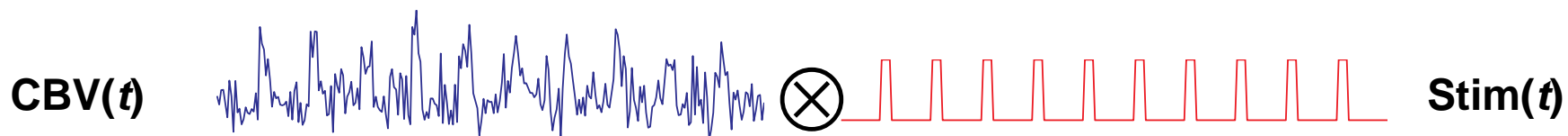
Stimulus pattern



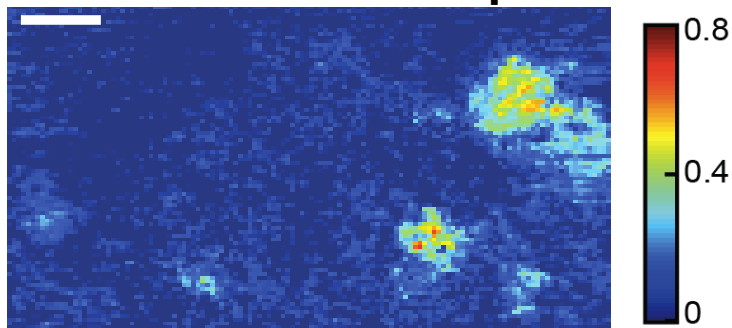
Increased CBV during stimuli

Brain activation maps

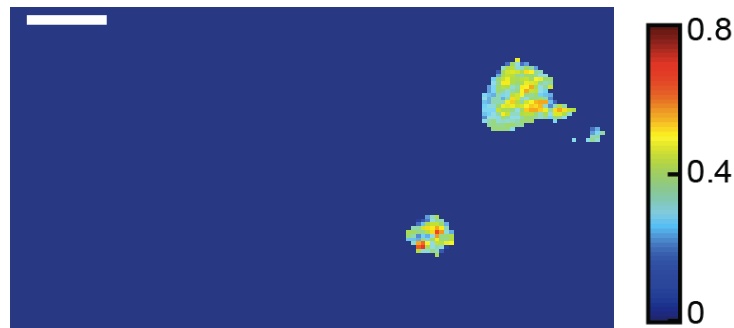
Correlation coefficient r for each pixel



Correlation map



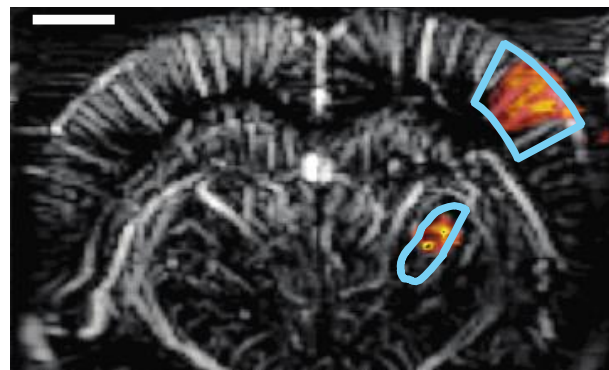
Activated pixels (t-test, $p > 0.001$)



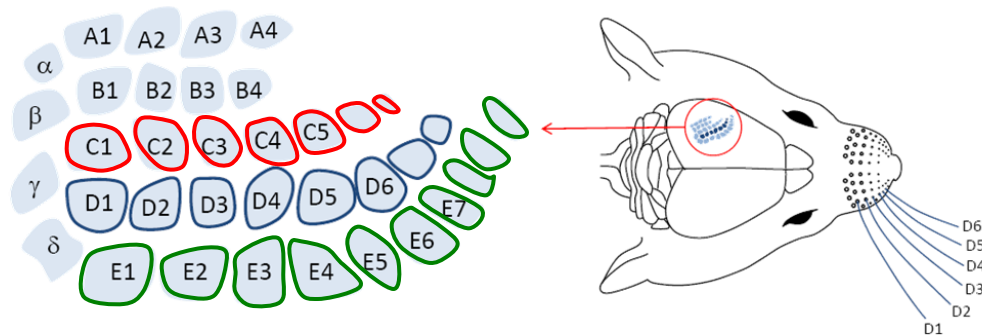
Superposition



Identification



Can we detect smaller activated areas?

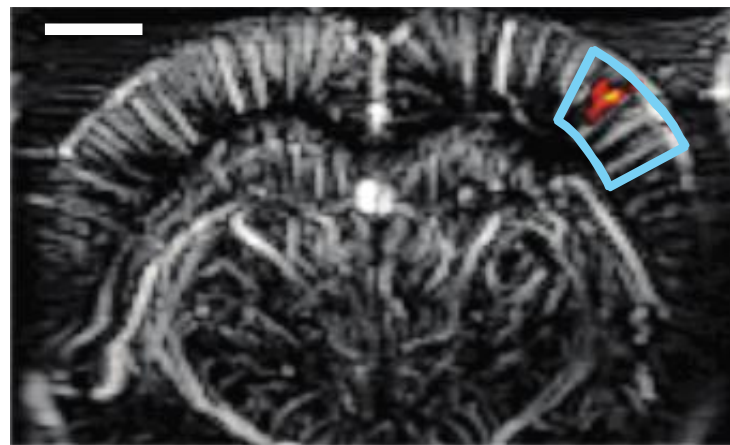
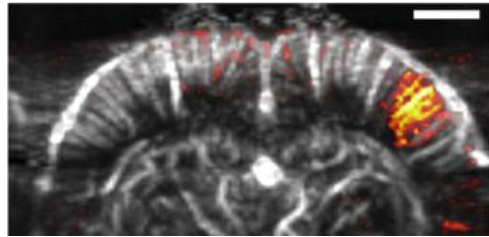
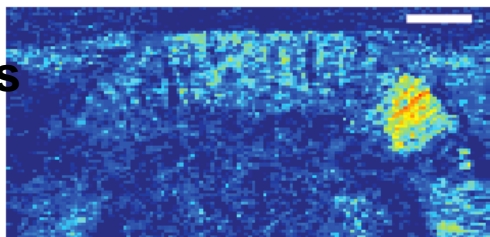


Correlation maps

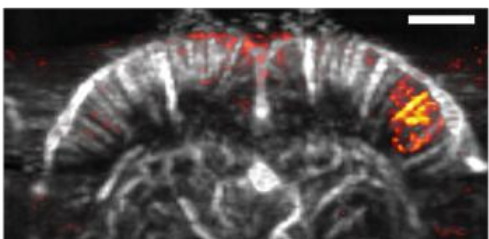
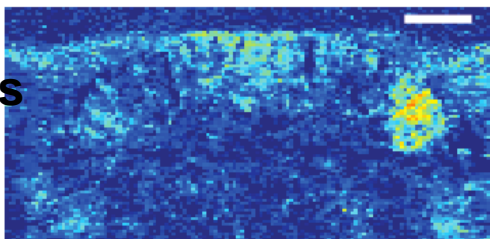
Activation maps

One whisker (D2)

Rows
CDE



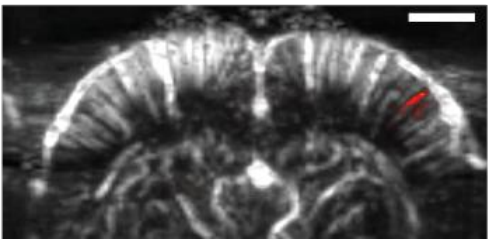
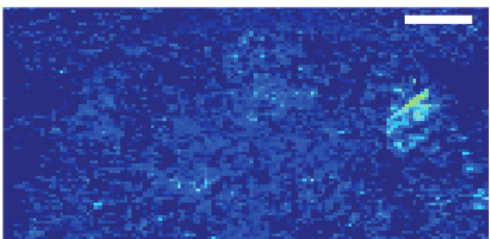
Rows
CD



Only 10 cycles!



Row
D



**Less invasive?
Other areas?**

Epilepsy: A Challenge for neuroimaging techniques

SEIZURE

- Whole brain
- Complex spatiotemporal dynamics
- Not reproducible

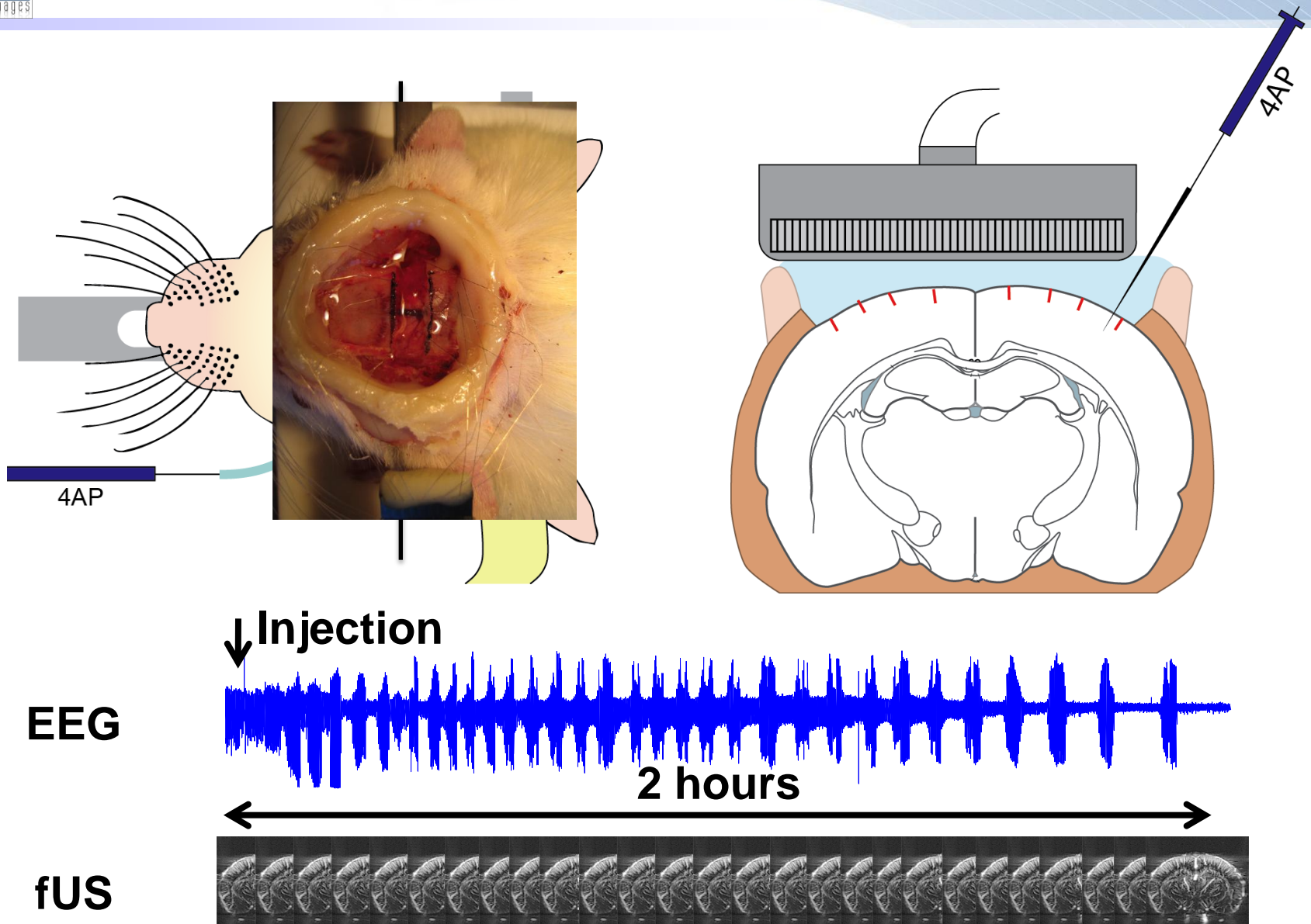
IMAGING MODALITY

- Penetration
- Large field of view
- High spatiotemporal resolution
- High sensitivity

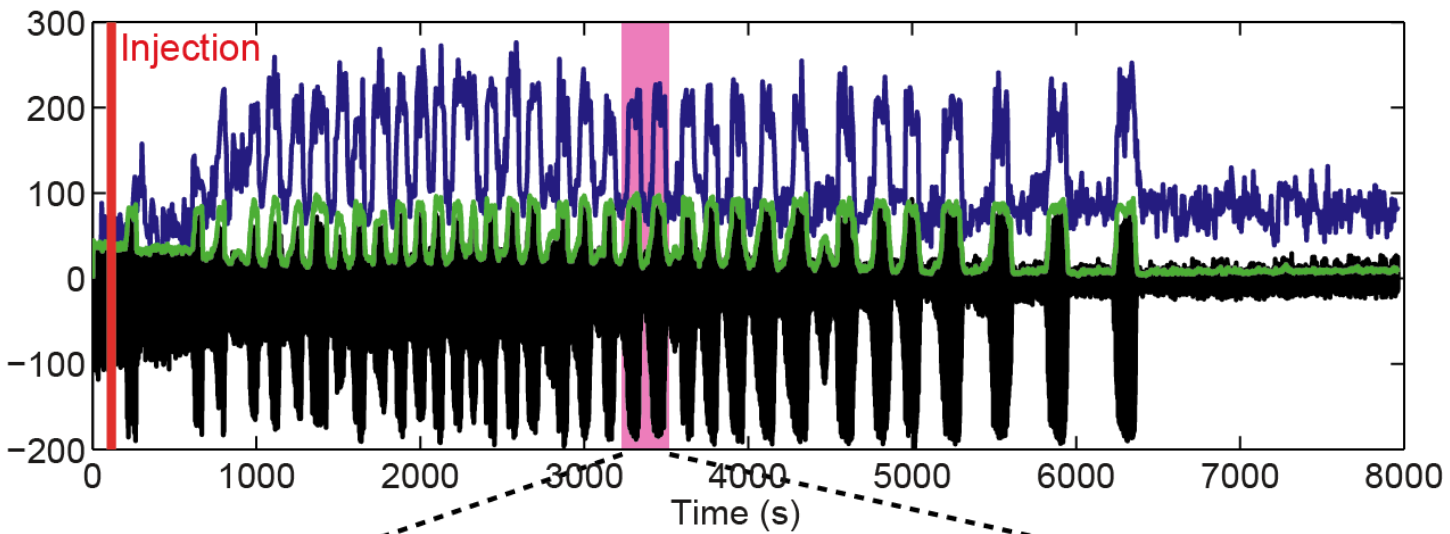
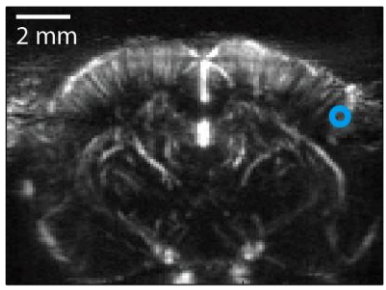


	EEG-fMRI		PET	Optics
Penetration/field of view	✗	✓	✓	✗
Spatial resolution	only few points	✓	✗	✓
Temporal resolution	✓	✗	✗	✓
Sensitivity (SNR)	✓	✗	✓	✓

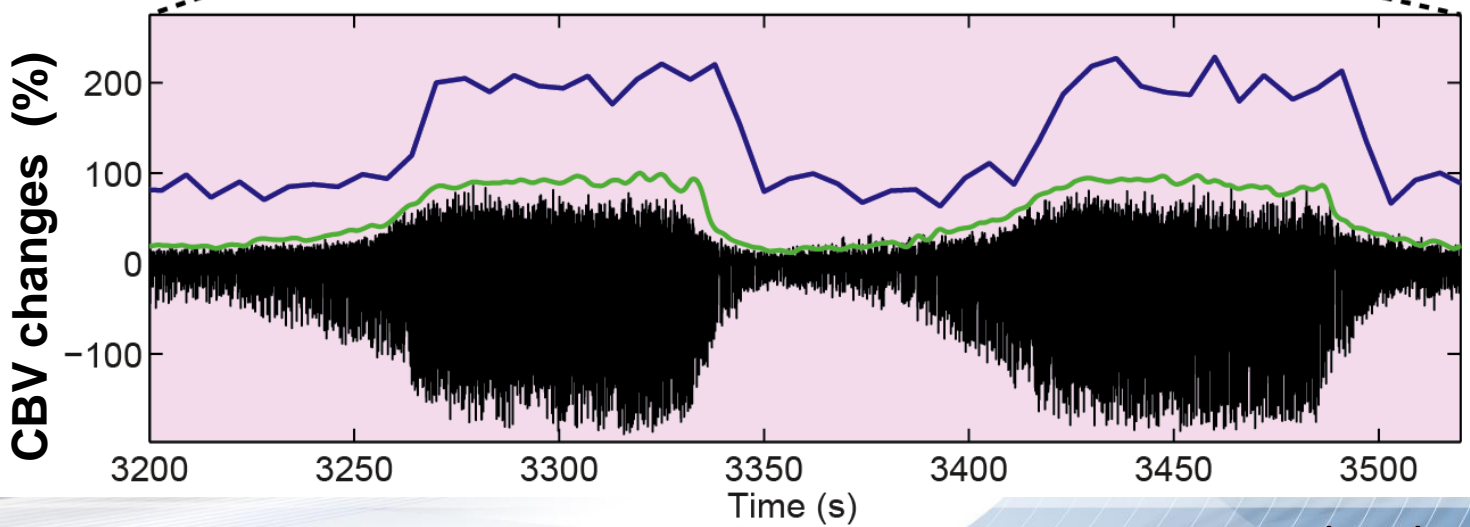
Experimental procedure



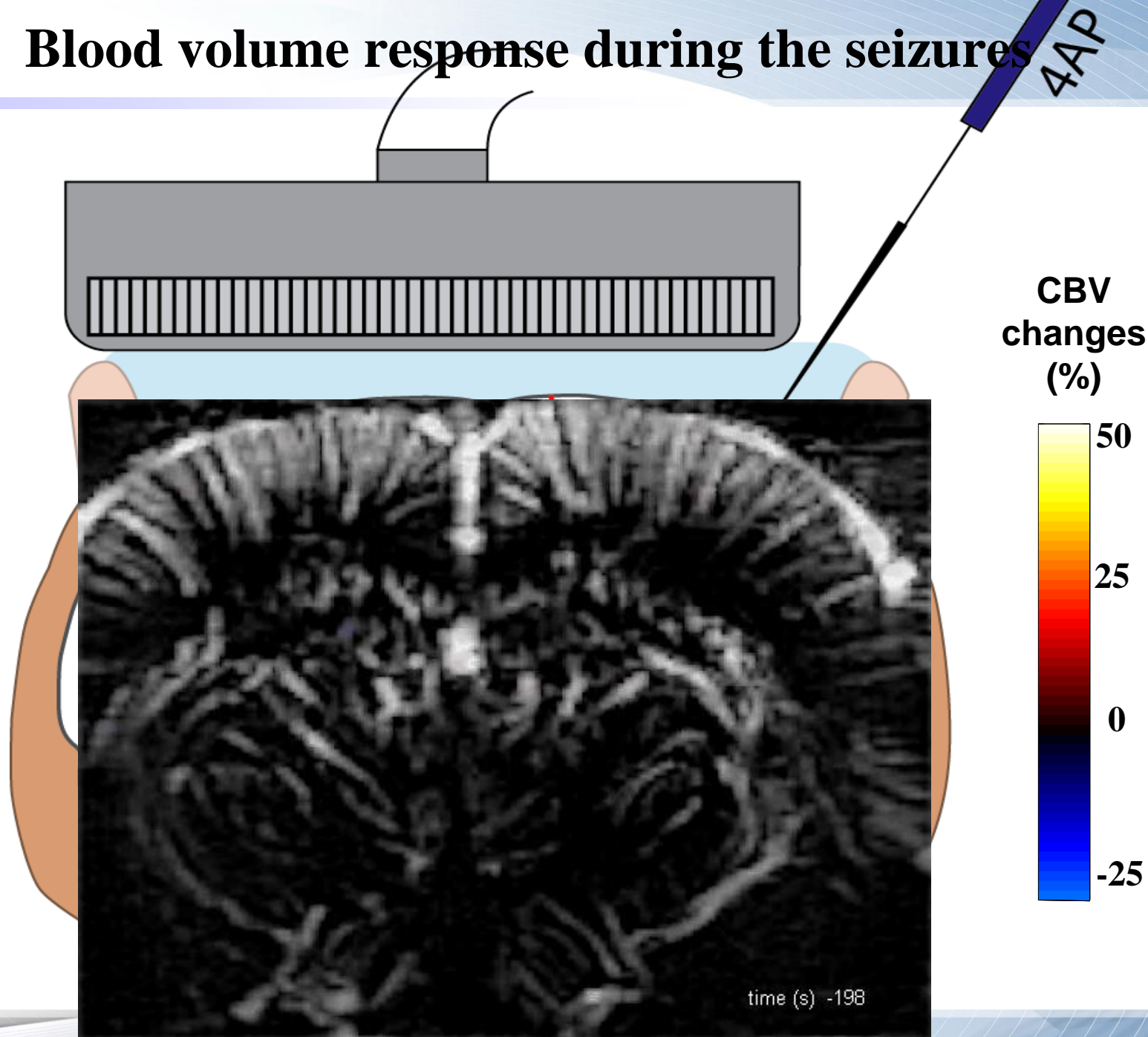
Correlated with neuronal activity?



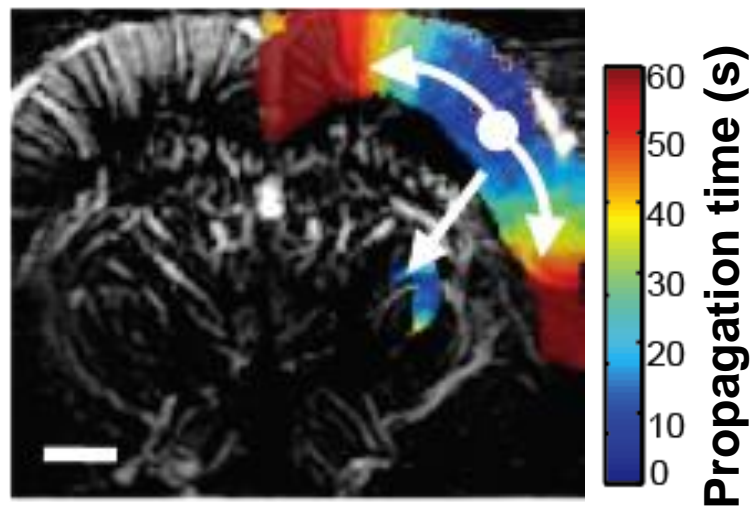
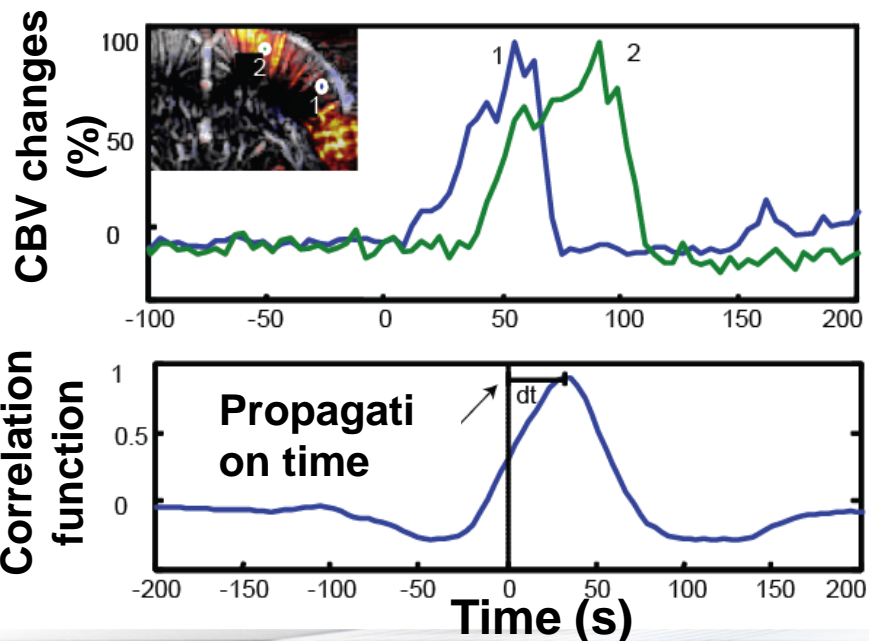
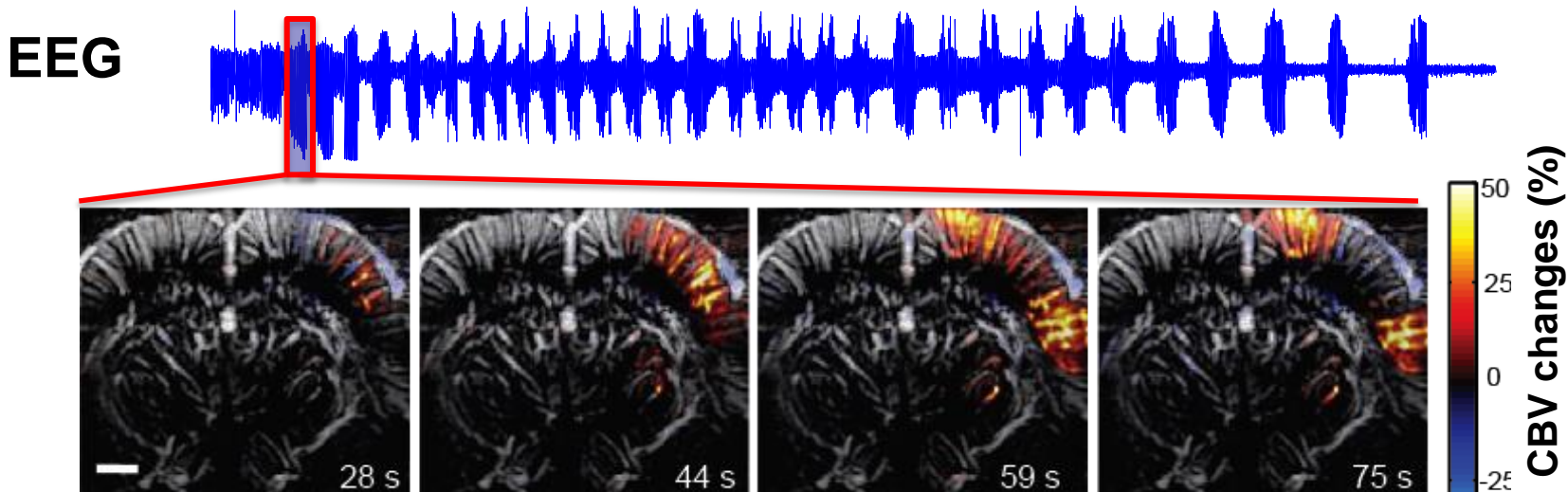
— CBV
— EEG
— EEG envelope



Blood volume response during the seizures



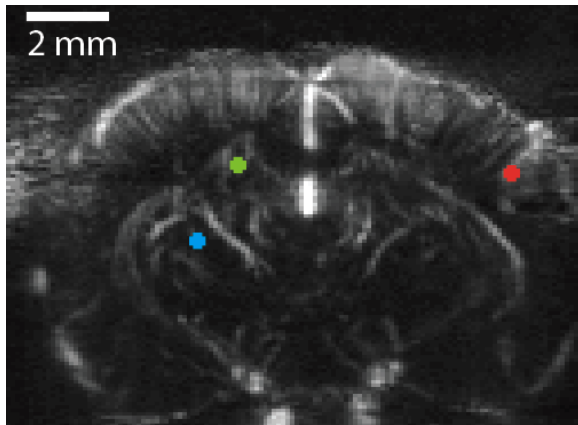
Propagation speed of epileptic seizures



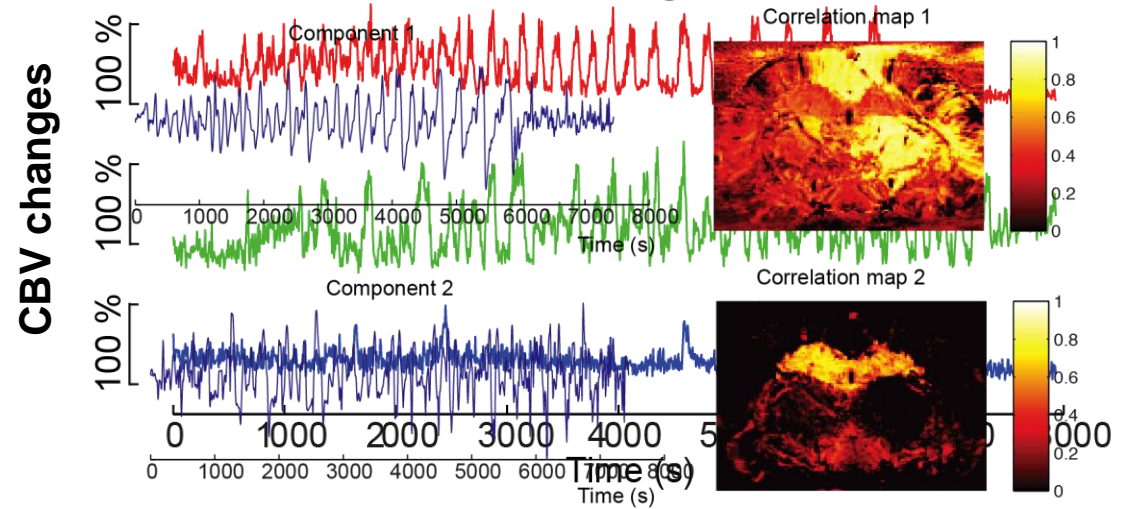
Cortical “wave” speed
3.2 ± 0.3 mm/min

Spatial extension of synchronous activity

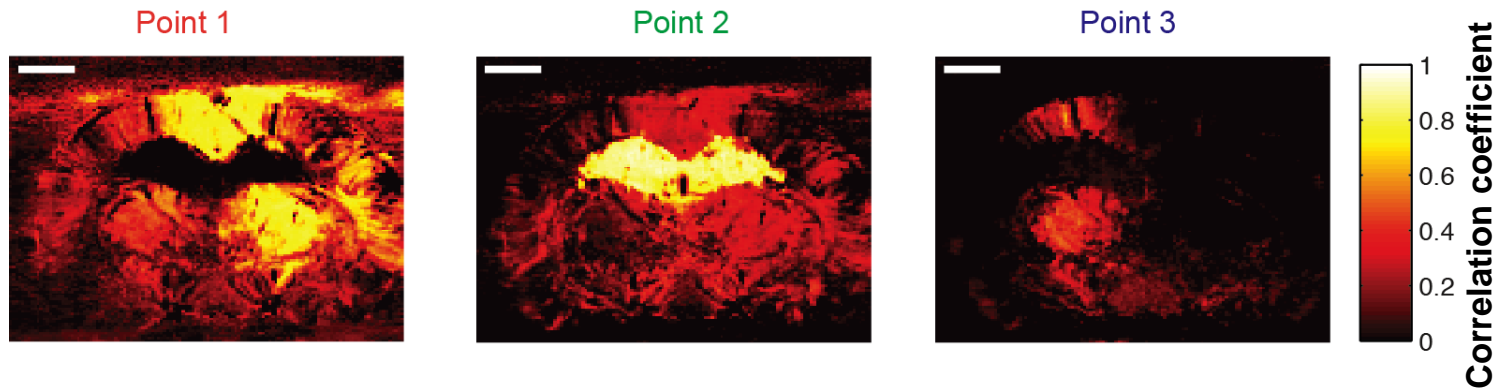
Reference points



Principal component analysis (PCA) fUS signals

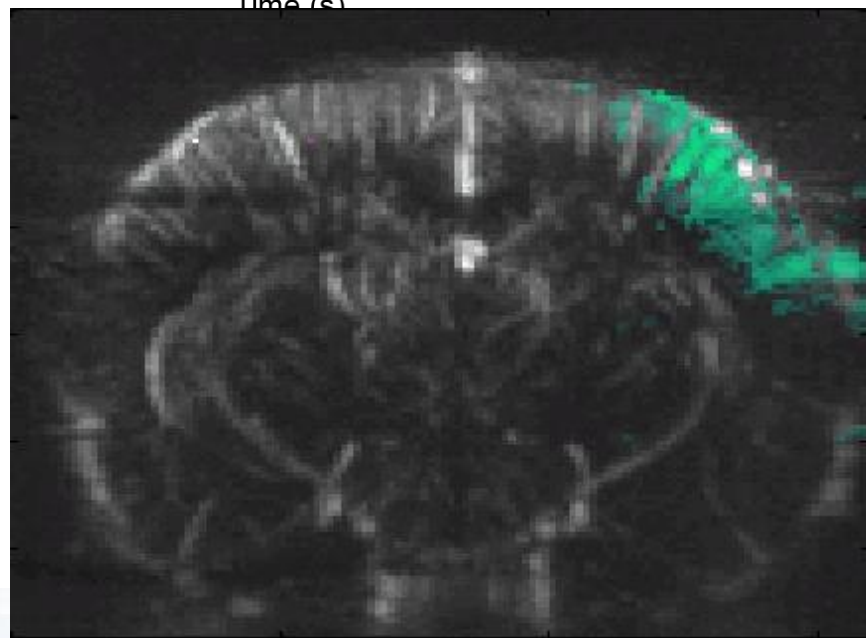
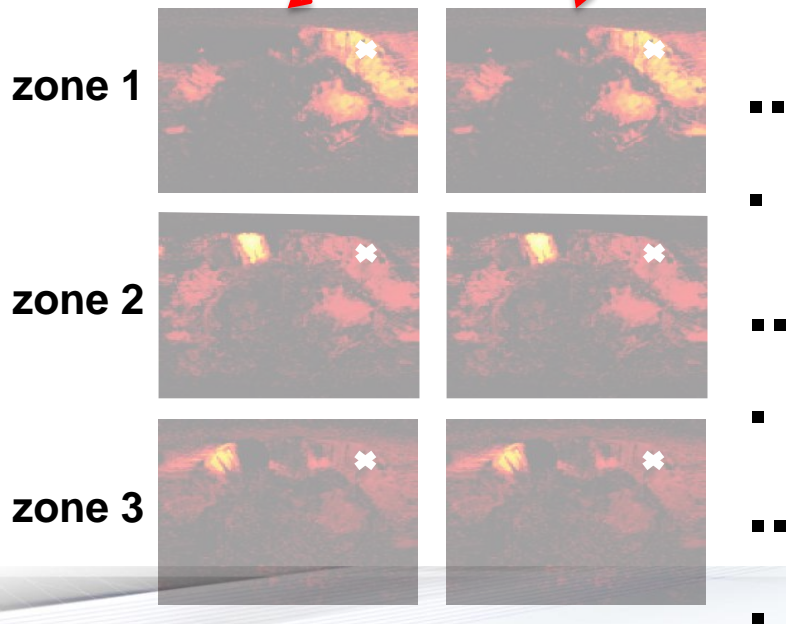
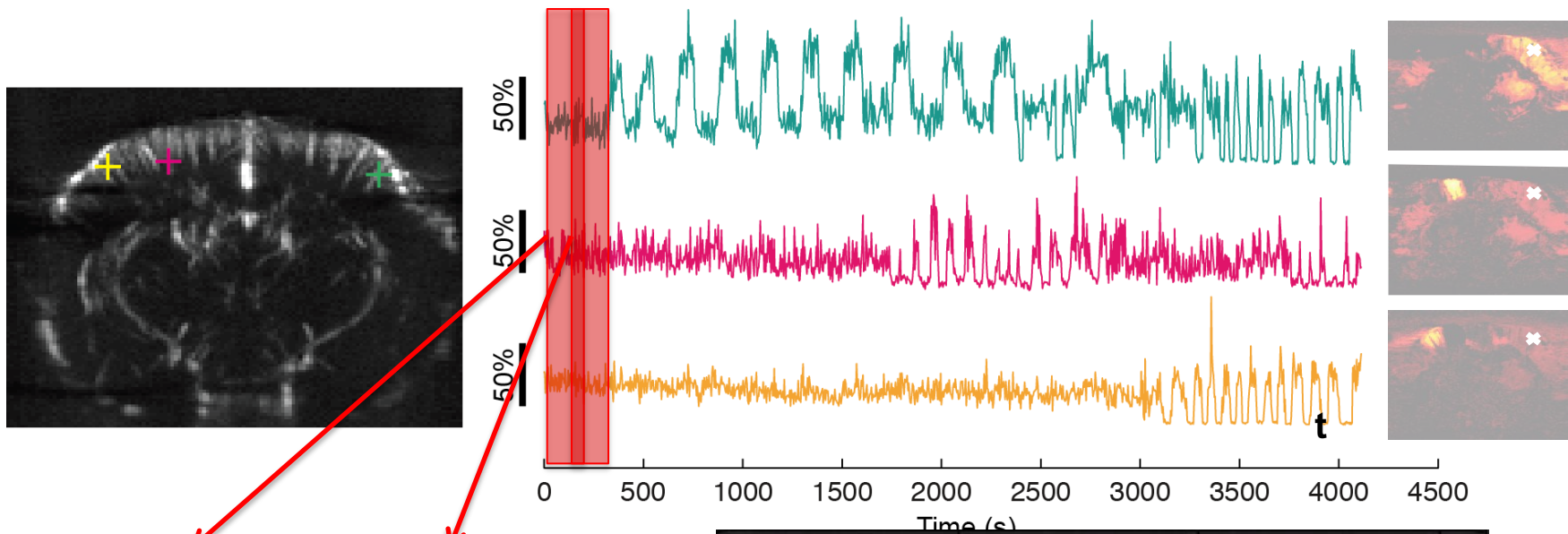


Correlation maps

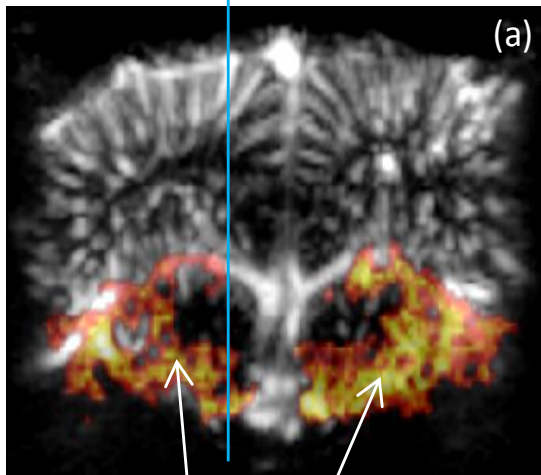
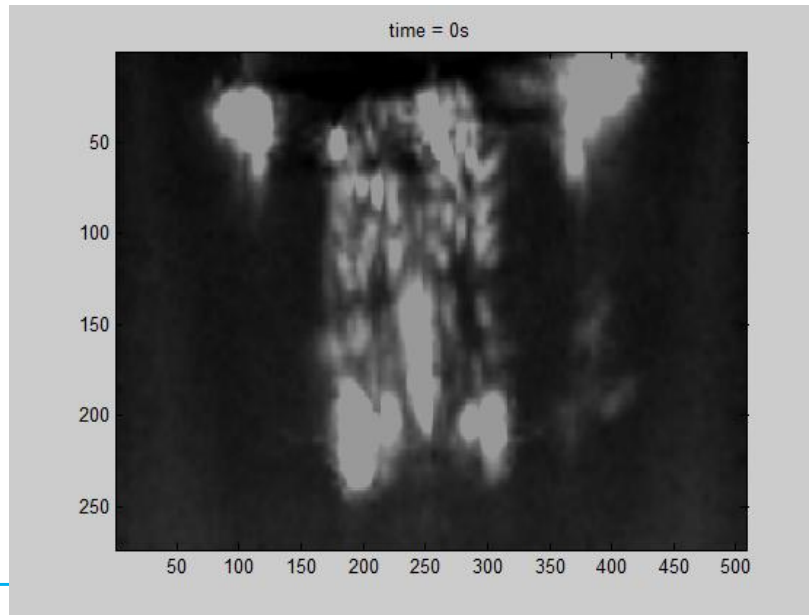


- Large synchronous areas matching with anatomical features
- Areas of independent seizing patterns

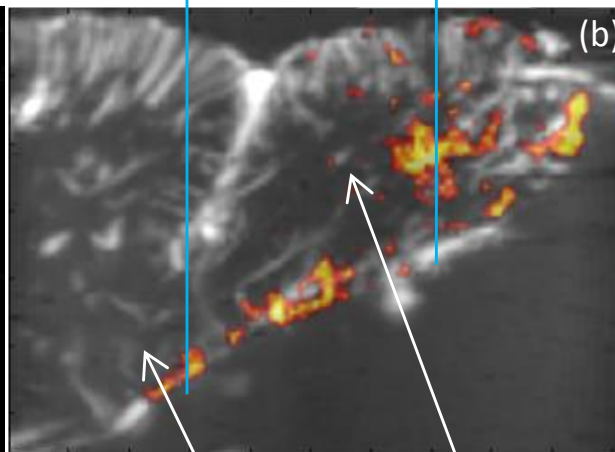
Secondary foci



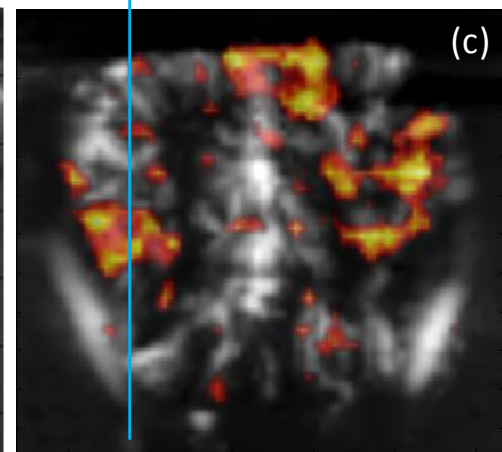
Other functional sensorial activity : following the olfactory track



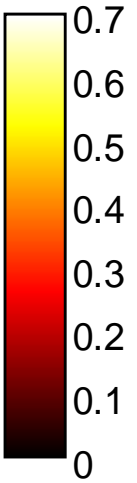
Piriform cortex



Piriform cortex and olfactory bulb

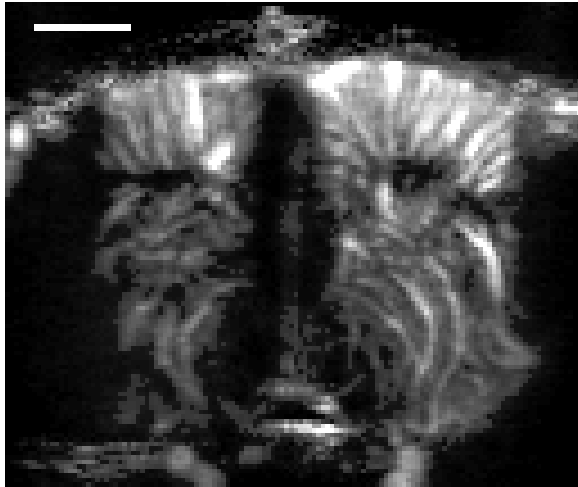


Olfactory bulb

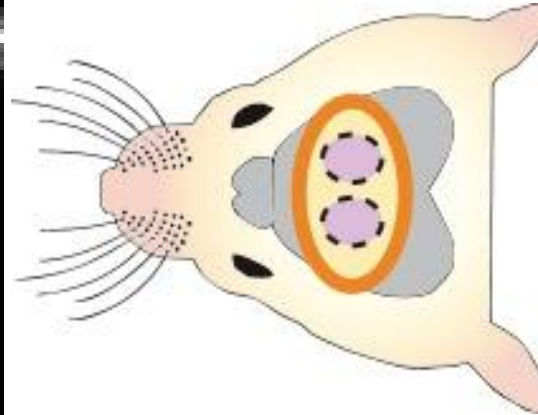


Ongoing work (II) : Development of Chronic and awake fUltrasound

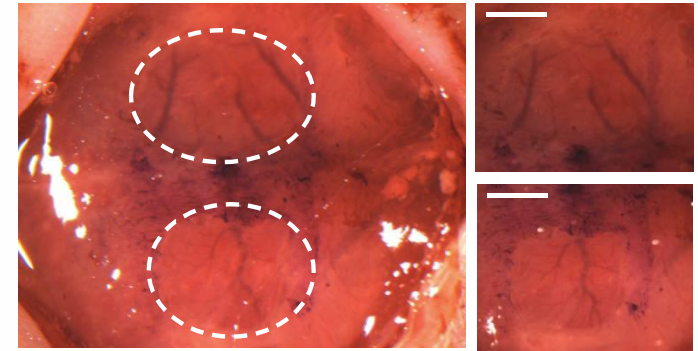
Thinned-skull surgical procedure



Thinned-skull



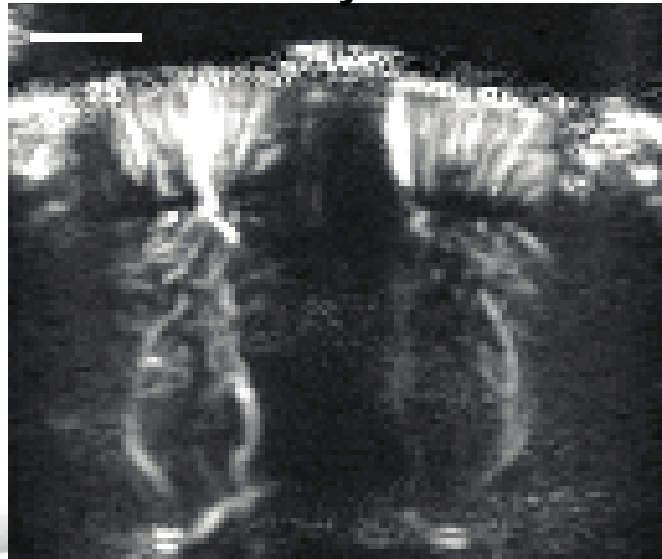
Craniotomy



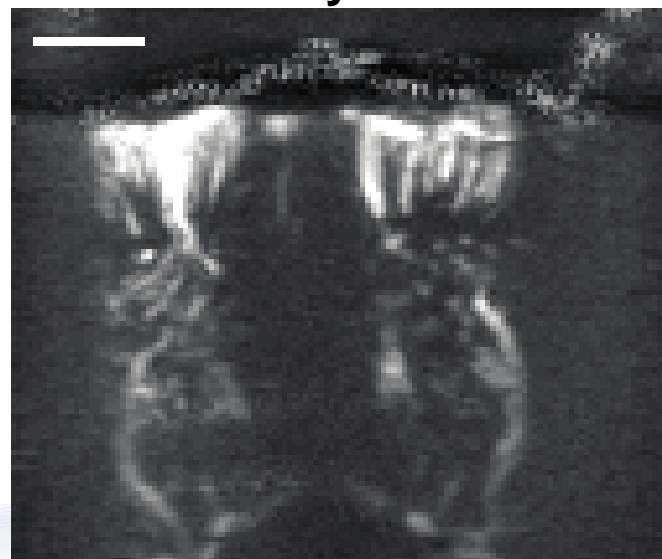
Thinned skull $\approx 50 \mu\text{m}$

$\mu\text{Doppler}$

Day 0

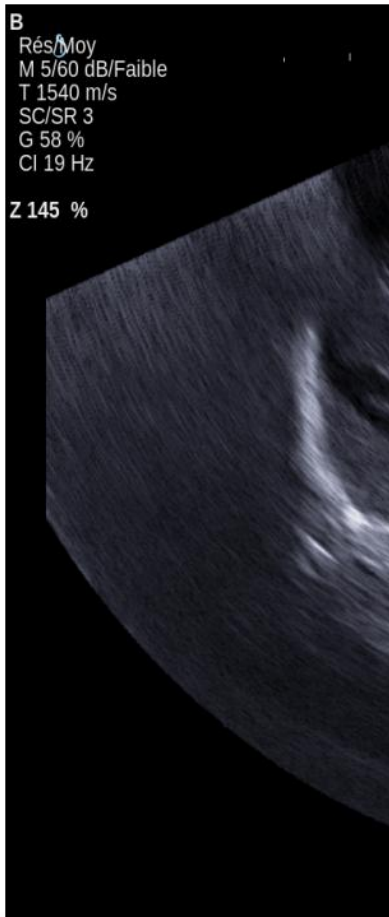


Day 7

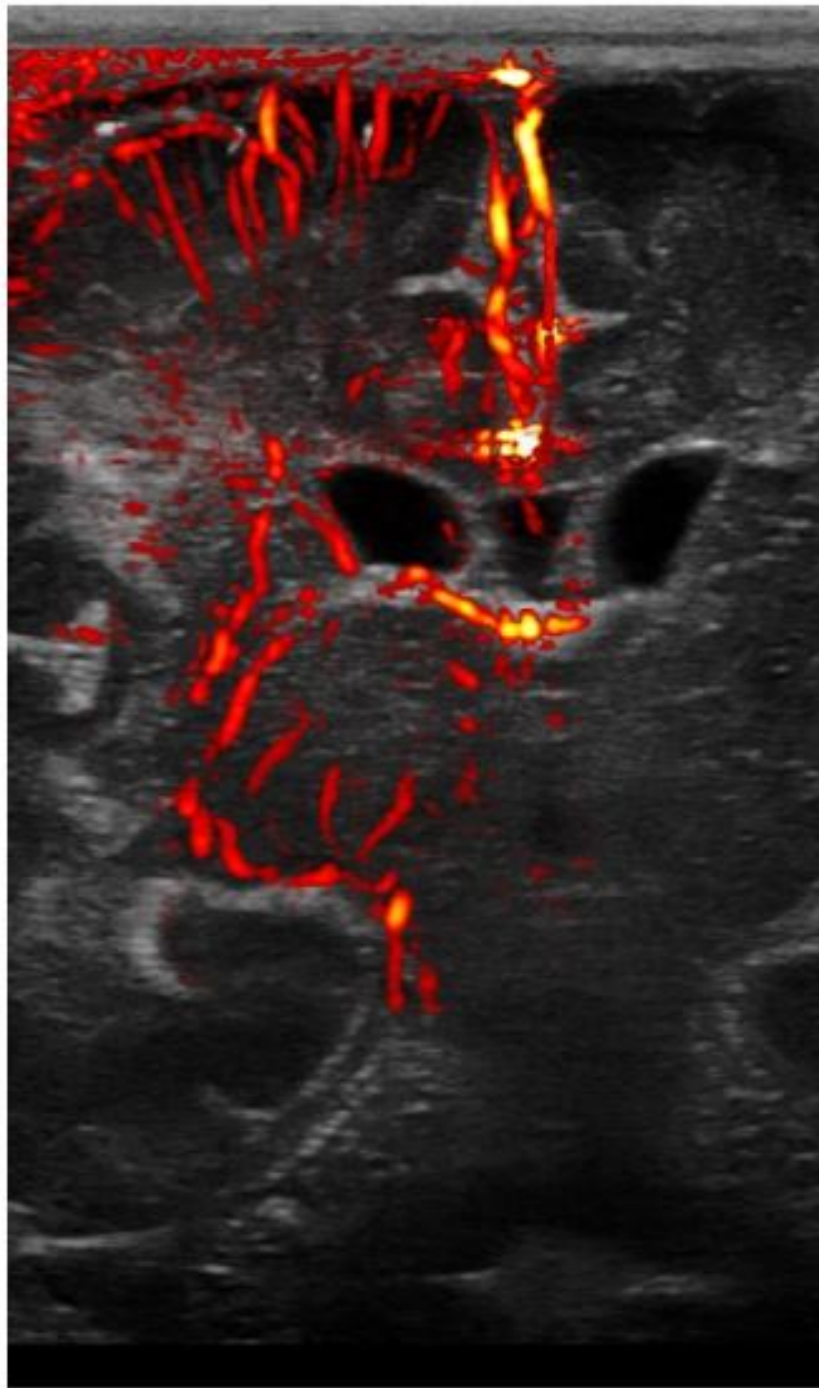


- ✓ Minimally invasive
- ✓ Quick recovery
- ✓ No sign of bone regrowth
- ✓ Low attenuation
- ! Smaller field of view

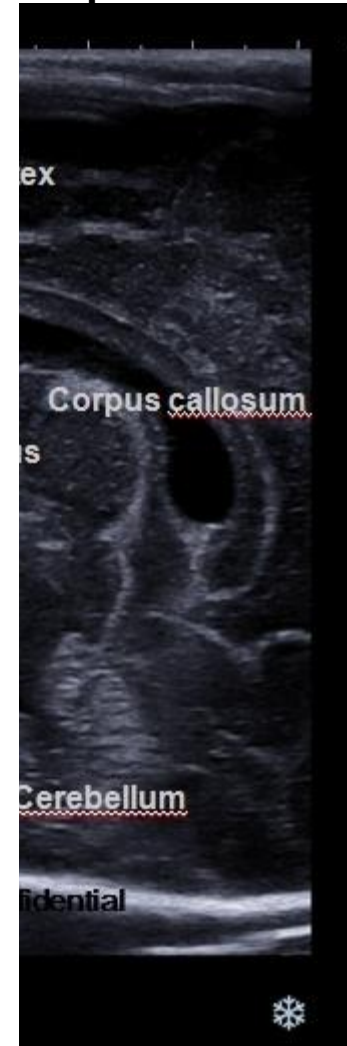
- Implementation
- First clinical st



Typical Bmode

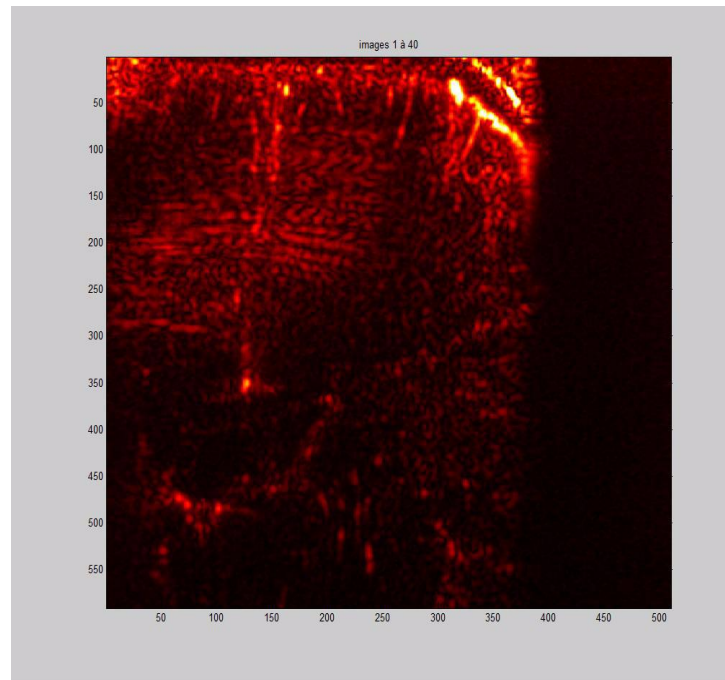
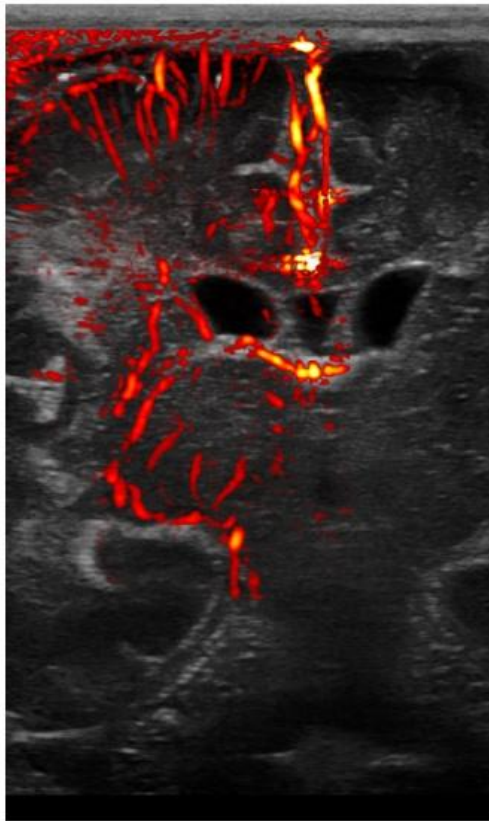


ear probe

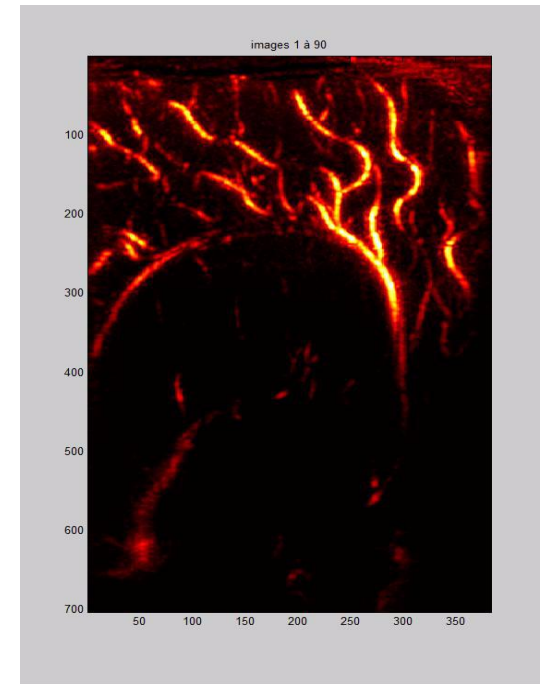


Ongoing work (III) : Proof of concept of clinical fUS

First in vivo data on preterm infants (transfontanel imaging)



Coronal view



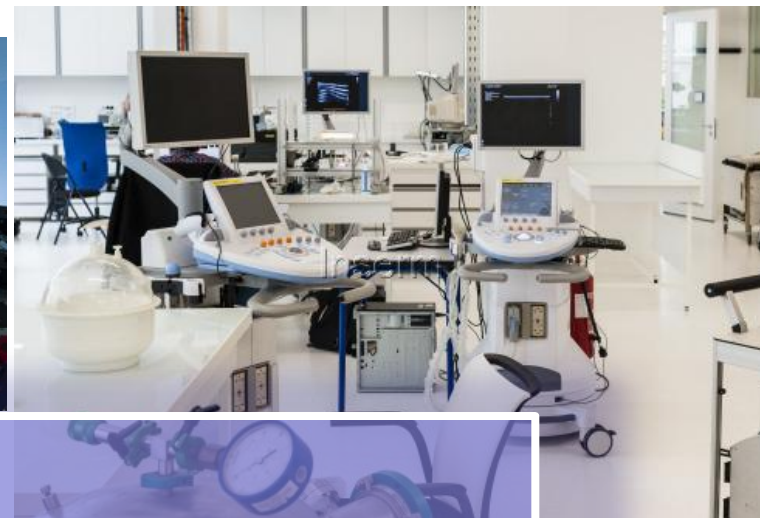
Sagittal view

Pulsatility on one single cardiac cycle

Summary

- Ultrafast ultrasound imaging is linked to the concept of **Holography in Optics**
- Ultrafast imaging using the concept of plane or circular waves paves the way **to tremendous applications for medical ultrasound**
- Ultrafast plane wave imaging was initially **introduced for Transient Elastography**
- Ultrafast imaging is the key for **quantitative and real time Elastography**
- Ultrafast imaging technology has emerged thanks to **video game industry**
- **Supersonic Shear Wave Elastography** was **the first clinical application** of ultrafast imaging and led to the first ultrafast imaging commercial device
- Beyond Elastography, new modalities are already emerging today :
 - **Ultrafast Doppler** for complex flows or small vessels imaging
 - Conventional Bmode will be replaced by **Coherent plane wave compounding**
 - **Ultrafast Cavitation Imaging**
 - **Ultrafast Contrast imaging**
 - **fUltrasound** : functional ultrasound imaging of brain activation

Thank You very much !



Join us !
PhD and PostDocs positions available
At Institute Langevin, Paris

